Stationary Subdivision and Multiresolution Surface Representations

Thesis by

Denis N. Zorin

In Partial Fulfillment of the Requirements

for the Degree of

Doctor of Philosophy

California Institute of Technology

Pasadena, California

1998

(Submitted September 23, 1997)

Report Documentation Page

Form Approved
OMB No. 0704-0188

Public reporting burden for the collection of information is estimated to average 1 hour per response, including the time for reviewing instructions, searching existing data sources, gathering and maintaining the data needed, and completing and reviewing the collection of information. Send comments regarding this burden estimate or any other aspect of this collection of information, including suggestions for reducing this burden, to Washington Headquarters Services, Directorate for Information Operations and Reports, 1215 Jefferson Davis Highway, Suite 1204, Arlington VA 22202-4302. Respondents should be aware that notwithstanding any other provision of law, no person shall be subject to a penalty for failing to comply with a collection of information if it does not display a currently valid OMB control number.

1. REPORT DATE	2. REPORT TYPE	3. DATES COVERED
1998		**00-00-1998 to 00-00-1998**

4. TITLE AND SUBTITLE	5a. CONTRACT NUMBER
Stationary Subdivision and Multiresolution Surface Representation	5b. GRANT NUMBER
	5c. PROGRAM ELEMENT NUMBER
6. AUTHOR(S)	5d. PROJECT NUMBER
	5e. TASK NUMBER
	5f. WORK UNIT NUMBER
7. PERFORMING ORGANIZATION NAME(S) AND ADDRESS(ES) **Air Force Office of Scientific Research,875 North Randolph Street Suite 325,Arlington,VA,22203-1768**	8. PERFORMING ORGANIZATION REPORT NUMBER
9. SPONSORING/MONITORING AGENCY NAME(S) AND ADDRESS(ES)	10. SPONSOR/MONITOR'S ACRONYM(S)
	11. SPONSOR/MONITOR'S REPORT NUMBER(S)

12. DISTRIBUTION/AVAILABILITY STATEMENT
Approved for public release; distribution unlimited

13. SUPPLEMENTARY NOTES
The original document contains color images.

14. ABSTRACT
see report

15. SUBJECT TERMS

16. SECURITY CLASSIFICATION OF:			17. LIMITATION OF ABSTRACT	18. NUMBER OF PAGES	19a. NAME OF RESPONSIBLE PERSON
a. REPORT	b. ABSTRACT	c. THIS PAGE			
unclassified	**unclassified**	**unclassified**		**302**	

© 1998
Denis N. Zorin
All Rights Reserved

Acknowledgements

I would like to thank my advisors, Alan H. Barr and Peter Schröder, and all people of the Caltech Computer Graphics Group: Cindy Ball, Dave Breen, Bena Currin, Dave Felt, Dan Fain, Louise Foucher, Kurt Fleischer, David Laidlaw, Alf Mikula, Mark Montague, Preston Pfarner, Eric Winfree and all the other people who made the lab a great place to work.

Special thanks go to Andrei Khodakovsky and Gary Wu for their help with implementing the mulitresolution editing system.

I am grateful to Wim Sweldens for his contribution to the papers that we have co-authored and for the opportunity to spend a summer at Bell Laboratories. I am also grateful to Jeff Lagarias for his suggestions.

I would like to thank Tom Duchamp, who has suggested to me some of the ideas presented in this thesis, and has provided a lot of valuable feedback.

I would like to thank Venkat Krishnamurthy for providing the Armadillo dataset, and Hughes Hoppe for the mannequin head.

And, finally, I would like to thank Isabella Goldmints; without her, my life would be very boring.

The research was supported in part through grants from Pixar, the Intel Corporation, Microsoft, the Charles Lee Powell Foundation, the Sloan Foundation, an NSF CAREER award (ASC-96-24957), the NSF STC for Computer Graphics and Scientific Visualization (ASC-89-20219), the Office of the Director, Defense Research and Engineering, the Air Force Office of Scientific Research (F49620-96-1-0471), as part of the MURI program,

Abstract

Stationary subdivision is an important tool for generating smooth free-form surfaces used in CAGD and computer graphics. One of the challenges in the construction of subdivision schemes for arbitrary meshes is to guarantee that the surfaces produced by the algorithm are C^1-continuous. First results in this direction were obtained only recently. In this thesis we derive necessary and sufficient criteria for C^k-continuity that generalize and extend most known conditions.

We present a new method for analysis of smoothness of subdivision which allows us to analyze subdivision schemes which do not generate surfaces admitting closed-form parameterization on regular meshes, such as the Butterfly scheme and schemes with modified rules for tagged edges.

The theoretical basis for analysis of subdivision that we develop allows us to suggest methods for constructing new subdivision schemes with improved behavior. We present a new interpolating subdivision scheme based on the Butterfly scheme, which generates C^1-continuous surfaces from arbitrary meshes.

We describe a multiresolution representation for meshes based on subdivision. Combining subdivision and the smoothing algorithms of Taubin [61] allows us to construct a set of algorithms for interactive multiresolution editing of complex hierarchical meshes of arbitrary topology.

Contents

Acknowledgements **iii**

Abstract **v**

Notation **xxi**

1 Introduction **1**

1.1 Subdivision 2

1.2 Multiresolution Representations and Editing 4

1.3 Contributions 5

1.3.1 Theory of Subdivision 5

1.3.2 Multiresolution Representations 7

1.4 Related Work: Construction of Subdivision Schemes 7

1.4.1 Approximating Subdivision Schemes 7

1.4.2 Interpolating Subdivision Schemes 8

1.5 Related Work: Analysis 9

1.6 Related Work: Surface Editing 10

1.6.1 Comparison with Previous Work 11

1.7 Overview 13

2 Basic Properties of Stationary Subdivision **15**

2.1 Summary 15

2.1.1 Subdivision on Complexes. 15

2.1.2 Subdivision Matrices 19

2.2 Subdivision of Abstract Simplicial Complexes 22

2.2.1 Definitions 23

2.2.2 Control and Localization Sets 34

2.2.3 Properties of Neighborhoods 36

2.3 Convergence of Subdivision 38

2.3.1 Definition of Convergence 39
2.3.2 Basis Function Decomposition 41
2.3.3 Reduction to the k-regular Complexes 44
2.4 Subdivision Matrix 47
2.4.1 Subdivision Matrix and Layers 47
2.4.2 Eigenbasis Functions and Scaling Relations 50
2.4.3 Jordan Normal Form of the Subdivision Matrix 54
2.4.4 Convergence Criterion for Subdivision 56
2.4.5 Extension of the Eigenbasis Functions 57

3 Smoothness of Stationary Subdivision 61

3.1 Definitions of Tangent Plane Continuity and C^k-continuity 63
3.1.1 C^1-continuous Surfaces 63
3.1.2 Constructing C^1-Continuous Subdivision Schemes 66
3.1.3 Tangent Plane Continuity 66
3.1.4 C^1-continuous Subdivision Schemes 70
3.2 Singular Parameterizations and a Nondegeneracy Condition 72
3.3 Subdivision on k-regular Complexes as Projection 74
3.4 Reduction to the Analysis of the Universal Surfaces 77
3.5 Tangent Plane Continuity Criterion 80
3.6 Tangent Plane Continuity of Schemes with Nondegenerate Directional Sets 84
3.7 Sufficient Conditions for Tangent Plane Continuity 88
3.8 A Necessary Condition 91
3.9 Interpretation of the Tangent Plane Continuity Criterion 93
3.10 Criteria for C^1 and C^k-continuity 95
3.10.1 Limit Values, Tangents and Normals 100
3.10.2 Degree Estimate for Piecewise Polynomial Subdivision 101
3.11 Proof of Lemma 3.3 102
3.12 Linear Transformations on $\Lambda^2(\mathbf{R}^p)$ 104
3.13 Scaling Relations 108
3.13.1 Two Real Eigenvalues 110
3.13.2 Complex-Conjugate Eigenvalues 117

3.13.3 Jordan Block of Size 2 119

4 Constructive Conditions for Smoothness 125

4.1 Injectivity of the Characteristic Map 126

4.1.1 Lipschitz Norms 126

4.1.2 Injectivity Criterion 129

4.2 Covering Conditions 133

4.3 Convergence Rates for Uniform Schemes on Regular Complexes 138

4.4 Convergence Rates for Schemes with Creases on Regular Complexes 147

4.4.1 Definitions 147

4.4.2 Commutation Formulas 151

4.5 The Algorithm for Checking C^1-continuity of a Subdivision Scheme 157

4.6 Continuity with Respect to the Control Values 158

5 Algorithms for Verification of C^1-continuity 163

5.1 Error Types 163

5.2 Interval Representations 165

5.3 Input of the Algorithms 169

5.4 Algorithm for Testing C^1-Continuity for Fixed Valence 171

5.5 Algorithm for Testing Regularity 173

5.6 Algorithm For Testing Isolation from Zero 175

5.7 Algorithm for Testing Injectivity 176

5.8 Conditions for Successful Completion 180

6 Analysis of Specific Schemes 181

6.1 Invariant Schemes 181

6.2 Single Ring Schemes 189

6.2.1 Algorithms for Testing C^1-Continuity of Invariant Schemes 192

6.3 Butterfly Scheme 195

6.3.1 Definition of the Scheme 195

6.3.2 Analysis of the Eigenvalues 196

6.4 Modified Butterfly Scheme 204

6.4.1 Definition of the Scheme 204

6.4.2 Subdivision Matrices, Eigenvectors and Convergence Rates 208
6.4.3 C^1-Continuity Analysis 210
6.4.4 Tangents, Normals and Degeneracy Conditions 213
6.5 Loop Scheme 218
6.5.1 Eigenvalues, Eigenvectors, Convergence Rates 218
6.6 Modification of Loop Scheme 222
6.7 Crease Subdivision 225

7 Multiresolution Representations 233

7.0.1 Structure of the Editng System 234
7.1 Multiresolution Representation 234
7.2 Algorithms and Implementation 237
7.2.1 Adaptive Analysis 240
7.2.2 Adaptive Synthesis 241
7.2.3 Local Synthesis 244
7.2.4 Local Incremental Analysis 245
7.2.5 Adaptive Rendering 249
7.2.6 Data Structures and Code 250
7.3 Results 253

8 Conclusions and Future Work 257

8.1 Summary 257
8.1.1 Subdivision Theory 257
8.1.2 Multiresolution Editing 257
8.2 Future Work 258
8.2.1 Subdivision 258
8.2.2 Multiresolution Representations and Editing 261

A Reduction of Subdivision of Polyhedra to Subdivision of Complexes 263

B Classification of Quasihomogeneous Polynomials 267

Bibliography 269

Index **274**

List of Figures

1.1 Insertion of new vertices for a triangular mesh. 2

1.2 The dark lines partition the mesh into 3 pieces. Each piece of the subdivided mesh, except for the shaded ones, can be mapped to the regular grid with a boundary. 3

1.3 An edit of a complex mesh. The original is on the right (courtesy Venkat Krischnamurthy). The edited version on the left illustrates large scale edits, such as his belly, and smaller scale edits such as his double chin; all edits were performed at about 5 frames per second on an Indigo R10000 Solid Impact. 5

1.4 Example of failure around vertex valence 3. 9

2.1 Neighborhoods of vertices A, B and C isomorphic to neighborhoods in regular (A and C) and k-regular complexes; $L = 2$. 19

2.2 Left: Excluded configurations of triangles around a vertex. Right: These configurations are allowed. 24

2.3 Left: enumeration of vertices of the regular complex. Right: enumeration of vertices of a k-regular complex for $k = 5$. 25

2.4 2 faces corresponding to each vertex in a k-regular complex. 26

2.5 Insertion of new vertices for a triangle (u, v, w). 27

2.6 Refinement of k-regular complexes. 28

2.7 Locality and finite support for the Loop scheme, $L = M = 2$. The larger gray disks mark vertices of the stencils $S[K, v]$. Left: $N_M(v)$ for a new vertex v; Right: N_M for an old vertex v. 31

2.8 Loop scheme. Gray vertices of K^j are elements of $\mathrm{St}(K^j, v)$ for vertices v marked with circles. Black vertices are vertices inserted by refinement (only two are shown). The numbers next to vertices are coefficients used to compute the value $p^{j+1}(v)$ from the values $p^j(v_i)$ for $v_i \in \mathrm{St}(K^j, v)$; $c_0 = \alpha(n)/(n + \alpha(n))$, $\alpha(n) = n((5/8 - (3 + 2\cos(2\pi/n))^2/64)^{-1} - 1)$, $d = 1/(1 + \alpha(n))$. 33

2.9 Left: Control set $Ctrl^0(V_T^\infty)$ for the Loop scheme, $M = 2$. Right: Control set for the Butterfly scheme, $M = 3$. 35

2.10 Types of points of $|K|$. Non-dyadic vertices are not vertices of a triangle on any level of subdivision, not only on the levels shown in the picture. 45

2.11 Non-dyadic points, reduction to the regular case, $L = 3$. 45

2.12 Non-dyadic boundary point, reduction to the regular case case, $L = 3$. . . . 46

2.13 Dyadic points, reduction to the regular case, $L = 3$, $j = 2$. 46

2.14 Subdivision matrix operates on the values of p^j on N_L^j (left) and produces the values of p^{j+1} on N_L^{j+1} (right). In the picture, $L = 2$, as for the Loop scheme. The numbers shown in the picture are used to arrange the values at vertices of N_L^j into one vector. 48

2.15 Layers Lr^0,Lr^1,Lr^2 for $L = 3$ (Butterfly scheme). 49

3.1 Relations between the main results presented in this chapter. 62

3.2 Definition of a simple C^1-continuous surface 63

3.3 A surface with a self-intersection. 64

3.4 Definition of a C^1-continuous surface. 65

3.5 Right: parametric surface $(s^2 - t^2, 2st, s + t)$. The complex form of $(s, t) \to (s^2 - t^2, 2st)$ is $z \to z^2$. The surface does not have a regular parameterization around 0. Left: two sheets of the surface with incision along the ray $s = 0$. One of the sheets is displaced. 68

3.6 Mapping of a pair of adjacent triangles of U_1 to two adjacent triangles of the regular complex. 72

3.7 Construction of the singular parameterization κ. 73

3.8 Conditions of Theorem 3.6 illustrated graphically. Each column corresponds to a Jordan subspace. Each cell in the columns corresponds to a generalized eigenvector (pair of generalized eigenvectors for complex eigenvalues) of matrix S^T. The generalized eigenvectors generating the parametric map are marked with black squares. 88

3.9 Three types of characteristic maps: control points after 4 subdivision steps are shown. a. Two real eigenvalues. b. A pair of complex-conjugate eigenvalues. c. single eigenvalue with Jordan block of size 2. 96

3.10 Subspace of $\Lambda^2(\mathbf{R}^p)$ generated by two cyclic subspaces J^i_j, J^k_l. The pairs of numbers correspond to the basis vectors $e^i_{jr} \wedge e^k_{lt}$, $r = 0 \dots n^i_j$, $t = 0 \dots n^k_l$; arrows indicate the components that are generated by each vector after one application of $\Lambda B - \lambda_i \lambda_k I$, as given by (3.20); after m steps, if we start in the bottom right corner, we only have components above the line given by equation $r + t \leq n^i_j + n^k_l - m$. 105

3.11 Subspace of $\Lambda^2(\mathbf{R}^p)$ generated by a single cyclic subspace J^i_j. The pairs of numbers correspond to the basis vectors. 106

3.12 (a) $|\lambda'| < |\lambda_2|^k$; All variables up to order k exist. (b) $|\lambda'| > |\lambda_2|^k$, $j_{min} = 0$; The function f_m has to be a polynomial. (c) $|\lambda'| > |\lambda_2|^k$, $j_{min} \neq 0$; derivative $\partial_2^{j_{min}} f_m$ has to be a polynomial. 113

4.1 Domains of the basis functions $\varphi_{i,j}$ for $H^{l,m}$, $(l, m) = (1, 0)$, $(0, 1)$, $(1, 1)$ (first row) $(-1, 0)$, $(0, -1)$, $(-1, -1)$ (second row). Thick triangle boundaries are included in the domain; each function is 1 inside the domain and 0 outside. 130

4.2 134

4.3 An example of a map which does not satisfy the conditions of Lemma 4.6. Infinitely many points on a line on the right map to 0, and the image of the line has to return to zero infinitely many times. While the points that map to zero do not have to be on one line, any regular characteristic map which has infinitely many points mapping to zero has to have similar structure for some curve. 136

4.4 Computing the winding number of a piecewise linear curve. 139

5.1 The ring Ring_7 for the Loop scheme and 3 scaled copies of the ring; the ring coincides with the domain of the characteristic map in the sense of Reif. The union of all scaled copies is the interior of the 7-gon bounded by the outer boundary of Ring_7 excluding 0. 171

5.2 Projecting an interval point onto the unit square. For the interval point A unique side is defined; for the interval point B two adjacent sides intersect the projection. For the point C there are 3 sides intersecting projection. In this case, precision is insufficient, and the algorithm fails completely: it is unlikely that the problem disappears with further subdivision. The absence of cases of this type can be guaranteed if the characteristic map on the ring is sufficiently well separated from 0 and the intervals for the control points are small. 177

5.3 Projecting an interval into the unit square. The algorithm computes projected length for interval A, but not for the interval B. It is possible to estimate the upper and lower bounds for projected length in some cases of type B, but it may also happen that the interval passes through 0 and its projected length is undefined. Rather than further analyzing this case, we choose to refine the mesh further to reduce the length of the interval. . . . 179

6.1 This diagram shows the maps used in the proof of Lemma 6.1 for the case $k = 7$. In this case the characteristic map Φ is generated by the eigenvectors of the blocks $B(4\pi/7)$ and $B(10\pi/7)$. 188

6.2 Coefficients for a single ring scheme in the regular case; a,b,c,d satisfy $2a + 2b + 4c + 2d = 1$ by affine invariance. 191

6.3 6 symmetry types of vertices with respect to rotations for single ring schemes and stencils for each type. 191

6.4 The stencil of the Butterfly scheme. 196

6.5 Eigenvalues of the subdivision matrix for the Butterfly scheme for valence 3. There are 2 eigenvalues with Jordan blocks of size 2 (dots with circles), 1 eigenvalue with a Jordan block of size 3 (the dot with a double circle) and 2 single eigenvalues. All eigenvalues with nontrivial Jordan blocks happen to coincide and are equal to 1/4. The dominant eigenvalue in this case is the one with the largest Jordan cell and belongs to $B(0)$. 199

6.6 One sector of the control net of the characteristic map for the Butterfly scheme. 200

6.7 Eigenvalues of the subdivision matrix for the Butterfly scheme for valence 6. 201

6.8 Eigenvalues of the subdivision matrix for the Butterfly scheme for valence 8. The magnitude for the largest eigenvalue of the first block $B(\pi/8)$ is less than the magnitude of the largest eigenvalue for the second block $B(2\pi/8)$. 201

6.9 Characteristic maps for the Butterfly scheme, valences 4,5,7. 202

6.10 The difference in the behavior of a C^1-continuous scheme (Modified Butterfly) and non-C^1-continuous scheme (Butterfly). The latter has close eigenvalues in $B(\pi/8)$ and $B(2\pi/8)$. The ring of points around the vertex of valence 8 was generated using the formula $e^{2m\pi/8} + 0.7e^{4m\pi/8+0.2}$, to introduce a significant component at the "frequency" $4\pi/8$. 203

6.11 Example of failure around valence 3 vertices 204

6.12 Left: for this initial mesh (all vertices around the extraordinary vertex of valence 8 are on a circle) the Butterfly scheme generates a smooth-looking surface, although it is not formally C^1-continuous. Right: for valence 17, the surface generated by the Butterfly scheme is close to conical. 205

6.13 Top row: pipe joint. Note the difference between Butterfly and Modified Butterfly. Lower left: mannequin head. Lower right: torso. 206

6.14 Stencil for a vertex in the 1-neighborhood of an extraordinary vertex . . . 207

6.15 Control nets of the rings of characteristic maps for the Modified Butterfly scheme. 210

6.16 Convergence of normalized control nets of one segment of the characteristic maps for the Modified Butterfly scheme as valence increases. Only the boundaries of the nets are shown. 212

6.17 Valences tested by algorithm; note that only few large valences need to be tested. Total number of tested valences is 440. Data for valences 3, 4, 5 are not shown. 212

6.18 Distance from normalized control net to the limit control net as a function of valence. 214

6.19 Upper and lower bounds for the Jacobians; error bars indicate the size of the interval; the *interval_size* argument for the algorithm was chosen to be 2.6^{-6} so that lower bound of the interval for J_{min} is close to zero. 214

6.20 Linear approximation errors for Modified Butterfly scheme; ϵ_1, ϵ_2 are errors for components of the map, ϵ_{12}, ϵ_{12}, ϵ_{12}, ϵ_{12} are errors for the partial derivatives. Note that errors level out quite quickly; this indicates that the difference between normalized maps for large valences is quite small. 217

6.21 One sector of the control net of the characteristic map for Loop scheme. . 218

6.22 Valences tested by algorithm; note that only few large valences need to be tested. Total number of tested valences is 55. Data for valences 3,4,5 are not shown. 221

6.23 Distance from normalized control net to the limit control net as a function of valence. 222

6.24 Upper and lower bounds for the Jacobians; error bars indicate the size of the interval; the *interval_size* argument for the algorithm was chosen to be 0.0004 so that lower bound of the interval for J_{min} is close to zero. 223

6.25 Linear approximation errors for Loop scheme; ϵ_1, ϵ_2 are errors for components of the map, and ϵ_{12}, ϵ_{12}, ϵ_{12}, ϵ_{12} are errors for the partial derivatives. ϵ_1 and ϵ_2 for valences close to 6 are large because J_{min} is sufficiently far away from zero, and the errors were computed using fewer subdivision levels. 224

6.26 Left: ripples on a surface generated by Loop scheme near a vertex of large valence; Right: mesh structure for Loop scheme near an extraordinary vertex with significant "high-frequency" component; a crease starting at the extraordinary vertex appears. 225

6.27 Upper and lower bounds for the Jacobians for Modified Loop scheme; error bars indicate the size of the interval; the *interval_size* argument for the algorithm was chosen to be 0.0013 so that lower bound of the interval for J_{min} is close to zero. 226

6.28 Normalized control nets for Modified Loop scheme and the limit control net. 226

6.29 Left: mesh structure for Loop scheme and Modified Loop scheme near an extraordinary vertex; a crease does not appear for the Modified Loop. Right: shaded images of the surfaces for Loop and Modified Loop; ripples are more apparent for Modified Loop. 229

6.30 Comparison of control nets for Loop scheme and Modified Loop scheme. Note that for Loop scheme the size of the hole in the ring (1-neighborhood removed) is very small relatively to the surrounding triangles for valence 3 and becomes larger as k grows. For Modified Butterfly this size remains constant. 230

6.31 Coefficients for Loop scheme with creases (regular case). 231

6.32 Three edges were assigned tensions 0.2, 0.5 (top row), and 0.7, 0.9 (bottom row). 231

6.33 Three edges were assigned "parallel" tensions 0.2, 0.5 (top row), and 0.7, 0.9 (bottom row). 232

7.1 The relationship between various procedures as the user moves a set of vertices. 234

7.2 Computing approximate frame; the tangents at $m(v, w)$ are taken to be $t_1 = w - v$ and $t_2 = u_2 - u_1$; the normal n is their cross-product; the frame is the coordinate system obtained from (t_1, T_2, n) by orthonormalization. 235

7.3 Wiring diagram of the multiresolution transform. 237

7.4 Wireframe renderings of virtual surfaces representing the first three levels of control points. 238

7.5 Analysis propagates the changes on finer levels to coarser levels, keeping the magnitude of details under control. Left: The initial mesh. Center: A simple edit on level 3. Right: The effect of the edit on level 2. A significant part of the change was absorbed by higher level details. 238

7.6 A restricted mesh: the center triangle is in T^i and its vertices in V^i. To subdivide it we need the 1-rings indicated by the circular arrows. If these are present the graph is restricted and we can compute s^{i+1} for all vertices and middle vertices of the center triangle. 241

7.7 The mesh on the top is adaptively subdivided; middle image shows the mesh after subdivision but before any temporary triangles are removed; in the bottom image the mesh has all temporary triangles removed. Temporary triangles are shown in light gray; temporary triangles that were fixed due to restriction and subdivided triangles are shown in dark gray. 246

7.8 Sets of even vertices affected through smoothing by either an even v or odd m vertex. 247

7.9 Adaptive rendering: On the left 6 triangles from level i, one has a covered child from level $i+1$, and one has a T-vertex. On the right the result from applying `Render` to all six. 249

7.10 Notation of the function `ExpandMesh`. 253

7.11 On the left are two meshes which are uniformly subdivided and consist of 11k (upper) and 9k (lower) triangles. On the right another pair of meshes mesh with approximately the same numbers of triangles. Upper and lower pairs of meshes are generated from the same original data but the right meshes were optimized through suitable choice of ϵ_S. See the color plates for a comparison between the two under shading. 254

7.12 It is easy to change ϵ_S locally. Here a "lens" was applied to the right eye of the Mannequin head with decreasing ϵ_S to force very fine resolution of the mesh around the eye. 255

7.13 Shaded rendering (OpenGL) of the meshes in Figure 7.11. 256

7.14 Shaded rendering (OpenGL) of the meshes in Figure 7.12. 256

8.1 Several different topological rules on regular grids and near an extraordinary vertex of valence 7. 259

A.1 Reducing refinement rules of the Catmull-Clark scheme to simplicial complex refinement. 264

A.2 Reducing refinement rules of the Doo-Sabin scheme to the Catmull-Clark refinement. a. The original polyhedron. b. One step of the Doo-Sabin subdivision. c. The original polyhedron with the centers of the faces added. d. The polyhedron subdivided using the Catmull-Clark refinement, with the edges of the polyhedron obtained using Doo-Sabin refinement (b) shown as dashed lines. e. The polyhedron converted to a simplicial complex. The picture in the center shows how vertex tags are propagated. Each quadrilateral has two tagged vertices; in the subdivided quadrilateral all old vertices are tagged, all new vertices are not tagged. 265

Notation

$[\cdot]_+$	normalization, p. 67
Δ_j	abbreviation for $\Delta_{(i,j)}$, p. 149
$\Delta_{(i,j)}$	difference in the direction (i,j), $i,j \in \{0,1\}$, p. 138
Φ	characteristic map, p. 90
φ	smooth parameterization of the universal surface $\psi \circ \kappa^{-1}$, p. 76
$\varphi_v(y)$	basis function at the vertex v, p. 43
κ	transformation $U_1 \to \mathbf{R}^2$, p. 73
$\Lambda^2(\mathbf{R}^p)$	space of wedge products of vectors from $\mathbf{R}^p$, p. 69
λ_i	eigenvalues of the subdivision matrix, p. 51
Ψ	parametric map, p. 87
ψ	universal surface $U_1 \to \mathbf{R}^p$, p. 76
A_{ij}	a cyclic block of the subdivision matrix, p. 184
$B(\omega)$	a block of the subdivision matrix reduced to block-diagonal form, p. 185
b_i, b_{ij}	piecewise constant schemes, p. 144
b^i_{jr}	complex generalized eigenvectors of the subdivision matrix, p 51
c^i_{jr}	real generalized eigenvectors of the subdivision matrix, p 51
$\mathrm{Ctrl}^j(V)$	control set of a set of vertices V , p. 34
$D(p)$	a contraction function for $p \in \mathcal{R}$, p. 138
$D_j(p)$	a contraction function for differences, p. 142
$D_{ij}(p)$	another notation for contraction functions p. 157
$D^j(K)$	result of subdividing K j times, also denoted K^j, p. 26
D_ψ	directional set, p. 81
D_k	DFT matrix, p. 185
$\mathcal{D}_k$	block matrix with DFT matrices on the diagonal, p. 185
e^i_{jr}	basis vectors of the basis for the subdivision matrix S^T, 74
$F^i(v)$	the frame on level i at vertex v, p. 235

$f[p]$	limit function $f : \|K\| \to B$ generated by subdivision from $p \in \mathcal{P}(V, B)$, p. 40
f^i_{jr}	complex eigenbasis functions, p. 51
g^i_{jr}	real eigenbasis functions, p. 51
h^i_{jr}	basis vectors of the basis for the subdivision matrix S, 74
$J[\cdot, \cdot]$	the Jacobian of a pair of functions $\mathbf{R}^2 \to \mathbf{R}$
$J[\cdot]$	the Jacobian of a mapping $\mathbf{R}^2 \to \mathbf{R}^2$
J^i_j	a cyclic subspace of a matrix with eigenvalue λ_i, p. 51
K	abstract complex, p. 23
K^j	the result of subdividing K j times, also denoted $D^j(K)$ p. 26
$L[p^j]$	linear approximation to f on the subdivision level j, p. 41
$\mathrm{Loc}^j(V)$	localization set of a set of vertices V , p. 35
Lr^j	layer in a k-regular complex, p. 2.12
$N^j_m(v), N_m(v, K)$	m-neighborhood of the vertex v, p. 24
N^j_m	m-neighborhood of the central vertex of a k-regular complex, p. 47
n^i_j	order of the cyclic subspace J^i_j p. 50
$\mathbf{P}(p, q)$	quasihomogeneous polynomials, p. 97
$\bar{\mathbf{P}}(p, q)$	complex quasihomogeneous polynomials, p. 97
$\mathcal{P}(V, B)$	the space of functions on the set of vertices of V with values in B, p. 28
$\mathrm{Proj}(v, W)$	projection of a vector onto the subspace W spanned by a set of basis vectors, p. 3.5
$\mathcal{R}$	regular complex, p. 25
$\mathcal{R}_k$	k-regular complex, p. 25
Ring_k	domain of an annular portion of the characteristic map, p. 170
S	subdivision matrix or subdivision scheme 47
S'	subdivision scheme for differences corresponding to S, p. 149
$S^j[K, v](p)$	subdivision function $\mathcal{P}(V) \to B$, p. 31
$S^j[K]$	subdivision operator $\mathcal{P}(V^j) \to \mathcal{P}(V^{j+1})$, p. 30
$\mathrm{St}(K, v)$	stencil of a scheme on K at the vertex v, p. 31
ΛS	tangent subdivision matrix, p. 80
$\|K\|$	topological complex, p. 39
$U^j_m(v)$	topological m-neighborhood of the vertex v, p. 39

U_m^j	topological m-neighborhood of the central vertex of a k-regular complex, p. 39
$w(y)$	$p(p-1)/2$-vector $\partial_1\psi \wedge \partial_2\psi$, p. 77
$\mathfrak{Z}_{(a,b)}$	shift operator, p. 150

Chapter 1 Introduction

Subdivision is a method for generating smooth surfaces, which first appeared as an extension of splines to arbitrary topology control nets. Efficiency of subdivision algorithms, their flexibility and simplicity make them suitable for many interactive computer graphics applications.

Although the basic subdivision algorithms are simple, the properties of limit surfaces generated by subdivision may be quite complicated and difficult to analyze. In this thesis our main focus is on the analysis of C^1-continuity and construction of *stationary* subdivision algorithms. This class of algorithms is particularly important because all classical subdivision schemes [13, 5, 20, 40] are stationary. Understanding the algorithms in this class is essential for understanding more general forms of subdivision.

Although subdivision was introduced as a generalization of knot insertion algorithms for splines, it is much more general and allows considerable freedom in the choice of subdivision rules. These degrees of freedom can be used to obtain surfaces with specific properties (varying degree of smoothness, interpolation) or with features such as creases and cusps. To take advantage of this flexibility we have to understand the dependence between the subdivision rules and the behavior of the limit surface. Because these dependences are difficult to analyze, most of the work on subdivision on meshes of arbitrary topology was centered on analysis of spline-based schemes, which constrained the variety of surfaces that could be generated.

One of the goals of this work is to develop a framework for analysis of general subdivision. We prove general necessary and sufficient conditions for tangent plane and C^k-continuity of subdivision and describe practical methods for analyzing C^1-continuity. We have implemented algorithms that allow us to perform C^1-continuity analysis automatically, potentially for whole families of subdivision schemes and prove C^1-continuity for all valences of extraordinary vertices.

Another goal was to design practical algorithms for manipulation of subdivision surfaces. We have chosen a particularly challenging application, multiresolution editing, to demonstrate how theoretical properties of subdivision lead to efficient adaptive and local

algorithms.

In the next sections we introduce the subject of this thesis and discuss the related work.

1.1 Subdivision

Given an initial mesh, subdivision computes a sequence of refined meshes converging to a limit surface. The refined meshes are obtained by adding new vertices to the mesh and connecting them with old vertices. The positions of new vertices are computed as functions of positions of the old vertices; the positions of old vertices in the refined mesh can be modified. To specify a subdivision scheme, we need to describe two rules: a topological rule for obtaining the graph of the refined mesh from the graph of the initial mesh and a rule for computing the positions of new vertices and modifying positions of the old vertices.

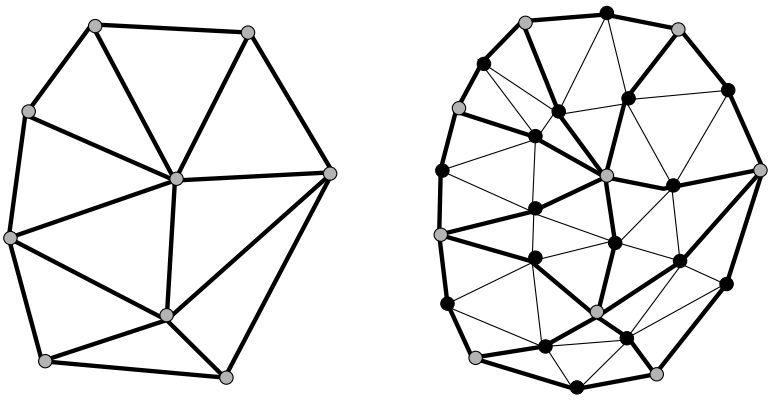

Figure 1.1: Insertion of new vertices for a triangular mesh.

The topological rule has primary importance; only several rules where ever used for construction of subdivision schemes for surfaces. We will mostly consider the schemes that use probably the simplest possible rule that works on arbitrary triangular meshes: one new vertex is added for each old edge, all old edges are replaced by a pair of edges and the new vertices for each old face are connected (Figure 1.1).

This rule is general enough to serve as a basis for a variety of subdivision algorithms. An important property of this rule is that all new vertices, unless they are on the boundary of the mesh, have valence 6.

The new vertices on the boundary have valence four. The number of *extraordinary*

vertices, which have valence other than 6 (4 on the boundary), remains constant on all subdivision levels. For the type of schemes that we consider, this fact means that almost everywhere a small part of the mesh is in one-to-one correspondence with a piece of the regular three-directional grid (Figure 1.1).

Analysis for other types of rules, such as topological rules used in Catmull-Clark and Doo-Sabin schemes, is similar (see Chapter 8 for discussion) and only minor adjustments are needed in the derivations. We choose to concentrate on the triangle-based schemes because the initial formalization (Chapter 2) is more transparent for these schemes. Once the triangular case is understood, it is relatively easy to adapt the derivations for the quadrilateral schemes.

Powerful tools exist for analysis and construction of subdivision schemes on regular grids (see [6]). We concentrate on the analysis of the behavior of subdivision near the extraordinary vertices.

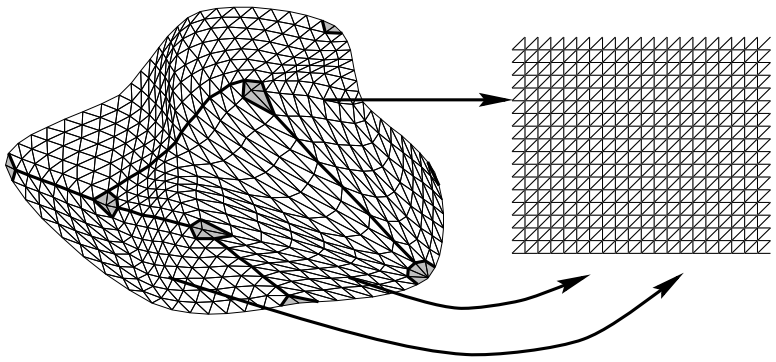

Figure 1.2: The dark lines partition the mesh into 3 pieces. Each piece of the subdivided mesh, except for the shaded ones, can be mapped to the regular grid with a boundary.

To specify a complete subdivision scheme, we need a set of functions for computing the positions of vertices on successive approximation levels. For the scheme to be practical, these functions should be as simple as possible, yet capable of generating a smooth limit surface. We will consider subdivision schemes for which all refinement functions are linear. Moreover, we will assume that the choice of function that is used to compute a value at a vertex depends only on the local topology of the mesh around this vertex, and the function itself depends only on a finite number of neighbors (*locality and finite support.*)

Linear and finitely supported functions can be computed very efficiently, which makes

the schemes of this type particularly promising for computer graphics applications.

We consider primarily *stationary* schemes, which implies that the choice of the refinement functions does not depend on the subdivision level. Once a mesh is refined, we "forget" about the old mesh and base our choice of functions for the next subdivision step only on the topology of the current mesh. This restriction makes the implementation highly efficient and also makes the analysis of the schemes much simpler. Following the pattern that was established in the analysis of subdivision on regular grids [19], one may hope to extend this analysis to the case of non-stationary subdivision.

1.2 Multiresolution Representations and Editing

An important part of this thesis is dedicated to the applications of subdivision.

Subdivision in its pure form is useful for generating smooth surfaces. However, applications such as special effects and animation require creation and manipulation of complex geometric models, which, like real world geometry, carry detail at many scales (cf. Figure 1.3). We extend subdivision to a more general multiresolution representation for surfaces. The advantage of our approach is that it allows us to implement level-of-detail rendering, multiresolution editing and animation using highly efficient subdivision algorithms.

We focus on interactive multiresolution editing of complex models, a particularly challenging application. Complex geometric models might be constructed from scratch (*ab initio* design) in an interactive modeling environment or be scanned-in either by hand or with automatic digitizing methods. The latter is a common source of data. If a model is obtained using a laser range scanners it is often composed of high resolution meshes with hundreds of thousands to millions of triangles.

Manipulating such fine meshes can be difficult, especially when they are to be edited or animated. Interactivity, which is crucial in these cases, is challenging to achieve. Even without accounting for any computation on the mesh itself, available rendering resources alone may not be able to cope with the sheer size of the data. Possible approaches include mesh optimization [33, 31] to reduce the size of the meshes and using hierarchical representations, such as the subdivision-based representation that we propose. Our representation is more suitable for editing and animation applications: different levels of resolution can be extracted on the fly, even if the geometry changes. In addition, our representation provides

Figure 1.3: An edit of a complex mesh. The original is on the right (courtesy Venkat Krischnamurthy). The edited version on the left illustrates large scale edits, such as his belly, and smaller scale edits such as his double chin; all edits were performed at about 5 frames per second on an Indigo R10000 Solid Impact.

multiresolution editing semantics: it is possible to control the geometry at a large scale; at the same time, minute features of the model can be modified if necessary.

1.3 Contributions

In this section we summarize the contributions of the thesis. Our results are compared to the previous work is discussed in Section 1.6.1.

1.3.1 Theory of Subdivision

The goal of this thesis is to build a systematic theory of stationary subdivision surfaces on arbitrary meshes. We find necessary and sufficient conditions for tangent plane continuity and C^k-continuity of subdivision schemes. These conditions can be used to determine smoothness of particular schemes; more importantly, they provide us with a more explicit description of whole classes of tangent plane continuous and C^k-continuous schemes; it is our hope that such description can be used for finding schemes in the class that are optimal in other senses, for example, schemes that produce surfaces with improved fairness.

Our analysis of stationary subdivision around extraordinary vertices builds on the ideas from the work of Warren [63, 62], Reif [55, 54, 56] and Cavaretta, Dahmen and Miccelli [6].

Our main results include

- A formalism for description of subdivision schemes on arbitrary meshes in terms of graph neighborhoods (Section 2.2), which allows us to define such crucial concepts as control sets (extension to the case of general subdivision of the idea of the set of control points of a spline patch).

- An approach to analysis of local properties of subdivision schemes near extraordinary points based on the idea of the universal surface (Section 3.4). This approach is crucial for developing geometric intuition about the behavior of subdivision surfaces.

- Necessary and sufficient conditions for tangent plane continuity given by Theorem 3.4 and under additional nondegeneracy assumptions by Corrolary 3.5 and equivalent Theorem 3.7.

- Necessary and sufficient conditions for C^k-continuity of subdivision schemes at extraordinary vertices (Section 3.10).

- Practical sufficient criteria for C^1-continuity of a subdivision scheme at an extraordinary vertex (Chapter 4);

- Algorithms for verifying C^1-continuity of general subdivision schemes (Chapter 5); the same algorithms can also be used for stability analysis.

- Construction and analysis of several specific schemes; we present a complete analysis of the Butterfly scheme and propose a new scheme based on the Butterfly which we prove to be C^1-continuous for vertices of arbitrary valence. We also present analysis of the Loop scheme for arbitrary valence and propose a way of introducing soft creases into the Loop scheme.

The sufficient conditions of Chapter 4 do not require knowledge of the explicit formula for the limit surface, which makes it useful for analysis of interpolating subdivision schemes, such as the Butterfly scheme [20].

The connection to the singularity theory, briefly discussed in Appendix B, suggests that some results from that area can be applied to the study of subdivision surfaces, stationary as well as non-stationary.

1.3.2 Multiresolution Representations

We propose a multiresolution representation for surfaces based on subdivision and describe algorithms for fast update and rendering of subdivision and multiresolution surfaces. Efficiency is achieved by using adaptive and local algorithms whenever possible.

We present an editing system which possesses the following properties

- **Multiresolution control:** Both broad and general handles, as well as small knobs to tweak minute detail, are available.
- **Speed/fidelity tradeoff:** All algorithms dynamically adapt to available resources to maintain interactivity.
- **Simplicity/uniformity:** A single primitive, triangular mesh is used to represent the surface across all levels of resolution.

It should be noted that our methods rely on the finest-level mesh having subdivision connectivity. This requires a remeshing step before external high resolution geometry can be imported into the editor. Eck et al. [22], have described a possible approach to remeshing arbitrary finest level input meshes fully automatically. A method that relies on a user's expertise was developed by Krishnamurthy and Levoy [37].

1.4 Related Work: Construction of Subdivision Schemes

In this section we briefly review a number of subdivision algorithms. These come in two principal varieties, approximating and interpolating. The former are typically based on generalizations of spline patch-based schemes, while the latter are related to 1D interpolating schemes [9, 10, 11, 14, 16].

1.4.1 Approximating Subdivision Schemes

The first subdivision algorithms for meshes of arbitrary topology were given by Doo and Sabin [12, 13, 57] and Catmull and Clark [5]. These were based on generalizations of quadratic and cubic B-spline subdivision for meshes consisting of quadrilaterals. The behavior around extraordinary vertices was first analyzed by Doo and Sabin [13] using Fourier

transforms and an analysis of the eigenvalues and eigenvectors of a matrix associated with the subdivision process.

A first scheme for arbitrary meshes consisting of triangles was given by Loop [40]. It is based on a generalization of quartic triangular B-splines.

Another class of approaches to generating smooth surfaces from arbitrary topology meshes attempts to directly derive a set of spline patches which globally achieve some order of continuity. Most of these approaches are based on some number of initial "corner cuttings" to regularize the topology, or alternatively place some restrictions on the mesh connectivity [8, 41, 47, 48]. The output of these algorithms is a set of patches of varying, at times rather high, polynomial order and varying shape, typically triangles and quadrilaterals. Once these patches have been generated, the surface can be built by subdivision through the de Casteljau algorithm.

1.4.2 Interpolating Subdivision Schemes

Since the ability to control the resulting surface exactly is very important in many practical applications, a number of modifications of approximating schemes have been developed to force the limit surface to interpolate particular points. Nasri [45] gives modifications to the quadratic scheme of Doo-Sabin to enforce interpolation of vertices and normals by solving a linear system which is global but sparse. Similarly, Halstead, Kass and DeRose [29] give an algorithm modifying the cubic scheme of Catmull-Clark to enforce positional and normal constraints, again by solving a global and sparse linear system. In both cases there are a number of limitations. For example, it is unclear under what conditions the linear system to be solved for the interpolation constraints can become singular. Additionally, the interpolation conditions are only satisfied in the limit. Among the patch-based schemes only Peters [47] recently gave one which can incorporate interpolation constraints without requiring the solution of a global linear system.

Until recently the only known interpolating scheme was the Butterfly scheme of Dyn, Gregory and Levin [20] and a later variant [17]. These schemes are interpolating by design, local, and simple in terms of the required data structures and algorithms. They are also known to be smooth in the regular setting, where they lead to C^1-continuous limit functions [17, 21]. Topological regularity, however, is a rather severe restriction since all vertices must be of valence six for these results to be applicable. The failure to be C^1-continuous

for vertices of valence other than six is easily observed in practice as can be seen in the example of Figure 1.4. Simultaneously with this work a new quadrilateral-based interpolating scheme was developed by Kobbelt [35].

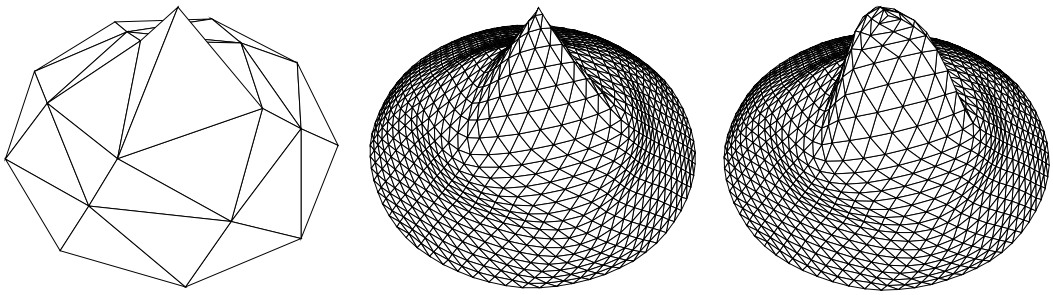

Figure 1.4: On the left a control mesh with a vertex of valence 3. In the middle the result after several levels of subdivision using the Butterfly scheme. The surface loses C^1-continuity around the vertex of valence 3. On the right the result achieved in the same situation with our modified scheme. The behavior around the extraordinary vertex remains C^1-continuous and no cusp is formed.

1.5 Related Work: Analysis

The subdivision literature is quite extensive, but until recently, surprisingly little was known about subdivision surfaces built on meshes with arbitrary topology. Already in the work of Doo and Sabin [12, 13] and Catmull and Clark [5] attempts were made to analyze smoothness properties of the subdivision surfaces around extraordinary vertices. A more systematic approach was taken by Ball and Storry [2], who established conditions for tangent plane continuity of Catmull-Clark subdivision. A similar analysis was performed by Loop [41].

Most recently, important results were obtained by Reif [54, 55, 56]. In [55] Reif points out that tangent plane continuity does not adequately reflect the intuitive idea of smoothness and establishes sufficient conditions for a stronger notion of smoothness (C^1-continuity) which requires existence of a local regular parameterization. The important concept of a characteristic map is introduced. Reif [56] demonstrates that polynomial patches of order 6 are required to achieve C^2-continuity of a surface — an important result showing limitations of stationary subdivision. The result requires establishing a necessary condition for C^2-continuity in a special case. In [54] asymmetric schemes are considered and somewhat more general sufficient conditions are proposed. Our work extends and generalizes the work of Reif. Another important source of ideas for this work was the manuscript by Warren [63],

where he noted the importance of scaling relations for understanding behavior of subdivision schemes around extraordinary vertices.

Reif's criterion was used to analyze C^1-continuity of subdivision schemes by Habib and Warren [28], Schweitzer [59], Peters and Reif [49].

Prautzsch [50] presents sufficient conditions for C^k-continuity that form a subset of our conditions. The differences between our work and the work of Prautzsch are discussed in Section 1.6.1. A degree estimate for C^k-continuous polynomial schemes was published by Prautzsch and Reif [51].

Reif's sufficient conditions for C^1-continuity of subdivision schemes requires establishing injectivity and regularity of the characteristic map. In [28] and [49] this was achieved using explicit representation of the surface with polynomial patches. Techniques developed by Schweitzer [59] are more subtle, but still rely on closed-form expressions. These approaches cannot be used to analyze schemes that do not have explicit formulas for parameterizations in the regular case.

1.6 Related Work: Surface Editing

Our system is inspired by a number of earlier approaches. We mention multiresolution editing [23, 25, 27], arbitrary topology subdivision [5, 13, 20, 35, 40, 66], wavelet representations [7, 22, 42, 58], and mesh simplification [31, 37]. Independently, an approach similar to ours was developed by Pulli and Lounsbery [52].

H-splines were presented in pioneering work on hierarchical editing by Forsey and Bartels [25]. Briefly, H-splines are obtained by adding finer resolution B-splines onto an existing coarser resolution B-spline patch relative to the coordinate frame induced by the coarser patch. Repeating this process, one can build very complicated shapes which are entirely parameterized over the unit square. Forsey and Bartels observed that the hierarchy induced coordinate frame for the offsets is essential to achieve correct editing semantics.

H-splines provide a uniform framework for representing both the coarse and fine level details. Note, however, that as more detail is added to such a model, the internal control mesh data structures more and more resemble a fine polyhedral mesh.

Forsey and Bartels' original work focused on *ab initio* design. The user's help is enlisted

in defining what is meant by different levels of resolution. The levels of the hierarchy are hand built by a human user and the representation of the final object is a function of its editing history.

To edit a given model, it is important to have a general procedure to define coarser levels and compute details between levels. We refer to this as the *analysis* algorithm. An H-spline analysis algorithm based on weighted least squares was introduced [24], but is too expensive to run interactively. Note that even in for *ab initio* design online analysis is needed, since after a long sequence of editing steps the H-spline is likely to be overly refined and needs to be consolidated.

Wavelets provide a framework in which multiresolution approximations can be rigorously defined. Finkelstein and Salesin [23], for example, used B-spline wavelets to describe multiresolution editing of curves. As in H-splines, parameterization of details with respect to a coordinate frame induced by the coarser level approximation is required to get correct editing semantics. Gortler and Cohen [27] pointed out that wavelet representations of detail tend to behave in undesirable ways during editing and returned to a pure B-spline representation as used in H-splines.

Carrying these constructions over into the arbitrary topology surface framework is not straightforward. In the work by Lounsbery et al. [42] the connection between wavelets and subdivision was used to define the different levels of resolution. The original constructions were limited to piecewise linear subdivision, but smoother constructions are possible [58, 66].

An approach to surface modeling based on variational methods was proposed by Welch and Witkin [64]. An attractive characteristic of their method is flexibility in the choice of control points. However, they use a global optimization procedure to compute the surface which is not suitable for interactive manipulation of complex surfaces.

1.6.1 Comparison with Previous Work

Subdivision Theory. Our criteria generalize and unify most of the known smoothness conditions at extraordinary points. Our main result is a set of necessary and sufficient conditions for tangent plane continuity and C^1-continuity. While various conditions were known before [2, 29, 55], they typically required some strong additional assumptions on the structure of the subdivision matrix, which we eliminate. We prove two sets of necessary and

sufficient conditions: Theorem 3.4, and Corollary 3.5 with equivalent Theorem 3.7. Theorem 3.4) gives necessary and sufficient conditions with minimal assumptions. Corollary 3.5 identifies a broad class of schemes for which more explicit conditions can be stated.

Reif [55] proved a sufficient condition for C^1-continuity of subdivision surfaces and introduced the characteristic maps for a restricted type of subdivision matrices. We generalize the definition to arbitrary matrices and introduce the parametric map, which coincides with the characteristic map given Reif's assumptions on eigenvalues, and defines singular (regular away from the extraordinary vertex) parameterizations for any tangent plane continuous scheme.

Some of the conditions for C^k-continuity proved in this thesis are similar to the conditions of Prautzsch [50], which were unknown to us when this work was done. However, our work improves the results obtained by [50] in a significant way. Prautzsch formulates sufficient and partial necessary conditions for C^k-continuity assuming that the scheme is C^1-continuous. We do not assume C^1-continuity. Our conditions are simultaneously necessary and sufficient. We consider the third possible type of characteristic map which was not considered by Prautzsch.

Prautzsch and Reif [51] consider conditions similar to the degree estimate of Section 3.10.2 in greater detail and provide better degree estimates. It is important to keep in mind that they assume that the characteristic map of the scheme is regular and injective, which makes the results slightly less general: in principle, there could be a scheme with non-injective or singular characteristic map for which the estimate does not hold. We show that this is not the case under weaker assumptions.

Analysis of specific schemes. Smoothness of Catmull-Clark and Doo-Sabin subdivision schemes was analyzed in [49]. Unfortunately, the analysis was based on several theorems that are not formally correct; this does not invalidate the proof of C^1-continuity, as these theorems can be proved under certain additional assumptions which hold for the schemes considered in [49]. C^1-continuity of Loop scheme was analyzed by Schweitzer [59]. Both approaches ([49] and [59]) rely on the closed form expression for the limit surface on the regular grid and symbolic calculation of the Jacobian of the characteristic map. Both [59] and [49] prove smoothness only for a finite number of valences, although this number is sufficiently large for practical purposes. In contrast, our approach is more general and

allows us to prove smoothness of schemes which do not generate surfaces with closed form parameterization on regular grids and for arbitrary valence.

Multiresolution surface representations. Our work extends H-splines of Forsey and Bartels to arbitrary topology meshes. Similar work was independently done by Pulli and Lounsbery [52]; our work also bears similarity to an earlier paper of Kurihara [38]. Most of the previous work focused on *ab initio* design with the exception of [24]. We introduce efficient algorithms for analysis based on Taubin's smoothing, which are essential for manipulating high-resolution meshes. All our algorithms are local and adaptive, which allows us to achieve interactive performance even with low-end graphics hardware.

1.7 Overview

In **Chapters 2 and 3** we present the theory of smoothness of stationary subdivision near extraordinary vertices.

In Chapter 2 we discuss the structure of the complexes generated by subdivision and prove some basic facts about dependencies of vertices generated by subdivision on the vertices on coarser levels.

Section 2.3 introduces topology on the complexes and defines convergence of subdivision. In the same section we show that the analysis of any local and finitely supported stationary scheme on arbitrary complexes can be reduced to the analysis of that scheme on k-regular complexes, which have only one extraordinary vertex.

Section 2.4 introduces the *subdivision matrix*. It is shown that the limit functions generated by the eigenvectors of the matrix satisfy *scaling relations*.

In Section 3.4 we introduce the universal surfaces, and show that analysis of subdivision schemes can be reduced to analysis of the corresponding universal surfaces.

Some of the main results are contained in Sections 3.5 and Sections 3.10. We formulate criteria for tangent plane continuity, C^1-continuity and C^k-continuity of a subdivision scheme.

Section 3.13 contains a discussion of the properties of the functions satisfying scaling relations.

In **Chapters 4 and 5** we develop practical algorithms for analysis of C^1-continuity of

subdivision schemes. In Chapter 4 we derive expressions for convergence rates for certain general types of schemes, including schemes that we call "crease schemes." We show how one can use these estimates to prove regularity of the characteristic map using linear approximations to this map. We show that under certain assumptions the characteristic map is a covering if it is a local homeomorophism and thus the question of injectivity of the characteristic map can be reduced to computation of the winding number for a curve.

In Chapter 5 we use facts proven in Chapter 4 to describe algorithms for verification of smoothness of subdivision schemes based on interval arithmetic.

Specific schemes are analyzed in **Chapter 6**. We also prove some general results on symmetric schemes; for this types of schemes injectivity is necessary for smoothness under certain assumptions. This result corrects the results reported by Peters and Reif [49] by adding several assumptions.

Finally, in **Chapter 7** we describe a multiresolution representation based on subdivision, and a number of efficient algorithms for manipulating and rendering subdivision and multiresolution surfaces.

Chapter 2 Basic Properties of Stationary Subdivision

In this chapter we introduce a formalism for describing general subdivision on simplicial complex. Our notation is similar to the notation of Warren [63]. Exposition in the chapter is rather detailed; some of the constructions are more general than it is required in the rest of the thesis. We have chosen this level of generality to clarify the relations between different properties of subdivision schemes such as finite support, local definition, invariance, stationarity etc. For example, the basis function decomposition requires only finiteness of the stencil for each vertex, but does not require finite support or local definition. These basic questions were mostly ignored in the literature, and we find it necessary to describe all these concepts in considerable detail.

For readers interested primarily in smoothness results described in Chapter 3, we provide a brief summary of this chapter in Section 2.1. This section contains all definitions and fact that are necessary for understanding the rest of the thesis.

2.1 Summary

2.1.1 Subdivision on Complexes.

Simplicial complexes. Subdivision surfaces are naturally defined as functions on two-dimensional simplicial complexes. Recall that a simplicial complex K is a set of vertices, edges and triangles in $\mathbf{R}^N$, such that for any triangle all its edges are in K, and for any edge its vertices are in K. We assume that there are no isolated vertices or edges. $|K|$ denotes the union of triangles of the complex regarded as a subset of $\mathbf{R}^N$ with induced metric. We say that two complexes K_1 and K_2 are *isomorphic* if there is a homeomorphism between $|K_1|$ and $|K_2|$ that maps vertices to vertices, edges to edges and triangles to triangles.

A *subcomplex* of a complex K is a subset of K that is a complex. A 1-neighborhood $N_1(v, K)$ of a vertex v in a complex K is the subcomplex formed by all triangles that have v as a vertex. An m-neighborhood is defined recursively as a union of all 1-neighborhoods of

vertices in $(m-1)$-neighborhood. We will omit K in the notation for neighborhoods when it is clear what complex we refer to.

Recall that a *link* of a vertex is the set of edges of $N_1(v, K)$ that do not contain v. We will consider only complexes with all vertices having links that are connected simple polygonal lines, open or closed. If the link of a vertex is an open polygonal line, this vertex is a boundary vertex, otherwise it is an internal vertex.

Most of our constructions will use two special types of complexes — *k-regular complexes* $\mathcal{R}_k$ and the *regular complex* $\mathcal{R}$. Each complex is simply a triangulation of the plane consisting of identical triangles. In the regular complex each vertex has exactly 6 neighbors. In a k-regular complex all vertices have 6 neighbors, except one vertex C, which has k neighbors. We will call C the central vertex of a k-regular complex and identify it with zero in the plane.

Subdivision of simplicial complexes. We can construct a new complex $D(K)$ from a complex K by subdivision, adding a new vertex for each edge of the complex and replacing each old triangle with four new triangles. Let m_{vw} be the midpoint of the edge (v, w); if (u, v, w) is a triangle of K, then (u, m_{uv}, m_{uw}), (v, m_{vw}, m_{uv}), (w, m_{uw}, m_{vw}) and (m_{uv}, m_{vw}, m_{uw}) are triangles of $D(K)$. Note that k-regular complexes are self-similar, that is, $D(\mathcal{R}_k)$ and $\mathcal{R}_k$ are isomorphic.

We will use notation K^j for j times subdivided complex $D^j(K)$ and V^j for the set of vertices of K^j. Note that the sets of vertices are nested: $V^0 \subset V^1 \subset \ldots$. We will call the elements of the union $\cap_{i=0}^{\infty} V^i$ the *dyadic points* of K.

Subdivision schemes. Next, we attach values to the vertices of the complex; in other words, we consider the space of functions $V \to B$, where B is a vector space over $\mathbf{R}$. The range B is typically $\mathbf{R}^l$ or $\mathbf{C}^l$ for some l. We denote this space $\mathcal{P}(V, B)$, or $\mathcal{P}(V)$, if the choice of B is not important.

A *subdivision scheme* for any function $p^j(v)$ on vertices V^j of the complex K^j computes a function $p^{j+1}(v)$ on the vertices of the subdivided complex $D(K) = K^1$. More formally, a subdivision scheme is a collection of operators $S[K]$ defined for every complex K, mapping $\mathcal{P}(K)$ to $\mathcal{P}(K^1)$. We consider only subdivision schemes that are linear, that is, the operators $S[K]$ are linear functions on $\mathcal{P}(K)$. In this case, each component of a subdivision operator

computing the value at a fixed vertex v is a linear function $\mathcal{P}(V) \to B$, and is defined by equations

$$p^1(v) = \sum_{w \in V} a_{vw} p(w)$$

for all $v \in V^1$. We restrict our attention to subdivision schemes which are finitely supported, locally defined, invariant with respect to a set of isomorphisms of complexes and affinely invariant.

A subdivision scheme is *finitely supported* if there is an integer M such that $a_{vw} \neq 0$ only if $w \in N_M(v, K^1)$ (note that the neighborhood is taken in the complex K^1) for any complex K. It is possible to show that the values $p^j(v)$ on all dyadic points of a subcomplex $K' \subset K$ depend only on the values $p^0(v)$ on the vertices of $N_M(K', K)$. We call $N_M(K', K)$ the *control set* of K'. This set is similar to the control set of a patch.

We assume our schemes to be *locally defined* and *invariant with respect to a set G of isomorphisms of complexes*. This means that there is an integer$L$, such that if for two complexes K_1 and K_2 and two vertices $v_1 \in V_1$ and $v_2 \in V_2$ there is an isomorphism $\rho : N_L(v_1, K_1) \to N_L(v_2, K_2)$, $\rho \in G$ such that $\rho(v_1) = v_2$, then $a_{v_1 w} = a_{v_2 \rho(w)}$. If for subcomplexes $K_1' \subset K_1$ and $K_2' \subset K_2$ there is a isomorphism ρ mapping $N_L(K_1', K_1)$ to $N_L(K_2', K_2)$ and ρ is from G, then the values computed by subdivision on all dyadic points of K_1' are identical to the values computed by subdivision on corresponding points of K_2'.

We assume that the set G contains isomorphisms of 1-neighborhoods of any vertex of any complex with a subcomplex of a k-regular complex or the regular complex, possibly with boundary. In addition, if it contains an isomorphism $\rho : K_1 \to K_2$, it also contains the induced isomorphism of $D(K_1) \to D(K_2)$, as well as the restrictions of ρ to subcomplexes of K_1.

An example of a nontrivial set G is the set of isomorphisms of tagged complexes: we can tag some edges of the complex, and propagate the tags to the edges of the subdivided complex. We can allow only isomorphisms that map tagged edges to tagged edges. Analysis of quadrilateral-based schemes, such as Catmull-Clark and Doo-Sabin, can be reduced to analysis of subdivision schemes on complexes introducing auxiliary vertices into complexes and tagging certain edges. Schemes on tagged complexes also can be used to create surfaces with creases. The requirement that we impose on the set G guarantees that the surfaces gen-

erated by subdivision on arbitrary complexes are locally identical to the surfaces generated by subdivision on a k-regular complex, possibly with boundary (see below).

The final requirement that we impose on subdivision schemes is *affine invariance*: if T is a linear transformation $B \to B$, then for any v $Tp^{j+1}(v) = \sum a_{vw} Tp^j(v)$. This is equivalent to requiring that all coefficients a_{vw} for a fixed v sum up to 1.

Limit functions. For each vertex $v \in \cup_{i=0}^{\infty} V^i$ there is a sequence of values $p^j(v)$, $p^{j+1}(v)$, ... where j is the minimal number such that V^j contains v.

Definition 2.1. *A subdivision scheme is called* **convergent** *on a complex K, if for any function $p \in \mathcal{P}(K, B)$ there is a continuous function f defined on $|K|$ with values in B, such that*

$$\lim_{i \to \infty} \sup_{v \in V^i} \left\| p^i(v) - f(v) \right\|_2 \to 0$$

The function f is called the limit function of subdivision.

Notation: $f[p]$ is the limit function generated by subdivision from the initial values $p \in \mathcal{P}(K)$.

It is easy to show that if a limit function exists, it is unique. A *subdivision surface* is the limit function of subdivision on a complex K with values in $\mathbf{R}^3$. In this case we will call the initial values $p^0(v)$ the *control points* of the surface.

Similar to Theorem 2.1 of [6] we can represent any limit function of subdivision as a linear combination of *basis functions*. A basis function $\varphi_v(y) : |K| \to \mathbf{R}$ at vertex v is obtained from the initial values $\delta_v \in \mathcal{P}(K, \mathbf{R})$, $\delta_v(v) = 1$, $\delta_v(w) = 0$ if $w \neq 0$. Let p^0 be some initial values on a complex K. If subdivision converges,

$$f[p^0](y) = \sum_{v \in V^0} p^0(v) \varphi_v(y) \tag{2.1}$$

Reduction to k-regular complexes. Locally any surface generated by a subdivision scheme on an arbitrary complex can be thought of as a part of a subdivision surface defined on a k-regular complex, if the set of isomorphisms G, with respect to which the scheme is invariant, satisfies the requirements above. The reason for this can be easily understood from Figure 2.3.3. More formally this can be proved by establishing isomorphisms between

neighborhoods $N_L(v, K^j)$ of any vertex of K^j for sufficiently large j and neighborhoods $N_L(0, \mathcal{R}_k)$ of the central vertex of the k-regular complex or regular complex and proving that they are in G.

Note that this fact alone does not guarantee that it is sufficient to study subdivision schemes only on k-regular complexes (see Section 3.1).

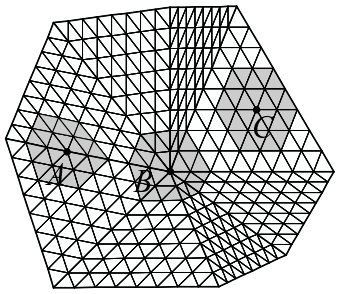

Figure 2.1: Neighborhoods of vertices A, B and C isomorphic to neighborhoods in regular (A and C) and k-regular complexes; $L = 2$.

If the complex has boundary, we also need to consider regular and k-regular complexes with boundaries. We mostly concentrate on the analysis for closed surfaces, and do not consider the boundary case.

The schemes for subdivision surfaces are typically constructed from schemes that generate C^k-continuous limit functions $f[p]$ on a regular complex. We will assume that this is the case, and focus on C^k-continuity near extraordinary points.

2.1.2 Subdivision Matrices

We have already observed that we have to consider primarily k-regular complexes, which are just triangulations of the plane. Consider the part of a subdivision surface $f[y]$ with $y \in U_1^j = |N_1(0, \mathcal{R}_k^j)|$, defined on the k-gon formed by triangles of the subdivided complex $\mathcal{R}_k^j$ adjacent to the central vertex. It is straightforward to show that the values at all dyadic points in this k-gon can be computed given the initial values $p^j(v)$ for $v \in N_L(0, \mathcal{R}_k^j)$. In particular, the control points $p^{j+1}(v)$ for $v \in N_L(0, R_k^{j+1})$ can be computed using only control points $p^j(w)$ for $w \in N_L(0, \mathcal{R}_k^j)$. Let $\bar{p}^j$ be the vector of control points $p^j(v)$ for $v \in N_L(0, \mathcal{R}_k^j)$. Let $p + 1$ be the number of vertices in $N_L(0, \mathcal{R}_k)$.

As the subdivision operators are linear, $\bar{p}^{j+1}$ can be computed from $\bar{p}^j$ using a $(p+1) \times$

$(p+1)$ matrix S^j:

$$\bar{p}^{j+1} = S^j \bar{p}^j$$

If for some m and for all $j > m$, $S^j = S^m = S$, we say that the subdivision scheme is *stationary on the k-regular complex*, or simply stationary, and call S the *subdivision matrix* of the scheme. Note that in the case $k = 6$ (regular complex) our definition is weaker than the standard definition of stationary subdivision on regular complexes [6].
As we will see, eigenvalues and eigenvectors of the matrix have fundamental importance for smoothness of subdivision.

Eigenbasis functions. let $\lambda_0, \lambda_i, \ldots \lambda_J$ be different eigenvalues of the subdivision matrix. The following lemma can be easily proved

Lemma 2.1. *If a subdivision scheme converges on the regular complex, it is necessary and sufficient for convergence on a k-regular complex that the subdivision matrix S has eigenvalue 1 with a single cyclic subspace of size 1 and all other eigenvalues have magnitude less than 1.*

Let $\lambda_0 = 1$. For any λ_i let J^i_j, $j = 1 \ldots P_i$ be the complex cyclic subspaces corresponding to this eigenvalue.

Let n^i_j be the *orders* of these cyclic subspaces; the order of a cyclic subspace is equal to its dimension minus one.

Let b^i_{jr}, $r = 0 \ldots n^i_j$ be the complex generalized eigenvectors corresponding to the cyclic subspace J^i_j. The vectors b^i_{jr} satisfy

$$\begin{aligned} Sb^i_{jr} &= \lambda_i b^i_{jr} + b^i_{j\,r-1} \quad \text{if } r > 0 \\ Sb^i_{j0} &= \lambda_i b^i_{j0} \end{aligned} \tag{2.2}$$

We use the following rules for enumerating the cyclic subspaces of S:

- All eigenvalues are enumerated in the order of nonincreasing magnitude.
- If the magnitudes of eigenvalues are equal, they are enumerated in the order of nonincreasing order of the largest cyclic subspace.

- If the eigenvalues have equal magnitudes, and equal orders of highest-order cyclic subspace, real eigenvalues have smaller numbers than complex; the real positive eigenvalue if there is one, has number less than real negative; two complex-conjugate eigenvalues have sequential numbers; the order of complex-conjugate pairs of eigenvalues is insignificant for our purposes.

- For each eigenvalue the cyclic subspaces are enumerated in nonincreasing order, i.e., $n^i_1 \geq n^i_2 \geq n^i_3 \geq \dots n^i_{P_i}$.

The complex *eigenbasis functions* are the limit functions defined by $f^i_{jr} = f[b^i_{jr}] : U_1 \to \mathbf{C}$

It immediately follows from (2.13) that any subdivision surface $f[p] : U_1 \to \mathbf{R}^3$ can be represented as

$$f[p](y) = \sum_{i,j,r} \beta^i_{jr} f^i_{jr}(y) \tag{2.3}$$

where $\beta^i_{jr} \in \mathbf{C}^3$, and if $b^i_{jr} = \overline{b^k_{lt}}$, $\beta^i_{jr} = \overline{\beta^k_{lt}}$, where the bar denotes complex conjugation.

One can show using the definition of limit functions of subdivision and (2.17) that the eigenbasis functions satisfy the following set of *scaling relations*:

$$\begin{aligned} f^i_{jr}(y/2) &= \lambda_i f^i_{jr}(y) + f^i_{j\,r-1}(y) \quad \text{if } r > 0 \\ f^i_{j0}(y/2) &= \lambda_i f^i_{j0}(y) \end{aligned} \tag{2.4}$$

Real eigenbasis functions. As we consider real surfaces, it is often convenient to use real Jordan normal form of the matrix rather than the complex Jordan normal form. For any pair of the complex conjugate eigenvalues λ_i, λ_k, we can choose the complex cyclic subspaces in such a way that they can be arranged into pairs J^i_j, J^k_j, and $b^i_{jr} = \overline{b^k_{jr}}$ for all j and r. Then we can introduce a single real subspace for each pair, with the basis c^i_{jr}, c^k_{jr}, $r = 0 \dots n^i_j$, where $c^i_{jr} = \Re b^i_{jr}$, and $c^k_{jr} = \Im b^i_{jr}$. We will call such subspaces *Jordan subspaces.* Then we can introduce real eigenbasis functions $g^i_{jr}(y) = f^i_{jr}(y)$ for real λ_i, and $g^i_{jr}(y) = \Re f^i_{jr}(y)$, $g^k_{jr}(y) = \Im f^i_{jr}(y)$ for a pair of complex conjugate eigenvalues (λ_i, λ_k). For a Jordan subspace corresponding to pairs of complex eigenvalues the order is the same as

the order of one of the pair of cyclic subspaces corresponding to it. We will follow the same rules for enumerating Jordan spaces, with one alteration: instead of two sequences of cyclic subspaces corresponding to a pair of complex Jordan eigenvalues we have a single sequence of Jordan subspaces.

Similar to (2.18) we can write for any surface generated by subdivision on U_1:

$$f[p](y) = \sum_{i,j,r} \alpha^i_{jr} g^i_{jr}(y) \tag{2.5}$$

Now all coefficients α^i_{jr} are real. Eigenbasis functions corresponding to the eigenvalue 0 have no effect on tangent plane continuity or C^k-continuity of the surface at zero. From now on we assume that $\lambda_i \neq 0$ for all i.

2.2 Subdivision of Abstract Simplicial Complexes

In this section we define subdivision schemes on abstract simplicial complexes; abstract simplicial complexes are simply a class of graphs with values attached to the vertices — no topology or metrics is defined. While it is possible to define subdivision directly on simplicial complexes described in the next section, starting with abstract simplicial complexes allows us to separate discrete and continuous aspects of subdivision. Abstract complexes closely match data structures used for implementation of subdivision, and in this sense our somewhat more abstract approach turns out to be more practical. Our definitions are similar to those found in introductory algebraic topology texts such as Giblin [26].

The only non-trivial restriction that we impose on the complex is that the triangles of the complex adjacent to a vertex should form one ring. It is easy to see that any mesh can be converted to a mesh of this type by replicating some vertices and triangles.

We define a formal language for describing local parts of a simplicial complex (neighborhoods) and derive their elementary properties.

Subdivision schemes that we consider are *finitely supported*, *locally defined* and *affine-invariant.* Informally, finite support means that only a finite number of vertices are used to compute the value at a new vertex. Local definition means that coefficients used to compute the new value depend only on the structure of a finite part of the complex. Stationarity

means that the rules do not change from one level to the next.

We show that if a scheme is finitely supported, then all new values that are computed as the result of subdivision of a triangle depend only on the values at the original vertices in a finite neighborhood of the triangle.

This neighborhood is called *control set* of the triangle and is similar to the set of control points of a spline patch. Similarly, a *localization set* is the neighborhood of the triangle whose topology influences the choice of functions for subdivision on all levels.

The distinction between localization and control sets is subtle; the rest of the material presented in this thesis would not loose much generality if this distinction is ignored and control and localization sets are identified. We make the distinction because these properties are in fact different and potentially there are useful subdivision schemes for which the difference is important.

2.2.1 Definitions

Definition 2.2. *An* **abstract simplicial 2D complex** $K = (V, E, F)$ *is a set of vertices* V*, a set of abstract edges, which are unordered pairs of vertices,* $E \subset \{(v, w)|\ v, w \in V\}$ *and a set of abstract triangles which are unordered triples of vertices,* $F \subset \{(u, v, w)|\ u, v, w \in V\}$*, satisfying the conditions below.*

In this section we omit the word "abstract" in the terms "abstract edge," abstract triangle" and "abstract simplicial complex".

The first three conditions formalize the intuitive idea of the complex consisting of triangles that are glued together. The last two conditions ensure that the neighborhood of any vertex has simple structure.

1. All edges of a triangle are in E: if $(u, v, w) \in F$, then $(u, v), (v, w), (w, u) \in E$.

2. No "dangling" edges: if $(v, w) \in E$, then there is $u \in V$ such that $(u, v, w) \in F$. If an edge is shared by two triangles, it is called an *internal* edge. Otherwise, it is called a *boundary* edge.

3. No isolated vertices: If $v \in V$, there is $w \in V$ such that $(v, w) \in E$.

4. No more than two triangles share an edge: If $(v, w) \in E$, there are no more than two vertices u_1, u_2 such that $(u_1, v, w) \in F$ and $(u_2, v, w) \in F$.

5. Consider the set of all triangles containing the vertex v. Consider the set of all edges of these triangles not containing v itself: $N(v) = \{e_0, e_1, ...e_{k-1}\}$; this set is called the *link* of v. We assume that this set is finite and there is a permutation π such that e_i and e_{i+1} share a vertex and no non-consecutive edges do not share a vertex except possibly e_0 and e_{k-1}. If e_0 and e_{k-1} share a vertex, the vertex v is called a *boundary vertex*; otherwise, the vertex is called an *internal* vertex (Figure 2.2).

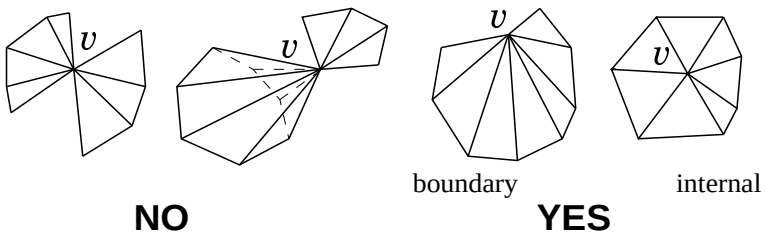

Figure 2.2: Left: Excluded configurations of triangles around a vertex. Right: These configurations are allowed.

A *simplicial map* $K_1 \to K_2$ is a map $V_1 \to V_2$ which maps edges to edges and triangles to triangles.

Definition 2.3. *We call two simplicial complexes K_1 and K_2* **isomorphic** *if there is there is a bijective simplicial map $K_1 \to K_2$.*

A *subcomplex* $K' = (V', E', F')$ of a complex K is a complex that satisfies $V \subseteq V'$, $E \subseteq E'$, $F \subseteq F'$.

A complex is *closed* if all edges are internal. It is easy to show that all vertices are also internal in this case.

If for a pair of complexes K_1 and K_2 there are subcomplexes $K_1' \subset K_1$ and $K_2' \subset K_2$ such that K_1' is isomorphic to K_2', K_1 and K_2 are called *locally isomorphic* on (K_1', K_2').

Definition 2.4. *A* 1**-neighborhood** $N_1(W)$ *of a set of vertices $W \in V$ is the subcomplex of K consisting of all triangles with at least one vertex in W, their edges and vertices. An* m**-neighborhood** $N_m(W)$ *is defined recursively as a 1-neighborhood of the $(m-1)$-neighborhood. We also use notation $N_m(W, K)$ when the want to emphasize in which complex we find the neighborhoods.*

$N_i^j(A)$ where A is a subcomplex of K^j denotes the i-neighborhood of the set of vertices of A; $N_i^j(A) = N_i(A, K^j)$.

k-regular complexes. Most of our constructions use special types of complexes — *regular* and *k-regular*.

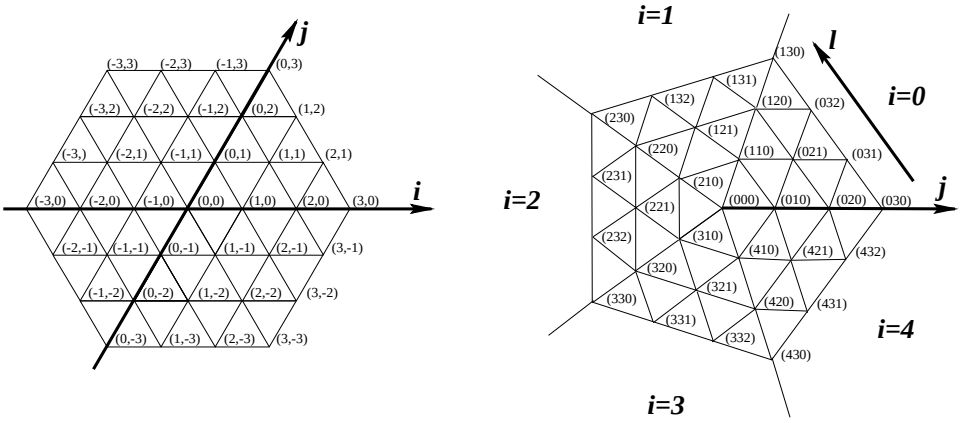

Figure 2.3: Left: enumeration of vertices of the regular complex. Right: enumeration of vertices of a k-regular complex for $k = 5$.

The standard k-regular complex $\mathcal{R}_k$ is shown in Figure 2.3. To specify the complex exactly, we need to enumerate its vertices and faces — all edges of each face are automatically included into the set of edges.

The set of vertices can be enumerated using three indices (i, j, l): the first index indicates the "sector," and the other two define the position of the vertex in the sector. Indices satisfy $i = 0 \dots k-1$, $j > 0$, $l = 0 \dots j-1$. There is also a special central vertex $v_{0,0,0}$. A pair of faces is defined for each vertex $v_{i,j,l}$ except $v_{0,0,0}$ (Figure 2.4): for $l < j-1$ the triangles

$$\left\{\left(v_{i,j,l}, v_{i,j+1,l+1}, v_{i,j,l+1}\right),\ \left(v_{i,j,l}, v_{i,j-1,l}, v_{i,j,l+1}\right)\right\} \in F$$

are in F; for $l = j-1$, the triangles

$$\left\{\left(v_{i,j,j-1}, v_{i,j+1,j}, v_{i+1,j,0}\right),\ \left(v_{i,j,j-1}, v_{i+1,j-1,0}, v_{i+1,j,0}\right)\right\} \in F$$

are in F.

Index i is incremented modulo k, i.e., $v_{k,j,l} = v_{0,j,l}$.

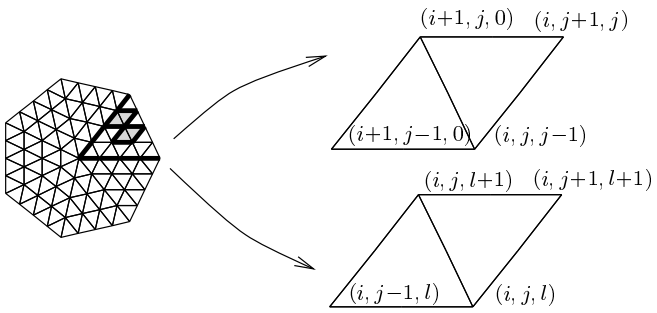

Figure 2.4: 2 faces corresponding to each vertex in a k-regular complex.

A standard k-regular complex with boundary $\mathcal{R}_k^B$ is defined in a similar way: the vertices of the complex are numbered using the same three-index scheme, but the last sector with $i = k - 1$ contains only vertices with $l = 0$.

The faces of the k-regular complex with boundary are defined exactly in the same way, but i varies in the range $0 \dots k - 2$.

If $k = 6$, there is a simpler way to enumerate the vertices of complex: they can be identified with the vertices of an integer grid on the plane. The vertex $v_{i,j}$ corresponds to the point (i, j) (Figure 2.3).

We use this numbering for the 6-regular complex; we call a 6-regular complex simply regular.

Similar numbering can be introduced for the 4-regular complex with boundary: the vertices are $v_{i,j}$, where i is any integer, j is non-negative. We call a 4-regular complex with boundary a regular complex with boundary.

Complex refinement. First we introduce *complex refinement* which describes how new vertices are added to a complex (this part of the subdivision process was called "topological rule" in the introduction).

The procedure is an abstraction of the midpoint subdivision: insert a new vertex at the middle of each edge and connect the midpoints for each triangle. We call this procedure complex refinement.

Let $D(K)$ be a new complex obtained in the following way: The new set of vertices $V' = V \cup V(E)$ where $V(E)$ is a set of vertices which has one vertex per edge of the complex K; let m_{vw} be the vertex in $V(E)$ corresponding to the edge (v, w).

The new set of edges E' is defined as $\{(v, m_{vw}) | (v, w) \in E\}$. For each old edge (v, w)

there are two new edges (v, m_{vw}) and (w, m_{vw}) in E'.

The new set of triangles F' consists of four new triangles for each triangle in F: if $(u, v, w) \in F$, then (u, m_{uv}, m_{uw}), (v, m_{vw}, m_{uw}), (w, m_{uw}, m_{vw}) and (m_{uv}, m_{vw}, m_{uw}) are in F' (Figure 2.5).

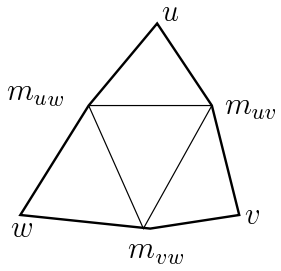

Figure 2.5: Insertion of new vertices for a triangle (u, v, w).

The new triangles are called *children* of the original triangle (u, v, w). The triangles of the complexes $D^j(K)$, $j = 0, 1 \ldots$ form a quadtree with no terminal nodes.

We use K^j as a notation for $D^j(K)$. The vertices of K^j are also vertices of K^{j+1}.

Notation for sets of vertices:

V_T^j is the set of vertices of all children of a triangle T in K^j.

V_T^∞ is the union of V_T^j for all j.

$V^j(A)$ is the union of V_T^j for all triangles T of a subcomplex A of K^j For $i < j$, $V^i(A)$ means $V^j(A) \cap V^i$ — the set of vertices of A that are vertices of K^i.

An simplicial map $\rho : K_1 \to K_2$ can be extended to K_1^j and K_2^j inductively:

$$\begin{aligned} \rho^j(v) &= \rho^{j-1}(v) \quad \text{for } v \in V_1^{j-1} \\ \rho^j(m_{uv}) &= m_{u'v'}, \quad \text{if } \rho^j(u) = u' \text{ and } \rho^j(v) = v'. \end{aligned} \tag{2.6}$$

where V_1 is the set of vertices of K_1. We denote the extension of ρ to $D(K_1)$ by ρ^D.

A complex K is *self-similar*, if the complexes K and $D(K)$ are isomorphic. k-regular complexes and k-regular complexes with boundary are all self-similar. Recall that the set of vertices of $D(\mathcal{R}_k)$ by definition consists of all vertices $v_{i,j,l}$ of $\mathcal{R}_k$ and vertices m_{uv} for

all edges (u, v) of $\mathcal{R}_k$. For each vertex $v_{i,j,l}$ there are 3 new vertices in $D(\mathcal{R}_k)$, shown in Figure 2.6.

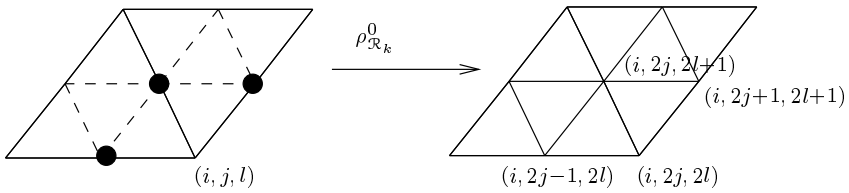

Figure 2.6: Refinement of k-regular complexes.

An isomorphism $\rho^0_{\mathcal{R}} :\ D(\mathcal{R}_k) \to \mathcal{R}_k$ is given by

$$\begin{aligned} \rho^0_{\mathcal{R}_k}(v_{i,j,l}) &= v_{2i,2j,2l} \\ \rho^0_{\mathcal{R}_k}(m(v_{i,j,l}, v_{i,j,l+1})) &= v_{i,2j,2l+1} \\ \rho^0_{\mathcal{R}_k}(m(v_{i,j,l}, v_{i,j,l+1})) &= v_{i,2j,2l+1} \\ \rho^0_{\mathcal{R}_k}(m(v_{i,j,l}, v_{i,j+1,l+1})) &= v_{i,2j+1,2l+1} \end{aligned} \tag{2.7}$$

where l is incremented modulo j as above.

Isomorphisms $\rho^j_{\mathcal{R}_k} : \mathcal{R}^{j+1}_k \to \mathcal{R}^j_k$ are derived from ρ using formulas (2.6).

Functions on complexes. Next we attach values to the vertices of the complex. A set of values defined at each vertex of the complex can be regarded as a function on the set of vertices of this complex.

For a fixed complex K, the linear vector space $\mathcal{P}(V, B)$ is defined as the space of functions on the set of vertices of the complex V with values in a vector space B over $\mathbf{R}$, with operations defined in the natural way. We are interested in the cases when B is $\mathbf{R}^n$ or $\mathbf{C}^n$ for $n = 1, 2, 3$. If $\rho : K_1 \to K_2$ is a simplicial map, it induces a homomorphism of linear spaces $\rho_* :\ \mathcal{P}(K_2) \to \mathcal{P}(K_1)$ defined by $(\rho_*(p))\,(v) = p(\rho(v))$ for $p \in \mathcal{P}(K_2)$, and $v \in V_1$. If ρ is injective, then ρ_* is surjective. If ρ is an isomorphism, then ρ_* is an isomorphism.

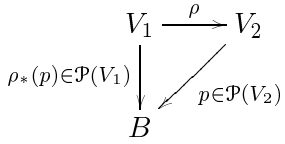

If two complexes are isomorphic, an isomorphism $\rho : V_1 \to V_2$ induces an isomorphism ρ^* of linear spaces $\mathcal{P}(V_1, B)$ and $\mathcal{P}(V_2, B)$ via $\rho^*(p)(v) = p(\rho^{-1}(v))$ for $v \in V_2$.

Typically we omit B in $\mathcal{P}(V, B)$, as the range is often obvious from the context.

Categories of complexes. In addition to abstract complexes described above, we would like to consider other types of complexes such as *tagged complexes*. For example, a set of edges can be designated as tagged, and two complexes are considered as isomorphic only if there is an isomorphism that maps tagged edges to tagged edges. Tagging can be viewed as a constraint on the set of simplicial maps of complexes. Let $\mathrm{Ob}(\mathcal{K})$ be the class of all abstract simplicial complexes and let $\mathrm{Mor}(K_1, K_2)$ be the set of simplicial maps from the complex K_1 to the complex K_2 for any K_1 and K_2, and $\mathrm{Ar}(\mathcal{K})$ the class of all simplicial maps. This defines the category of simplicial complexes. We consider various subcategories $\mathcal{K}'$ of K with $\mathrm{Ob}(\mathcal{K}') = \mathrm{Ob}(\mathcal{K})$, and $G = \mathrm{Ar}(\mathcal{K}') \subset \mathrm{Ar}(\mathcal{K})$. We call the elements of G the admissible simplicial maps of $\mathcal{K}'$. If $\rho \in G$ is an isomorphism of complexes K_1 and K_2 we call K_1 and K_2 G-isomorphic. Locally G-isomorphic complexes are defined in a similar way.

Of course, not all possible sets G are useful. We consider sets G that in addition to the maps required by the category axioms (the identity map $K \to K$, for any K, compositions of maps) also contains the following maps:

- if K_2 is a subcomplex of K_1, G contains the inclusion map $K_2 \to K_1$;
- for any $\rho : K_1 \to K_2$, G contains $\rho^D : D(K_1) \to D(K_2)$.
- If two complexes K_1 and K_2 are locally isomorphic on (K_1', K_2'), $K_1' \subset K_1$, $K_2' \subset K_2$ then there is a complex K_3 with subcomplex K_3' such that K_3 is isomorphic to K_2, and K_1 and K_3 are locally G-isomorphic on (K_1', K_3').

The first two requirements are obvious. To understand the last requirement, note that the whole class of complexes can be separated into nonintersecting equivalence classes of isomorphic complexes. If we eliminate those isomorphisms that are not in G, then each equivalence class is separated into subclasses of G-isomorphic complexes. Suppose we know that we can analyze invariant subdivision locally, using only certain equivalence classes of complexes (specifically, regular and k-regular). Then the third requirement ensures that subclasses of these classes produced by G can be used for the same purpose.

For example, for some G there may be more than one nonisomorphic class of k-regular complexes in $\mathcal{K}'$: we can tag one, two three etc. edges in a k-regular complex and if G

contains only isomorphisms that map tagged edges to tagged edges, all these complexes are not isomorphic in $\mathcal{K}'$. The requirement is a formal way of saying that if some complex K is locally isomorphic to a k-regular complex, then no matter how we tag complex K, it is locally isomorphic to a tagged k-regular complex.

Tagged complexes can be used to define schemes with creases such as the one described in [32], and to reduce other types of refinement rules (Catmull-Clark, Doo-Sabin) to refinement of simplicial complexes (Appendix A).

Subdivision schemes. The most general definition of subdivision simply states that a subdivision scheme computes values at finer subdivision levels from the values at the top level for any complex and any initial set of values.

Definition 2.5. *A* **subdivision scheme** $\mathcal{S}$ *is a map from the class of complexes to the linear operators* $S[K] : \mathcal{P}(V)$ *to* $\mathcal{P}(V^1)$*, where* V^1 *is the set of vertices of* $D(K)$*. We call the operators* $S[K]$ *subdivision operators.*

We say that a scheme is G-invariant, if it commutes with the isomorphisms in G. If $\rho K_1 \to K_2$ is an isomorphism from G, then $S[K_1](\rho_*(p)) = \rho_*^D(S[K_2](p))$:

$$\begin{array}{ccc} \mathcal{P}(K_1) & \xrightarrow{S[K_1]} & \mathcal{P}(D(K_1)) \\ \Big\downarrow{\scriptstyle \rho^*} & & \Big\downarrow{\scriptstyle \rho_*^D} \\ \mathcal{P}(K_2) & \xrightarrow{S[K_2]} & \mathcal{P}(D(K_2)) \end{array}$$

Definition 2.5 is too general to be useful. In addition, we require schemes to have a number of properties. These properties have two origins: most of them are motivated by practical considerations. One property (stationarity), while being practically useful, also makes theoretical analysis much easier.
We consider subdivision schemes having the following properties:

- finite support;
- local definition;
- stationarity;
- affine invariance.

Any locally defined scheme is finitely supported, but not every finitely supported scheme is locally defined.

Before defining these properties, we define *stencils*. Because a subdivision operator $S[K]$ is linear on $\mathcal{P}(K)$, it can be written as

$$(S[K](p))(v) = \sum_{w \in V} a_{wv} p(w),$$

where a_{vw} are coefficients which depend on K. If we fix v, we can consider $S[K, v](p) = (S[K](p))(v)$ as a function $\mathcal{P}(V) \to B$. We call this function the *subdivision function*. Then the *stencil* at v $\mathrm{St}(K^j, v)$ is the set of all w such that the coefficient a_{wv} is not zero.

Note that the vertices of the stencil are vertices of K^j, but due to the inclusion $V^j \subset V^{j+1}$, they may be regarded also as vertices of K^{j+1}.

Example. Figure 2.8 shows the stencils of the Loop scheme for various vertices.

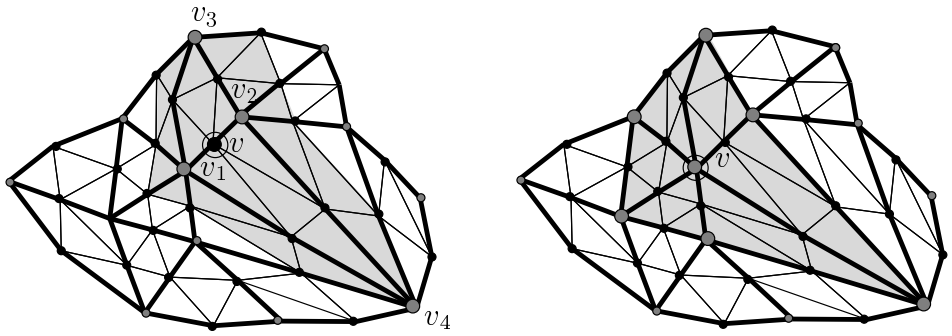

Figure 2.7: Locality and finite support for the Loop scheme, $L = M = 2$. The larger gray disks mark vertices of the stencils $S[K, v]$. Left: $N_M(v)$ for a new vertex v; Right: N_M for an old vertex v.

Condition 1: Finite support. The new value at any vertex depends only on the finite number of values on the coarser level in the neighborhood of the vertex.

Formally, suppose for any j and $v \in K^{j+1}$ there is a neighborhood $N^{j+1}_{M(v)}(v)$ containing the stencil $\mathrm{St}(K^j, v)$. If the set of all $M(v)$ for all K and j is bounded by a constant M, the scheme has finite support:

$$\text{for all } K, v \quad \mathrm{St}(K^j, v) \subset N^{j+1}_M(v)$$

We call the minimal M the *support size* for the subdivision scheme. Figure 2.7 shows stencils and neighborhoods N_m for the Loop scheme (see example below).

Condition 2: Local definition. The scheme has *local definition* if the subdivision rule at any vertex depends only on the structure of a finite part of the complex around this vertex.

More precisely, suppose two subdivided complexes $D(K_1)$ and $D(K_2)$ for some L_1 have isomorphic L-neighborhoods $N_L(v_1)$ and $N_L(v_2)$ of vertices $v_1 \in V_1^1$ and $v_2 = \rho(v_1) \in V_2^1$, and ρ is an admissible isomorphism of $N_L(v_1)$ and $N_L(v_2)$. Then if for any $p \in \mathcal{P}(V_2)$ $S[K_1, v_1](\rho_*(p)) = S[K_2, v_2](p)$, and if L can be chosen to be the same for all vertices of all complexes the scheme is said to be *locally defined* and L is called the *localization size* of the scheme. If a scheme is finitely supported, in general it is possible for schemes with small support (for example, midpoint subdivision) that $L < M$. These cases are not particularly interesting, so we assume that $L \geq M$.

As we will see, for local schemes it is sufficient to study surfaces defined over k-regular complexes and k-regular complexes with boundary.

Condition 3: Affine invariance with respect to the values. A natural geometric property of subdivision is invariance with respect to rotations and translations of the space of initial values B. Due to linearity of subdivision, this is equivalent to requiring invariance with respect to the class of all affine transformations.

Let A be an affine transformation on B. Then a subdivision scheme S is called *affine invariant with respect to the values* if for any complex K, for any j, for any $p \in \mathcal{P}(K, B)$, $S^j[K](Ap) = AS^j[K](p)$. Above, the transformation A is applied to the values of p at the vertices of K and to the values of $S^j[K](p)$ at the vertices of $D(K)$.

The properties of subdivision schemes defined above are all independent, except the dependence between finite support and locality: a scheme can be finitely supported, and not locally defined, but not the other way around.

Example. One of the simplest and useful subdivision schemes satisfying Conditions 1–3 is the Loop scheme (Loop [40]). The stencils and coefficients for a variant of the scheme are shown in Figure 2.8. Different stencils are used for computing values at four types of vertices:

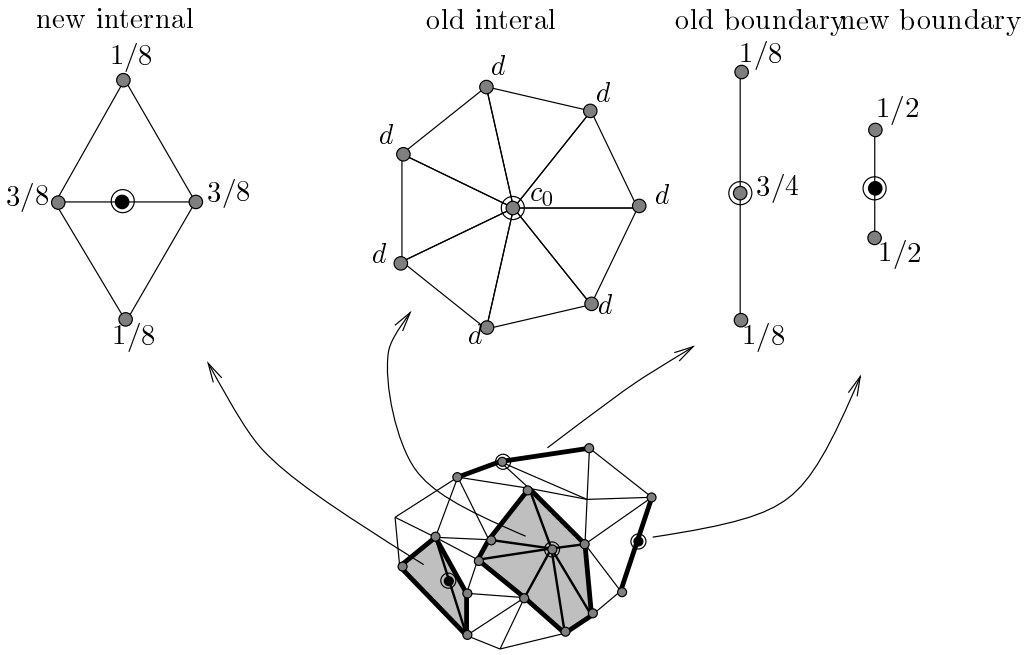

Figure 2.8: Loop scheme. Gray vertices of K^j are elements of $\mathrm{St}(K^j, v)$ for vertices v marked with circles. Black vertices are vertices inserted by refinement (only two are shown). The numbers next to vertices are coefficients used to compute the value $p^{j+1}(v)$ from the values $p^j(v_i)$ for $v_i \in \mathrm{St}(K^j, v)$; $c_0 = \alpha(n)/(n+\alpha(n))$, $\alpha(n) = n((5/8-(3+2\cos(2\pi/n))^2/64)^{-1}-1)$, $d = 1/(1+\alpha(n))$.

- "old" internal: a vertex inherited from the previous subdivision level which has a closed ring of triangles around it;
- "new" internal: a vertex generated by complex refinement;
- "old" boundary: a vertex from the previous subdivision level which has an open strip of triangles around it;
- "new" boundary: a vertex inserted by complex refinement on the edge connecting two boundary "old" vertices.

This list exhausts all possible positions of vertices. For example, the formula used to compute a new value at a "new" internal vertex is

$$p^{j+1}(v) = 3/8p^j(v_1) + 3/8p^j(v_2) + 1/8p^j(v_3) + 1/8p^j(v_4)$$

Vertices v_1, v_2, v_3, v_4 are the vertices of triangles adjacent to the edge of v (Figure 2.8. Details about the scheme can be found in Loop [40]).

2.2.2 Control and Localization Sets

In this section we introduce the *control sets* of sets of vertices of subdivided complexes.

It is sufficient to define the values at the control set of a set W to compute with subdivision all values on W.

This idea generalizes the sets of control points of splines: if we know the positions of control points, all points of a spline patch can be computed.

Definition 2.6. *Define the* **control set** $\mathrm{Ctrl}^j(W)$ *where* $W \subset V^{j+1}$ *to be* $V^j\left(N_M^{j+1}(W)\right)$, *where* M *is the support size defined in Condition 1, Section 2.2.1.*

The values $p^{j+1}(v)$ for $v \in W$ depend only on the values $p^j(v)$ for $v \in \mathrm{Ctrl}^j(W)$.

We define $\mathrm{Ctrl}^i(W)$ for $W \in V^{j+1}$, $i \leq j$ recursively:

$$\mathrm{Ctrl}^i(W) = \mathrm{Ctrl}^i(\mathrm{Ctrl}^{i+1}(W))$$

For a subset W of V^∞, the control set on level i is the union of control sets $\cup_j \mathrm{Ctrl}^i(W \cap V^j)$. For $i > j$ a control set $\mathrm{Ctrl}^i(W)$ is defined using inclusion $V^j \subset V^i$.

For subsets of $W \subset V^\infty$ we define control sets as

$$\mathrm{Ctrl}^i(W) = \cup_j \mathrm{Ctrl}^i(W \cap V^j)$$

Note that the control set may include vertices which are not actually used to compute values on W; an alternative definition could be based on stencils. Our definition has the advantage of giving control sets more regular structure at the expense of increasing the size.

There is no guarantee that this set is finite. We are primarily interested in control sets of V_T^∞; $\mathrm{Ctrl}^0(V_T^\infty)$ is the direct analog of the set of control points of a spline patch; in fact, if subdivision produces a triangular spline patch (for example, Loop scheme on the regular complex), the set of values of $p^0(v)$ on $\mathrm{Ctrl}^0(V_T^\infty)$ is exactly the set of control points of the patch.

The control sets for a triangle for the Loop scheme and for the Butterfly scheme of Dyn, Gregory and Levin [20] are shown in Figure 2.9.

Lemma 2.2. *Control set* $\mathrm{Ctrl}^j(V_T^\infty)$ *is finite for schemes with finite support and is a subset of* $V^j\left(N_{M-1}^j(V_T^j)\right)$, *where* M *is the support size of the scheme.*

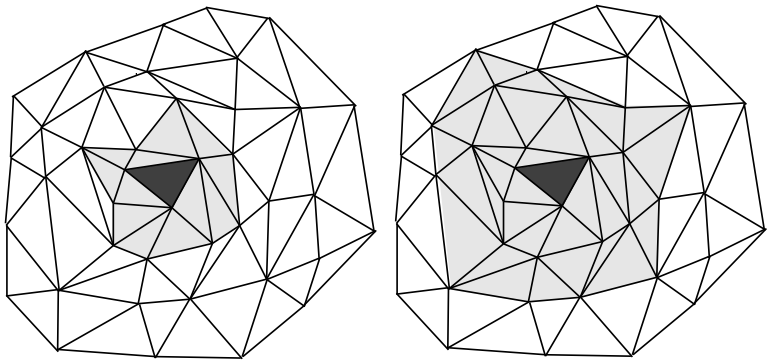

Figure 2.9: Left: Control set $Ctrl^0(V_T^\infty)$ for the Loop scheme, $M = 2$. Right: Control set for the Butterfly scheme, $M = 3$.

Proof. We use Lemma 2.5 from the next section.

Observe that if there is a sequence of sets C^j, $j = 0, 1 \dots$ such that for any $j > 0$ $\mathrm{Ctrl}^j(V_T^{j+1}) \subset C^j$ and $\mathrm{Ctrl}^j(C^{j+1}) = C^j$, then $\mathrm{Ctrl}^i(V_T^\infty) \subset C^i$. Indeed, $\mathrm{Ctrl}^i(V_T^{j+1}) \subset \mathrm{Ctrl}^i(C^j) = C^i$ (the last inclusion is easy to show by induction). As this is true for any j, $\mathrm{Ctrl}^i(V_T^\infty) \subset C^i$.

Take $C^j = N_{M-1}^j(V_T^j)$. Then from the definition of the control set and Lemma 2.5, we get

$$\begin{aligned} \mathrm{Ctrl}^j(C^{j+1}) &= V^j\left(N_M^{j+1}\left(N_{M-1}^{j+1}\left(V_T^{j+1}\right)\right)\right) \\ &= V^j\left(N_{2(M-1)+1}^{j+1}\left(V_T^{j+1}\right)\right) = N_{M-1}^j\left(V_T^j\right) = C^j \end{aligned}$$

.

It is easy to see that $M - 1$ is the minimal possible size of C^j.

□

Note that both Conditions 2 and Condition 1 define a fixed-size neighborhood for any vertex in V^∞.

Exactly the same construction can be used to define *localization sets*:

Definition 2.7. *Let L be the localization size defined in Condition 2, Section 2.2.1 Define the* **localization set** $\mathrm{Loc}^j(W)$ *where $W \subset V^{j+1}$ to be $V^j\left(N_L^{j+1}(W)\right)$.*

Significance of localization sets is different; they can be used to establish equivalence of subdivision on parts of two complexes (Lemma 2.3).

The values $p^{j+1}(v)$ for $v \in W$ depend only on the values $p^j(v)$ for $v \in \mathrm{Loc}^j(W)$.

We define $\mathrm{Loc}^i(W)$ for $W \in V^{j+1}$, $i > j$ recursively: $\mathrm{Loc}^i(W) = \mathrm{Loc}^i(\mathrm{Loc}^{i+1}(W))$. The rest of the definitions for control sets are transferred to the localization sets in the same way.

Note that the sets $\mathrm{Ctrl}^i(V_T^\infty)$ and $\mathrm{Loc}^i(V_T^\infty)$ are sets of vertices of subcomplexes. We use the same names for these complexes.

The following fact is the basis for reducing the study of finitely supported schemes with local definition on arbitrary complexes to the case of k-regular complexes. It follows immediately from the definition of localization sets:

Lemma 2.3. *Suppose K_1 and K_2 have isomorphic subcomplexes $\mathrm{Loc}^0(V_{T_1}^\infty)$ and $\mathrm{Loc}^0(V_{T_2}^\infty)$, where T_1 is a triangle of K_1 and T_2 is a triangle of K_2 and $\rho(T_1) = T_2$. If the initial values p_1 and p_2 satisfy $p_2 = \rho^*(p_1)$ on $\mathrm{Ctrl}^0(V_{T_1}^\infty)$ and $\mathrm{Ctrl}^0(V_{T_2}^\infty)$, then for all vertices v in $V_T^j \subset V_T^\infty$, $p_2^i(\rho(v)) = p_1^i(v)$ for $i \geq j$.*

A proposition similar to Lemma 2.2 holds for localization sets:

Lemma 2.4. *Localization set $\mathrm{Loc}^j(V_T^\infty)$ is finite for schemes with local definition and is a subset of $N_{L-1}^j(V_T^j)$, where L is defined in Condition 2.*

As L is always no less than M, $\mathrm{Ctrl}^j(V_T^\infty) \subset \mathrm{Loc}^j(V_T^\infty)$.

2.2.3 Properties of Neighborhoods

We start with several elementary properties which are straightforward to prove using the definition of the neighborhood and induction.

1. $N_1(\cup_i A_i) = \cup_i N_1(A_i)$, $A_i \subset V$
2. if $A \subset B$, $N_1(A) \subset N_1(B)$, $A, B \subset V$
3. The sets V_T^j have the following property: if $v_i \in V_T^{j+1} \setminus V^j$ (i.e., it is a new vertex created on jth subdivision step) then vertices $v_a, v_b \in V^j$ such that (v_i, v_a), (v_i, v_b) are edges of K^{j+1}, also are in V_T^{j+1}. This property immediately follows from the construction of V_T^j.

The following fact is easy to show:

$$N_1^{j+1}(v) \subset N_1^{j+1}(v_a) \cup N_1^{j+1}(v_b) \tag{2.8}$$

Using property 2 and induction, we can show that

$$N_m^{j+1}(v) \subset N_m^{j+1}(v_a) \cup N_m^{j+1}(v_b) \tag{2.9}$$

for any m.

Now we are ready to prove the following lemma:

Lemma 2.5. *For any m and any $j \geq 0$,*

$$\begin{aligned} V^j\left(N_{2m}^{j+1}\left(V_T^{j+1}\right)\right) &= V^j\left(N_m^j\left(V_T^j\right)\right) \quad \textit{and} \\ V^j\left(N_{2m+1}^{j+1}\left(V_T^{j+1}\right)\right) &= V^j\left(N_m^j\left(V_T^j\right)\right) \end{aligned}$$

Proof. First we show that $D(N_m^j(W^j)) = N_{2m}^{j+1}(W^{j+1})$ for any subcomplex W^j.

A straightforward check shows that $D(N_1^j(v)) = N_2^{j+1}(v)$ for any $v \in V^j$. It is also straightforward to show that $D(\cup_i A_i) = \cup_i D(A_i)$, where A_i are subcomplexes of a complex. Therefore, for any W^j,

$$D(N_1^j(W^j)) = D(\cup_{v \in W^j} N_1^j(v)) = \cup_{v \in W^j} N_2^{j+1}(v) \tag{2.10}$$

Using (2.9) with $m = 2$, we obtain

$$D(N_1^j(W^j)) = \cup_{v \in D(W^j)} N_2^{j+1}(v) = N_2^{j+1}(W^{j+1})$$

Suppose $D(N_{m-1}^j(W^j)) = N_{2(m-1)}^{j+1}(W^{j+1})$. Then taking $\tilde{W}^j = N_{m-1}^j(W^j)$ and applying (2.9), we obtain

$$\begin{aligned} D\left(N_m^j(W^j)\right) &= D\left(N_1^j(\tilde{W}^j)\right) = N_2^{j+1}(D(\tilde{W}^j)) \\ &= N_2^{j+1}\left(N_{2(m-1)}^{j+1}(W^j)\right) = N_{2m}^{j+1}(W^{j+1}) \end{aligned}$$

which proves our proposition by induction.

Now the first formula becomes obvious: $V^j(D(A^j)) = A^j$ for any subcomplex A^j by definition of D.

Now we can prove the second formula. Let $W^{j+1} = N_{2m}^{j+1}(V_T^{j+1})$, $W^j = N_m^j(V_T^j)$.

Write $N_{2m+1}^{j+1}(V_T^{j+1})$ as $N_1^{j+1}(N_{2m}^{j+1}(V_T^{j+1}))$ which coinsides with $N_1^{j+1}(W^{j+1})$. For any vertex $v \in V^j(W^{j+1})$ $N_1^{j+1}(v)$ does not contain vertices in V^j except v. For any vertex $v \in V^{j+1}(W^{j+1}) \setminus V^j(W^{j+1})$ v_a and v_b are in $V^j(W^{j+1})$. Using (2.8), we conclude that for v $N_1(v)$ doesn't contain vertices of V^j other than v_a and v_b, which are in W^j, and therefore

$$V^j\left(N_{2m+1}^{j+1}\left(V_T^{j+1}\right)\right) = V^j\left(N_m^j\left(V_T^j\right)\right)$$

□

2.3 Convergence of Subdivision

The goal of this section is to introduce some basic constructions for analysis of convergence of subdivision. To define convergence, we need a parameter domain for subdivision which has topological structure.

We introduce topology on abstract simplicial complexes. Once topology is specified, we can define continuous functions on simplicial complex. A *subdivision surface* is such a function with values in $\mathbf{R}^3$.

A simple, but very useful fact (Theorem 2.8) provides us with a representation of limit functions of subdivision as linear combinations of a set of *basis functions*. This is a straightforward generalization of a similar fact proved for regular complexes in [6].

We show that for locally defined subdivision the questions of convergence and tangent plane continuity and C^k-continuity of subdivision surfaces can be answered for any complex if the answer is known for k-regular complexes. This is a consequence of local definition and finite support. (but see Section 3.1 for a caveat).

2.3.1 Definition of Convergence

Most of the constructions in this section are routine formalizations of the intuitive concepts described in the introduction.

Topology on Simplicial Complexes. A 2D simplicial complex in a Euclidean space $\mathbf{R}^N$ can be defined as a set of triangles in $\mathbf{R}^N$ that satisfy the following conditions:

- Any two triangles are either disjoint, or have one vertex in common, or have two vertices and the edge joining them in common.
- Define the link of a vertex v as the union of edges of triangles that have v as a vertex. A link of any vertex is either open or closed connected simple polygonal line.

It is clear that for any simplicial complex we can construct a corresponding abstract simplicial complex, assigning an abstract triangle to each triangle of the simplicial complex and abstract edge to each edge. The converse is not obvious. A realization of an abstract simplicial complex K is a simplicial complex such that the corresponding abstract simplicial complex is isomorphic to K. A well-known theorem says that any finite abstract simplicial complex has a realization in $\mathbf{R}^4$ (but not necessarily in $\mathbf{R}^3$; non-orientable complexes cannot be realized in $\mathbf{R}^3$). As we are interested primarily in finite complexes we can use simplicial complexes to introduce topology on abstract complexes. We also use k-regular complexes, which are not finite, but they clearly can be realized as triangulations of the plane. We use notation K_S to denote a realization of an abstract simplicial complex K. The union of all triangles of a simplicial complex K_S regarded as a subset of of R^N with induced topology is denoted $|K_S|$. We use notation $|T|$ for a triangle of K_S corresponding to the abstract triangle T of K.

For any abstract complex neighborhood $N_m(v)$, there is a corresponding topological closed neighborhood $U_m(v) = |N_m(v)|$, which is the union $\cup_i |T_i|$ for all abstract triangles in $N_m(v)$.

Refinement of simplicial complexes: midpoint subdivision. Refinement of abstract complexes produces a new complex $D(K)$ from an old complex K. The vertices of K are also vertices of the new complex $D(K)$. Given a simplicial complex K_S, we can produce a new complex $D(K_s)$ using midpoint subdivision: replace each triangle of K_S with vertices

$v_1, v_2, v_3 \in \mathbf{R}^N$, with four new triangles obtained by adding vertices $(v_1+v_2)/2$, $(v_2+v_3)/2$, $(v_1+v_3)/2$, and connecting the new vertices. Clearly, $|D(K_S)| = |K_S|$, and $D(K_S)$ is a realization of $D(K)$. In this way, $\left|K^j\right|$, $j = 0\dots$ are identified. If we map a triangle $|T|$ to the triangle $((0,0),(1,0),(1,1))$, the *dyadic points* (the points corresponding to vertices of K^j, $j = 0\dots$) map to the points with coordinates of the form $i/2^j, k/2^j$ for some integer i, k. From now on we identify abstract simplicial complexes with their realizations and drop the subscript in the notation K_S.

For each dyadic point v of $|K|$ we have a sequence of values $p^j(v), p^{j+1}(v), \dots$ defined by subdivision, where j is the minimal number such that $v \in V^j$.

Definition 2.8. *A subdivision scheme is called* **convergent**, *if for any pair* (K,p), $p \in \mathcal{P}(K,B)$ *there is a continuous function* f *defined on* $|K|$ *with values in* B, *such that*

$$\lim_{i\to\infty} \sup_{v\in V^i} \left\|p^i(v) - f(v)\right\|_2 \to 0$$

The function f *is called the limit function of subdivision.*

Notation: $f[p]$ is the limit function generated by subdivision from the initial values $p \in \mathcal{P}(K)$.

Isomorphism of simplicial complexes. An isomorphism ρ of abstract complexes K_1 and K_2 induces a unique homeomorphism ρ' of corresponding simplicial complexes: as induced isomorphisms are defined for all subdivided complexes K^j, ρ' is already defined on a dense set in $|K_1|$. It is easy to show that ρ coincides with the restriction to V^∞ of a mapping of topological spaces which is an affine mapping for each triangle of $|K_1|$. Uniqueness of continuous extension of ρ to the immediately follows from density of V^∞ in $|K_1|$. We identify isomorphisms of abstract complexes with their extensions to the topological spaces.

Identification of k-regular simplicial complexes with the plane. For k-regular abstract simplicial complex $\mathcal{R}_k$, $|\mathcal{R}_k|$ can be realized as a triangulation of the plane. Consider the triangulation of the plane with vertices $v_{i,j,l}$. Let $v_{0,0,0}$ be the point $(0,0)$ and $v_{i,j,l}$ to the point $R_i[j - l + l\cos 2\pi/k, l\sin 2\pi/k]^T$, where R_i is the rotation by $2i\pi/k$ around zero. It is easy to see that the abstract complex of this triangulation is exactly the k-regular complex. This identification is shown in Figure 2.3.

The vertices of subdivided complexes $\left|\mathcal{R}_k^j\right|$ are identified with points of the plane obtained by midpoint subdivision. Note that the isomorphism $\rho^0_{\mathcal{R}_k}$, defined in Section 2.2.1, becomes the restriction to the set of vertices of $\mathcal{R}_k^1$ of the scaling of the plane $\sigma : \mathbf{R}^2 \to \mathbf{R}^2$,$\sigma(y) = 2y$. Extension of $\rho^0_{\mathcal{R}_k}$ to the plane is exactly σ.

2.3.2 Basis Function Decomposition

In this section we derive a decomposition of the limit function of converging subdivision into the sum of *basis functions,* which can be obtained as limit functions of subdivision with initial value 1 at one of the vertices of a complex and 0 at all other vertices. The lemmas in this section are proved with the only assumption that the stencil of the subdivision scheme is finite for any point of any complex. The scheme is not required to be either finitely supported or locally defined.

First, we show that linear and piecewise constant approximations to the limit function defined below converge to the limit function in L_∞ norm on any compact subset of $|K|$.

Definition 2.9. *Let $T = (v_1, v_2, v_3)$ be a triangle of K^j, $y \in |T|$. Let $\alpha_1, \alpha_2, \alpha_3$ be the barycentric coordinates of y in the triangle T, $\alpha_1+\alpha_2+\alpha_3 = 1$. Define $L[p^j](y) = \alpha_1 p^j(v_1)+ \alpha_2 p^j(v_2) + \alpha_3 p^j(v_3)$,* **$j$th linear approximation** *of $f[p^0](y)$.*

Clearly, $L[p^j](y)$ is continuous, and the definition is consistent on common edges of triangles.

Lemma 2.6. *On any compact subset A of K*

$$\lim_{j\to\infty} \|L^j(y) - f[p^0](y)\|_{\infty,A} = 0 \tag{2.11}$$

Proof. We denote $f[p^0](y)$ by $f(y)$, $L[p^j](y)$ by $L^j(y)$. For any compact set $A \subset |K|$, there is only a finite number of triangles T of K^j such that $A \cap |T| \neq \emptyset$. Thus,

$$\|L^j(y) - f(y)\|_{\infty,A} < \max_{|T|\cap A\neq\emptyset} \|L^j(y) - f(y)\|_{\infty,T}$$

and it is sufficient to show convergence only for $A = |T|$, where

T is a triangle of K, $T = (v_1, v_2, v_3)$.

$$\begin{aligned}\left\|L^j(y)-f(y)\right\|_\infty &\leq \max_{s\in|T|}\max_{y\in|T|}\left|L^j(y)-L^j(s)\right| \\ &\leq \max_{s\in|T|}\max_{i\in\{1,2,3\}}\left|L^j(v_i)-f(s)\right| \\ &= \max_{s\in|T|}\max_{i\in\{1,2,3\}}\left|p^j(v_i)-f(s)\right|\end{aligned}$$

As $|T|$ is compact, $f(y)$ is uniformly continuous on $|T|$ in the standard metrics on T, i.e., for any $\epsilon > 0$ there is a $\delta > 0$ such that for any s_1, s_2 satisfying $|s_1 - s_2| < \delta$, $|f(s_1) - f(s_2)| < \epsilon$.

As the maximal distance between points of $|T|$ for a triangle T of K^m is $\frac{\sqrt{2}}{2^m}$, then for any $\epsilon > 0$ there is m_1 such that for all triangles T of K^j, $j > m_1$, for any $s_1, s_2 \in |T|$, $|f(s_1) - f(s_2)| < \epsilon$.

By definition, $f(v_i) = \lim_{l\to\infty} p^l(v_i)$. Therefore, there is a number m_2 such that for all $l > m_2$ $\left|p^l(v_i) - f(v_i)\right| < \epsilon$ for $i \in \{1, 2, 3\}$.

Let $m = \max(m_1, m_2)$. Then for $j > m$

$$\max_i \left|p^j(v_i) - f(s)\right| < \max_i(\left|p^j(v_i) - f(v_i)\right| + |f(v_i) - f(s)|) < 2\epsilon$$

We conclude that (2.11) is true.

□

A similar statement holds for piecewise constant approximations, defined in the following way.

Definition 2.10. *Suppose for each triangle T of K^j we choose a vertex v, and define* **piecewise contstant** *$C^j(t)$, for t in the interior of $|T|$ to be equal to $p^j(v)$. On the intersections of triangles $C^j(y)$ is defined by arbitrarily picking a triangle "responsible" for the intersection.*

Lemma 2.7. *On any compact subset A of K*

$$\lim_{j\to\infty} \|C^j(y) - f[p^0](y)\|_{\infty,A} = 0 \tag{2.12}$$

The proof of this lemma is exactly the same as the proof of Lemma 2.6.

Now we can prove the following theorem:

Theorem 2.8. *Suppose a subdivision scheme S converges on a complex K for any initial values $p^0 \in \mathcal{P}(K, \mathbf{R})$. Then*

$$f[p^0](y) = \sum_{v \in V^0} p^0(v)\varphi_v(y) \tag{2.13}$$

where $\varphi_v(y)$ is continuous and $\varphi_v(y) = f[\delta_v](y)$, $\delta_v(v) = 1$ and $\delta_v(w) = 0$ for $w \neq v$.

Proof. It follows from Lemma 2.7 that

$$\varphi_v(y) = \lim_{j \to \infty} L^j[\delta_v](y) \tag{2.14}$$

For any vertex $v \in V^j$,

$p^j(v) = \sum_{w \in V^{j-1}} a_{wv}^{j-1} p^{j-1}(w)$, where only a finite number of $a_{wv}^{j-1} \neq 0$.

By induction, $p^j(v) = \sum_{w \in V^{j-l}} a_{wv}^{j-l} p^{j-l}(w)$ for all $l < j$, i.e., $p^j(v) = \sum_{w \in V^0} a_{wv}^0 p^0(w)$, with only finite number of $a_{wv}^0 \neq 0$.

In particular, for $p^0 = \delta_u^0$, $\delta_u^j(v) = a_{uv}$, i.e.,

$$p^j(v) = \sum_{w \in V^0} \delta_w^j(v) p^0(w)$$

$L[p^j](y) = \alpha_1 p^j(v_1) + \alpha_2 p^j(v_2) + \alpha_3 p^j(v_3)$, if $y \in |T|$, T is a triangle of K^j and $\alpha_1, \alpha_2, \alpha_3$ are barycentric coordinates of y. Then

$$L^j[p](y) = \sum_{w \in V^0} \left(\alpha_1 \delta_w^j(v_1) + \alpha_2 \delta_w^j(v_2) + \alpha_3 \delta_w^j(v_3)\right) p^0(w) = \sum_{w \in V^0} p^0(w) L[\delta_w^j](y)$$

The limits of the right and of the left side exist by Lemma 2.6. Taking limits and using (2.14), we get (2.13). □

2.3.3 Reduction to the k-regular Complexes

In this section we reduce local analysis of the limit surfaces generated by a scheme satisfying Conditions 1 and 2 to the analysis of limit surfaces on k-regular complexes. By local analysis we mean analysis of properties that can be determined from arbitrarily small neighborhood of a point in $|K|$ where K is the simplicial complex over which the surface is defined.

Suppose we can demonstrate that for a certain subcomplex K_y such that y is an interior point of $|K_y|$, there is an isomorphism ρ_y of K_y and K_{std} where K_{std} is a subcomplex of a standard complex, and any limit function $f[p]$, $p \in \mathcal{P}(K)$ can be represented locally on $|K_y|$ as $f[\rho_y^*(p)] \circ \rho_y$:

$$\begin{array}{ccc} |K_y| & \xrightarrow{\rho_y} & |K_{std}| \\ & \searrow^{f[\rho_y^*(p)]} & \downarrow{\scriptstyle f[p]} \\ & & B \end{array} \tag{2.15}$$

We use the k-regular complexes, possibly with boundary, as K_{std}. Then the analysis of all local properties of f, of C^k-continuity in particular, can be done on k-regular (possibly with boundary) complexes.

We consider the case of schemes invariant with respect to all isomorphisms of complexes. Constructions for G-invariant schemes for sets G satisfying the requirements stated in Section 2.2.1 is similar.

In order to demonstrate existence of the isomorphisms ρ_y described above, we consider several types of points of $|K|$, shown in Figure 2.10.

Non-dyadic, non-edge, internal. Suppose ϵ is the distance from y to the boundary of $\left|T^0\right|$. Let T^j be the triangle of K^j such that $y \in \left|T^j\right|$. There is j such that $\left|N_{L-1}^j(T^j)\right| \subset B_\epsilon(y)$, where B_ϵ is a disk of radius ϵ centered at y. Therefore, $N_{L-1}^j(T^j)$ doesn't contain any extraordinary vertices and it is isomorphic to a subcomplex of the regular complex. Explicit enumeration of the vertices in $N_{L-1}^j(T^j)$ establishes the isomorphism. The fact that the localization set doesn't contain extraordinary vertices guarantees that the mapping induced by the isomorphism satisfies (2.15).

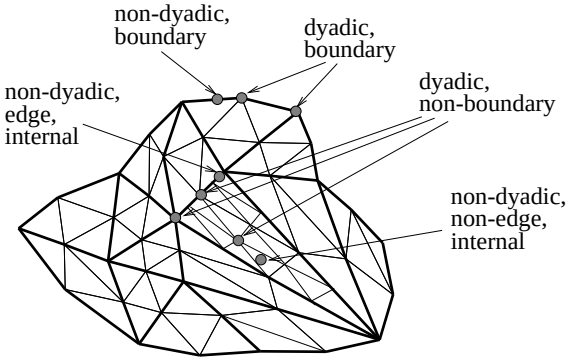

Figure 2.10: Types of points of $|K|$. Non-dyadic vertices are not vertices of a triangle on any level of subdivision, not only on the levels shown in the picture.

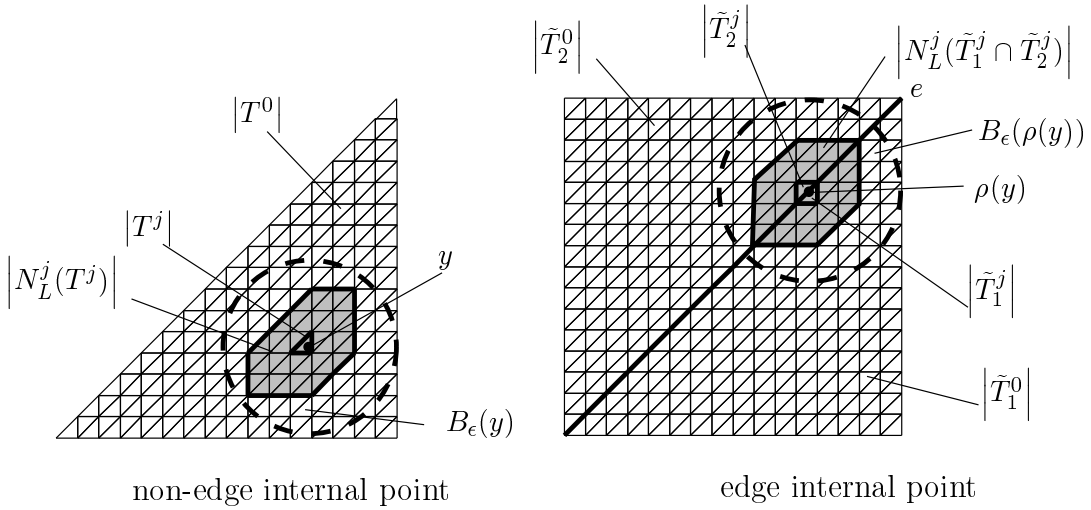

Figure 2.11: Non-dyadic points, reduction to the regular case, $L = 3$.

Non-dyadic, edge, internal. Suppose $y \in |T_1^0| \cup |T_2^0|$. For any j, there is an isomorphism ρ between $D^j(T^0) \cup D^j(T^1)$ and the subcomplex of the regular complex consisting of $v_{i,k}$, $0 \le i, k \le 2^j$,induced by the map from $|T_1^0| \cup |T_2^0|$ to the square $[0,1] \times [0,1]$, which is identity for T_1^0, and reflection across $e = [(0,0),(1,1)]$ for T_2^0, assuming that e is the edge of T_1^0 identified with the same edge of T_2^0. Let $\tilde{T}_i^0 = \rho(T_i^0)$, $i = 1, 2$.

Suppose ϵ is the distance from $\rho(y)$ to the boundary of the square formed by $\tilde{T}_1^0$ and $\tilde{T}_2^0$. Then there is j such that $N^j(\tilde{T}_1^j) \cup N^j(\tilde{T}_2^j) \subset B_\epsilon(\rho(y))$. Then we proceed as in case 1.

Non-dyadic, boundary. Suppose $y \in |T^0|$. Assume $[(0,0),(1,0)]$ is on the boundary. Map T_1^0 to the triangle (v_{00}, v_{01}, v_{11}) in the regular complex with boundary. The rest of the argument is similar to case 1.

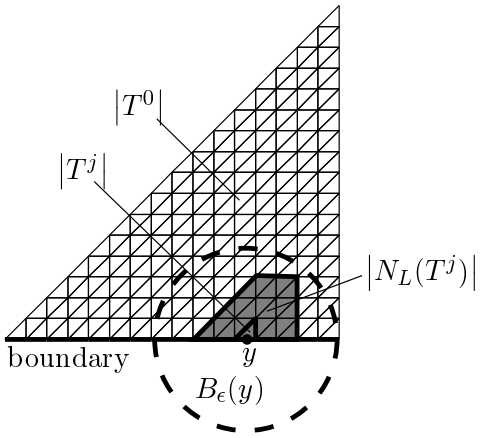

Figure 2.12: Non-dyadic boundary point, reduction to the regular case case, $L = 3$.

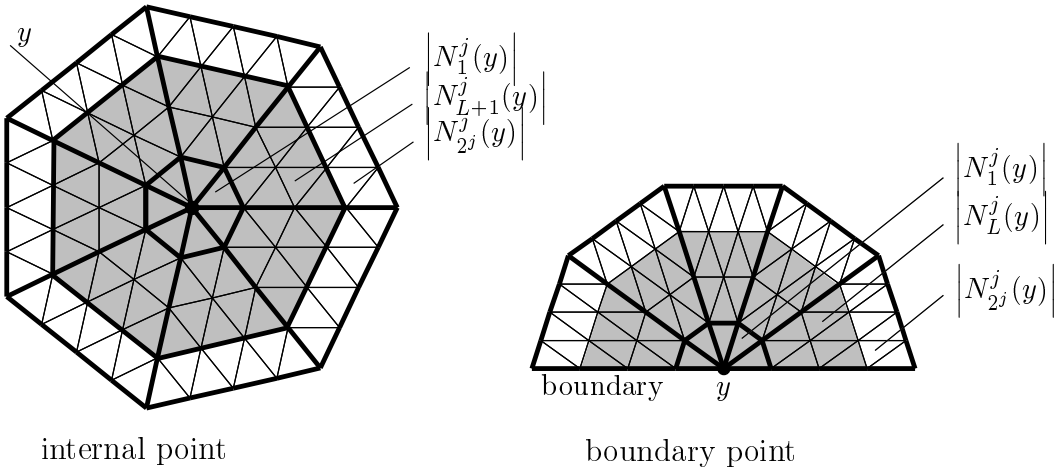

Figure 2.13: Dyadic points, reduction to the regular case, $L = 3$, $j = 2$.

Dyadic, internal. Clearly, $N_1^0(y)$ is isomorphic to N_1^0 in the k-regular complex, where k is the valence of the vertex. Therefore, $N_{2^j}^j$ in K is isomorphic to a similar neighborhood in the k-regular complex $\mathcal{R}_k$. Choosing sufficiently large j, we obtain the required isomorphism.

Dyadic boundary. This case is similar to the previous one, but the k-regular complex with boundary is used instead of the k-regular complex.

In the case of internal non-dyadic and regular dyadic points of $|K|$, it is sufficient to analyze C^k-continuity of the surface on the regular complex.

In the case of internal extraordinary points, it is sufficient to analyze C^k-continuity the k-regular complexes.

Thus, analysis of C^k-continuity of the scheme at internal points of $|K|$ is reduced to two cases: the regular case, for which the scheme is defined with a finite mask, and k-regular case, for which the scheme is defined with a finite number of finite masks, corresponding to different symmetry classes of vertices.

On the boundary, it is also sufficient to analyze two cases: regular and k-regular complexes with boundary.

The regular case is described in detail for functional subdivision by Cavaretta, Dahmen and Micchelli [6].

The second case did not receive much attention until recently. Relevant literature includes works by Loop, Warren, Kobbelt, Reif [40, 63, 36, 55].

2.4 Subdivision Matrix

In this section we introduce the subdivision matrix, which is the matrix that relates the values on the localization set of the topological 1-neighborhood of zero in the k-regular complex to the values on the similar neighborhood on the next subdivision level. This matrix is defined only for stationary schemes.

As the localization set of 1-neighborhood of zero $\dot{U}_1$ is contained in N_L, the limit function on $\dot{U}_1$ is completely defined by values p^0 on N_L. In particular, if we take the initial values to be equal to the values of an eigenvector of the subdivision matrix, subdivision will produce a limit function called *eigenbasis function.* These functions satisfy scaling relations which will be used in the next section to derive a criterion for C^k-continuity.

We introduce layers of a k-regular complex, which are rings of triangles around a vertex, where only regular subdivision rules are used.

Finally, we prove a simple condition on the eigenvalues of the subdivision matrix that is sufficient for convergence of subdivision.

2.4.1 Subdivision Matrix and Layers

Let L be the localization size for $\mathcal{S}$.

Definition 2.11. *Consider $N^0_{L-1}(N^0_1) = N^0_L$ in the k-regular complex $\mathcal{R}_k$. As $N^j_L \simeq N^{j+1}_L$ and $\mathrm{Ctrl}^j(N^{j+1}_L) \subset N^j_L$, the values of $p^{j+1}|_{N^{j+1}_L}$ can be computed from $p^j|_{N^j_L}$ only, using a matrix S^j. If there is an m such that for all $j > m$ $S^j = S^m = S$ we say that the*

subdivision scheme is stationary on the k-regular complex, or simply **stationary**. *We call S the* **subdivision matrix** *of $\mathcal{S}$ on $\mathcal{R}_k$.*

Note that our definition differs from the definition of stationary subdivision on regular complexes which can be found for example in [6]. Our definition is somewhat weaker.

Example. The following matrix is the subdivision matrix for the Loop scheme on the 3-regular complex. The vertices are indexed as it is shown in Figure 2.14.

$$\left(\begin{array}{c|ccc|ccc|ccc}
7/16 & 3/16 & 3/16 & 3/16 & 0 & 0 & 0 & 0 & 0 & 0 \\ \hline
3/8 & 3/8 & 1/8 & 1/8 & 0 & 0 & 0 & 0 & 0 & 0 \\
3/8 & 1/8 & 3/8 & 1/8 & 0 & 0 & 0 & 0 & 0 & 0 \\
3/8 & 1/8 & 1/8 & 3/8 & 0 & 0 & 0 & 0 & 0 & 0 \\ \hline
1/16 & 5/8 & 1/16 & 1/16 & 1/16 & 0 & 0 & 1/16 & 0 & 1/16 \\
1/16 & 1/16 & 5/8 & 1/16 & 0 & 1/16 & 0 & 1/16 & 1/16 & 0 \\
1/16 & 1/16 & 1/16 & 5/8 & 0 & 0 & 1/16 & 0 & 1/16 & 1/16 \\ \hline
1/8 & 3/8 & 3/8 & 0 & 0 & 0 & 0 & 1/8 & 0 & 0 \\
1/8 & 0 & 3/8 & 3/8 & 0 & 0 & 0 & 0 & 1/8 & 0 \\
1/8 & 3/8 & 0 & 3/8 & 0 & 0 & 0 & 0 & 0 & 1/8
\end{array}\right)$$

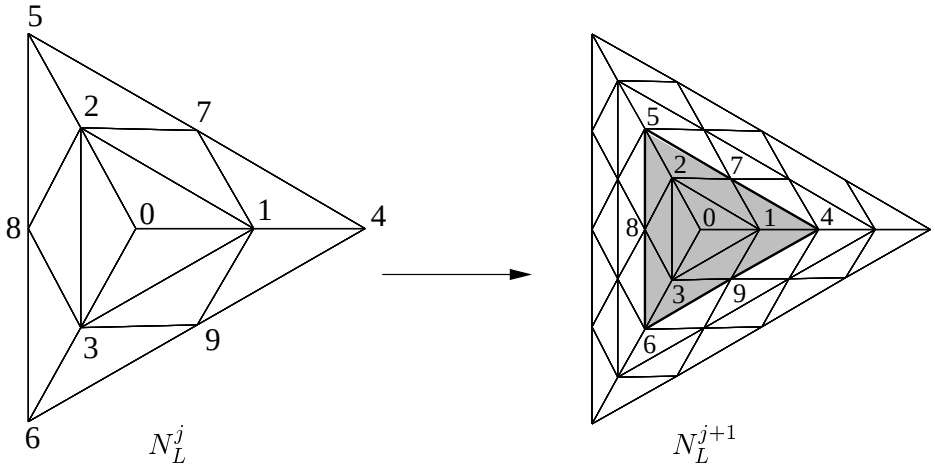

Figure 2.14: Subdivision matrix operates on the values of p^j on N_L^j (left) and produces the values of p^{j+1} on N_L^{j+1} (right). In the picture, $L = 2$, as for the Loop scheme. The numbers shown in the picture are used to arrange the values at vertices of N_L^j into one vector.

Conditions 1–3 from Section 2.2 are reflected in the properties of the matrix. For example, Condition 3 (affine invariance) implies that the subdivision matrix has eigenvalue 1 with eigenvector $x(v) = 1$ for all $v \in N_L$. Indeed, let $p'(v) = p(v) - 1$ for $p \in N_m$, i.e., $p' = p - x$. Then $Sp' = Sp - x$ by affine invariance. But by linearity $Sp' = Sp - Sx$, thus $Sx = x$.

Next we define the *layers* of k-regular complexes. For any triangle T, $T \cap N_L = \emptyset$, convergence of $\mathcal{S}$ on $|T|$ is equivalent to convergence of $\mathcal{S}$ on a triangle of the regular complex (Lemma 2.4). By assumption, $\mathcal{S}$ converges there. Thus the scheme converges on $\mathcal{R}_k \setminus N_L$. Note that $D(\mathcal{R}_k^j \setminus N_L^j) = \mathcal{R}_k^{j+1} \setminus N_{2L}^{j+1}$.

Definition 2.12. *A* **Layer** Lr^j *of the subdivided k-regular complex $\mathcal{R}_k^j$ is defined as $N_{2L}^j \setminus N_L^j$.*

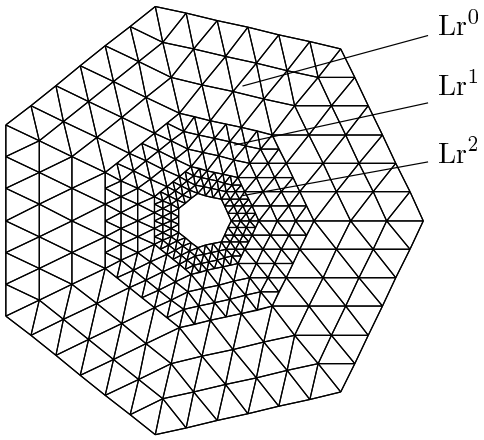

Figure 2.15: Layers Lr^0,Lr^1,Lr^2 for $L = 3$ (Butterfly scheme).

The union of all layers covers a neighborhood of zero in $|\mathcal{R}_k|$, except for zero itself:

$$\bigcup_{j=0}^{\infty} \left|\mathrm{Lr}^j\right| = \dot{U}_{2(L+1)}^0 \tag{2.16}$$

We use notation $\dot{U}_l^j$ for $U_l^j \setminus \{(0,0)\}$.

By construction of the layers, functions $f[p^n]$ are defined on $\cup_{j=0}^m \mathrm{Lr}^j$ for $n \geq m$, and $f[p^n] = f[p^m]$ on $\cup_{j=0}^m \mathrm{Lr}^j$. Thus, we can define $f^\circ(y) = f[p^n](y)$ for $y \in \cup_{j=0}^n \mathrm{Lr}^j$. If the subdivision scheme converges on $\mathcal{R}_k$, the limit function $f[p^0]$ coincides with $f^\circ[p^0]$ on $\left|N_{2L}^0\right|$.

We summarize the observations above in the following

Lemma 2.9. *On a k-regular complex $\mathcal{R}_k$ for a subdivision scheme $\mathcal{S}$ converging on the regular complex, for any $p \in \mathcal{P}(N_L)$ there is a continuous limit function $f^\circ[p]$ defined on $\dot{U}_1$; at dyadic points v, the sequences of values $p^i(v)$ converge to $f^\circ[p]$. If the scheme converges on $\mathcal{R}_k$, $f^\circ[p]$ coincides with $f[p]$ on $\dot{U}_1$.*

2.4.2 Eigenbasis Functions and Scaling Relations

The limit functions generated by the eigenvectors of the subdivision matrix have an important property: they satisfy scaling relations described in this section. This property will be used in Section 3.10 to derive a criterion for C^k-continuity of subdivision.

Let $\lambda_0, \lambda_i, \ldots \lambda_J$ be different eigenvalues of the subdivision matrix. The following lemma can be easily proved

Lemma 2.10. *If a subdivision scheme converges on the regular complex, it is necessary and sufficient for convergence on a k-regular complex that the subdivision matrix S has eigenvalue 1 with a single cyclic subspace of size 1 and all other eigenvalues have magnitude less than 1.*

Let $\lambda_0 = 1$. For any λ_i let J^i_j, $j = 1 \ldots P_i$ be the complex cyclic subspaces corresponding to this eigenvalue.

Let n^i_j be the *orders* of these cyclic subspaces; the order of a cyclic subspace is equal to its size minus one.

Let b^i_{jr}, $r = 0 \ldots n^i_j$ be the complex generalized eigenvectors corresponding to the cyclic subspace J^i_j. The vectors b^i_{jr} satisfy

$$\begin{aligned} Sb^i_{jr} &= \lambda_i b^i_{jr} + b^i_{j\,r-1} \quad \text{if } r > 0 \\ Sb^i_{j0} &= \lambda_i b^i_{j0} \end{aligned} \tag{2.17}$$

We use the following rules for enumerating the cyclic subspaces of S:

- All eigenvalues are enumerated in the order of nonincreasing magnitude.
- If the magnitudes of eigenvalues are equal, they are enumerated in the order of nonincreasing order of the largest cyclic subspace.

- If the eigenvalues have equal magnitudes, and equal orders of highest-order cyclic subspace, the real positive eigenvalue if there is one, has number less than real negative; complex eigenvalues are enumerated after real; two complex conjugate eigenvalues have sequential numbers; the order of complex-conjugate pairs of eigenvalues is insignificant for our purposes.

- For each eigenvalue the cyclic subspaces are enumerated in nonincreasing order, i.e., $n^i_1 \geq n^i_2 \geq n^i_3 \geq \dots n^i_{P_i}$.

Definition 2.13. *Suppose S is the subdivision matrix of a subdivision scheme $\S$ on the k-regular complex, and b^i_{jr} are the vectors of the Jordan basis of S. Then the limit functions $f[b^i_{jr}](y)$ defined on U_1 are called* **complex eigenbasis functions.**

Eigenbasis function $f[b^i_{jr}]$ is also denoted f^i_{jr}.

It immediately follows from Theorem 2.8 that any function on U_1 can be written as a linear combination

$$f[p](y) = \sum_{i,j,r} \beta^i_{jr} f^i_{jr}(y) \tag{2.18}$$

where $\beta^i_{jr} \in \mathbf{C}^3$, and if $b^i_{jr} = \overline{b^k_{lt}}$, $\beta^i_{jr} = \overline{\beta^k_{lt}}$, where the bar denotes complex conjugation.

One can show using the definition of limit functions of subdivision and (2.17) that the eigenbasis functions satisfy the following set of *scaling relations*:

$$\begin{aligned} f^i_{jr}(y/2) &= \lambda_i f^i_{jr}(y) + f^i_{j\,r-1}(y) \quad \text{if } r > 0 \\ f^i_{j0}(y/2) &= \lambda_i f^i_{j0}(y) \end{aligned} \tag{2.19}$$

Real eigenbasis functions. As we consider real surfaces, it is convenient to use real Jordan normal form of the matrix rather than the complex Jordan normal form. For any pair of the complex conjugate eigenvalues λ_i, λ_k, we can choose the complex cyclic subspaces in such a way that they can be arranged into pairs J^i_j, J^k_j, and $b^i_{jr} = \overline{b^k_{jr}}$ for all j and r. Then we can introduce a single real subspace for each pair, with the basis

c^i_{jr}, c^k_{jr}, $r = 0 \dots n^i_j$, where $c^i_{jr} = \Re b^i_{jr}$, and $c^k_{jr} = \Im b^i_{jr}$. We will call such subspaces *Jordan subspaces.* Then we can introduce real eigenbasis functions $g^i_{jr}(y) = f^i_{jr}(y)$ for real λ_i, and $g^i_{jr}(y) = \Re f^i_{jr}(y)$, $g^k_{jr}(y) = \Im f^i_{jr}(y)$ for a pair of complex conjugate eigenvalues (λ_i, λ_k). For a Jordan subspace corresponding to pairs of complex eigenvalues the order is the same as the order of one of the pair of cyclic subspaces corresponding to it. We will follow the same rules for enumerating Jordan spaces, with one alteration: instead of two sequences of cyclic subspaces corresponding to a pair of complex Jordan eigenvalues we have a single sequence of Jordan subspaces.

Similar to (2.18) we can write for any surface generated by subdivision on U_1:

$$f[p](y) = \sum_{i,j,r} \alpha^i_{jr} g^i_{jr}(y) \tag{2.20}$$

Now all coefficients α^i_{jr} are real. Eigenbasis functions corresponding to the eigenvalue 0 have no effect on tangent plane continuity or C^k-continuity of the surface at zero. From now on we assume that $\lambda_i \neq 0$ for all i.

Trivial eigenbasis functions and eigenvalues. Some of the eigenbasis functions of a subdivision scheme may be identically equal to zero. These eigenbasis functions do not affect the limit functions of subdivision in any way. If an eigenbasis function corresponds to the eigenvalue $\lambda = 0$, it also cannot affect convergence or C^1-continuity of subdivision surfaces. Although it need not be identically zero on U_1, it is identically zero on a smaller neighborhood U^1_1. Eigenbasis functions which are identically equal to zero or correspond to the eigenvalue zero are called *trivial.*

If all eigenbasis functions corresponding to an eigenvalue λ are trivial, λ is said to be a *trivial eigenvalue.*

The non-trivial eigenvectors of the subdivision matrix span a subspace of $\mathcal{P}(N_L, \mathbf{R})$ or $\mathcal{P}(N_L, \mathbf{C})$ that we call the *non-trivial subspace.* The limit function generated by any $x \in \mathcal{P}(N_L, \mathbf{R})$ is equal to the limit function generated by the projection of x onto the non-trivial subspace.

Constant eigenvectors and eigenbasis functions. We have observed that if the subdivision scheme is affine invariant, S has eigenvalue $\lambda_i = 1$ with eigenvector constant on N_L. Note that S cannot have generalized eigenvectors of order greater than 0 corresponding to the eigenvalue 1: if x is such eigenvector, $S^m x$ diverges. Any eigenvector with eigenvalue 1 should produce a constant eigenbasis function. Note that for any eigenvector x of the eigenvalue 1 $S^m x$ does not converge to zero as $m \to \infty$. Therefore, the corresponding eigenbasis function cannot be trivial. By Lemma 3.14 the eigenbasis function corresponding to eigenvalue 1 should be a constant. Consider two eigenvectors b^i_{10} and b^i_{20} of the eigenvalue 1. if they generate eigenbasis functions equal to C_1 and C_2 respectively, then $C_2 b^i_{10} - C_1 b^i_{20}$ generates a trivial eigenbasis function, which means that the $C_2 b^i_{10} - C_1 b^i_{20} = 0$ (it is also an eigenvector of eigenvalue 1). We conclude that the eigenvalue 1 has a single cyclic subspace of size 1 with constant eigenvector and constant eigenbasis function.

Suppose the set of vectors b_m $m = 0 \dots n$ are generalized eigenvectors of S for the eigenvalue λ, $Sb_m = \lambda b_m + b_{m-1}$ for $m > 0$, $Sb_0 = \lambda b_0$.

In Section 2.3.1 we have introduced an identification of the k-regular complex and the plane. Recall that the map $y \to y/2$ of the plane to itself maps $N^j_i \to N^{j+1}_i$ for any m.

Theorem 2.11. *For a subdivision scheme $\mathcal{S}$, the functions $f[b_m] = f_m$ defined on $\dot{U}_1$ in the k-regular complex $\mathcal{R}_k$ satisfy scaling relations*

$$\begin{aligned} f_m(y/2) &= \lambda f_m(y) + f_{m-1}(y) \quad \textit{for } m > 0 \\ f_0(y/2) &= \lambda f_0(y) \end{aligned} \tag{2.21}$$

Proof. By linearity of subdivision, if $b^j_m = \lambda b^j_m + b^j_{m-1}$, $b^j_m \in \mathcal{P}(D^j(N^0_L))$, then $b^{j+1}_m = \lambda b^{j+1}_m + b^{j+1}_{m-1}$, $b^{j+1}_m \in \mathcal{P}(D^{j+1}(N^0_L))$. As $L^j_m(y) := L[b^j_m](y)$ is linear in y on each triangle $|T|$, where T is a triangle of $D^j(N_1)$, then

$$L^j_m(\frac{y}{2}) = \lambda L^j_m(y) + L^j_{m-1}(y) \tag{2.22}$$

For any complex $\mathcal{R}^p_k \setminus N^p_L$ $\lim_{j\to\infty} L_m(y) = f(y)$. Therefore, $\lim_{j\to\infty} L_m(y) = f(y)$ everywhere, and (2.21) follows from (2.22).

□

2.4.3 Jordan Normal Form of the Subdivision Matrix

Let $\{b^i_{jr} | i = 0 \dots J,\ j = 1 \dots P_i,\ r = 0 \dots n^i_j\}$ be a basis in which the subdivision matrix S has Jordan normal form. Any vector x can be written in the form

$$x = \sum_{i=0}^{J} \sum_{j=1}^{P_i} \sum_{r=0}^{n^i_j} \beta^i_{jr} b^i_{jr},$$

and b^i_{jr} satisfies $S b^i_{jr} = \lambda_i b^i_{jr} + b^i_{j(r-1)}$ for $r \geq 0$, $S b^i_{j0} = \lambda_i b^i_{j0}$.

We are interested in the expression for the vector $S^l x$. We assume that $l \geq n^i_j$ for all i, j.

First, we consider a matrix with one Jordan block. In this case the subscripts i, j can be dropped.

We introduce a formal operator N, acting on eigenvectors of S. $N b_m = b_{m-1}$ for $m > 0$ and $N b_0 = 0$. The action of S is just $\lambda I + N$. Clearly, multiplication by a constant and N commute. Therefore,

$$S^l x = (\lambda I + N)^l \sum_{j=0}^{n} \beta_m b_m = \sum_{j=0}^{n} \sum_{q=0}^{j} \binom{l}{q} \lambda^{l-q} b_{j-q} \beta_j$$

Changing indexing and the order of summation, we get

$$\sum_{j=0}^{n} \sum_{q=0}^{j} \binom{l}{q} \lambda^{l-q} b_{j-q} \beta_j = \sum_{m=0}^{n} \sum_{q=0}^{m} \binom{l}{m-q} \lambda^{l-m+q} b_q \beta_m = \sum_{q=0}^{n} b_q \sum_{m=0}^{n-q} \binom{l}{m} \lambda^{l-m} \beta_{m+q}$$

Thus,

$$S^l x = \lambda^{l-n} \sum_{q=0}^{n} b_q \left(\sum_{m=0}^{n-q} \binom{l}{m} \lambda^{n-m} \beta_{m+q} \right) \tag{2.23}$$

In the general case,

$$S^l x = \sum_{i=0}^{J} \sum_{j=1}^{P_i} \lambda_i^{l-n_j^i} \sum_{q=0}^{n_j^i} b_{jq}^i a_{jq}^{il} \tag{2.24}$$

where $a_{jq}^{il} = \sum_{m=0}^{n_j^i - q} \binom{l}{m} \lambda^{n_i^j - m} \beta_{j(m+q)}^i$.

Estimating $|a_{jq}^{il}|$, we get

$$|a_{jq}^{il}| \leq \max_m \beta_{jm}^i \sum_{m=0}^{n_j^i - q} \binom{l}{m} \lambda^{n_j^i - m} \leq \max_m |a_{jm}^i| \sum_{m=0}^{n_i^j - q} \binom{l}{m}$$

for $|\lambda_i| \leq 1$.

$$|a_{jq}^{il}| \leq \max_m |\beta_{jm}^i| l^{n_j^i - q + 1} = O(l^{n_j^i - q + 1})$$

Finally,

$$S^l x = \sum_{i=0}^{J} \sum_{j=0}^{P_i} \lambda_i^{l-n_j^i} \sum_{q=0}^{n_j^i} b_{jq}^i O(l^{n_j^i - q + 1}) \tag{2.25}$$

In certain cases we have to use bases consisting of real vectors. Generalized eigenvectors corresponding to complex eigenvalues can be complex. As the matrix is real, complex eigenvalues come in conjugate pairs and the same is true for complex eigenvectors. Further, if the decomposition (2.23) is written for a real vector x, the coefficients of a pair of conjugate vectors of the Jordan basis are complex conjugate.

Let $\lambda = |\lambda| \exp(i\varphi_\lambda)$, $\beta_{m+q} = |\beta_{m+q}| \exp(i\varphi_{m+q})$ and $b_q^j = |b_q^j| \exp(i\psi_q^j)$, where b_q^j is j-th component of b_q.

Using Equation (2.24) for a matrix with 2 Jordan blocks corresponding to λ and $\bar{\lambda}$, we obtain an analog of (2.23).

$$[S^l x]^j = 2|\lambda^{l-n}| \sum_{q=0}^{n} |b_q^j| \sum_{m=0}^{n-q} \binom{l}{m} |\lambda^{n-m}| |\beta_{m+q}| \cos(\varphi_\lambda (l-m) + \varphi_{m+q} + \psi_q^j) \tag{2.26}$$

This decomposition of x is real.

2.4.4 Convergence Criterion for Subdivision

The idea of layers introduced in Section 2.4.1 can be used to prove a criterion for convergence of subdivision. This criterion is very similar to Theorem 3.2 [55] by Reif. We do not make any assumptions about the range of p and f — it can be $\mathbf{R}^n$ or $\mathbf{C}^n$. For the second part of the lemma, we use a fact that will be proven in Section 3.13.

Theorem 2.12. *Suppose* $\mathcal{S}$ *converges on the regular complex.* $\mathcal{S}$ *converges on* $\mathcal{R}_k$ *if and only if the eigenvalues of the subdivision matrix* S *have magnitudes less than one, except* $\lambda_0 = 1$*, which has a single cyclic subspace of size 1 with a constant eigenvector.*

Proof. Sufficiency. Suppose $\lambda_0 = 1$, and all other eigenvalues satisfy $|\lambda_i| < 1$. By assumptions of the lemma, λ_0 has a single eigenvector which is constant on N_L. Consider a sequence of points $s_i \in \mathcal{R}_k$ such that $\lim_{i\to\infty} s_i = 0$. By Lemma 2.9, the limit function $f[p](y)$ is defined everywhere except 0. For a triangle T of $\mathcal{R}_k$ such that $\mathrm{Loc}^j|T|$ doesn't contain 0,

$$f[p](y)\,\big|_{|T|} = \sum_{v\in \mathrm{Ctrl}^j|T|} p(v)\varphi_v(y)$$

Suppose that for all v $\|p(v) - a\|_2 < \epsilon$ for some a. For any y, $\|\sum_v p(v)\varphi_v(y) - a\|_2 = \|\sum_v (p(v) - a)\varphi_v(y)\|_2$ by affine invariance.

Hence,

$$\left\|\sum_v p(v)\varphi_v(y) - a\right\|_2 \le \epsilon \sum_v |\varphi_v(y)| < \epsilon C \tag{2.27}$$

where $C = \max_{y\in|T|}\sum_v |\varphi_v(y)|$. C is finite, because $\varphi_v(y)$ are continuous and $|T|$ is compact. Clearly, (2.27) is also true for any union of triangles T.

Consider the sequence p^j, $p^j \in \mathcal{P}(N^j_{2(L+1)+M})$. The control set $\mathrm{Ctrl}(\left|Lr^j\right|)$ is contained in $\mathcal{P}(N^j_{2(L+1)+M})$: the limit function restricted to $\left|\mathrm{Lr}^j\right|$ depends only on the values of p^j.

There is a matrix S_{lr} such that $S_{lr}p^j = p^{j+1}$. As the subdivision matrix takes $\tilde{p}^j = p^j|_{N_L}$ to $\tilde{p}^{j+1}$, eigenvalues of S_{lr} are also eigenvalues of S and have to satisfy the conditions of the theorem. Let b^i_{jr}, $i \in \{0\ldots J\}$, $j \in \{1\ldots P_i\}$, $r \in \{0\ldots n^i_j\}$, be the the Jordan basis of S_{lr}. Write

$$p^j = \beta_0 b_0 + \sum_{i=1}^{J}\sum_{j=1}^{P_i} \lambda_i^{l-n^j_i} \sum_{q=0}^{n^j_i} b^i_{jq} O(l^{n^i_j - q+1}),$$

using (2.25) and $\lambda_0 = 1 > |\lambda_1|$.

Thus, as $j \to \infty$ $p^j \to \beta_0 b_0$; in particular, $\lim_{j\to\infty} p^j(0) = f[p_0](0) = \beta_0$

For any $\epsilon > 0$ there is l such that $\|s_j\|_2 < \epsilon$ for $j > l$. Therefore, for any n there is l such that $s_j \in \cup_{i=n}^{\infty} \left|\mathrm{Lr}^i\right|$ for $j > l$, unless $s_j = 0$.

Choose l' so that $\left\|p^j - \beta_0 b_0\right\|_\infty < \delta/C$, for a given δ. Then $\|f[p](s) - \beta_0\|_2 < \delta$ for $s \in \mathrm{Lr}^{n'}$ for $n' > l'$; if $s_j = 0$, this is also true.

We conclude that $f[p](s_j)$ converges to β_0, and the scheme converges on $\mathcal{R}_k$.

Necessity. In the previous section, we have already proved that the eigenvalue 1 should be a non-trivial eigenvalue of the matrix and have a single cyclic subspace of size 1 with constant eigenvector.

Suppose $|\lambda_i| > 1$ or $|\lambda_i| = 1$, but $\lambda_i \neq 1$; clearly, $S^m b_{10}^i$ does not converge; and the scheme is not convergent. □

2.4.5 Extension of the Eigenbasis Functions

Sometimes it is more convenient to consider functions defined on the plane rather than on U_1. In this section we show that any eigenbasis vector b_{jr}^i can be extended to the whole k-regular complex $\mathcal{R}_k$ in such a way that when restricted to any neighborhood N_m, $m \geq L$, it is an eigenbasis vector for the subdivision matrix S_m mapping $\mathcal{P}(N_m)$ to itself. Consequently, any eigenbasis function can be extended to the whole plane and will satisfy scaling relations everywhere.

In this lemma we omit the subscripts i, j for b_{jr}^i and f_{jr}^i.

Lemma 2.13. *Any set of eigenbasis functions f_r, $r = 0 \ldots n$ defined on U_1 can be extended in a unique way to the whole plane; the extended functions satisfy the scaling relations*

$$\begin{aligned} f_r(\frac{y}{2}) &= \lambda f_r(y) + f_{r-1}(y), \textit{for } r > 0 \\ f_0(\frac{y}{2}) &= \lambda f_0(y) + f_0(y) \end{aligned} \tag{2.28}$$

Proof. Throughout this proof we will assume the standard identification of $\mathcal{R}_k$ and $\mathcal{R}_k^1$.

Consider the set of eigenvectors b_r, $r = 0 \ldots n$. If the localization size of the scheme is L, for any neighborhood N_p, $p \geq L$, the values on N_{2p-L} can be computed using only the values from $\mathcal{P}(N_p)$;

We extend the vectors b_r to the whole complex $\mathcal{R}_k$ recursively. Suppose we have extension $b_r^{[p]}$ to N_p, $p \geq L$. It can be extended in arbitrary way to the vector $b_r^{\mathbf{ext}}$ defined on the whole complex $\mathcal{R}_k$.

Note that $S[\mathcal{R}_k]b_r^{\text{ext}}$ restricted to N_{2p-L} depends only on the values of b_r^{ext} on N_p, i.e., only on $b_r^{[p]}$.

Define

$$\widehat{b}_r = S[\mathcal{R}_k]b_r^{\text{ext}} \,\big|_{N_{2p-L}}$$

$\widehat{b}$ can be extended in arbitrary way to the whole complex $\mathcal{R}_k$ and considered to be an element of $\mathcal{P}(\mathcal{R}^k)$. Let S^n be the subdivision matrix for N_n, $n \geq p$. Then

$$S^{2p-L}\widehat{b}_r = S[\mathcal{R}_k]\widehat{b}_r \,\big|_{N_{2p-L}}$$

depends only on the values of $\widehat{b}_r$ on N_p. By construction of $\widehat{b}_r$ and the assumption of induction

$$\widehat{b}_r \,\big|_{N_p} = S^p b_r^{[p]} = \lambda b_r^{[p]} + b_{r-1}^{[p]}$$

Define

$$\tilde{b}_r = \sum_{s=0}^{r} (-1)^s \frac{1}{\lambda^{s+1}} \widehat{b}_{r-s}$$

As $\widehat{b}_r$, $\tilde{b}_r$ is defined on N_{2p-L} which is larger than N_p. A direct check shows that $\tilde{b}\,\big|_{N_p} = b_r^{[p]}$.

At the same time,

$$S^{2p-L}\tilde{b}_r = \sum_{s=0}^{r-1} (-1)^s \frac{1}{\lambda^{s+1}} \left(\lambda \widehat{b}_{r-s} + b_{r-s-1}\right) + \frac{(-1)^r}{\lambda^r}\widehat{b}_0 = \lambda \tilde{b}_r + \tilde{b}_{r-1}$$

Therefore, $\tilde{b}_r$ extends $b_r^{[p]}$ to N_{2p-L} and satisfies the same relation with respect to S^{2p-L} as $b_r^{[p]}$ satisfies with respect to S^p.

By induction, we extend b_r to a vector $b_r^{[\infty]}$ defined on the whole plane and satisfying

$$S[\mathcal{R}_k]b_r^{[\infty]} = \lambda b_r^{[\infty]} + b_{r-1}^{[\infty]} \tag{2.29}$$

The argument of Theorem 2.11 still applies, and the limit functions $f_r^\infty(y)$ generated by subdivision from b_r satisfy scaling relations (2.28).

We have established existence of the extension, now we prove that it is unique.

For any point y and $p \geq n$

$$f_r^\infty\left(\frac{y}{2^p}\right) = \sum_{s=0}^{r} \binom{s}{p} \lambda^{p-s} f_{r-s}^\infty(y)$$

For sufficiently large p, $y/2^p$ is in U_1, and $f^\infty(y/2^p) = f(y/2^p)$. Then $f_r^\infty(y)$ can be found as a solution of a triangular linear system with non-zero entries on the diagonal. The solution is unique, hence the values of f_r^∞ are uniquely defined by the scaling relations.

□

Chapter 3 Smoothness of Stationary Subdivision

In this chapter we establish criteria for tangent plane continuity and C^k-continuity of subdivision schemes at extraordinary points. The chapter is subdivided into four parts.

Part I establishes the framework for discussing smoothness of subdivision. In Section 3.4 we show that any subdivision surface near an extraordinary point can be represented as a projection of a higher-dimensional space $\mathbf{R}^p$ into $\mathbf{R}^3$. We will call this surface the *universal surface*. We show that a subdivision scheme is tangent plane or C^k-continuous if and only if the universal surface is tangent plane or C^k-continuous.

In Part II we discuss the criteria for tangent plane continuity. This is the heart of the theory presented in this chapter. In Section 3.5 we show how tangent plane continuity of the universal surface is related to the eigenstructure of a matrix derived from the subdivision matrix. We call this matrix the *tangent subdivision matrix*. The eigenstructure of this matrix is determined by the eigenstructure of the subdivision matrix; the relation between the two structures is discussed in Section 3.12. These observations lead us to the necessary and sufficient conditions for geometric smoothness of subdivision in terms of the eigenstructure of the subdivision matrix and properties of the eigenbasis functions.

We introduce two maps: the parametric map, which gives a local parameterization of almost all surfaces generated by subdivision, and characteristic map, which is a self-similar map that can be used to establish properties of the parametric map.

Theorem 3.4 is the most general result of this part. Corollary 3.5 and equivalent Theorem 3.7 provide an characterization of an important class of geometrically smooth schemes.

In Part III we consider C^1 and C^k continuity. In Section 3.10 we show how to augment the conditions for geometric smoothness to ensure that the surface is C^1-continuous. We formulate the conditions for C^k-continuity, which easily follow once the conditions for C^1-smoothness are established.

Part IV is a collection of technical proofs that were omitted in the first three parts to improve presentation.

Figure 3.1 shows the structure of this chapter.

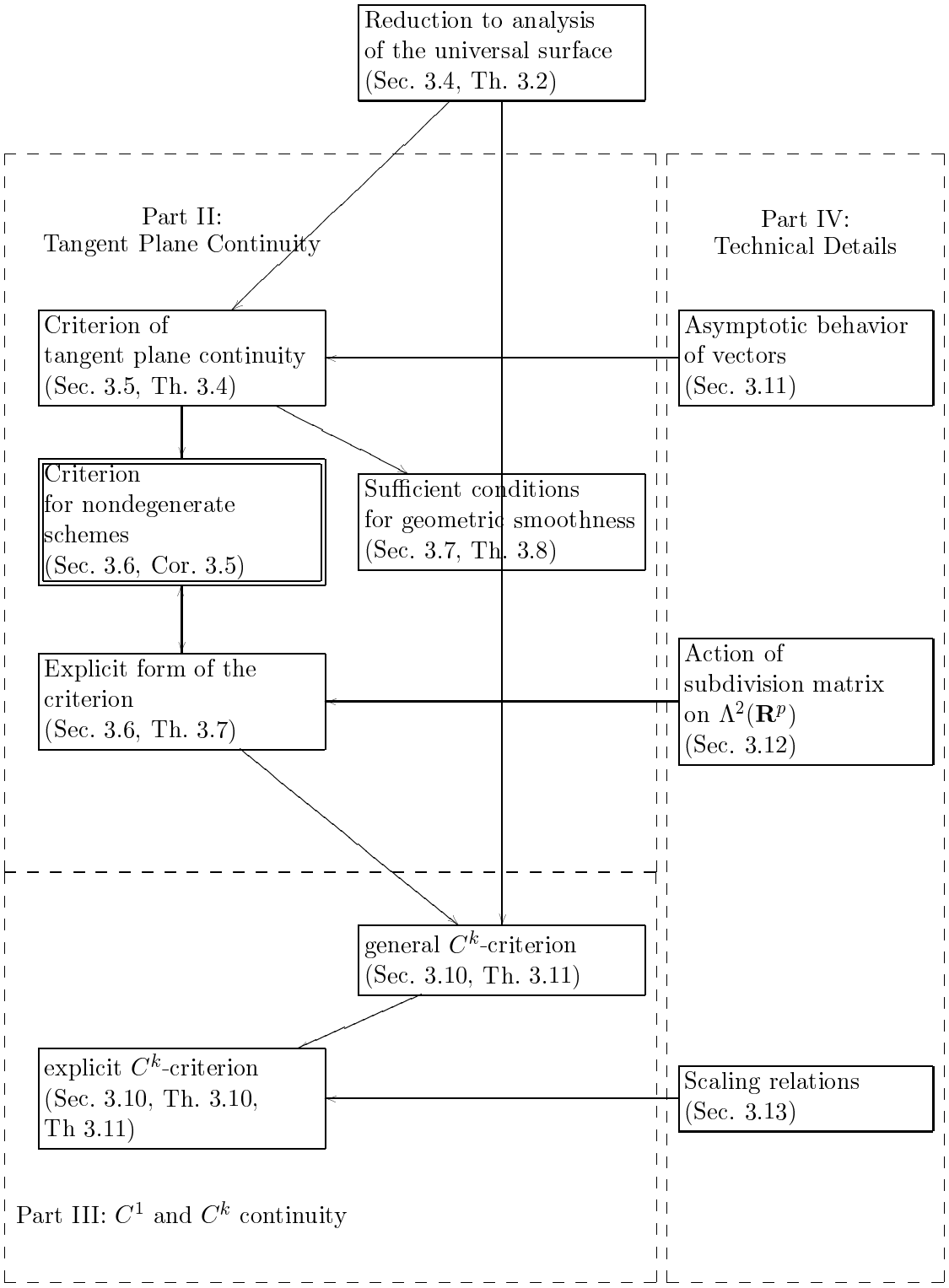

Figure 3.1: Relations between the main results presented in this chapter.

Part I: Preliminaries

3.1 Definitions of Tangent Plane Continuity and C^k-continuity

To avoid ambiguity, we describe the definitions of tangent plane continuity and C^k-continuity that we are going to use in detail, and provide motivations for the choices that we have made. The discussion in this section is quite general and applies to a variety of parametric surfaces rather than only surfaces constructed using stationary subdivision.

3.1.1 C^1-continuous Surfaces

The simplest definition of a C^1-continuous surface A is a "locally C^1-continuous two-dimensional" subset of $\mathbf{R}^3$: if we take a small ball B centered at any point of A, and look at the part of A enclosed in the ball B, then it can be obtained from a disk in the plane by a C^1-continuous deformation. More formally, there is a C^1 map p from a disk D in the plane to $A \cap B$ with Jacobi matrix of maximal rank. We will call surfaces satisfying this condition *simple C^1-continuous surfaces*. We will call maps with Jacobians of maximal rank regular. The definition is illustrated in Figure 3.2. Surfaces satisfying this definition are 2-dimensional manifolds embedded in $\mathbf{R}^3$.

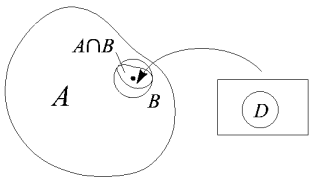

Figure 3.2: Definition of a simple C^1-continuous surface

However, this definition is not convenient for reasoning about surfaces obtained using subdivision and parametric surfaces in general; (recall that a subdivision surface by construction is parameterized over its topological complex). The problems with the definition above can be seen best from an example, such as the surface depicted in Figure 3.3. If we regard the surface in Figure 3.3 as a subset of $\mathbf{R}^3$, clearly point A does not have a neighborhood that can be deformed into a disk. But we can look at this surface in a different way. Suppose we start with a flat sheet, and then deform it into the shape shown in the figure.

In this case, we can think about the point A as being two separate points of the sheet that happen to coincide for this particular deformation. We can still consider the surface to be C^1-continuous: we can take a small neighborhood of A on the original sheet and see that its image under the deformation can be parameterized with a regular map over a disk.

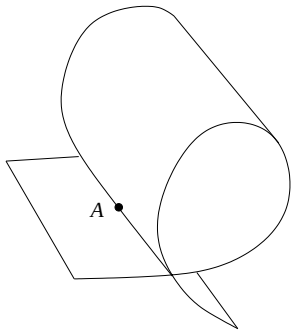

Figure 3.3: A surface with a self-intersection.

Note that we needed the original sheet and the deformation to separate the parts of the surface that intersect at A. While they are close in $\mathbf{R}^3$, from the point of view of the surface they are far away. The parameter domain (the sheet) is used to define the neighborhoods of all points. It need not be a subset of $\mathbf{R}^3$: we can use any topological space. We only need it to define neighborhoods on the surface independently from the way the surface is mapped into $\mathbf{R}^3$. In the case of subdivision surfaces we already have a convenient domain: the topological complex $M = |K|$. A subdivision surface is the domain M together with a map f from M to $\mathbf{R}^3$. This leads us to the following definition of C^1-continuity and C^k-continuity:

Definition 3.1. *Consider a surface (M, f) where M is a topological space, and f is a map $f : M \to \mathbf{R}^3$. This surface is* **C^1-continuous** *if for any point $x \in M$ there is a neighborhood $U_x \subset M$ such that there is a regular parameterization of $f(U_x)$ over a disk in the plane, that is, a map $p : D \to f(U_x) \subset \mathbf{R}^3$ which is C^1 and has Jacobi matrix of maximal rank (2). If the parameterization p can be chosen to be C^k, then the surface is C^k-continuous.*

The mappings that are used in this definition are shown in Figure 3.4.

Note that parameterization p and the map f are not necessarily related: in fact, for f C^1-continuity may not even be defined, because we assume very little about M: it only has to have a system of neighborhoods defined for each point. In contrast, the domain of p is a

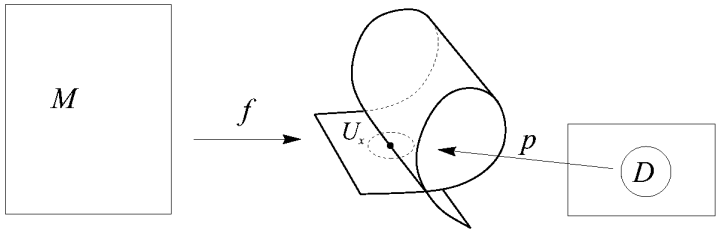

Figure 3.4: Definition of a C^1-continuous surface.

disk in the plane, which inherits the metric of the plane. We use f to separate the surface into small pieces; then we parameterize each piece p separately in the same way as we did it for simple surfaces.

Example. The fact that p and f in our definition are unrelated leads to some complications. Consider, for example, the map from the unit disk D in x, y plane to the same disk defined by $x' = x^2 - y^2, y' = 2xy$. If we identify the plane with the complex plane, this is simply the map $f(z) = z^2$. It is easy to check that the map is onto; thus, $f(D) = D$. We can look at the pair (D, f) as the pair (M, f) in the definition above. This map is not one-to-one: f "wraps" the disk around itself twice, and has a singularity at zero. However, clearly there is a nice regular parameterization of $f(D) = D$: we can take the identity as a parameterization. Although f is not one-to-one anywhere, we still get a C^1-continuous surface. If we are trying to determine if a subdivision surface (M, f) is C^1-continuous by constructing a C^1-continuous parameterization p, our example shows that f might be a bad starting point, which makes analysis of subdivision surfaces somewhat more difficult.

An alternative to our definition is to require p to be a mapping of the form $f \circ p'$, for some $p' : D \to M$. This approach allows constructing parameterizations from f, and automatically excludes cases when f locally is not one-to-one. While being somewhat easier to use, this definition would give f a special role in determining C^1-continuity: returning to the example discussed above, according to the alternative definition the parameterized disk may be not a C^1-continuous surface. We use the weaker definition to include such cases.

3.1.2 Constructing C^1-Continuous Subdivision Schemes

Typically, subdivision schemes are constructed starting with the rules for the regular complex. These rules are chosen so that if we identify each triangle of the topological complex with a triangle in the plane using a mapping p, then the mapping $f \circ p$ is C^1-continuous in the interior of the triangle. Moreover, if we use the same rules for refining the boundaries of the triangles, it is easy to construct C^1 parameterizations of the same type near any point of the edge except the endpoints. Note that continuously differentiable parameterization does not guarantee yet that the surface is C^1-continuous in the sense defined above: the parameterization may be C^1 but singular, i.e., have Jacobi matrix of rank 1 or 0. It is possible to show that this problem cannot be completely avoided due to linearity of subdivision. However, for a good choice of subdivision rules on the regular part of the complex (for example, spline subdivision rules or interpolating subdivision rules) we can ensure that the surfaces are singular only for a nowhere dense set of configurations of control points.

Assume that the control points are chosen in such a way that the surface is C^1-continuous everywhere except the corners of the triangles of the topological complex M, i.e., vertices of the complex. It is easy to see that we can construct a parameterization of a part of the surface adjacent to a vertex v of M (to be more precise, of the union of images $f(T)$ of all triangles T of M adjacent to v) which will be C^1-continuous and nonsingular everywhere except at the vertex v. This parameterization is described in greater detail in Section 3.2. Thus, we are particularly interested in surfaces which are known to be locally C^1-continuous everywhere except at a set of isolated points (extraordinary vertices).

It is important to note that the for C^1-continuity of the surface the parameterization of Section 3.2 need not be regular or even C^1-continuous at extraordinary vertices; moreover, this parameterization need not even be one-to-one.

3.1.3 Tangent Plane Continuity

It turns out to be useful to split the task of establishing C^1-continuity of a subdivision surface at extraordinary vertices into two steps: first, check the existence of a tangent plane, then determine if the projection into the tangent plane is injective. To make this idea formal, we need to describe the tangent planes as functions on the surface more precisely.

Recall that the tangent plane is the span of all tangent vectors, which are defined as

directional derivatives of the parameterization. If regular parameterizations are defined everywhere except a set of isolated points, so are tangent planes. In $\mathbf{R}^3$, a tangent plane at a given point is uniquely determined by its unit normal; however, each tangent plane has two unit normals. We use the regular parameterization near the extraordinary vertex, to guarantee a consistent choice of the orientation of normals: the normal can be computed as a cross product of directional derivatives in the parametric domain. In this case we can identify each tangent plane with one of its unit normals. This leads us to the following definition of tangent plane continuity:

Definition 3.2. *Let D be the unit disk in the plane. Suppose a surface (M, f) in a neighborhood of a point $x \in M$ is parameterized by $p : D \to \mathbf{R}^3$, which is regular everywhere except 0, and $p(0) = f(x)$. Let $n(y)$, $y \in D$ be the unit normal defined as $[\frac{\partial p}{\partial x_1} \times \frac{\partial p}{\partial x_2}]_+$, where (x_1, x_2) is a coordinate system in the plane of the disk D and $[\cdot]_+$ denotes normalization. The surface is called* **tangent plane continuous** *at x if the limit $\lim_{y \to 0} n(y)$ exists.*

The orientation of the normals is a subtle question. It is possible to characterize tangent planes in such a way that no orientation is specified; then the limit plane might exist, even if the limit of consistently oriented normals does not. One can show that such surfaces will not be C^1-continuous (Definition 3.1); as we regard tangent plane continuity as an intermediate stage on the way to C^1-continuity, we choose somewhat stronger definition including orientation.

Tangent plane continuity is clearly a weaker notion than C^1-continuity. A typical example of a surface, which is not C^1-continuous but is tangent plane continuous, is shown in Figure 3.5. The local structure of the surface near the singularity can be very complicated; this is the reason why requiring just tangent plane continuity is not sufficient.

Tangent plane continuity in $\mathbf{R}^p$. A surface in $\mathbf{R}^3$ is tangent plane continuous at a point, if the normals to the surface have a limit at that point. In $\mathbf{R}^3$, there is a one-to-one correspondence between planes and their normals. This is not the case for $p > 3$: the orthogonal space to a plane is not one-dimensional. A normal to a plane can be obtained by computing the cross product of any two independent vectors in the plane. The crucial property of the normal is that up to a constant, it does not depend on the choice of vectors. The cross product has a well-known generalization to $\mathbf{R}^p$, called the wedge product, which we describe here for completeness.

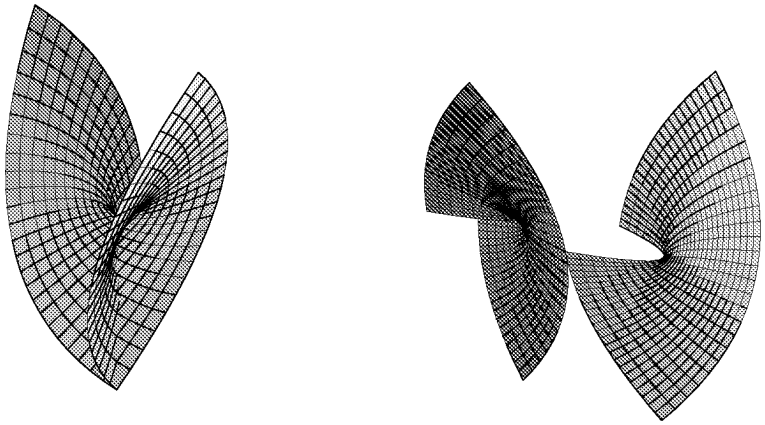

Figure 3.5: Right: parametric surface $(s^2 - t^2, 2st, s + t)$. The complex form of $(s, t) \to (s^2 - t^2, 2st)$ is $z \to z^2$. The surface does not have a regular parameterization around 0. Left: two sheets of the surface with incision along the ray $s = 0$. One of the sheets is displaced.

The key to generalizing the definition of a normal is the relation between normals to a surface and Jacobians: each component of the normal is the Jacobian of a pair of coordinate functions, assuming that the coordinate functions are C^1-continuous and at least one of the three pairwise Jacobians is not zero. This is just a special case of the general observation that the components of the normal to a plane defined by vectors t^1 and t^2 are determinants of two-by-two matrices

$$n_k = \begin{pmatrix} t_i^1 & t_j^1 \\ t_i^2 & t_j^2 \end{pmatrix}, \quad (i, j, k) \in \{(2, 3, 1), (3, 1, 2), (1, 2, 3)\}$$

Once we have described the normal in this way, we can see that given a plane in $\mathbf{R}^p$, we can consider the vector of Jacobians for all possible pairs of components, which will have length $p(p-1)/2$. Each such component is invariant with respect to planar affine transformations, hence the whole vector is invariant. For two vectors $x^1, x^2 \in \mathbf{R}^p$ this vector of determinants is called the wedge product and denoted $x^1 \wedge x^2$. As elements of $\mathbf{R}^{p(p-1)/2}$, such products have well-defined sums, but not every element of $\mathbf{R}^{p(p-1)/2}$ corresponds to a wedge product for $p > 3$ (example: $e_1 \wedge e_2 + e_3 \wedge e_4$, where $e_i, i = 1 \ldots 4$, are the basis vectors in $\mathbf{R}^p$). Although our definition clarifies how wedge products generalize normals, a

more natural and invariant definition is the space of all antisymmetric bilinear functions of two vectors from $\mathbf{R}^p$. It is straightforward to check that these spaces are isomorphic. The space of wedge products of vectors is denoted $\Lambda^2(\mathbf{R}^p)$.

In the three-dimensional space a surface is tangent plane continuous at a point if the normals have a limit at that point. Using the wedge product, we can define tangent plane continuity is $\mathbf{R}^p$ in a way similar to the definition in $\mathbf{R}^3$:

Definition 3.3. *Let D be the unit disk in the plane, M a topological space. Suppose a surface (M, f), $f : M \to \mathbf{R}^p$, in a neighborhood of a point x is parameterized by $g : D \to \mathbf{R}^p$, which is regular everywhere except 0, and $p(0) = f(x)$. The the surface is* **tangent plane continuous** *at the point x if the limit of $[\partial_1 g \wedge \partial_2 g]_+ : D \to \Lambda^2(\mathbf{R}^p)$ exists at that point. $[\cdot]_+$ denotes normalization to unit length.*

The following Proposition shows the relation between tangent plane continuity and C^1-continuity:

Proposition 3.1. *Suppose a surface is tangent plane continuous at zero. Let τ be the limit at zero of the oriented tangent planes, and let $P_\tau : \mathbf{R}^p \to \mathbf{R}^2$ be the projection of $\mathbf{R}^p$ onto the plane τ. Then the surface is C^1-continuous if and only if there is a neighborhood D of zero, such that P_τ restricted to $f(D)$ is injective.*

Proof. Necessity is obvious; we prove sufficiency. Suppose P_τ is injective on $f(D)$. We are going to show that the inverse of $P_\tau|_{f(D)}$ is regular as a function on the tangent plane in a neighborhood of $f(0)$.

By assumption, there is a parameterization p of the surface defined on a neighborhood of zero in the plane, which is regular away from zero, and the limit $\lim_{y\to 0}[\partial_1 p(y) \wedge \partial_2 p(y)]_+ = u_0$ exists. Choose the basis in $\mathbf{R}^p$ in such a way that $u_0 = e_1 \wedge e_2$. As any nondegenerate projections into a plane differ by a nondegenerate affine transformation which does not affect injectivity, we can assume that $P_\tau(a) = (a^1, a^2)$ for any $a \in R^p$, if $a = \sum_i a^i e_i$. Let $p^i(y)$ be the i-th coordinate function of p. Let $\Phi(y) = (p^1(y), p^2(y))$. Note that the components of $\partial_1 p(y) \wedge \partial_2 p(y)$ are the Jacobians of the pairs of coordinate functions $J[p^i, p^j]$. As $\lim_{y\to 0}[\partial_1 p(y) \wedge \partial_2 p(y)]_+ = e_1 \wedge e_2$, for a sufficiently small neighborhood of zero U $(\partial_1 p(y) \wedge \partial_2 p(y), e_1 \wedge e_2) > 0$; but this component of $\partial_1 p(y) \wedge \partial_2 p(y)$ is exactly the Jacobian of Φ. We conclude that Φ is regular on U away from zero.

Therefore, for any point $x \in U$, $x \neq 0$, there is a neighborhood U_x of x such that Φ is invertible.

Also note that $[\partial_1 p(y) \wedge \partial_2 p(y)]_+ = \partial_1 p(y) \wedge \partial_2 p(y) / \left\|\partial_1 p(y) \wedge \partial_2 p(y)\right\|$. Writing the components of the equation $\lim_{y\to 0}[\partial_1 p(y) \wedge \partial_2 p(y)]_+ = e_1 \wedge e_2$ explicitly, we obtain

$$\lim_{y\to 0} \frac{J[\Phi]}{\left\|\partial_1 p(y) \wedge \partial_2 p(y)\right\|} = 1 \tag{3.1}$$

$$\lim_{y\to 0} \frac{J[p^i, p^k]}{\left\|\partial_1 p(y) \wedge \partial_2 p(y)\right\|} = 0 \quad \text{for } (i,k) \neq (1,2) \tag{3.2}$$

combining (3.1) with (3.2) we obtain

$$\lim_{y\to 0} \frac{J[p^i, p^k]}{J[\Phi]} = 0 \quad \text{for } (i,k) \neq (1,2)$$

Let $P_\tau|_{f(D)} = \pi$. As $\Phi = P_\tau \circ p$, then on U_x we can write $\pi = p \circ \Phi^{-1}$. Observe that $\partial_1\pi \wedge \partial_2\pi = J[\Phi]^{-1}\partial_1 p \wedge \partial_2 p$. Let M_J be the Jacobi matrix of Φ.

Note that the we can write the vector $\left[\frac{J[p^i,p^k]}{J[\Phi]}, \frac{J[p^i,p^k]}{J[\Phi]}\right]^T$ as

$$\frac{1}{J[\Phi]} \begin{bmatrix} J[p^i, p^1] \\ J[p^i, p^2] \end{bmatrix} = M_J^{-1} \begin{bmatrix} \partial_1 p^i \\ \partial_2 p^i \end{bmatrix} \tag{3.3}$$

which is exactly the gradient $[\partial_1\pi^i\, \partial_2\pi^i]^T$ of the i-th component of π. As we have observed, each component of the left-hand side of (3.3) converges to zero for $i \neq 1, 2$. For $i = 1, 2$ the components of π are just linear functions away from zero and their gradients have limits $[1, 0]$ and $[0, 1]$ at zero.

If the limit of a derivative exists at zero, the derivative itself exists at zero and is continuous. We conclude that π is a regular parameterization of the surface. □

3.1.4 C^1-continuous Subdivision Schemes

It would be natural to say that a subdivision scheme is C^1-continuous if all surfaces generated by a scheme are C^1-continuous. However, this requirement is too restrictive: in general, it is impossible to construct schemes of this type; even for spline surfaces we can find configurations of control points that lead to non-C^1-continuous surfaces. We adopt a

weaker notion of C^1-continuity of a scheme. Recall that the collections of control values for a given complex can be regarded as elements of a linear space $\mathcal{P}(V)$. As we consider only local schemes, it is sufficient to consider only finite complexes. For such complexes, the spaces $\mathcal{P}(V)$ are finite-dimensional, and we can define a distance on $\mathcal{P}(V)$ identifying it with a Euclidean space. We will consider a subdivision scheme C^1-continuous on a complex K if it generates C^1 continuous surfaces for all initial values $p \in \mathcal{P}(V)$ exclusing a nowhere dense subset of $\mathcal{P}(V)$.

This approach introduces a new problem. For a vertex v, $\mathrm{Ctrl}(N_1(v_K))$ be the set of vertices $w \in V$ such that the values of the limit function $f[p]$ on $|N_1(v, K)|$ depend only on the vertices from $\mathrm{Ctrl}(N_1(v, K))$. Recall that we reduce the analysis of subdivision on arbitrary complexes to analysis on k-regular complexes using an isomorphism ρ between $N_L(v, K^j)$ and $N_L(0, \mathcal{R}_k)$ for some j. Clearly, the values $p^j(v)$ on $N_L(v, K^j)$ can be computed from the values $p^0(v)$ on $\mathrm{Ctrl}(N_1(v, K))$. By linearity of subdivision, there is a matrix (not necessarily square) A such that $p^j(v) = Ap^0(v)$. If the rank of A is less than $p + 1$, then the dimension of the space of $p^j(v)$ on $N_L(v, K^j)$ is less than the maximal dimension $p + 1$ and it can be identified with a proper subspace $\tilde{\mathcal{P}}$ of the space $\mathcal{P}_k$ of functions on the vertices of $N_L(0, \mathcal{R}_k)$, rather than with the whole space. The simplest example of such complex is a tetrahedron: the dimension of $\tilde{\mathcal{P}}$ cannot be more than 4, but even for Loop scheme $p = 9$ for a vertex of valence 3. It might happen that the subspace $\tilde{\mathcal{P}}$ is contained inside the nowhere dense subset of $\mathcal{P}_k$ for which subdivision generates surfaces that are not C^1-continuous. We will call complexes for which this occurs *constraining.* It is difficult to characterize constraining complexes for arbitrary schemes. We simplify our task by excluding such complexes.

This leads us to the following definition:

Definition 3.4. *A subdivision scheme is* C^1**-continuous** *on a complex K if it generates C^1-continuous surfaces for any choice of control points on K, except a nowhere dense set of configurations. A subdivision scheme is C^1-continuous, if it is C^1-continuous for any non-constraining complex.*

Tangent plane continuity of a subdivision scheme is defined in a similar way. This definition allows us to consider only subdivision on k-regular complexes. If a subdivision scheme is C^1-continuous according to our criteria additional analysis is needed to identify

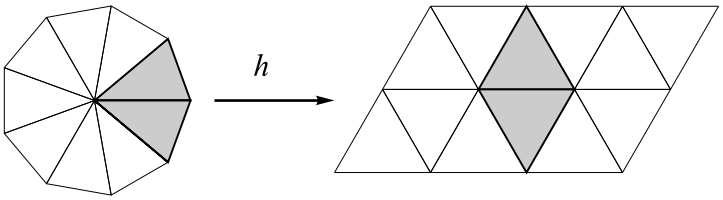

Figure 3.6: Mapping of a pair of adjacent triangles of U_1 to two adjacent triangles of the regular complex.

constraining complexes.

3.2 Singular Parameterizations and a Nondegeneracy Condition

We have already mentioned that any subdivision surface has a natural parameterization near extraordinary vertices, which is C^1-continuous everywhere except the extraordinary point itself. In this section we describe this parameterization in greater detail. This construction is similar but not identical to the complex-analytic structure on complexes described by Duchamp and others [15].

Consider the 1-neighborhood U_1 of the extraordinary vertex of the k-regular complex. This neighborhood is identified with a regular k-gon in the plane centered at zero. The surface $f : U_1 \to \mathbf{R}^3$ defined by subdivision is piecewise C^1-continuous on U_1: it is C^1-continuous in the interior of the triangles of U_1 and may be not C^1-continuous on the boundaries between triangles. However, assuming C^1-continuity of the scheme on the regular complex, we can map any pair of adjacent triangles to two adjacent triangles of the regular complex using a piecewise linear mapping h (Figure 3.6). Then $f \circ h^{-1}$ has to be C^1 on the interior of the quadrilateral formed by the two triangles of the regular complex.

Note that any deformation of the two triangles of U_1 that agrees with h in the limit near the boundary between the two triangles can be used instead. We describe a mapping κ defined on the whole neighborhood U_1 that agrees with mappings h constructed as above for each pair of adjacent triangles of U.

Each triangle has angle $2\pi/k$ at the extraordinary vertex. The map κ first maps each triangle of U_1, equilateral triangle, then "squeezes" the equilateral triangle back into the an-

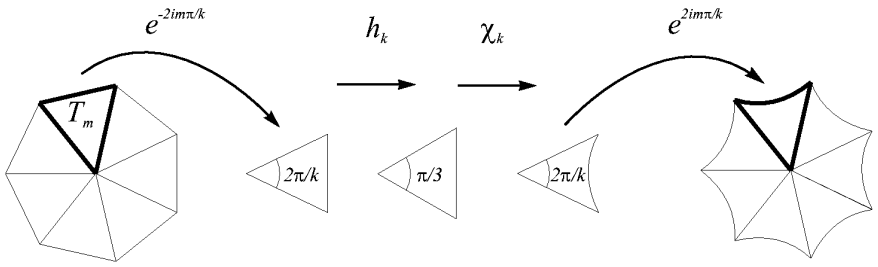

Figure 3.7: Construction of the singular parameterization κ.

gle $2\pi/k$ conformally. Conformality guarantees that near the boundary of any two triangles the map looks exactly like the piecewise linear map h defined above.

Formally, the map κ can be defined as follows; identify the plane with the complex plane. Suppose the vertices of the k-gon identified with U_1 are π/k, $3\pi/k$, ... $(2k-1)\pi/k$. Let H_k be the linear transformation with the matrix

$$\begin{pmatrix} \frac{\sqrt{3}}{2\cos\pi/k} & 0 \\ 0 & \frac{1}{2\sin\pi/k} \end{pmatrix}$$

Let $\chi(z)$ be the map $\chi_k(z) = z^{6/k}$. The image of the equilateral triangle with vertices 0, $e^{\pi/6}$, $e^{-\pi/6}$ is contained in the triangle T_0, with two of the edges adjacent to 0 mapping to the edges of T_0.

Then on the triangle T_m with vertices 0, $(2m-1)\pi/k$, $(2m+1)\pi/k$ the map κ can be defined as

$$\kappa(z) = e^{-2im\pi/k}\left(\chi_k\left(h_k(e^{2im\pi/k}z)\right)\right) \tag{3.4}$$

The structure of the mapping κ is shown in Figure 3.7.

Then for any surface $f : U_1 \to \mathbf{R}^3$ generated by subdivision, the parameterization $f \circ \kappa^{-1}$ is C^1-continuous everywhere except 0.

Nondegeneracy condition. It is straightforward to show that the *parameterization* $f \circ \kappa^{-1}$ *is regular away from zero* for all configurations of control points except for a set of

configurations of measure zero, if the following nondegeneracy condition holds:

Condition A. *For any point y in a triangle $T \subset U_1$ there is a pair of eigenbasis functions g^i_{jr}, g^k_{lt} such that the Jacobian $J[g^i_{jr}, g^k_{lt}]$ is not zero.*

In this condition we assume that the Jacobian is defined on the boundaries of the triangles using one-sided derivatives. Note that these derivatives need not coincide for adjacent triangles, thus we are talking about Jacobians only for eigenbasis functions restricted to a single triangle. It is easy to check, however, that although the derivatives may not coincide, the Jacobians on different sides of the boundary have to coincide. *This means that we can consider the Jacobian to be defined everywhere on U_1 except zero.*

If Condition A is violated, then there is a point in U_1 such that any surface generated by the subdivision scheme would have a singularity there. Moreover, one can see from scaling relations for wedge products of tangents (3.9), that there will be a singularity arbitrarily close to zero. In this work we consider only schemes satisfying Condition A.

3.3 Subdivision on k-regular Complexes as Projection

To analyze C^1-continuity of a subdivision scheme it is necessary to examine C^1-continuity of all surfaces generated by subdivision. Moreover, we may have to exclude a nowhere dense set of surfaces. The problem can be simplified if we regard any subdivision surface as a projection into $\mathbf{R}^3$ of a single surface in a higher-dimensional space.

We have observed that any surface generated by subdivision on a 1-neighborhood of zero in the k-regular complex is just a linear combination of the eigenbasis functions g^i_{jr}, with coefficients from $\mathbf{R}^3$.

Let $p+1$ be the size of the localization set of U_1, i.e., of N_L. As the eigenbasis function corresponding to the eigenvalue 1 is constant we will assume the corresponding coefficient to be zero, and consider only the surfaces mapping zero to the origin in $\mathbf{R}^3$. For our purposes, it is convenient to consider the coefficients as three vectors x^1, x^2, x^3 from $\mathbf{R}^p$, rather than p vectors from $\mathbf{R}^3$. Let h^i_{jr} be an orthonormal basis in $\mathbf{R}^p$, with one vector per each generalized real eigenvector c^i_{jr} of S. Denote the vector of all eigenbasis functions g^i_{jr} by $\psi(y) : U_1 \to \mathbf{R}^p$, $\psi(y) = \sum_{i,j,r} g^i_{jr}(y) h^i_{jr}$. Then any surface in $\mathbf{R}^3$ is given by

$$((x^1, \psi), (x^2, \psi), (x^3, \psi)) \tag{3.5}$$

Note that by definition of S for any $x \in \mathbf{R}^p$

$$(x, \psi(y/2)) = (Sx, \psi(y))$$

Using the well-known formula for inner products, $(Su, v) = (u, S^T v)$, we get

$$(x, \psi(y/2)) = (x, S^T \psi(y)), \quad \text{for any } x$$

This means that the scaling relations can be jointly written as

$$\psi(y/2) = S^T \psi(y)$$

where S is the subdivision matrix; in our basis, the matrix S is in real normal Jordan form. Although S^T is not in Jordan normal form, a simple permutation of the vectors of the basis will reduce S^T to Jordan normal form; specifically, for a Jordan subspace of a real eigenvalue λ_i of order n_j^i, introduce a new basis $e_{jr}^i = h_{j\, n_j^i - r}^i$, that is, simply reverse the order of the generalized eigenvectors. Similarly, reverse the order of vectors for Jordan subspaces corresponding to pairs of complex conjugate eigenvalues. It is easy to see that in the new basis S^T has Jordan normal form. An important consequence of this fact is that $h_{j n_j^i}^i$ is an eigenvector of S^T. The transposed matrix S^T is more important for most of our constructions, so we will primarily use the basis e_{jr}^i obtained by reordering the vectors of the basis h_{jr}^i.

From (3.5) we can see that any surface generated by subdivision can be regarded as a projection of a unique surface $\psi : U_1 \to \mathbf{R}^p$ into $\mathbf{R}^3$. Rather than studying all such projections, we would like to relate C^1-continuity of projected surfaces to C^1-continuity of the unique surface in $\mathbf{R}^3$, and then establish C^1-continuity criteria directly for ψ. The advantage of this approach is that it becomes unnecessary to consider singular surfaces that are generated for some special directions of projection, as long as this set of projections is known to be nowhere dense.

In the previous section we have described a transformation κ of the parametric domain

U_1 that gives a regular away from zero parameterization of almost any surface generated by subdivision, if Condition A is satisfied. As we will see later, this condition also guarantees that the parameterization of the surface ψ given by $\psi \circ \kappa^{-1}$ is regular away from 0.

Definition 3.5. *For a subdivision scheme S let ψ be the vector of the eigenbasis functions on the 1-neighborhood of zero U_1 in the k-regular complex. The* **universal surface** *is the surface in $\mathbf{R}^p$ defined by $\psi = \psi : U_1 \to \mathbf{R}^p$. Let κ be the transformation of U_1 defined in Section 3.2. Then the universal surface has a parameterization $\varphi = \psi \circ \kappa^{-1} : \kappa(U_1) \to \mathbf{R}^p$, which is C^1-continuous away from 0.*

Note that while we define a unique surface ψ, any surface obtained from ψ by nondegenerate affine transformation of $\mathbf{R}^p$ would also characterize the subdivision scheme completely.

The advantage of using φ rather than ψ is that partial derivatives of φ are well-defined everywhere on $\kappa(U_1)$ except 0. The drawback of using φ is that the scaling relation has a somewhat more complex form; instead of simply scaling the argument by 1/2, we have to use a mapping given by $Ty = \kappa(1/2(\kappa^{-1}(y)))$, $y \in \kappa(U_1)$. Then the scaling relation for φ has the form

$$\varphi(Ty) = S^T \varphi(y) \tag{3.6}$$

Tangent plane continuity of the universal surface. Note that Condition A in the wedge-product notation can be written as $\partial_1\psi(y) \wedge \partial_2\psi(y) \neq 0$ for any y in a triangle T of U_1. As the Jacobian of κ is not zero anywhere including the boundaries of the triangles of U_1, and the composition $\varphi = \psi \circ \kappa^{-1}$ is differentiable on $\kappa(U_1)$, we can restate Condition A as

Condition A. $\partial_1\varphi(y) \wedge \partial_2\varphi(y) \neq 0$ *for any y in $\kappa(U_1)$, $y \neq 0$.*

If we assume Condition A, the parameterization φ is not only continuously differentiable, but is also regular at any point $y \in \kappa(U)$, $y \neq 0$, hence can be used as g in the definition of the tangent plane continuity of the universal surface at 0.

There is a simple formula relating the Jacobian of a mapping $U_1 \to \mathbf{R}^2$ generated by subdivision to the wedge product $\partial_1\psi \wedge \partial_2\psi$. The Jacobian of a mapping $((x^1, \psi), (x^2, \psi)) : U_1 \to \mathbf{R}^2$ can be computed as

$$(x^1, \partial_1\psi)(x^2, \partial_2\psi) - (x^1, \partial_2\psi)(x^2, \partial_1\psi)$$

It is easy to check that this expression can be transformed to the following simple form:

$$J[F[x^1, x^2]] = (x^1 \wedge x^2, \partial_1\psi \wedge \partial_2\psi) \tag{3.7}$$

where the dot product is defined by the standard basis $e^i \wedge e^j, i < j \leq p$, with $e^1 \dots e^p$ being the basis in $\mathbf{R}^p$.

Note that the partial derivatives of ψ are defined only on the interior of the triangles of U_1; on the boundaries only one-sided derivatives exist, excluding zero. However, using the argument that was used to establish C^1-continuity of φ in Section 3.2, we can see that the Jacobian of ψ is continuous on $\dot{U}_1$. Equation 3.7 is valid on the boundaries too, if one-sided derivatives of ψ are used.

Equation 3.7 is useful for relating the normals of surfaces in $\mathbf{R}^3$ defined by subdivision to the normals of the universal surface. For a surface $f[x^1, x^2, x^3] : U_1 \to \mathbf{R}^3$ a normal at any point except zero can be written as

$$N(y) = [(x^2 \wedge x^3, w(y)), (x^3 \wedge x^1, w(y)), (x^1 \wedge x^2, w(y))], \quad y \in \kappa(U) \tag{3.8}$$

where $w(y) = \partial_1\psi(y) \wedge \partial_2\psi(y)$. Note that by assumption $w(y) \neq 0$ for all y. Therefore, for any choice of x^1, x^2, x^3, such that at least 2 vectors are independent, the vector above is not zero and the unit normal can be obtained by normalizing the vector above.

3.4 Reduction to the Analysis of the Universal Surfaces

Our goal is to relate tangent plane continuity and C^k-continuity of the universal surface in $\mathbf{R}^p$ and tangent plane continuity of the subdivision scheme at an extraordinary vertex of valence k. It turns out that the following theorem holds under our assumptions:

Theorem 3.2. *For a subdivision scheme satisfying Condition A to be tangent plane continuous, it is necessary and sufficient that the universal surfaces for all valences are tangent*

plane continuous; for the subdivision scheme to be C^k-continuous, it is necessary and sufficient that the universal surfaces are C^k-continuous.

Proof. Sufficiency is straightforward.

Necessity: tangent plane continuity. Suppose the universal surface for some valence is not tangent plane continuous at zero, that is, the limit $\lim_{y\to 0}[w(y)]_+$ does not exist.

Note that $[w(y)]_+ \in S^{p(p+1)/2-1}$, the unit sphere in $\Lambda^2(\mathbf{R}^p)$. As the sphere is compact, there are two sequences y_s^1, y_s^2, $s \in \mathbf{N}$ such that $\lim_{s\to\infty}[w(y_s^1)]_+ = u_1$, $\lim_{s\to\infty}[w(y_s^2)]_+ = u_2$, and $u_1 \neq u_2$. As the set of all decomposable elements in $\Lambda^2(\mathbf{R}^p)$ is closed, $u_1 = u_1^1 \wedge u_1^2$ and $u_2 = u_2^1 \wedge u_2^2$ for some u_1^1, u_1^2, u_2^1, $u_2^2 \in \mathbf{R}^p$. As both u_1 and u_2 are unit vectors and are not equal, at least 3 out of 4 vectors u_1^1, u_1^2, u_2^1, u_2^2 are linearly independent, or $u_1 = -u_2$.

For the purposes of this proof it is convenient to fix a basis such that $u_j^i, i, j = 1, 2$ are vectors of the basis (if some u_j^i are linearly dependent, we can always modify our choices of u_j^i so that the only ones that are dependent, are equal). We assume that u_1^i, and u_2^i are independent for $i = 1, 2$. If there are three independent vectors, we assume that u_1^1 and u_2^2 are independent. Otherwise, $u_1^1 = u_2^2$ and $u_2^1 = u_1^2$.

First, assume that at least 3 vectors u_j^i are independent. For any basis e_i, $i = 1 \dots p$ in $\mathbf{R}^p$ we can construct a basis in $\Lambda^2(\mathbf{R}^p)$ out of vectors $e_i \wedge e_j$, $i < j$. For the dual basis $\tilde{e}_i$, the corresponding basis $\tilde{e}_i \wedge \tilde{e}_j$ in $\Lambda^2(\mathbf{R}^p)$ is dual to the basis $e_i \wedge e_j$. Let $\tilde{u}_j^i$ be the vectors dual to u_j^i, that is, satisfying $(\tilde{u}_j^i, u_l^k) = \delta(i-k)\delta(j-l)$, and orthogonal to other vectors of the basis.

Consider the surface $[\tilde{u}_1^1, \tilde{u}_2^1 + \tilde{u}_1^2, \tilde{u}_2^2]$. The normals to this surface are given by

$$N(y) = \left[((\tilde{u}_2^1 + \tilde{u}_1^2) \wedge \tilde{u}_2^2, [w(y)]_+), (\tilde{u}_2^2 \wedge \tilde{u}_1^1, [w(y)]_+), (\tilde{u}_1^1 \wedge (\tilde{u}_2^1 + \tilde{u}_1^2), [w(y)]_+)\right]$$

Note that the limit $\lim_{s\to\infty} N(y_s^1)$ is $[0, 0, 1]$ if all four vectors are independent; if $u_2^1 = u_1^2$, the limit is $[0, 0, 2]$. For $N(y_s^2)$ we get $[1, 0, 0]$ if all four vectors are independent; if $u_2^1 = u_1^2$, we get $[2, 0, 0]$. In either case, the sequences of unit normals $[N(y_s^1)]_+$ and $[N(y_s^2)]_+$ converge to different limits.

In the case of two independent vectors among u_i^j the argument is similar.

In both cases it is easy to see that any surface obtained from the described surfaces by small perturbation of the vectors defining the surface will not be tangent plane continuous.

Therefore, there is a set of surfaces of measure greater the zero that are not tangent plane continuous, and the scheme is not tangent plane continuous.

Necessity, C^k-continuity. We assume that the universal surface is tangent plane continuous; for the surface to be C^1-continuous, it is necessary and sufficient for the projection of the surface into the tangent plane to be injective in a neighborhood of zero (Proposition 3.1). Suppose the projection of the universal surface into the tangent plane is not injective arbitrarily close to zero. As we have seen, the tangent plane is spanned by two basis vectors in $\mathbf{R}^p$. Suppose these vectors are u_1^0 and u_2^0, and ψ_1, ψ_2 are the corresponding components of the universal map $\psi : U_1 \to \mathbf{R}^p$. Let map Ψ be the map $(\psi_1, \psi_2) : U_1 \to \mathbf{R}^p$. Let τ be the tangent plane, $P_\tau : \mathbf{R}^p \to \tau$ be the projection into the tangent plane defined by $x \in \mathbf{R}^p \to ((u_1^0, x), (u_1^0, x))$. If $P_\tau|_{\psi(U_1)}$ is not injective arbitrarily close to zero, then there are two sequences of points $y_s^1, y_s^2 \in U_1,\ s = 1\ldots$, such that $\psi(y_s^1) \neq \psi(y_s^2)$ for all s, $\lim_{s\to\infty} y_s^1 = \lim_{s\to\infty} y_s^2 = 0$ and $\Psi(y_s^1) = \Psi(y_s^2)$. We can choose a component ψ_i of ψ that has different values at infinitely many pairs of points y_s^1, y_s^2. Consider a surface in $\mathbf{R}^3$ defined by (ψ_1, ψ_2, ψ_i). The tangent plane to this surface is obtained by projecting u_1^0 and u_2^0 into $\mathbf{R}^3$; this plane coincides with the plane of the first two coordinate axes in $\mathbf{R}^3$. Clearly, projection into this plane is not injective. Now consider arbitrary projection of ψ into $\mathbf{R}^3$. By a change of coordinates, we can always reduce it to the form (ψ_1, ψ_2, f) where f is a linear combination of components of ψ. If this linear combination is sufficiently close to ψ_i, the projection is not injective again. We have constructed an open set of surfaces generated by subdivision that are not C^1-continuous, and the scheme cannot be C^1-continuous.

The argument is easily extended to C^k-continuous surfaces: for the universal surface to be C^k-continuous it is necessary and sufficient that the inverse projection to the tangent plane is C^k-continuous. As any subdivision surface in $\mathbf{R}^3$ can be obtained by applying a linear mapping $P : \mathbf{R}^p \to \mathbf{R}^3$ to the universal surface, the projection of the surface in $\mathbf{R}^3$ into its tangent plane is obtained in the same way. We have shown that if the universal surface is C^1-continuous for almost any linear mapping P the projection into the tangent plane is injective. Then its inverse is well defined and its derivatives can be computed as linear combinations of the derivatives of the parameterization of the universal surface over its tangent plane. If the universal surface is not C^k, for almost any choice of P the subdivision surface in $\mathbf{R}^3$ is not C^k-continuous. □

Part II: Tangent Plane Continuity

3.5 Tangent Plane Continuity Criterion

In this section we are going to formulate a general criterion for tangent plane continuity of the universal surface. We make very few assumptions about the eigenbasis functions: we assume only

- Condition A
- the scaling relation $\psi(y/2) = S^T\psi(y)$, $y \in U_1$.

It is important to keep in mind that although eigenbasis functions for a stationary subdivision scheme necessarily satisfy scaling relations, the converse is not true, that is, not every set of functions satisfying scaling relations can be generated by subdivision. We primarily explore properties of the universal surface that do not depend on the fact the coordinate functions of the surface were obtained by subdivision.

Action of the subdivision matrix on 2-vectors. As we are interested in the behavior of the normals to the universal surface, rather than using the scaling relation for the surface, it is convenient to formulate a scaling relation for the elements of $\Lambda^2(\mathbf{R}^p)$.

We obtain the action of S on $\Lambda^2(\mathbf{R}^p)$ by setting

$$\Lambda S(u_1 \wedge u_2) = Su_1 \wedge Su_2$$

This defines the action on decomposable elements. It is easy to see that ΛS is linear and can be extended by linearity to the whole space $\Lambda^2(\mathbf{R}^p)$. We call the matrix of ΛS with respect to the basis $h^i_{jr} \wedge h^k_{lt}$ the *tangent subdivision matrix*.

Recall that the scaling relations can be written as $\psi(y/2) = S^T\psi(y)$. Differentiating and taking wedge products, we obtain

$$w(y/2) = 4\Lambda S^T w(y) \tag{3.9}$$

where $w(y) = \partial_1\psi(y) \wedge \partial_2\psi(y)$. Again, although only one-sided partial derivatives exist

on the boundaries of triangles of U_1, the wedge product does not depend on the chosen triangle; thus, $w(y)$ is well-defined on U_1 away from zero.

The matrix $\Lambda S(y)$ is uniquely determined by the subdivision matrix S. Tangent plane continuity of a subdivision scheme is naturally related to the eigenstructure of the matrix ΛS.

If the 2-vectors $w(y)$, $y \in U_1$ span the whole space $\Lambda^2(\mathbf{R}^p)$, as we will see below, the smoothness properties of the scheme are mostly determined by the eigenstructure of ΛS. In general, however, this is not the case: it is possible that two or more functions generated by subdivision are dependent, i.e., $J\big[f[x^1], f[x^2]\big](y) = 0$ for all y. In this case the tangents to the surface are constrained to the directions perpendicular to the plane $x^1 \wedge x^2$. Writing the Jacobian above as $(x^1 \wedge x^2, \partial_1\psi \wedge \partial_2\psi)$ we can see that the condition for dependence of two functions generated by subdivision can be written in $\Lambda^2(\mathbf{R}^p)$ as orthogonality to the space spanned by vectors $w(y)$, $y \in U_1$. The set of all directions of $w(y)$ is the p-dimensional analog of the set of the directions of normals, i.e., the image of the Gauss map of the surface.

Definition 3.6. *The* **directional set** D_ψ *is the image of the Gauss map* $[\partial_1\psi(y) \wedge \partial_2\psi(y)]_+ : U_1 \to S^{p(p-1)/2-1}$.

The crucial property of the directional set D_ψ trivially follows from the scaling relation for tangents: *If* $v \in D_\psi$, *then* $[\Lambda S^T v]_+ \in D_\psi$.

Asymptotic behavior of vectors under iterated linear transforms. It follows from relations (3.9) that sequences of 2-vectors of the form $[(\Lambda S^T)^s u]_+$ are important for analysis of tangent plane continuity. The behavior of such sequences is best understood if we identify $\Lambda^2(\mathbf{R}^p)$ with the Euclidean space $\mathbf{R}^{p(p-1)/2}$ and regard 2-vectors just as vectors. We need to determine the conditions on a matrix A and vector $v \in \mathbf{R}^k$ that are necessary and sufficient for convergence of the sequence $[A^s v]_+$ as $s \to \infty$. The conditions for convergence of such sequences are quite general and have little to do with subdivision. Here we just state the main definitions and the condition for convergence (Lemma 3.3). We make only one assumption on A: all eigenvalues of A are not equal to zero and less than 1. This assumption does not lead to a loss of generality: components of v from the kernel of A do not contribute to the asymptotic behavior of $A^s v$ for any v, unless $v \in \mathrm{Ker}A$; in the latter case, for some s $A^s v = 0$.

For each eigenvalue μ of A let V_μ be the corresponding invariant space, that is, the subspace of vectors that are annulled by $(A-\mu I)^j$ for some j. The **order** of any vector v in the invariant subspace V_μ of a matrix A is the minimal number j such that $v \in \mathrm{Ker}(A-\mu I)^{j+1}$.

If a vector $v \in V_\mu^j$ has order k, then $Av = \mu v + v'$ where v' has order $k-1$. By induction we obtain the following decomposition of $A^s v$ for $s \geq k$:

$$A^s v = \mu^s \sum_{q=0}^{k} \mu^{q-k} \begin{pmatrix} s \\ k-q \end{pmatrix} v^{(q)} \tag{3.10}$$

where $v^{(q)}$ is in V_μ^q, and $v^{(q)} \neq 0$. As $s \to \infty$, the direction of Av converges to the direction of $v^{(0)}$.

A decomposition similar to (3.10) can be written for complex eigenvalues. Let χ be the complex phase of the eigenvalue μ, let $v_1^{(q)} = \Re v^{(q)}$, $v_2^{(q)} = \Im v^{(q)}$. where $v^{(q)}$ are complex generalized eigenvectors of order q; note that the vectors $v_1^{(q)}$, $v_2^{(q)}$, $q = 0 \ldots k$ are linearly independent.

$$A^s v = |\mu|^s \sum_{q=0}^{k} |\mu|^{q-k} \begin{pmatrix} s \\ k-q \end{pmatrix} v_1^{(q)} \cos((s+q-k)\chi) - v_2^{(q)} \sin((s+q-k)\chi) \tag{3.11}$$

Consider an arbitrary vector v in $\mathbf{R}^k$. The vector v can be written as a linear combination of the vectors in the invariant subspaces V_μ of A:

$$v = \sum_{\mu} v_\mu \tag{3.12}$$

where $v_\mu \in V_\mu$. This decomposition is unique. Let k_μ be the order of the vector v_μ, if $v_\mu \neq 0$.

The following definition identifies the set $\mathcal{M}(v)$ of components of $A^s v$ that determine the asymptotic behavior of the direction of $A^s v$. These are the components with coefficients changing as $|\mu|^s k^s$, with maximal possible $|\mu|$ and k.

Definition 3.7. *For a given vector v, Let $M = \max\{|\mu| \,\big|\, v_\mu \neq 0\}$, and $k_M = \max\{k_\mu \,\big|\, v_\mu \neq 0,\ |\mu| = M\}$. Define $\mathcal{M}(v)$ as $\{\mu \,\big|\, \mu = M, k_\mu = k_M\}$.*

Lemma 3.3. *If there is a complex or negative $\mu \in \mathcal{M}(v)$, $A^s v$ does not have a limit direction as $s \to \infty$. Otherwise, $\mathcal{M}(v)$ has a single positive element M and the limit direction is given by $u^0(v) = \left[v_M^{(0)}\right]_+$; The sequence $\left\|u^0(v) - [A^s v]_+\right\|$ converges to zero no slower than Cs^{-1}, where C does not depend on v.*

The proof of Lemma 3.3 can be found in Section 3.11.

We apply this Lemma to the tangent subdivision matrix ΛS acting on 2-vectors.

Tangent plane continuity criterion. We are ready to state a general criterion for tangent plane continuity. Recall $[4\Lambda S^T w(y)]_+ = [\Lambda S^T w(y)]_+ = [w(y/2^n)]_+$, $s = 0\ldots$, is a sequence of normals at points y, $y/2$ ... in U_1. It is clearly necessary for existence of a limit tangent plane that all such sequences converge to the same limit. It turns out to be sufficient. Note that the factor 4 in (3.9) has no effect on the limit direction, therefore, we can drop it and consider sequences $(\Lambda S^T)^s w(y)$. From now on we will drop this factor.

Let V_μ be the invariant subspace of $\Lambda^2(\mathbf{R}^p)$ corresponding to the eigenvalue μ. Let $u_\mu = \mathrm{Proj}(u, V_\mu)$ be the component of a 2-vector u from the invariant subspace V_μ of ΛS. For a set of 2-vectors X, $\mathrm{Proj}(X, V_\mu)$ is the set of $\mathrm{Proj}(u, V_\mu)$ for all $u \in X$.

Lemma 3.3 allows us to prove the following general condition for tangent plane continuity:

Theorem 3.4. *The universal surface and hence the corresponding subdivision scheme is tangent plane continuous at zero, if and only if there is a real positive eigenvalue M of ΛS^T and an eigenvector u^0 of M such that the following conditions hold for all u from the directional set D_ψ:*

1. *the set $\mathcal{M}(u)$ contains a single element M;*
2. *For any 2-vector $u \in D_\psi$, let $u_M = \mathrm{Proj}(u, V_M)$; then the term $u_M^{(0)}$ in decomposition (3.10) is au^0 for some $a \neq 0$; in other words, if the order of u_M is k, then u_M is in the preimage $(\Lambda S^T - MI)^{-k}(\mathrm{span}\langle u^0\rangle)$ and is not zero.*

Proof. Necessity. The first condition immediately follows from Lemma 3.3. By definition of $\mathcal{M}$, the projection u_μ is non-zero. In addition, the limit direction is the same for all

2-vectors; this means that in the expansion (3.10) $u^{(0)}$ is the same for all $u \in D_\psi$ up to a scaling factor. Given that $u_M^{(0)} = (S - MI)^k u_M$ for an element of order k, we obtain the second condition of the lemma.

Sufficiency. The conditions of the lemma guarantee that for any 2-vector u, $[(\Lambda S^T)^s u]_+$ converges to the same limit u^0. Lemma 3.3 gives us a uniform estimate for the convergence rate of the direction of $(\Lambda S^T)^s u$. Consider a ring R^0 in U_1 with outer radius $2r$ and inner radius r. The distance to the limit direction $\left\|[w(y)]_+ - u^0\right\|$ is bounded by some constant K on the ring R^0. Let R^j be the ring with inner radius $r/2^j$ and outer radius $r/2^{j-1}$. Then on R^j the distance to the limit direction can be estimated from above by CKj^{-1}, where C is a constant not depending on y or j. The same estimate applies to the union of rings R^s, $s = j \ldots$, that is, to a punctured neighborhood of zero. We conclude that the direction of $w(y)$ regarded as a function of y has a limit at 0. □

3.6 Tangent Plane Continuity of Schemes with Nondegenerate Directional Sets

The results presented in this section, while being less general than the results of the previous sections, are of primary importance both for practical purposes and for understanding the geometry of subdivision surfaces near extraordinary vertices.

A geometrically natural assumption on the directional set D_ψ is that $\operatorname{span}\langle D_\psi \rangle$ has maximal possible dimension, that is, coincides with $\Lambda^2(\mathbf{R}^p)$. This assumption means that the universal surface is in a general position — any surface can be deformed into a general position surface by arbitrarily small perturbation. In three dimensions, this is equivalent to requiring that the surface is not a cylinder: there is no plane such that the projection of ψ into this plane is a curve. In this case for any generalized eigenvector e of ΛS we are guaranteed to have 2-vectors $\partial_1\varphi \wedge \partial_2\varphi \in D_\psi$ with non-zero component along e.

Corollary 3.5. *Suppose that for a subdivision scheme with universal map ψ* $\operatorname{span}\langle D_\psi \rangle = \Lambda^2(\mathbf{R}^p)$ *Then the subdivision scheme is tangent plane continuous if and only if*

1. *the subdivision matrix ΛS^T has an eigenvalue of maximal magnitude M which is positive and real, and this eigenvalue has a single Jordan subspace J_M of maximal*

order k_M (dominant Jordan subspace); for any eigenvalue μ such that $|\mu| = M$, the maximal order of a Jordan subspace is less than k_M.

2. *For any $u \in D_\psi$,* $\mathrm{Proj}(u, J_M) \neq 0$.

Proof. If $\mathrm{span}\langle D_\psi \rangle = \Lambda^2(\mathbf{R}^p)$ then for any 2-vector u and hence for any invariant subspace $V_\mu \in \Lambda^2(\mathbf{R}^p)$, $\mathrm{Proj}(D_\psi, V_\mu) \neq 0$. Then the first condition follows from the first condition of Theorem 3.4.

If the eigenvalue M has two Jordan subspaces of maximal order k_M, there is a subspace W of V_M with all 2-vectors of order k_M of dimension at least two. The projection of D_ψ on that subspace should span a two-dimensional subspace. Therefore, we can find two 2-vectors u_1 and u_2 from D_ψ such that $u_1' = \mathrm{Proj}(u_1, W)$ and $u_2' = \mathrm{Proj}(u_2, W)$ are linearly independent. By construction of W, $\alpha_1 u_1' + \alpha_2 u_2'$ also has order k_M for any α_1, α_2 unless both are 0. Note that the limit directions of $[(\Lambda S^T)^s u_1]_+$ and $[(\Lambda S^T)^s u_2]_+$ are $u_1^\infty = \left[(\Lambda S - MI)^{k_M} u_1\right]_+$ and $u_2^\infty = \left[(\Lambda S - MI)^{k_M} u_2\right]_+$ respectively. As $\alpha_1 u_1' + \alpha_2 u_2'$ has order k_M, $\alpha_1 u_1^\infty + \alpha_2 u_2^\infty \neq 0$ if one of α_1, α_2 is not zero. Therefore, $(\Lambda S^T)^s u_1$ and $(\Lambda S^T)^s u_2$ have different limit directions. We conclude that the Jordan subspace of maximal order must be unique.

The second condition of the corollary directly follows from Theorem 3.4. □

There are some interesting cases for which the assumptions of Corollary 3.5 are not satisfied; most notable exception are piecewise smooth schemes of the type described by H.Hoppe and others [32]. The assumption is easy to verify for piecewise polynomial schemes, as for such schemes Jacobians also can be expressed in polynomial bases, and the nondegeneracy assumption is reduced to checking independence of vectors of control values for the Jacobians.

The conditions on D_ψ and ΛS^T required by Corollary 3.5 are quite simple. In practice, however, it is more useful to have explicit conditions on eigenbasis functions rather than on the directional set D_ψ, and on the matrix S^T, rather than on the larger matrix ΛS^T. There are three parts of Corollary 3.5 that have to be restated: the assumption about $\mathrm{span}\langle D_\psi \rangle$, the conditions on the eigenstructure of ΛS^T and the condition on the projection of D_ψ on the largest Jordan subspace of ΛS^T. Now we consider these parts one by one.

Linear independence of Jacobians. First, we reformulate the assumption of Corollary 3.5 in terms of eigenbasis functions. Observe that the components of the vectors $w(y) \in D_\psi$ are $J[g^i_{jr}, g^k_{lm}](y)$. $\mathrm{span}\langle D_\psi \rangle \neq \Lambda^2(\mathbf{R}^p)$, if and only if for any vector $u \in \Lambda^2(\mathbf{R}^p)$ there is y such that $(u, w(y)) = 0$; the latter inequality means that for any linear combinations of Jacobians $J[g^i_{jr}, g^k_{lm}](y)$ there is a point y such that this linear combination is not zero, that is, the set of functions $J[g^i_{jr}, g^k_{lm}](y)$ is linearly independent.

Eigenstructure of ΛS^T. To interpret the condition imposed by Corollary 3.5 on the tangent subdivision matrix, we use a Lemma relating the eigenstructure of a matrix ΛB acting on $\Lambda^2(\mathbf{R}^p)$ to the eigenstructure of the matrix B acting on $\mathbf{R}^p$. This Lemma is a general algebraic fact and is not specific to subdivision. We use the notation for eigenvalues and Jordan subspaces of B introduced in Section 2.4 for the subdivision matrix and the order of cyclic subspaces fixed there. We use an ordering of pairs (λ_i, n^i_j) corresponding to the order of Jordan subspaces: $(\lambda_i, n^i_j) > (\lambda_k, n^k_l)$, if $|\lambda_i| > |\lambda_k|$, or $|\lambda_i| = |\lambda_k|$ and $n^i_j > n^i_k$.

Let $\Pr\left(J^i_j \wedge J^k_l\right)$ be the real cyclic subspace generated by the vector $e^i_{j\,n^i_j} \wedge e^k_{l\,n^k_l}$ if $J^i_j \neq J^k_l$, and by $e^i_{j\,n^i_j} \wedge e^i_{j\,n^i_j - 1}$ otherwise (we assume that $\lambda_i \lambda_k$ is real).

Lemma 3.6. *Suppose the Jordan subspaces of a matrix B are numbered following the rules described in Section 2.4. The dominant Jordan subspace J_M for the matrix ΛB acting on $\Lambda^2(\mathbf{R}^p)$ is unique and corresponds to a real positive eigenvalue exactly in one of the following cases.*

1. *$J_M = \Pr\left(J^1_1 \wedge J^1_1\right)$, if λ_1 real, $(\lambda_i, n^i_1) < (\lambda_1, n^1_1 - 2)$ for all $i > 1$. If λ_1 has more than one cyclic subspace, then $n^1_2 < n^1_1 - 2$.*

2. *$J_M = \Pr\left(J^1_1 \wedge J^1_2\right)$, if λ_1 real, has at least two cyclic subspaces, $n^1_2 = n^1_1$ or $n^1_2 = n^1_1 - 1$, $(\lambda_i, n^i_1) < (\lambda_1, n^1_2)$ for all $i > 1$. If λ_1 has more than two cyclic subspaces, $n^1_3 < n^1_2$.*

3. *$J_M = \Pr\left(J^1_1 \wedge J^2_1\right)$, if λ_1 and λ_2 real, of the same sign and consequently $\lambda_1 > \lambda_2$. The eigenvalue λ_1 has a single cyclic subspace of order $n^1_1 = 0$, and $n^2_2 < n^2_1$ if n^2_2 is defined, and $(\lambda_i, n^i_1) < (\lambda_2, n^2_1)$ for all $i > 2$.*

4. *$J_M = \Pr\left(J^1_1 \wedge J^1_2\right)$, if (λ_1, λ_2) are a pair of complex-conjugate eigenvalues, and for all $i > 2$ $(\lambda_i, n^i_1) < (\lambda_1, n^1_1)$. If λ_1 has more than one cyclic subspace, then $n^1_1 > n^1_2$.*

The conditions on eigenvalues are illustrated in Figure 3.8. The proof of the lemma can be found in Section 3.12.

Parametric map. Suppose the universal surface is tangent plane continuous. The limit unit 2-vector u^0 is an eigenvector of ΛS^T. As it is the limit of sequences of decomposable 2-vectors and the set of decomposable 2-vectors is closed, it can be written as $u_1^0 \wedge u_2^0$, where $u_1^0, u_2^0 \in \mathbf{R}^p$. If $u_1^0 \wedge u_2^0$ is an eigenvector of a real eigenvalue u_1^0 and u_2^0 can be chosen in one of the following ways: u_1^0 and u_2^0 are both eigenvectors, u_1^0 and u_2^0 are linear combinations of a pair of complex eigenvectors, and u_1^0, u_2^0 satisfy $S^T u_1^0 = \lambda u_1^0 + u_2^0$. For a suitable choice of the basis c_{jr}^i, u^0 has one of the forms $e_{b0}^a \wedge e_{d0}^c$ (λ_a and λ_c real), or $e_{b0}^a \wedge e_{b0}^c$ (λ_a and λ_c complex-conjugate), or $e_{b0}^a \wedge e_{b1}^a$.

Definition 3.8. *Suppose the universal surface for a subdivision scheme is tangent plane continuous, and has limit tangent plane defined by $u_1^0 \wedge u_2^0$. Then we define the* **parametric map** *as*

$$((\psi, u_1^0), (\psi, u_2^0)) : U_1 \to \mathbf{R}^2$$

The second condition of Corollary 3.5 is equivalent to requiring the parametric map to have nonzero Jacobian $J(y)$ for sufficiently small y. Indeed, for any $u = w(y)$, $J(y) = (w(y), u^0)$. If $[w(y)]_+ \to u_0$ as $y \to 0$, then $J(y)$ has to be positive as $y \to 0$. Observing that if $\mathrm{Proj}(w(y), J_\mu) = 0$ then $\mathrm{Proj}(w(y/2^s), J_\mu) = \mathrm{Proj}((\Lambda S^T)^s w(y), J_\mu) = 0$, we get the converse.

Now we have all the ingredients required to restate the Corollary 3.5 in a more explicit form.

Theorem 3.7. *Suppose that the set of Jacobians $J[g_{jr}^i, g_{lm}^k](y)$ regarded as functions on U_1 is linearly independent. Let S be the subdivision matrix of the scheme with eigenvalues and Jordan subspaces numbered as described above.*

For the subdivision scheme to be tangent plane continuous, it is necessary and sufficient that the subdivision matrix satisfies the conditions of Lemma 3.6 and for a sufficiently small neighborhood of 0 the parametric map of the scheme should have positive Jacobian. The parametric map $U_1 \to \mathbf{R}^2$ is given by $(f^1_{1\,n_1^1}, f^1_{1\,n_1^1-1})$ in case 1 of Lemma 3.6, $(f^1_{1\,n_1^1}, f^1_{1\,n_2^1})$ in case 2, $(f^1_{1\,n_1^1}, f^2_{1\,n_1^2})$ in case 3, and $(\Re f^1_{1\,n_1^1}, \Im f^2_{1\,n_1^1})$ in case 4.

The conditions of the theorem are illustrated in Figure 3.8.

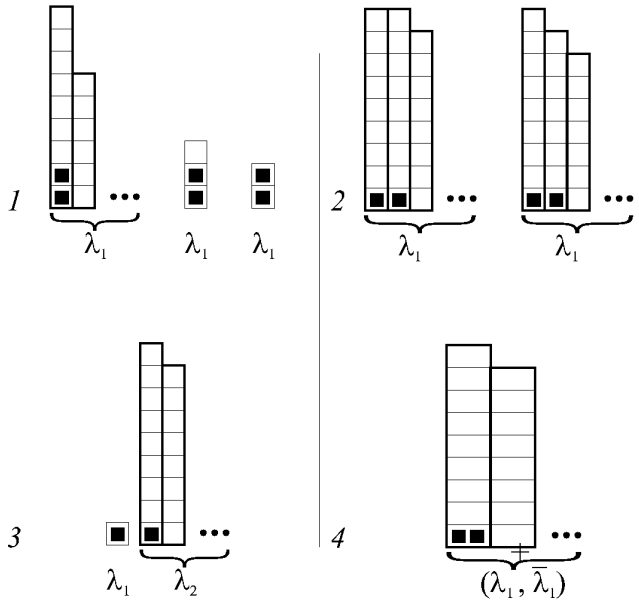

Figure 3.8: Conditions of Theorem 3.6 illustrated graphically. Each column corresponds to a Jordan subspace. Each cell in the columns corresponds to a generalized eigenvector (pair of generalized eigenvectors for complex eigenvalues) of matrix S^T. The generalized eigenvectors generating the parametric map are marked with black squares.

The theorem is just a restatement of Corollary 3.5 in a different language.

Comparison of Corollary 3.5 and equivalent Theorem 3.7 shows the advantage of using the tangent subdivision matrix ΛS for theoretical analysis: otherwise, the geometric properties of subdivision are obscured by the apparent complexity of the conditions on eigenvalues and generalized eigenvectors.

3.7 Sufficient Conditions for Tangent Plane Continuity

In the previous sections we have derived conditions for tangent plane continuity that are geometrically natural, but only in Theorem 3.5 we have made a step towards conditions that can be explicitly verified for specific subdivision schemes. Conditions which are simultaneously necessary and sufficient are important for understanding the structure of the class of tangent plane continuous subdivision schemes. However, for the purposes of verification of tangent plane continuity of specific schemes it is more useful to have conditions that are easier to check, even if they are less natural mathematically.

In this section we derive sufficient conditions extending those originally proposed by

Reif[55][1]

As a practical criterion, Theorem 3.7 suffers from two problems: first, the assumption of the Theorem is unnecessarily restrictive; second, it is likely to be difficult to evaluate Jacobian of the parametric map directly. We start with introducing a new map, called the *characteristic map*, which is closely related to the parametric map; this map is more suitable for explicit evaluation. Our definition is based on the definition proposed by Reif.

Characteristic map.

Suppose a surface is tangent plane continuous, and $u^0 = \lim_{y\to 0}[w(y)]_+$. Recall that for a suitable choice of the basis c^i_{jr}, u^0 has one of the forms $e^a_{b0} \wedge e^c_{d0}$ (λ_a and λ_c real), or $e^a_{b0} \wedge e^c_{b0}$ (λ_a and λ_c complex-conjugate), or $e^a_{b0} \wedge e^a_{b1}$. We consider only the first case, the other two are similar.

Note that for the parametric map at $y/2^s$ we have

$$(w(\frac{y}{2^s}), u^0) = ((\Lambda S^T)^s w(y), u^0) = (w(y), \Lambda S^s u^0) \tag{3.13}$$

Although ΛS in the basis of wedge products $e^i_{jr} \wedge e^k_{lt}$ does not have normal Jordan form, with proper choice of ordering it still has block-diagonal form, with each block corresponding to a Jordan subspace. It is easy to show that $u^0 = e^a_{b0} \wedge e^c_{d0}$ has order $n^a_b + n^c_d = k_M$ with respect to matrix ΛS. Therefore, as we can see from (3.10) (3.11), asymptotically $\Lambda S^s u^0$ behaves as

$$M^s \binom{s}{k_M} e^a_{bn_b} \wedge e^c_{dn_d} = M^s \binom{s}{k_M} h^a_{b0} \wedge h^c_{d0}$$

As we have observed, the 2-vector $u^{k_M} = e^a_{bn_b} \wedge e^c_{dn_d}$ is an eigenvector of ΛS. Suppose for all $y \in U_1$ the Jacobian $(w(y), u^{k_M})$ is not zero. Then for sufficiently large s, the Jacobian of the parametric map is arbitrarily well approximated by $M^s \binom{s}{k_M}(w(y), u^{k_M})$. If the Jacobian $(w(y), u^{k_M})$ is positive, this guarantees that the parametric map has positive Jacobian sufficiently close to zero. One can observe that it is also necessary for this Jacobian to be nonnegative, otherwise the parametric map will be negative arbitrarily close to zero.

[1] Reif's conditions guarantee C^1-continuity, not just tangent plane continuity; however, as we will see in Section 3.10 the difference between conditions for tangent plane continuity and C^1-continuity is small.

These considerations lead us to the following definition:

Definition 3.9. *The* **characteristic map** $\Phi : U_1 \to \mathbf{R}^2$ *is defined for a pair of cyclic subspaces* J^a_b, J^c_d *of the subdivision matrix as follows:*

1. *if* $J^a_b = J^c_d$, λ_a *is real, the characteristic map is* (f_{a0}, f_{a1});
2. *if* $J^a_b \neq J^c_d$, λ_a, λ_c *are real, the characteristic map is* (f_{a0}, f_{c0});
3. *if* $\lambda_a = \overline{\lambda_c}$, $b = d$, *the characteristic map is* $(\Re f_{a0}, \Im f_{a0}) = (g_{a0}, g_{c0})$.

Although a characteristic map is defined for many pairs of cyclic subspaces, only the map corresponding to the pair of cyclic subspace of the parametric map is of interest. The characteristic map has a remarkable property, which makes it particularly useful for proving tangent plane continuity and C^k-continuity of subdivision schemes:

The characteristic map Φ *for any pair of Jordan subspaces has self-similar Jacobian:*

$$J[\Phi](y/2) = J[\Phi](y)$$

This property can be easily proved using the scaling relation. Therefore, it is sufficient to verify that the characteristic map is regular on a suitably chosen annular compact set. Reif's original characteristic map is defined on such set. In our context it is more natural to consider the map defined on the whole neighborhood U_1.

Note that if the parametric map corresponds to a pair of distinct Jordan subspaces of order 0, to a Jordan subspace of a pair of complex eigenvalues of order 0, or a single Jordan subspace of a real eigenvalue of order 1, the characteristic map coincides with the parametric map.

Sufficient condition. Now we are ready to formulate the sufficient condition. The idea of the condition is to ensure that the parametric map corresponds to a given pair of Jordan subspaces of S and then to require the corresponding characteristic map to have positive Jacobian.

Suppose that for a given pair of cyclic subspaces J^a_b and J^c_d the characteristic map Φ has non-zero Jacobian everywhere. This guarantees that the projection of the any 2-vector in D_ψ on $\Pr(J^a_b \wedge J^c_d)$ has maximal possible order k_M, where $M = \lambda_a\lambda_c$ and $k_M = n^a_b + n^c_d$ if $J^a_b \neq J^c_d$ and $2n^a_b - 2$ otherwise.

By Theorem 3.4, it is sufficient for tangent plane continuity to ensure for any $u \in D_\psi$ that if $|\lambda_i\lambda_k| > M$, then $\mathrm{Proj}(u, J^i_j \wedge J^k_l) = 0$ and if $|\lambda_i\lambda_k| = M$, then the order of $\mathrm{Proj}(u, J^i_j \wedge J^k_l)$ is less than k_M for $(J^i_j, J^k_l) \neq (J^a_b, J^c_d)$.

The first part of this requirement is also necessary and is equivalent to $J[f^i_{jr}, f^k_{lt}] = 0$ if $|\lambda_i\lambda_k| > M$. For the second part it is sufficient to have $\mathrm{Proj}(u, e^i_{jr} \wedge e^k_{lt}) = 0$ for which the order of $e^i_{jr} \wedge e^k_{lt}$ is no less than k_M, i.e. $r + t \geq k_M$ if $(i, j) \neq (k, l)$, or $r + t - 1 \geq k_M$ if $r \neq t$ and $(i, j) = (k, l)$. However, this is not necessary: a linear combination of vectors of order k_M or higher may have order less than k_M; projections of 2-vectors from D_ψ can be such linear combinations.

Our observations lead to the following condition:

Theorem 3.8. *For a subdivision scheme to be tangent plane continuous on the k-regular complex it is sufficient that there is a basis b^i_{jr}, in which S has Jordan normal form, such that there is a pair of cyclic subspaces J^a_b, J^c_d in this basis, possibly coinciding, with $\lambda_a\lambda_c$ positive real, and the following conditions are satisfied:*

1. *For any pair of eigenbasis functions corresponding to eigenvalues λ_i and λ_k such that $|\lambda_i\lambda_k| > \lambda_a\lambda_c$ the Jacobian $J[f^i_{jr}, f^k_{lt}]$, is identically zero.*

2. *Let $\mathrm{ord}(b^i_{jr}, b^k_{lt}) = r + t$ if $J^i_j \neq J^k_l$, $\mathrm{ord}(b^i_{jr}, b^k_{lt}) = r + t - 1$ if $J^i_j = J^k_l$, and $r \neq t$. Let $\mathrm{ord}(b^i_{jr}, b^i_{jt}) = 0$. For any pair of eigenbasis functions of S f^i_{jr} and f^k_{lt} corresponding to eigenvalues λ_i and λ_k such that $|\lambda_i\lambda_k| = \lambda_a\lambda_c$ the Jacobian $J\big[f^i_{jr}, f^k_{lt}\big]$, is identically zero if $\mathrm{ord}(b^i_{jr}, b^k_{lt}) \geq \mathrm{ord}(b^a_{bn^a_b}, b^c_{dn^c_d})$.*

3. *The characteristic map of J^a_b, J^c_d has Jacobian of constant sign everywhere on U_1 except zero.*

Another condition, with stronger assumptions than the one above, but easier to check, can be obtained directly from Theorem 3.7 by relaxing the nondegeneracy assumptions; it is sufficient to assume that only the characteristic map corresponding to the dominant cyclic subspace of ΛS^T is nondegenerate.

3.8 A Necessary Condition

If we want to prove that a scheme is not tangent plane continuous, it is useful to have necessary conditions that are easier to check than the general conditions of Theorem 3.4, or

the assumptions of Theorem 3.7. Most of the schemes do satisfy these assumptions; however, to make the conditions of Theorem 3.7 necessary, weaker assumptions would suffice.

Define the decay exponent of a generalized eigenvector with eigenvalue μ oforder k as $(|\mu|, k)$. Define the decay exponent of a cyclic subspace of order k_μ of eigenvalue μ as $(|\mu|, k_m u)$. Decay exponents are ordered: $(\lambda, n) > (\lambda', n')$ if $\lambda > \lambda'$ or $\lambda = \lambda'$ and $n > n'$.

Define the *decay exponent* of a pair of basis vectors d.e. $\left(e^i_{jr}, e^k_{lt}\right)$ as the decay exponent of $e^i_{jr} \wedge e^k_{lt}$. Explicitly, the pair $(|\lambda_i \lambda_k|, r + t)$ if $J^i_j \neq J^k_l$, as the pair $(|\lambda_i|^2, r + t - 1)$ if $J^i_j = J^k_l$, $r \neq t$, and as $(0, 0)$ if $e^i_{jr} = e^k_{lt}$.

Suppose the tangent subdivision matrix has two cyclic subspaces J_M and $J_{M'}$ of equal sizes with $|M| = |M'|$. This happens if there are two pairs of cyclic subspaces of the subdivision matrix J^a_b, J^c_d and $J^{a'}_{b'}, J^{c'}_{d'}$ such that d.e. (J^a_b, J^c_d) = d.e. $\left(J^{a'}_{b'}, J^{c'}_{d'}\right)$; and $J_M = \Pr\left(J^a_b \wedge J^c_d\right)$ and $J_{M'} = \Pr\left(J^{a'}_{b'} \wedge J^{c'}_{d'}\right)$.

We can consider decompositions of the form (3.10), but with respect to the sum of subspaces $J_M \oplus J_{M'}$. If there are 2-vectors $w(y_1)$ and $w(y_2)$ such that their projections on $J_M \oplus J_{M'}$ have maximal order, and $w(y_1)^{(0)}$ and $w(y_2)^{(0)}$ are linearly independent, then $w(y_1/2^s)$ and $w(y_2/2^s)$ converge to different limits as $s \to \infty$. These projections have maximal order if and only if

$$\mathrm{Proj}(w(y_m), \mathrm{span}\langle e^a_{bn^a_b} \wedge e^c_{dn^c_d}, e^{a'}_{b'n^{a'}_{b'}} \wedge e^{c'}_{d'n^{c'}_{d'}}\rangle) \neq 0 \text{ for } m = 1, 2$$

This is equivalent to requireing that at least one of the Jacobians $J[g^a_{b0}, g^c_{d0}](y_m)$, $J[g^{a'}_{b'0}, g^{c'}_{d'0}](y_m)$ is not zero for $m = 1, 2$.

For $w(y_1)^{(0)}$ and $w(y_2)^{(0)}$ to be linearly independent, we require vectors of length 2 $[J[g^a_{bn^a_b}, g^c_{dn^c_d}](y_m), J[g^{a'}_{b'n^{a'}_{b'}}, g^{c'}_{d'n^{c'}_{d'}}](y_m)]^T$ for $m = 1, 2$ to be linearly independent.

The resulting necessary condition for tangent plane continuity is

Lemma 3.9. *Suppose for any pair of subspaces J^i_{jr}, J^k_{lt}*

$$\text{d.e.}\left(J^i_{jr}, J^k_{lt}\right) \leq \text{d.e.}\left(J^a_b, J^c_d\right) \quad \textit{and} \quad \text{d.e.}\left(J^a_b, J^c_d\right) = \text{d.e.}\left(J^{a'}_{b'}, J^{c'}_{d'}\right)$$

Suppose that at the points $y_1, y_2 \in U_1$ and vectors of length 2

$$\begin{bmatrix} J[g^a_{bn^a_b}, g^c_{dn^c_d}](y_m) \\ J[g^{a'}_{b'n^{a'}_{b'}}, g^{c'}_{d'n^{c'}_{d'}}](y_m) \end{bmatrix} \quad m = 1, 2$$

are linearly independent, and $J[g^{a'}_{b'0}, g^{c'}_{d'0}](y_m) \neq 0$ *or* $J[g^{a'}_{b'0}, g^{c'}_{d'0}](y_m)$ *is not zero for each* $m = 1, 2$. *Then the subdivision scheme is not tangent plane continuous.*

Note that the assumptions on the Jacobians are rather weak and are typically satisfied. In most cases, schemes with subdivision matrices violating conditions of Theorem 3.7 are not tangent plane continuous.

3.9 Interpretation of the Tangent Plane Continuity Criterion

In this section we discuss the meaning of Theorem 3.4 in terms of eigenbasis functions and subdivision matrices, without any additional assumptions. Our goal is to gain more understanding of the subdivision schemes that do not satisfy our sufficient conditions, but are nevertheless tangent plane continuous.

Note that the first part of Theorem 3.8 is also necessary. The "coarse structure" conditions on pairs of eigenfunctions with $|\lambda_i \lambda_k| \neq |\lambda_a \lambda_c|$ where λ_a, λ_c are the eigenvalues of the pair of cyclic subspaces J^a_b, J^c_d corresponding to the parametric map.

The crucial difference between Theorem 3.4 and Theorem 3.8 is the assumption that the characteristic map of the pair of blocks J^a_b, J^c_d is regular. This assumption is not necessary. However, it is easy to see that the characteristic map has to have a nonnegative Jacobian. Thus, the tangent plane continuous schemes that do not satisfy Theorem 3.8, have singular characteristic maps. If the characteristic map has zero Jacobian at a subset of U_1, then tangent plane continuity of the scheme depends on the "next slowest decreasing Jacobian" (we will make this idea precise below). If that map also has degeneracies, we have to consider the next Jacobian etc. We can separate the domain U_1 into subsets such that the number of "vanishing Jacobians" is constant for each subset. The rate at which the Jacobian vanishes is constant for each subset.

Partition of U_1. To make these ideas more precise, we consider the eigenspace V_μ of the tangent subdivision matrix ΛS^T. Let u_{jr}, $j = 1 \dots P_\mu$, $r = 0 \dots n_j$, be a Jordan basis for the matrix ΛS^T on V_μ.

We would like to describe more explicitly when an eigenvector u^0 with an eigenvalue M is the limit of all sequences $(\Lambda S^T)^s w(y)$. By Theorem 3.4, for any $y \in U_1$ the component $\mathrm{Proj}(w(y), V_\mu)$ should be in $(S - MI)^{-k}(\mathrm{span}\langle u^0 \rangle)$ for some k. To make this statement

more explicit, we define a decomposition of V_μ into subspaces W_k of elements of k-th order. Note that while V_μ is invariant, W_k depend on the choice of the Jordan basis.

Let W_k be the span of all vectors u_{jk} for all j such that the order of the j-th cyclic subspace $n_j \geq k$. Then

$$V_\mu = \sum_{k=0}^{m_\mu} W_k$$

Let $v(y) = \text{Proj}(w(y), V_\mu)$. Then v has order k if $\text{Proj}(v, W_r) = 0$ for all $r > k$. If v has order k then the limit of $[(\Lambda S^T)^s v]_+$, is u_{10} only if $\text{Proj}(v, W_k)$ is parallel to u_{1k}; in other words, $\text{Proj}(v, u_{jk}) = 0$ for all $j \neq 1$.

Let $Z(k)$ be the set of all points y such that $\text{Proj}(w(y), W_r) = 0$ for $r < k$ and $\text{Proj}(w(y), W_k) \neq 0$. This defines a partition of U_1:

$$U_1 = \cup_{k=0}^{k=m_\mu} Z(k)$$

For each $y \in Z(k)$, $\text{Proj}(w(y), u_{jk}) = 0$ for all $k \geq 0$.

Orthogonality conditions. Conditions of the type $\text{Proj}(w(y), v) = 0$ can be interpreted as conditions on Jacobians using the dual basis $\tilde{u}_{jr}$ of the basis u_{jr} in V_μ. Then $\text{Proj}(w(y), u_{jk}) = 0$ is equivalent to $(w(y), \tilde{u}_{jk}) = 0$.

Observe that each vector $\tilde{u}_{pq}$ can be written as a linear combination of vectors

$$\sum j, r, l, t \alpha_{jrlt} h^i_{jr} \wedge h^k_{lt}$$

where h^i_{ij} are vectors of the Jordan basis for the subdivision matrix. Therefore, all conditions on $w(y)$ can be written in the form

$$\sum_{jrlt} \alpha_{jrlt} J[f[x^i_{jr}], f[x^k_{lt}]] = 0$$

that is, a particular linear combination of Jacobians of maps generated by pairs of the vectors of the Jordan basis of S should be zero. It is easy to see that in general these linear combinations cannot be reduced to a single Jacobian of a certain map, because most vectors u_{pq} are not decomposable. For example, if $u_{pm_q} = h_{jn_j} \wedge h_{ln_l}$, then

$$u_{pm_q-1} = \Lambda S u_{pm_q} - \mu u_{pm_q} = h_{jn_j} \wedge h_{ln_l} + \lambda_i h_{jn_j} \wedge h_{ln_l-1} \lambda_k h_{jn_j-1} \wedge h_{ln_l} + h_{jn_j-1} \wedge h_{ln_l-1}$$

It is interesting to observe that without additional restrictions on the eigenbasis functions it is impossible to formulate any strong necessary conditions on the subdivision matrix: virtually for any structure of the subdivision matrix we can choose the eigenbasis functions in such a way that the resulting universal surface is tangent plane continuous.

Part III: C^k-continuity

3.10 Criteria for C^1 and C^k-continuity

Once tangent plane continuity is established, the only additional condition that is required for C^k-continuity is injectivity and C^k-continuity of the projection of the universal surface into the tangent plane.

This criterion for C^k-continuity can be obtained by reinterpreting the injectivity condition in terms of the eigenbasis functions. Let τ be the tangent plane, P_τ be the projection $\mathbf{R}^3 \to \tau$. Recall that $P_\tau \circ \psi$ is just the parametric map Ψ defined in Section 3.5. Suppose $\Psi(y_1) = \Psi(y_1)$. If $\psi(y_1) \neq \psi(y_2)$, the projection P_τ restricted to $\psi(U_1)$ is not injective.

To obtain conditions for C^k-continuity we only have to note that in this case the parameterization of the universal surface over the tangent plane can be written as $\psi \circ \Psi^{-1}$ where Ψ is the parametric map. Note that Ψ can be noninjective, but conditions of Theorem 3.10 guarantee that $\psi \circ \Psi^{-1}$ is well-defined.

Thus, we have the following criterion for C^k-continuity

Theorem 3.10. *A tangent plane continuous scheme with parametric map Ψ is C^1-continuous if and only if there is a neighborhood of zero U, such that for any $y_1, y_2 \in U$, $y_1, y_2 \neq 0$ for which $\Psi(y_1) = \Psi(y_2)$, and for any eigenbasis function g the values $g(y_1)$ and $g(y_2)$ coincide. A subdivision scheme is C^k-continuous if and only if the reparameterized eigenbasis functions $f^i_{jk}(\Psi^{-1}(\xi)) : \Psi(U) \to \mathbf{R}$ are C^k-continuous for some neighborhood of zero in U_1.*

This condition can be made much more explicit if the parametric map coincides with

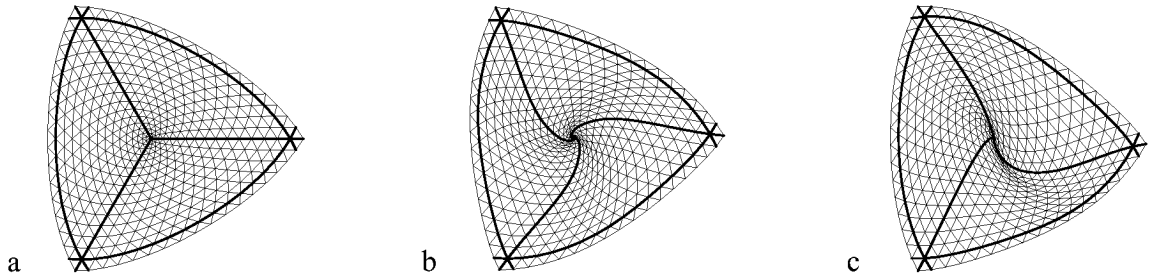

Figure 3.9: Three types of characteristic maps: control points after 4 subdivision steps are shown. a. Two real eigenvalues. b. A pair of complex-conjugate eigenvalues. c. single eigenvalue with Jordan block of size 2.

the characteristic map:

Condition C. The parametric map corresponds to a pair of cyclic subspaces of order 0 with real eigenvalues, or cyclic subspaces of a pair of complex-conjugate eigenvalues of order 0, or a single Jordan subspace of order 2. In other words, the sum of the pair of Jordan subspaces defining the parametric map has dimension 2.

Additional motivation for considering this case is that only in this case C^1-continuity of the subdivision scheme can be *stable with respect to perturbations of coefficients.* It is possible to show that under certain assumptions unless Condition C is satisfied, there is an arbitrary small perturbation of the entries of the subdivision matrix such that the resulting matrix violates the necessary conditions for tangent plane continuity. Three possible types of characteristic maps for which the subdivision scheme can be tangent plane continuous are shown in Figure 3.9.

In this case the complex eigenbasis functions reparameterized by the parametric map $f^i_{jr}(\xi) = f^i_{jr}(\Psi^{-1}(\xi))$ satisfy more general scaling relations of the form

$$f^i_{jr}(T\xi) = \lambda_i f^i_{jr}(\xi) + f^i_{j(r-1)}(\xi), \quad \text{for } r \geq 1$$
$$f^i_{j0}(T\xi) = \lambda_i f^r_{j0}(\xi)$$

where T is a nondegenerate linear transformation of the plane, which can be reduced to one of three normal forms: diagonal matrix with real eigenvalues λ_a, λ_c, rotation matrix

corresponding to a pair of complex eigenvalues $\lambda\exp(i\varphi), \lambda\exp(-i\varphi)$ or a Jordan block $J_2(\lambda)$ for a real λ. We assume that $|\lambda_1|$, $|\lambda_2|$, $|\lambda| < 1$ and $\lambda' \neq 0$.

Using the results about C^k-continuity of functions satisfying scaling relations (Section 3.13), we can formulate a general criterion of C^k-continuity of subdivision schemes.

Before stating the theorem, we need to define three special types of polynomials. Each type of polynomials corresponds to a particular type of characteristic map described above.

The first two types generalize the idea of homogeneous polynomials. Their definitions differ only slightly from the standard definitions of quasihomogeneous polynomials.

1. For T being the diagonal matrix with real eigenvalues λ_a, λ_c, we use the classes of polynomials $\mathbf{P}(p,q)$. Let $\mathbf{N}(p,q)$ be the set of all pairs of non-negative integers (i,j) such that $\lambda_a^i\lambda_c^j = \lambda_a^p\lambda_c^q$ for a fixed pair (p,q). Then $\mathbf{P}(p,q)$ is defined as

$$\mathbf{P}(p,q) = \Big\{ \sum_{i,j} \alpha_{ij}\xi_1^i\xi_2^j \;\Big|\; (i,j) \in N(p,q),\ \alpha_{ij} \in \mathbf{C} \Big\}$$

   Note that the set $N(p,q)$ depends on p, q and the ratio $\ln\lambda_a/\ln\lambda_c$. For example, if this ratio is $2/3$, then $\mathbf{P}(4,3)$ is spanned by the monomials ξ_1^6, $\xi_1^4\xi_2^3$, $\xi_1^2\xi_2^6$, ξ_2^{12}.

   We also define an integer constant j^i_{min} for all λ_i satisfying $|\lambda_i| \geq |\lambda_c|^k$ as

$$j^i_{min} = \min \Big\{ j \;\Big|\; \exists l:\ l + j \leq k,\ \text{and } |\lambda_a^l\lambda_c^j| \leq |\lambda_i| \Big\}$$

   Note that if $|\lambda_a| = |\lambda_c|$ and $|\lambda_i| \geq |\lambda_c^k|$, $j^i_{min} = 0$. The meaning of this constant is explained in Section 3.13.

2. If T has a pair of a pair of complex conjugate eigenvalues $\lambda_a = \lambda$, $\lambda_c = \bar{\lambda}$, we define $\bar{\mathbf{N}}(p,q)$ as the set of all pairs of integers (i,j) such that $\lambda^i\bar{\lambda}^j = \lambda^p\bar{\lambda}^q$ for a fixed pair (p,q). In this case we define the set of polynomials

$$\bar{\mathbf{P}}(p,q) = \Big\{ \sum_{i,j} \alpha_{ij}\xi_1^i\bar{\xi}_2^j \;\Big|\; (i,j) \in \bar{\mathbf{N}}(p,q),\ \alpha_{ij} \in \mathbf{C} \Big\}$$

3. If T is a Jordan block of size 2 with real eigenvalue λ, we use polynomials

$$F_m(t) = \frac{1}{m!}\prod_{i=0}^{m-1}(x-i) \text{for } m > 0;\ F_0(t) = 1 \tag{3.14}$$

Theorem 3.11. *Suppose a subdivision scheme $\mathcal{S}$ is C^k on the regular complex and the parametric map of the scheme coincides with the characteristic map Ψ. $\mathcal{S}$ is C^1-continuous on the k-regular complex if and only if Ψ has Jacobian of constant sign, and for any y_1 and y_2 for which $\Psi(y_1) = \Psi(y_2)$, and for any eigenbasis function g the values $g(y_1)$ and $g(y_2)$ coincide.*

$\mathcal{S}$ is C^k-continuous if in addition for $|\lambda_i| > |\lambda_c|^k$ any nontrivial set of complex eigenbasis functions $f^i_{jr}(\Phi^{-1}(\xi)) = f^i_{jr}(\xi)$, $r = 1..n_j$ corresponding to the eigenvalue λ_i satisfies one of the following conditions:

1. *If the characteristic map is (f^a_{b0}, f^c_{d0}) with λ_a, λ_c real and*

   (a) *$\lambda_i = \lambda_a^p \lambda_c^{q+j^i_{min}}$ for some nonnegative p, q , $p + q \le k - j^i_{min}$ and $\partial_2^{j^i_{min}} f^i_{jn^i_j}(\xi) \in \mathbf{P}(p, q)$, $\partial_2^{j^i_{min}} f^i_{jm}(\xi) \equiv 0$ for $m < n^i_j$.*

   (b) *OR $\partial_2^{j^i_{min}} f^i_{jr}(\xi) \equiv 0$ for all j.*

2. *If the characteristic map is $(\Re f^a_{b0}, \Im f^a_{b0})$ with complex eigenvalue λ_a, and $\lambda_i = \lambda_a^p \overline{\lambda_a}^q$ for some p, q, $p + q < k$, $f^i_{jn^i_j}(\xi) \in \bar{\mathbf{P}}(p, q)$, and $f^i_{jm}(\xi) \equiv 0$ for $m < n^i_j$.*

3. *If the characteristic map is (f^a_{b0}, f^a_{b1}) with eigenvalue λ_a real, $\lambda_i = \lambda_a^p$ for some $p \le k$ and*

$$f^i_{jr}(\xi) = \sum_{i=0}^{r-l} C_{r-l-m} \frac{\xi_2^p}{\lambda_a^{mp}} F_m\left(\frac{\lambda_a \xi_1}{\xi_2}\right)$$

   for $r \ge n^i_j - p$, where $l = \max(0, n^i_j - p)$. For $r < n^i_j - p$, $f^i_{jr}(\xi) \equiv 0$.

The theorem immediately follows from 3.10 combined with the criteria of C^k-continuity of functions satisfying scaling relations stated in Section 3.13.

In the first case, the eigenbasis functions can be specified in more explicit form integrating the relations given in the theorem, as it is described in Section 3.13.

An important special case of Theorem 3.11 occurs when $\lambda_a = \lambda_c$; in this case the eigenvalues are necessarily real and the criterion becomes

Corollary 3.12. *If a subdivision scheme satisfies conditions of Theorem 3.11 and* $\lambda_a = \lambda_c = \lambda$, *than the scheme is* C^k *if and only if any nonzero complex eigenbasis function* $f^i_{jn^i_j}$ *corresponding to an eigenvalue* $\lambda_i \geq \lambda^k$ *is a homogeneous polynomial of degree* d, $\lambda_i = \lambda^d$ *and for all* $r < n^i_j$ $f^i_{jr} \equiv 0$.

Another important special case are the conditions for C^1-continuity:

Corollary 3.13. *If for a tangent plane continuous subdivision scheme the characteristic map* Ψ *coincides with the parametric map, it is* C^1*-continuous if and only if for any* $y_1, y_2 \in U_1$, $y_1, y_2 \neq 0$, *such that* $\Psi(y_1) = \Psi(y_2)$, *for any eigenbasis function* $g(y_1) = g(y_2)$ *and the Jacobian of* Ψ *has constant sign.*

C^2-continuity. The conditions of Theorem 3.11 for $k = 2$ lead to the following constraints on the nontrivial eigenbasis functions.

- If the eigenvalues λ_a and λ_b are real and $|\lambda_a| > |\lambda_b|$, there are three distinct cases: $|\lambda_a|^2 > |\lambda_b|$, $|\lambda_a|^2 = |\lambda_b|$ and $|\lambda_a|^2 < |\lambda_b|$. For simplicity, we assume that both λ_a and λ_b are positive.

  In both cases, a nontrivial eigenbasis function $f(\xi)$ has to correspond to an eigenvalue λ' with $\lambda' < \lambda_a^2$, or $\lambda' \in \{\lambda_a, \lambda_b, \lambda_a\lambda_b, \lambda_a^2, \lambda_b^2\}$. In the latter case, if $\lambda' = \lambda_a$, $f(\xi) = C\xi_1$, if $\lambda' = \lambda_a\lambda_b$, $f(\xi) = C\xi_1\xi_2 + g(\xi_1)$, where $g(\xi)$ satisfies λ'-scaling relations for (λ_a, λ_b), if $\lambda' = \lambda_b^2$, $f(\xi) = C\xi_2^2 + g(\xi_1)$, and if $\lambda' = \lambda_a^2$, $f(\xi) = C\xi_1^2$.

  If $\lambda' = \lambda_b$, three cases are possible: if $\lambda_a^2 > \lambda_b$ then $f(\xi) = C\xi_2$; if $\lambda_a^2 = \lambda_b$ then $f(\xi) = C_1\xi_1^2 + C_2\xi_2$ and if $\lambda_a^2 < \lambda_b$ then $f(\xi) = C\xi_2 + g(\xi_1)$.

- If the eigenvalues λ_a and λ_c are complex conjugate, then a nontrivial eigenbasis function corresponds to an eigenvalue λ' with $|\lambda'| < |\lambda_a|$, or $\lambda' \in \{\lambda_a, \overline{\lambda_a}, \lambda_a^2, |\lambda_a|^2, \overline{\lambda_a}^2\}$, and $f(\xi)$ is $C\xi_1$, $C\xi_2$ $C\xi_1^2$, $C\xi_1\xi_2$ or $C\xi_2^2$ respectively.

- If the characteristic map is defined by a Jordan block of size 2 with real positive eigenvalue λ_a, then a nontrivial eigenbasis function corresponds to an eigenvalue λ' with $|\lambda'| < |\lambda_a|$, or $\lambda' \in \{\lambda_a, \lambda_a^2\}$. If $\lambda' = \lambda_a$, then there may be a pair of eigenbasis functions corresponding to a cyclic subspace of order $m \geq 1$ $f_m(\xi) = C_1\xi_2 + C_0\xi_1$ and $f_{m-1}(\xi) = C_0\xi_1$, or a single eigenbasis function $f_0(\xi) = C_0\xi_1$ for a a cyclic

subspace of order 0. if $\lambda' = \lambda_a^2$, then there may be three nontrivial eigenbasis functions corresponding to a cyclic subspace of order $m \geq 2$, $f_m(\xi) = C_2\xi_2^2 + C_1\xi_1\xi_2 + C_0\xi_1^2$, $f_{m-1}(\xi) = (\lambda C_1 + C_0)\xi_2^2 + 2C_0\xi_1\xi_2$ and $f_{m-2}(\xi) = 2C_0\lambda^2\xi_2^2$. For a cyclic subspace of order 1, there may be a pair of nontrivial eigenbasis functions $f_1(\xi) = (C_1 - C_0)\xi_2^2 + C_0\lambda\xi_1\xi_2$ and $f_0(\xi) = 2C_0\lambda^2\xi_2^2$, and for a cyclic subspace of size 1, $f_0(\xi) = C_0\xi_2^2$.

3.10.1 Limit Values, Tangents and Normals

When the subdivision surface is C^1-continuous or at least tangent plane continuous, it is possible to find explicit expressions for limit values, tangents and normals to the surface at vertices of V^∞. These expressions can be easily derived from decompositions given in Equations 2.24. Suppose the parametric map is defined by the pair of eigenbasis functions (g^1, g^2), corresponding to the generalized eigenvectors c^1, c^2. Recall that (c^1, c^2) is either $(c^a_{bn^a_b}, c^c_{dn^c_d})$ (real λ_a, λ_c), $(c^a_{bn^a_b}, c^c_{bn^c_b})$ (complex-conjugate λ_a, λ_c), or $(c^a_{bn^a_b}, c^a_{b\,n^a_b-1})$ (single real eigenvalue λ_a).

A vector of initial values $x \in \mathcal{P}(N_L, \mathbf{R}^3)$ can be decomposed with respect to the Jordan basis of the subdivision matrix:

$$x = \sum_{i,j,r} \beta^i_{jr} c^i_{jr}$$

where $\beta^i_{jr} \in \mathbf{R}^3$ for all i,j and r.

The tangent plane is spanned by the vectors β^1 and β^2, from $\mathbf{R}^3$ corresponding to c^1 and c^2 in the decomposition above unless $\beta^1 \times \beta^2 = 0$. In the latter case the generated surface may be not smooth (this is the subset that we allow to be excluded in our definition of smoothness of a scheme).

Let $\tilde{c}^1$ and $\tilde{c}^2$ be the left generalized eigenvectors of the subdivision matrix corresponding to c^1 and c^2. Then

$$\beta^1 = (\tilde{c}^1, x)\beta^2 = (\tilde{c}^2, x) \tag{3.15}$$

It is possible to compute β^1 and β^2 using vectors of smaller size; Let $L' \leq L$ be the size of the neighborhood $N_{L'}$ such that $\mathrm{Ctrl}_0(N^1_l) \subset N_{L'}$, we call such neighborhoods *invariant.*

Similar to Lemma 2.2, it is easy to see that minimal size of an invariant neighborhood is in general $L-1$. It can be further decreased in specific cases such as the Modified Butterfly scheme (Section 6.4).

For such neighborhood we can write a matrix S' such that $S'x^j = x^{j+1}$ for $x \in \mathcal{P}(N_{L'})$. Clearly, this matrix is a submatrix of the subdivision matrix, and subdivision matrix with appropriate reordering has the form

$$S = \left(\begin{array}{c|c} S' & 0 \\ \hline S^{r1} & S^{r2} \end{array}\right)$$

Each left generalized eigenvector of S can be taken in one of the two forms $[\tilde{y}'|\tilde{y}^r]$ or $[\tilde{y}'|\mathbf{0}]$ where $\tilde{y}'$ is a left generalized eigenvector of S'. Corresponding generalized right eigenvectors have forms $[0|y^r]$ and $[y'|y^r]$ respectively. Typically, the dominant eigenvectors have the second form. (Explicit reasons for this for single ring symmetric schemes are discussed in Section 6.2). If this is true, then corresponding left generalized eigenvectors can be written as $[\tilde{c'}^1|\mathbf{0}]$ and $[\tilde{c'}^2|\mathbf{0}]$, where $\tilde{c'}^1$ and $\tilde{c'}^2$ are generalized eigenvectors of S'. This means that β^1 an β^2 depend only on S' and can be computed using its left generalized eigenvectors. This makes formulas for computing tangents and normals for schemes with small support particularly simple (Sections 6.4,6.5).

3.10.2 Degree Estimate for Piecewise Polynomial Subdivision

A simple consequence of Theorem 3.11 is the following estimate for the minimal degree of the polynomial patches that is required to obtain C^k-continuous surfaces.

We derive these estimates for the case of two equal real eigenvalues, which is the most common case.

First, we note that if all eigenvalues are less than λ_c^k, then the scheme is C^k-continuous. But this also means that all partial derivatives up to the order k disappear at zero, i.e., the surface is "flat." Extending the definition of [53] we define a *non-flat surface* of order k as a C^k-continuous surface which has non-vanishing partial derivatives up to order k. In this case Corollary 3.12 tells us that the scheme should reproduce surfaces of the form

$$z = H^k(x, y)$$

where $H^k(x,y)$ is a homogeneous polynomial of degree k. x, y and z, in the case of piecewise polynomial schemes, are piecewise polynomials of degrees less than $d > k$. As it was shown by Reif, the degree of piecewise polynomials x and y should be at least $k+1$. Therefore, the degree of z is at least $k(k+1)$.

3.11 Proof of Lemma 3.3

Using (3.10) and (3.11) we can write an expression for $A^s v$ in terms of vectors $v_\mu^{(q)}$ (real μ) and $v_{1\mu}^{(q)}$, $v_{2\mu}^{(q)}$ (complex μ), $q = 0 \dots k_\mu$. Define $r_\mu(s,q) = |\mu|^{s-k_\mu+q} \begin{pmatrix} s \\ k_\mu - q \end{pmatrix}$. Then

$$\begin{aligned} A^s v = & \sum_{\text{real}\,\mu>0} \sum_{q=0}^{k_\mu} r_\mu(s,q) v_\mu^{(q)} \\ & + \sum_{\text{real}\,\mu<0} \sum_{q=0}^{k_\mu} (-1)^{s-k_\mu+q} r_\mu(s,q) v_\mu^{(q)} \\ & + \sum_{\text{complex}\,\mu} \sum_{q=0}^{k_\mu} r_\mu(s,q) (v_{\mu 1}^{(q)} \cos((s+q-k)\chi_\mu) - v_{\mu 2}^{(q)} \sin((s+q-k)\chi_\mu)) \end{aligned} \tag{3.16}$$

The set of vectors $v_\mu^{(q)}$, $v_{1\mu}^{(q)}$, $v_{2\mu}^{(q)}$, $\mu \in \mathcal{M}(v)$, is linearly independent. Therefore, we can construct a basis such that this set of vectors is a part of the basis. In a finite-dimensional space any basis is a Riesz basis, in particular, there is a constant B such that

$$\begin{aligned} \left\| A^s v \right\| \geq & B \Bigg(\sum_{\text{real}\,\mu} \sum_{q=0}^{k_\mu} r_\mu(s,q) \left\| v_\mu^{(q)} \right\| \\ & + \sum_{\text{complex}\,\mu} \sum_{q=0}^{k_\mu} r_\mu(s,q) (\left\| v_{\mu 1}^{(q)} \right\| |\cos((s+q-k)\chi_\mu)| + \left\| v_{\mu 2}^{(q)} \right\| |\sin((s+q-k)\chi_\mu)|) \Bigg) \end{aligned} \tag{3.17}$$

Consider the direction of $A^s v$, that is, $A^s v / \left\| A^s \right\|$. As all components of the vector are independent, this vector has a limit if and only if each component has a limit.

Suppose $\mu \in \mathcal{M}(v)$ is complex. Define

$$v(s) = v_{1\mu}^{(0)} \cos s\chi_\mu - v_{1\mu}^{(0)} \sin s\chi_\mu$$

Intuitively it is clear that this sequence of vectors does not have a limit direction; there are two sequences s_k^1, s_k^2 such that $v(s_k^1)$ and $v(s_k^2)$ converge to linearly independent limits as $k \to \infty$. For irrational $\chi_\mu/2\pi$, this follows from the well-known fact (see for example, Hardy [30]) that for any $\epsilon > 0$, $t \in [0, 2\pi]$ and arbitrary large s, there is an s' such that $|s\chi_\mu \bmod 2\pi - t| < \epsilon$. If $\chi_\mu/2\pi$ is rational, then the function is periodic, and unless it is constant, which is impossible, we can choose two constant subsequences of linearly independent vectors.

Let s_k^1, s_k^2 are two sequences such that $v(s_k^1)$ converges to c^1 and $v(s_k^2)$ converges to c^2 as $k \to \infty$, with c^1 and c^2 linearly independent.

Because $\mu \in \mathcal{M}(v)$, $k_\mu = k_M$ and the ratio $r_{\mu'}(s,q)/r_\mu(s,k_M)$ as $s \to \infty$ for all μ' and q. From (3.17) we have

$$\left\|A^{s_k^1} v\right\| \geq B r_M(s, k_M)(\left\|c^1\right\|(1-\epsilon)) \tag{3.18}$$

for arbitrary small ϵ and sufficiently large k. Similar statement is true for s_k^2. Therefore, all elements of the sequence $A^s v/\left\|A^s v\right\|$ are well-defined for sufficiently large k.

Also from definition of M and k_M it follows that

$$\left\|A^s v\right\| < K r_M(s, k_M) \text{ for some constant } K. \tag{3.19}$$

Observe that $v(s) r_\mu(s, k_M)/\left\|A^s v\right\|$ is a linearly independent component in the decomposition of $A^s v/\left\|A^s v\right\|$. To show that $A^s v/\left\|A^s v\right\|$ does not have a limit it is sufficient to show that $v(s) r_\mu(s, k_M)/\left\|A^s v\right\|$ does not have a limit.

For sufficiently large k and arbitrarily small ϵ

$$\frac{\left\|v(s_k^1) r_M(s_k^1, k_M)\right\|}{\left\|A^{s_k^1} v\right\|} \geq \frac{1}{K}\left\|c^1\right\|(1-\epsilon)$$

The direction of the vectors $v(s_k^1) r_\mu(s_k^1, k_M)/\left\|A^{s_k^1} v\right\|$ converges to $c^1/\left\|c^1\right\|$; the direction

of the vectors in the sequence $v(s_k^2)r_\mu(s_k^2, k_M)/\left\|A^{s_k^2}v\right\|$ converges to $c^2/\left\|c^2\right\|$. By linear independence of c^1 and c^2 these limits do not coincide.

Therefore, the component does not have a limit as $s \to \infty$ and we conclude that the sequence $A^s v$ does not have a limit direction.

Similar argument can be used to show that that $\mu \in \mathcal{M}$ cannot be negative.

Thus, if the sequence of vectors has a limit direction, the eigenvalues in $\mathcal{M}(v)$ are all positive and real. But the magnitudes of all eigenvalues in $\mathcal{M}(v)$ are equal, therefore, it may contain only a single element.

Convergence rate can be easily estimated observing that the ratio of the second slowest term to the dominant term decreases at least at the rate $O(s^{-1})$.

3.12 Linear Transformations on $\Lambda^2(\mathbf{R}^p)$

Complex Jordan structure of ΛB. We start with the complex Jordan structure of ΛB. It is straightforward to show that any eigenvalue μ of ΛB is a product of eigenvalues $\lambda_i\lambda_k$ of B (i and k may coincide). Suppose B has cyclic subspaces J_j^i and J_l^k corresponding to eigenvalues λ_i and λ_k, of orders n_j^i and n_l^k respectively.

Let $e_{j0}^i, \dots e_{jn_j^i}^i$ be the basis for the cyclic subspace J_j^i satisfying $Be_{jr}^i = \lambda_i e_{jr}^i + e_{jr-1}^i$, for $r > 0$, $Be_{j0}^i = \lambda_i e_{j0}^i$. Let $e_{l0}^k, \dots e_{ln_l^k}^k$ be a similar basis in J_l^k.

Two cases are possible: J_j^i and J_l^k are are different subspaces, or they coincide.

1. *Case 1: J_j^i and J_l^k are different.* In this case the cyclic subspaces J_j^i and J_l^k generate a subspace $J_j^i \wedge J_l^k$ of $\Lambda^2(\mathbf{R}^p)$ of dimension $(n_j^i+1)(n_l^k+1)$. For different cyclic subspaces J_j^i and J_l^k, $e_{jr}^i \wedge e_{lt}^k$ has order $r+t$. This can be shown by induction. For $r > 0$ and $t > 0$,

$$\begin{aligned}(\tilde{A} - \lambda_i\lambda_k I)e_{jr}^i \wedge e_{lt}^k =& Ae_{jr}^i \wedge Ae_{lt}^k - \lambda_i\lambda_k e_{jr}^i \wedge e_{lt}^k \\ =& \lambda_k e_{j\,r-1}^i \wedge e_{lt}^k + \lambda_i e_{jr}^i \wedge e_{l\,t-1}^k + e_{j\,r-1}^i \wedge e_{l\,t-1}^k\end{aligned} \tag{3.20}$$

   As we apply the transform $(\Lambda B - \lambda_i\lambda_k I)$ iteratively, on step m $(\Lambda B - \lambda_i\lambda_k I)^m e_{jr}^i \wedge e_{lt}^k$ would consist out of terms proportional to $e_{jq}^i \wedge e_{ls}^k$, where $q + s \le r + t - m$. After $r + t$ steps, we get $q + s \le 0$, that is, a single component $e_{j0}^i \wedge e_{l0}^k$. The components

that we get by repeatedly applying the transform to a vector $e^i_{jr} \wedge e^k_{lt}$ can be seen in the diagram on Figure 3.10

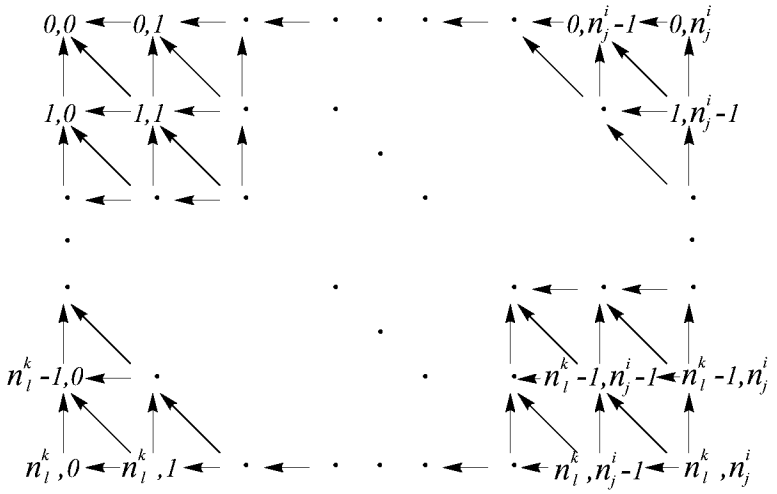

Figure 3.10: Subspace of $\Lambda^2(\mathbf{R}^p)$ generated by two cyclic subspaces J^i_j, J^k_l. The pairs of numbers correspond to the basis vectors $e^i_{jr} \wedge e^k_{lt}$, $r = 0 \ldots n^i_j$, $t = 0 \ldots n^k_l$; arrows indicate the components that are generated by each vector after one application of $\Lambda B - \lambda_i \lambda_k I$, as given by (3.20); after m steps, if we start in the bottom right corner, we only have components above the line given by equation $r + t \leq n^i_j + n^k_l - m$.

Clearly, there is a cyclic subspace of order $n^i_j + n^k_l$ generated by $e^i_{j\, n^i_j} \wedge e^k_{l\, n^k_l}$; we will denote this subspace $\Pr\left(J^i_j \wedge J^k_l\right)$ to find other cyclic subspaces, we should characterize eigenvectors of ΛB that are linear combinations of $e^i_{jr} \wedge e^k_{lt}$. Suppose $u = \sum_{r,t} c_{rt} e^i_{jr} \wedge e^k_{lt}$ is an eigenvector, that is, should satisfy $(\Lambda B - \lambda_i \lambda_k I)u = 0$. Then from (3.20) after trivial transformations, we get the following system of equations for coefficients c_{rt} of the eigenvector:

$$\begin{aligned} c_{rt} + \lambda_i c_{r-1\, t} + \lambda_k c_{r,\, t-1} = 0, \quad & r = 1 \ldots n^i_j,\ t = 1 \ldots n^k_l \\ c_{r\, n^k_l} = 0, \quad & r = 1 \ldots n^i_j \\ c_{n^i_j\, t} = 0, \quad & t = 1 \ldots n^k_l \end{aligned} \tag{3.21}$$

Note that if two out of three coefficients c_{rt},$c_{r-1\, t}$,$c_{r\, t-1}$ are zero, then the third one is also zero. An inductive argument starting with the triple $c_{n^i_j, n^k_l - m}$, $c_{n^i_j, n^k_l - m - 1}$, $c_{n^i_j - 1, n^k_l - m}$, $m = 0 \ldots n^k_l - 1$, shows that for $r + t > n^i_j$ the coefficient c_{rt} is zero, that is, all coefficients below $r + t = n^i_j$ the diagram in Figure 3.10. Similar statement is true for

n_l^k. We conclude that any eigenvector has coefficients $c_{rt} = 0$ for $r + t > \min(n_j^i, n_l^k)$. Assume $n_l^k \leq n_j^i$. Again, following the diagram it is easy to see that if we choose arbitrary values for $c_{n_j^i\, r}$ we can always construct a unique eigenvector. By choosing $c_{n_j^i\, r} = \delta(r - m)$, for $m = 0 \ldots n_l^k$ we get $n_j^k + 1$ eigenvectors $u_0, u_1, \ldots u_m$, with $u_0 = e_{j0}^i \wedge e_{l0}^k$. Clearly, the size of the cyclic subspace corresponding to u_0 is $n_j^i + n_j^k$. All other eigenvectors u_s are not decomposable, and corresponding cyclic subspaces are of little interest to us. We note however, that orders of the cyclic subspaces are $n_j^i + n_l^k - 2m$, $m = 0 \ldots n_l^k$.

2. *Case 2: J_j^i and J_l^k coincide.* This case is similar; however, because of dependencies between the basis vectors, we get smaller cyclic subspaces. The diagram for the basis of $J_j^i \wedge J_j^i$ is shown in Figure 3.11

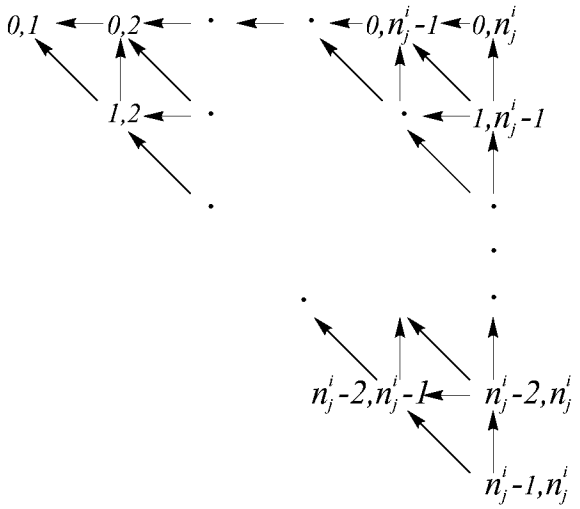

Figure 3.11: Subspace of $\Lambda^2(\mathbf{R}^p)$ generated by a single cyclic subspace J_j^i. The pairs of numbers correspond to the basis vectors.

In a similar way, we obtain a decomposition of $J_j^i \wedge J_j^i$ into a sum of $\lfloor (n_i+1)/2 \rfloor$ cyclic subspaces with orders from $2n_i - 2$, $2n_i - 6 \ldots$, down to 0 for odd n_i and down to 2 for even n_j^i. If $n_j^i = 0$, the cyclic subspace $J_j^i \wedge J_j^i$ does not exist. For $J_j^i \wedge J_j^i$ again the only cyclic subspace that has decomposable eigenvector has maximal order $2n_i - 2$, which we denote $\Pr\left(J_j^i \wedge J_j^i\right)$.

Conditions for existence of a single dominant cyclic subspace of ΛB. Recall that we call a cyclic subspace J_M of ΛB dominant, if it corresponds to a real positive eigenvalue M, and for any other cyclic subspace of order k corresponding to the eigenvalue μ, $(\mu, k) < (M, k_M)$ where k_M is the order of J_M.

We have observed that any eigenvalue of ΛB has the form $\lambda_i\lambda_k$ or λ_i^2; and the orders of cyclic subspaces are of the form $n_j^i + n_l^k - 2m$ and $2n_j^i - 2 - 4m$ $m = 0 \ldots$. Therefore, we need to assert that $(M, k_M) > (\lambda_i\lambda_k, n_j^i + n_l^k)$ and $(M, k_M) > (\lambda_i^2, 2n_j^i)$ for all other pairs of cyclic subspaces of B different from the pair of cyclic subspaces defining J_M.

We have to consider only subspaces $\Pr\left(J_j^i \wedge J_l^k\right)$; other cyclic subspaces of ΛB have smaller orders. With our ordering of cyclic subspaces M can be either λ_1^2 or $\lambda_1\lambda_2$. The dominant subspace is one of $\Pr\left(J_1^1 \wedge J_1^1\right)$, $\Pr\left(J_1^1 \wedge J_2^1\right)$, $\Pr\left(J_1^1 \wedge J_1^2\right)$ and $\Pr\left(J_1^1 \wedge J_1^2\right)$. The first two cases require λ_1 real, the third case requires λ_1 and λ_2 real, and the last case requires λ_1 and λ_2 to be complex conjugate with $\lambda_1\lambda_2$ real positive. These four possible cases correspond to the cases of Lemma 3.6.

1. $J_M = \Pr\left(J_1^1 \wedge J_1^1\right)$; this case implies that $M = \lambda_1^2$. Therefore, λ_1 is real. In addition, we need for any i, j, $(\lambda_i\lambda_j, n_1^i + n_1^k) < (\lambda_1, 2n_1^1 - 2)$ and $(\lambda_i, 2n_1^i - 2) < (\lambda_1, 2n_1^1 - 2)$. As $|\lambda_1| \geq |\lambda_i|$ for any $i > 1$, and $n_1^1 \geq n_j^1$ for any $j > 1$, it is sufficient to require $n_1^1 > n_2^1 + 2$, and $(\lambda_1, n_1^1) > (\lambda_i, n_1^i + 2)$ for all $i > 1$.

2. $J_M = \Pr\left(J_1^1 \wedge J_2^1\right)$; $M = \lambda_1^2$ and λ_1 are real. Similarly, the additional conditions are $n_1^1 < n_2^1 + 2$, $n_2^1 > n_3^1$ if n_3^1 is defined, and $(\lambda_1, n_1^2) > (\lambda_i, n_1^i)$ for all $i > 1$.

3. $J_M = \Pr\left(J_1^1 \wedge J_1^2\right)$, $M = \lambda_1\lambda_2$, and λ_1 and λ_2 both are complex and have opposite phase. Suppose that $|\lambda_1| \neq |\lambda_2|$; then $\bar{\lambda_1} = \lambda_i$ and $\bar{\lambda_2} = \lambda_k$ are also eigenvalues of B distinct from λ_1 and λ_2. Then eigenvalue $\lambda_1\lambda_2 = \lambda_i\lambda_k$ has a cyclic subspace $\Pr\left(J_1^i \wedge J_1^k\right)$ distinct from $\Pr\left(J_1^1 \wedge J_1^2\right)$ and of the same size, because $n_1^i = n_1^1$ and $n_1^k = n_1^2$. Therefore, there is no dominant subspace unless $\lambda_1 = \bar{\lambda_2}$. Suppose $\lambda_1 = \bar{\lambda_2}$. For $\Pr\left(J_1^1 \wedge J_1^2\right)$ to be dominant, we need $n_2^1 < n_1^1$ if n_2^1 is defined and $(\lambda_i, n_1^i) < (\lambda_1, n_1^i)$ for all $i > 2$.

4. If λ_1 and λ_2 are real, for M to be positive, they have to be of the same sign. Then necessarily $|\lambda_1| > |\lambda_2|$. To guarantee that $(lm_1\lambda_2, n_1^1 + n_1^2) > (lm_i\lambda_k, n_1^i + n_1^k)$ we need $n_1^1 < n_1^2 - 2$, $n_2^2 < n_1^2$ and $(\lambda_i, n_1^i) < (\lambda_2, n^2 - 1)$ for all i.

3.13 Scaling Relations

In this section we the prove the criteria for C^k-continuity of functions satisfying scaling relations. We consider the scaling relation of the form

$$f(T\xi) = J_{n+1}(\lambda')f(\xi) \tag{3.22}$$

where T is a nondegenerate linear transformation of $\mathbf{R}^2$, f is a map $\mathbf{R}^2 \to \mathbf{C}^{n+1}$, $J_{n+1}(\lambda')$ is a Jordan block with eigenvalue λ', possibly complex.

We assume that T is reduced to the real Jordan normal form; as T is nondegenerate, it can be reduced to one out of three possible forms:

$$\begin{pmatrix} \lambda_1 & 0 \\ 0 & \lambda_2 \end{pmatrix} \quad \text{or} \quad \begin{pmatrix} \lambda\cos\varphi & -\lambda\sin\varphi \\ \lambda\sin\varphi & \lambda\cos\varphi \end{pmatrix} \quad \text{or} \quad \begin{pmatrix} \lambda & 1 \\ 0 & \lambda \end{pmatrix}$$

where λ_1,λ_2, λ and φ are real and are not equal to zero; in addition, we assume that $|\lambda_1|$, $|\lambda_2|$, $|\lambda| < 1$. We assume that $\lambda' \neq 0$.

The following lemma is the basis of our derivations. This lemma extends a similar lemma by Warren [63].

Lemma 3.14. *Suppose $f(\xi) = [f_n, f_{n-1} \dots f_0]^T : \mathbf{R}^2 \to \mathbf{C}^{n+1}$ is a continuous function defined on $D \setminus \{0\}$, where D is a compact domain in $\mathbf{R}^2$ which contains the origin as an internal point and f satisfies* (3.22)

1. *If $|\lambda'| < |\lambda_{min}|^k$, where λ_{min} is the eigenvalue of T with minimal absolute value, then*

$$\lim_{|\xi|\to 0} \frac{\left\| f(\xi) \right\|}{\left\| \xi_i \right\|^k} = 0$$

2. *If $\lambda' = 1$, then f is continuous at 0 if and only if $f_n = const$ and $f_m = 0$ for $m < n$.*

3. *If $|\lambda'| \geq 1$, and $\lambda' \neq 1$, then f are continuous if and only if $f \equiv 0$.*

Proof. 1. Without the loss of generality we assume that f is defined on the whole plane except zero: using the scaling relation (3.22) we can extend f to the whole plane from

D.

For any ξ,

$$\frac{\left\|f(T^p\xi)\right\|}{\left\|T^p\xi\right\|^k} = \frac{\left\|(J_{n+1}(\lambda'))^p f(\xi)\right\|}{\left\|T^p\xi\right\|^k} \leq K\frac{|\lambda'|^p n^p}{|\lambda_{min}|^{pk}}\frac{\left\|f(\xi)\right\|}{\left\|\xi\right\|^k} \tag{3.23}$$

where K is a constant.

Suppose $\left\|\xi\right\| < \epsilon$. Then

$$\left\|T^{-n}\xi\right\| \leq (|\lambda_{min}|)^{-n} m^n \left\|\xi\right\| \tag{3.24}$$

where m is the size of the maximal Jordan block of T. On the other hand, for any ξ there is p such that $\left\|T^{-p}\xi\right\| > r_0$ for a fixed r_0. Let p_ϵ be the minimal p such that for some ξ with $\left\|\xi\right\| < \epsilon$, $\left\|T^{-p_\epsilon}\xi\right\| > r_0$. It follows from (3.24), that $p_\epsilon \to \infty$ as $\epsilon \to 0$. Suppose for some ξ $\left\|T^{-p}\xi\right\| > r_0$ and $\left\|T^{-p+1}\xi\right\| \leq r_0$ Then $\left\|T^{-p}\xi\right\| < Cr_0$, where C depends only on T. We conclude that for any $\epsilon > 0$ for any $\left\|\xi\right\| < \epsilon$ we can choose p such that $r_0 < \left\|T^{-p}\xi\right\| < R_0$, and if p_ϵ is minimal p defined as above, $p_\epsilon \to \infty$. As $\left\|f(\xi)\right\|/\left\|\xi\right\|^k$ is continuous away from zero, it is bounded on the ring $r_0 \leq \left\|xi\right\| \leq R_0$ by a constant K'.

Therefore, we can estimate

$$\frac{\left\|f(\xi)\right\|}{\left\|\xi\right\|^k} \leq KK'\frac{|\lambda'|_\epsilon^p n_\epsilon^p}{|\lambda_{min}|^{p_\epsilon k}} \tag{3.25}$$

for any $\xi \leq \epsilon$ for sufficiently small ϵ, if $|\lambda'| < |\lambda_{min}^k|$. Clearly, as $\epsilon \to 0$, the estimate in the right part of (3.25) converges to zero.

2. If $\lambda' = 1$, then $f(T^p(\xi)) = (J_{n+1}(1))^p f(\xi) = (I+N)^p f(\xi) = f(\xi) + pNf(\xi) + \ldots$, where N is a nilpotent matrix. Unless $Nf(\xi) = 0$, this sequence does not have a limit. This proves the second part of the lemma.

3. If $|\lambda'| > 1$, $f(T^p\xi) = J_{n+1}(\lambda')^p f(\xi)$ diverges whenever $f(\xi) \neq 0$; as $T^p\xi \to 0$, this proves that $f(\xi)$ is continuous at zero only if it is identically zero. If $|\lambda'| = 1$, consider

$f_0(T^p\xi) - f_0(T^{p-1}\xi) = (\lambda')^{p-1}(1-\lambda')f_0(\xi)$. Unless $f_0(\xi)$ is identically zero, this quantity does not converge to zero as $p \to \infty$. In a similar way we prove that $f_m(\xi)$ for $m > 0$ has to be identically zero for f to be continuous.

□

Remark: the proof of the lemma did not use the fact that T is a transformation of $\mathbf{R}^2$; it holds for f defined on $\mathbf{R}^k$ for any k, as long as T is contracting.

Using Lemma 3.14, we establish conditions for C^k-continuity of functions satisfying scaling relations. These conditions have different form depending on the type of the transformation T. We consider each of the three types separately.

3.13.1 Two Real Eigenvalues

First we consider the scaling relations of the form

$$\begin{aligned} f_m(\lambda_1\xi_1, \lambda_2\xi_2) &= \lambda' f_m(\xi) + f_{m-1}(\xi), \quad \text{for } m \geq 1 \\ f_0(\lambda_1\xi_1, \lambda_2\xi_2) &= \lambda' f_0(\xi) \end{aligned} \tag{3.26}$$

This case includes the case when $\lambda_1 = \lambda_2$, and the matrix has a single real eigenvalue but with two cyclic subspaces. We assume without the loss of generality that $|\lambda_1| \geq |\lambda_2|$. We say that a system of functions $f_m(\xi)$ satisfies (λ_1, λ_2)-scaling relation for λ' if it satisfies (3.26).

Functions of this type are well-know in singularity theory; Newton diagrams described below were used to study quasihomogeneous functions by Kushnirenko [39].

The derivatives of functions satisfying a scaling relation do not satisfy a scaling relation themselves, but their scaled versions do. This allows us to establish the following

Lemma 3.15. *If a system of functions $f_0(\xi), \ldots f_m(\xi)$ satisfies the (λ_1, λ_2)-scaling relation for λ', the functions are defined on a compact domain containing 0 as an internal point, and are C^k everywhere except 0, then the derivative $\partial_1^i\partial_2^j f_m(\xi)$, $i + j \leq k$, exists at 0 and is continuous if and only if one of the following conditions is met:*

1. $|\lambda'| < |\lambda_1^i\lambda_2^j|$
2. $\lambda' = \lambda_1^i\lambda_2^j$, $\partial_1^i\partial_2^j f_n(\xi) \equiv const$ *and* $\partial_1^i\partial_2^j f_m(\xi) \equiv 0$ *for all* $m < n$.

3. $\partial_1^i \partial_2^j f_m(\xi) \equiv 0$ *for all* m.

Proof. Differentiating the scaling relation, we obtain

$$\lambda_1^i \lambda_2^j \partial_1^i \partial_2^j f_m(\lambda_1 \xi_1, \lambda_2 \xi_2) = \lambda' \partial_1^i \partial_2^j f_m(\xi) + \partial_1^i \partial_2^j f_{m-1}(\xi) \quad \text{for } m > 0$$
$$\lambda_1^i \lambda_2^j \partial_1^i \partial_2^j f_0(\lambda_1 \xi_1, \lambda_2 \xi_2) = \lambda' \partial_1^i \partial_2^j f_0(\xi)$$

Define the functions

$$\tilde{f}_m(\xi) = \left(\lambda_1^i \lambda_2^j\right)^m \partial_1^i \partial_2^j f_m(\xi)$$

Then $\tilde{f}_m(\xi)$ satisfy

$$\tilde{f}_m(\lambda_1 \xi_1, \lambda_2 \xi_2) = \frac{\lambda'}{\lambda_1^i \lambda_2^j} \tilde{f}_m(\xi) + \tilde{f}_{m-1}(\xi) \quad \text{for } m > 0$$
$$\tilde{f}_0(\lambda_1 \xi_1, \lambda_2 \xi_2) = \tilde{f}_0(\xi)$$

which is the (λ_1, λ_2)-scaling relation for $\frac{\lambda'}{\lambda_1^i \lambda_2^j}$.

As the functions $\tilde{f}_m$ are just scaled versions of $\partial_1^i \partial_2^j f_m$, their properties are the same. Now we can apply Lemma 3.14.

Necessity immediately follows from Lemma 3.14, as the derivatives $\partial_1^i \partial_2^j f_m(\xi)$ and, therefore, $\tilde{f}_m(\xi)$ have to be continuous.

Sufficiency.

1. If both i and j are equal to zero, the statement of the lemma is reduced to the statement of Lemma 3.14.

   Assuming that $j \neq 0$, consider the derivative $\partial_1^i \partial_2^{j-1} f_m$. If $\left|\frac{\lambda'}{\lambda_1^i \lambda_2^j}\right| < 1$, then $\left|\frac{\lambda'}{\lambda_1^i \lambda_2^{j-1}}\right| < |\lambda_2|$. As the set of functions $\tilde{f}_m$ corresponding to $\partial_1^i \partial_2^{j-1} f_m$ satisfies the (λ_1, λ_2)-scaling relation for $\frac{\lambda'}{\lambda_1^i \lambda_2^{j-1}}$, by part 1 of Lemma 3.14, the limit

   $$\lim_{|\xi| \to 0} \frac{\tilde{f}_m(\xi)}{\xi_2}$$

   exists and is equal to 0. This limit is precisely the derivative $\partial_1^i \partial_2^j f_m(\xi)$.

Similarly, as $\left|\frac{\lambda'}{\lambda_1^i\lambda_2^j}\right| < 1$, the limit of $\partial_1^i\partial_2^j f_m(\xi)$ exists and is equal to 0. We conclude that the derivative $\partial_1^i\partial_2^j f_m(\xi)$ exists and is continuous.

2. If $\frac{\lambda'}{\lambda_1^i\lambda_2^j} = 1$, to be continuous, $\partial_1^i\partial_2^j f_n$ has to be constant. Therefore, $\partial_1^i\partial_2^{j-1} f_n$ is linear in ξ_2, for $\xi \neq 0$, and the appropriate limit clearly exists, and is equal to the same constant. Thus, the derivative in this case exists. For $m < n$ $\partial_1^i\partial_2^j f_m$ is 0 everywhere. Then $\partial_1^i\partial_2^{j-1} f_m$ is a constant for $\xi \neq 0$, and $\partial_1^i\partial_2^j f_m$ exists and is 0 at $\xi = 0$. This argument also applies to part 3.

□

The functions $f_m(\xi)$ are C^k-continuous if all derivatives

$$\partial_1^i\partial_2^j f_m(\xi)$$

with $i + j \leq k$ exist and are continuous. The derivative $\partial_1^i\partial_2^j f_m$ can be associated with the integer point (i, j) in the plane. Such representation is used for the *Newton diagrams* of quasihomogeneous polynomials (Appendix B).

We are interested in the existence and continuity of the derivatives which are represented by integer points inside the triangle bounded by $x = 0$, $y = 0$, $x + y = k$ (Figure 3.12).

According to Lemma 3.15, the derivatives $\partial_1^i\partial_2^j f_m$ are guaranteed to exist at 0 if $\left|\frac{\lambda'}{\lambda_1^i\lambda_2^j}\right| < 1$. Taking logarithms of both sides of this inequality, we can see that for all integer points below the line $l(\lambda')$ with equation $x \ln|\lambda_1| + y \ln|\lambda_2| = \ln|\lambda'|$, the derivatives are known to exist. The slope of $l(\lambda')$ is less than -1, because $|\lambda_2| < |\lambda_1|$.

For the points between the lines $l(\lambda')$ and $x + y = k$, the derivatives have to be either 0 or constants to exist and be continuous. For those that are constants, additional condition $\lambda' = \lambda_1^i\lambda_2^j$ have to be satisfied; only the derivatives of f_n can be constant; derivatives of f_m for $m < n$ are identically zero.

Note that if a derivative $\partial_1^i\partial_2^j f_m$ is 0 or constant, all derivatives to the right and upward from (i, j) are equal to zero everywhere. Suppose $|\lambda'| \geq |\lambda_2^k|$; this means that $l(\lambda')$ intersects the y axis below or at the point $(0, k)$.

In this case let j_{min} be the minimal integer value of y for which there is an integer point (x, j_{min}) between $l(\lambda')$ and $x + y = k$. All derivatives represented by integer points inside the area delimited by $x = 0$, $l(\lambda')$, $x + y = k$, $y = j_{min}$ are 0 (shaded area in Figure 3.12).

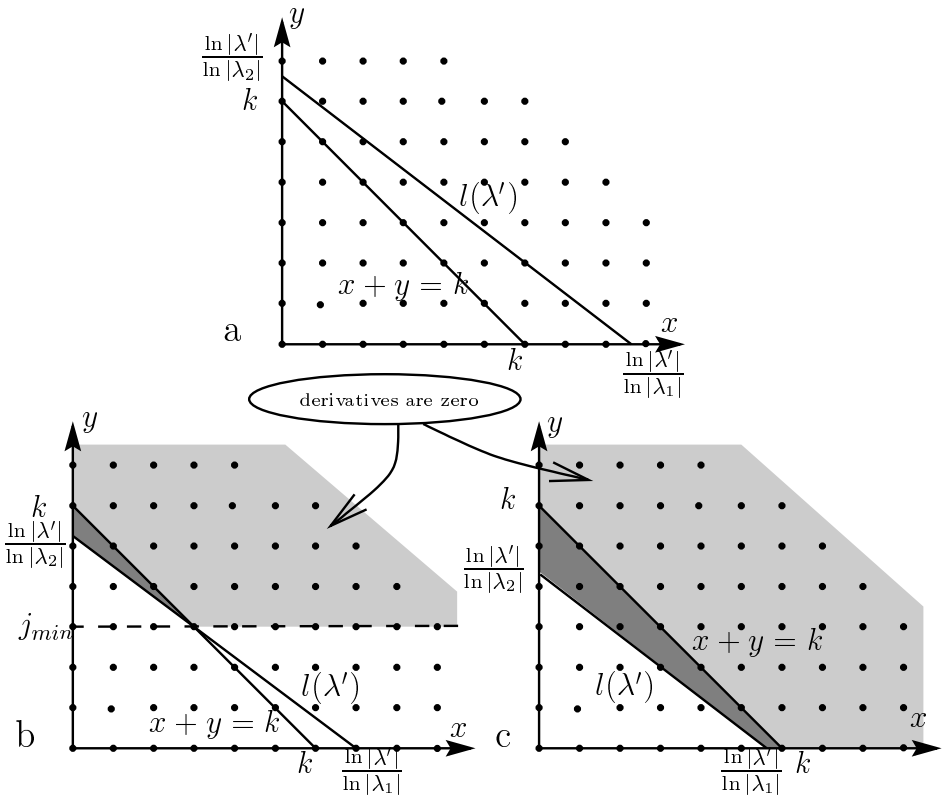

Figure 3.12: (a) $|\lambda'| < |\lambda_2|^k$; All variables up to order k exist. (b) $|\lambda'| > |\lambda_2|^k$, $j_{min} = 0$; The function f_m has to be a polynomial. (c) $|\lambda'| > |\lambda_2|^k$, $j_{min} \neq 0$; derivative $\partial_2^{j_{min}} f_m$ has to be a polynomial.

Before formulating the result following from these considerations, recall the definition of the sets of polynomials $\mathbf{P}(p,q)$, generalizing the idea of homogeneous polynomials to the case of nonuniform scaling of variables. Let $\mathbf{N}(p,q)$ be the set of all pairs of integers (i,j) such that $\lambda_1^i\lambda_2^j = \lambda_1^p\lambda_2^q$ for a fixed pair (p,q) Then

$$\mathbf{P}(p,q) = \left\{ \sum_{i,j} \alpha_{ij}\xi_1^i\xi_2^j \;\middle|\; (i,j) \in N(p,q),\ \alpha_{ij} \in \mathbf{C} \right\}$$

Lemma 3.16. *Suppose a set of functions $f_m(\xi)$, $m = 0 \ldots n$ satisfies the conditions of Lemma 3.15. If $|\lambda'| \geq |\lambda_2|^k$, set*

$$j_{min} = \min \{ j \in \mathbf{N} | \left| \lambda_1^i\lambda_2^j \right| \leq |\lambda'|,\ i+j \leq k, \quad \textit{for some } i \in \mathbf{N} \}$$

.

All functions are C^k-continuous at 0 if and only if one of the following conditions holds:

1. $|\lambda'| < |\lambda_2|^k$,
2. $\lambda' = \lambda_1^p\lambda_2^{q+j_{min}}$ *for some* p, q, $p+q \leq k-j_{min}$, $\partial_2^{j_{min}} f_n(\xi) \in \mathbf{P}(p,q)$, *and* $\partial_2^{j_{min}} f_m(\xi) \equiv 0$ *for* $m < n$.
3. $\partial_2^{j_{min}} f_m(\xi) \equiv 0$ *for all* m.

Proof.

Necessity. Suppose $|\lambda'| \geq |\lambda_2|^j$. As it was observed above, all derivatives corresponding to the integer points in the area between $l(\lambda')$ and $x+y=k$ should be constant. Note that all derivatives $\partial_1^i\partial_2^{j+j_{min}} f_m$ for all m and for $i+j > k-j_{min}$ are 0. This means that $\partial_2^j f_m$ is a polynomial because all its derivatives of order $k-j_{min}$ are zeros.

Suppose $\partial_1^p\partial_2^{q+j_{min}} f_n$ is not zero for some p and q satisfying $p+q \leq k-j_{min}$. Then it follows from Lemma 3.15 that $\lambda' = \lambda_1^p\lambda_2^{q+j_{min}}$.

Moreover, as the polynomial $\partial_1^{j_{min}} f_0(\xi)$ should satisfy the scaling relation for $\lambda'/\lambda_2^{j_{min}} = \lambda_1^p\lambda_2^q$, $\partial_1^{j_{min}} f_0(\xi)$ should be contained in $P(p,q)$. On the other hand, if for a pair i,j $|\lambda^i\lambda^j| \geq |\lambda^p\lambda^q|$, $\partial_1^{j_{min}} f_0$ cannot contain the monomial $C\xi_1^i\xi_2^j$ unless $n=0$. In particular, $\partial_1^{j_{min}} f_0$ cannot contain any monomials from $P(p,q)$; therefore, $f_0(\xi) \equiv 0$. By induction, all $\partial_1^{j_{min}} f_m$ for $m < 0$ are identically zero and $\partial_1 j_{min} f_n$ is contained in $P(p,q)$.

Sufficiency. If the first condition of the lemma is satisfied, the derivatives up to order k exist by Lemma 3.15.

Suppose the second or the third condition is satisfied. Then all derivatives $\partial_1^i \partial_2^j f_m$ exist for $j \geq j_{min}$. However, if $j < j_{min}$, the scaled versions of the derivatives $\tilde{f}_m$ satisfy scaling relation for $\frac{\lambda'}{\lambda_1^i \lambda_2^j}$, and $\left|\frac{\lambda'}{\lambda_1^i \lambda_2^j}\right| < 1$ by definition of j_{min}. Therefore, all other derivatives also exist.

□

The condition on $\partial_2^{j_{min}} f_m$ does not give the explicit form for the functions f_m unless $j_{min} = 0$. It is possible to find a more explicit expression for f_m that are C^k and satisfy scaling relation for λ'.

Integrate the expression for the derivative, we obtain the following formulas:

$$\begin{aligned} f_n(\xi) &= \xi_2^{j_{min}} p(\xi) + \sum_{s=0}^{j_{min}-1} h_n^s(\xi_1)\xi_2^s \\ f_m(\xi) &= \sum_{s=0}^{j_{min}-1} h_m^s(\xi_1)\xi_2^s \quad \text{for } m < n \end{aligned} \tag{3.27}$$

where h_m^s are some functions of ξ_1. The functions f_m satisfy

$$\begin{aligned} f_m(\lambda_1\xi_1, \lambda_2\xi_2) &= \lambda_1^p \lambda_2^{q+j_{min}} f_m(\xi) + f_{m-1}(\xi) \\ f_0(\lambda_1\xi_1, \lambda_2\xi_2) &= \lambda_1^p \lambda_2^{q+j_{min}} f_0(\xi) \end{aligned}$$

Regarding f_m as polynomials in ξ_2, we obtain equations for h_m^s:

$$\begin{aligned} \lambda_2^s h_m^s(\lambda_1\xi_1) &= \lambda_1^p \lambda_2^{q+j_{min}} h_m^s(\xi) + h_{m-1}^s(\xi) \\ \lambda_2^s h_0^s(\lambda_1\xi_1) &= \lambda_1^p \lambda_2^{q+j_{min}} h_m^s(\xi) \end{aligned}$$

Substituting $h_m^s = \lambda_2^{-sm} f_m^s(\xi)$, we can see that the set of functions $f_m^s(\xi)$, $m = 0 \ldots n$ satisfies one-dimensional λ_1-scaling relations for $\lambda_1^p \lambda_2^{q+j_{min}-s}$:

$$f_m^s(\lambda_1\xi_1) = \lambda_1^p\lambda_2^{q+j_{min}-s} f_m^s(\xi_1) + f_{m-1}^s(\xi_1) \quad \text{for } m > 0$$
$$f_0^s(\lambda_1\xi_1) = \lambda_1^p\lambda_2^{q+j_{min}-s} f_0^s(\xi_1)$$

Fixing ξ_2, at a set of values $x_1 \dots x_{j_{min}}$ such that the matrix

$$\begin{pmatrix} 1 & x_1 & x_1^2 & . & . & . & x_1^{j_{min}-1} \\ 1 & x_2 & x_2^2 & . & . & . & x_2^{j_{min}-1} \\ . & & & & & & . \\ . & & & & & & . \\ . & & & & & & . \\ 1 & x_{j_{min}} & x_{j_{min}}^2 & . & . & . & x_{j_{min}}^{j_{min}-1} \end{pmatrix}$$

has nonzero determinant, we can express $h_m^s(\xi_1)$ as linear combinations of $f_m(\xi_1, \xi_2)$ with $\xi_2 \in \{x_1 \dots x_{j_{min}}\}$. Therefore, the functions have to be C^k-continuous if f_m is C^k-continuous. Therefore, $f_m^s(\xi_1)$ also have to be C^k-continuous.

A direct computation shows that if f_m^s are C^k-continuous and satisfy λ^1-scaling relations for $\lambda_1^p\lambda_2^{q+j_{min}-s}$, then f_m, $m = 0 \dots n$ defined as above satisfy (λ_1, λ_2)-scaling relations for $\lambda_1^p\lambda_2^{q+j_{min}}$.

Therfore, we can restate Lemma 3.16 in the following more explicit form

Lemma 3.17. *The functions $f_m(\xi)$, $m = 0 \dots n$ that are C^k-continuous on a set $D \setminus \{0\}$, where D is a compact set containing zero as an internal point satisfy the (λ_1, λ_2)-scaling relation and are C^k-continuous at zero, if and only if one of the following conditions is satisfied:*

1. $|\lambda'| < |\lambda_2|^k$,

2. $\lambda' = \lambda_1^p\lambda_2^{q+j_{min}}$ *for some nonnegative* p, q, $p + q \le k - j_{min}$ *and*

$$f_n(\xi) = \xi_2^{j_{min}} p(\xi_1, \xi_2) + \sum_{s=0}^{j_{min}-1} \lambda_2^{-sn} f_n^s(\xi_1)\xi_2^s$$
$$f_m(\xi) = \sum_{s=0}^{j_{min}-1} \lambda_2^{-sm} f_m^s(\xi_1)\xi_2^s$$

where f_m^s are C^k-continuous and satisfy the λ_1-scaling relation for $\lambda_1^p \lambda_2^{j+j_{min}-s}$.

3.

$$f_m(\xi) = \sum_{s=0}^{j_{min}-1} \lambda_2^{-sm} f_m^s(\xi_1)\xi_2^s$$

where f_m^s are C^k-continuous and satisfy the λ_1-scaling relation for $\lambda' \lambda_2^{-s}$.

For $|\lambda' \lambda_2^{-s}| > 1$ this implies that $f_m^s(\xi) \equiv 0$ for all m; for $|\lambda' \lambda_2^{-s}| = 1$, $f_n^s(\xi) = const$ and $f_m^s(\xi) \equiv 0$ for $m < n$.

If $\lambda_1 = \lambda_2$, it is guaranteed that $j_{min} = 0$. Moreover, the set $\mathbf{P}(p, q)$ becomes simply the set of homogeneous polynomials of a given degree $p + q$.

This case is particularly important for the analysis of subdivision schemes, so we state is as a separate corollary.

Corollary 3.18. *Suppose a set of functions $f_m(\xi)$, $m = 0 \ldots n$ satisfies the conditions of Lemma 3.15 for $\lambda_1 = \lambda_2 = \lambda$. All functions are C^k-continuous at 0 if and only if one of the following conditions holds:*

1. *$|\lambda'| < |\lambda|^k$,*
2. *$\lambda' = \lambda^p$ for some p, $f_n(\xi)$ is a homogeneous polynomial of degree j, and $f_m(\xi) \equiv 0$ for all $m < n$.*
3. *$f_m(\xi) \equiv 0$ for all m.*

3.13.2 Complex-Conjugate Eigenvalues

In this section we consider the case of scaling relations

$$f_m(T\xi) = \lambda' f_m(\xi) + f_{m-1}(\xi), \quad \text{for } m \geq 1$$
$$f_0(T\xi) = \lambda' f_0(\xi)$$

with

$$T = \begin{pmatrix} \lambda\cos\varphi & -\lambda\sin\varphi \\ \lambda\sin\varphi & \lambda\cos\varphi \end{pmatrix}$$

In this case it is convenient to consider ξ to be a complex number.

We introduce operators $\partial = \partial_1 - i\partial_2$ and $\bar{\partial} = \partial_1 + i\partial_2$. Clearly, any derivative $\partial_1^i \partial_2^j$ can be expressed as a linear combination of operators $\partial^s \bar{\partial}^t$ with $s + t = i + j$. We examine conditions for existence and continuity of derivatives of the form $\partial^i \bar{\partial}^j$, for $i + j \leq k$, which is equivalent to C^k continuity.

Observe that $T\xi = \lambda\xi$, where $\lambda = \lambda \exp i\varphi$.

Thus, the scaling relation takes the form

$$\begin{aligned} f_m(\lambda\xi) &= \lambda' f_m(\xi) + f_{m-1}(\xi), \quad \text{for } m \geq 1 \\ f_0(\lambda\xi) &= \lambda' f_0(\xi) \end{aligned} \tag{3.28}$$

If the system of functions $f_m(\xi)$ satisfies (3.28) we say that it satisfies λ-scaling relation for λ'.

The following two equations make the transfer of Lemmas 3.14-3.17 a straightforward operation:

$$\begin{aligned} \partial(f(\lambda\xi)) &= \lambda(\partial f)(\lambda\xi) \\ \partial(f(\lambda\xi)) &= \bar{\lambda}(\partial f)(\lambda\xi) \end{aligned} \tag{3.29}$$

Lemma 3.15 becomes

Lemma 3.19. *If a system of functions satisfies the λ-scaling relation for λ', the functions are defined on a compact domain containing 0 as an internal point, and are C^k everywhere except 0, then the derivative $\partial^i \bar{\partial}^j f_m(\xi)$, $i + j \leq k$, exists at 0 and is continuous if and only if one of the following conditions is met:*

1. $|\lambda'| < |\lambda|^{i+j}$

2. $\lambda' = \lambda^i \bar{\lambda}^j$, $\partial_1^i \partial_2^j f_n(\xi) \equiv const$, *and* $\partial^i \bar{\partial}^j f_m(\xi) \equiv 0$ *for all* $m < n$.

3. $\partial_1^i \partial_2^j f_m(\xi) \equiv 0$ *for all* m.

The proof of this lemma exactly repeats the proof of Lemma 3.15, if λ_1 and λ_2 are replaced with λ and $\bar{\lambda}$ respectively, and ∂_1 and ∂_2 are replaced with ∂ and $\bar{\partial}$.

The analog of Lemma 3.16 is much simpler due to the fact that $|\lambda| = |\bar{\lambda}|$, and is more similar to the Corollary 3.18.

Recall the definition of $\bar{\mathbf{N}}$ and $\bar{\mathbf{P}}$: $\bar{\mathbf{N}}(p,q)$ is the set of all pairs of integers (i,j) such that $\lambda^i \bar{\lambda}^j = \lambda^p \bar{\lambda}^q$ for a fixed pair (p,q) Then

$$\bar{\mathbf{P}}(p,q) = \Big\{ \sum_{i,j} \alpha_{ij} \xi_1^i \bar{\xi}_2^j \;\Big|\; (i,j) \in \bar{\mathbf{N}}(p,q),\ \alpha_i j \in \mathbf{C} \Big\}$$

Lemma 3.20. *Suppose a set of functions* $f_m(\xi)$, $m = 0 \dots n$ *satisfies the conditions of Lemma 3.19.*

All functions are C^k*-continuous at 0 if and only if one of the following conditions holds*

1. $|\lambda| < |\lambda|^k$,

2. $\lambda' = \lambda^p \bar{\lambda}^q$ *for some* p, q, $f_n(\xi) \in \bar{\mathbf{P}}(p,q)$, $p+q \le k$, *and* $f_m(\xi) \equiv 0$ *for* $m < n$.

3. $f_m(\xi) \equiv 0$ *for all* m.

The crucial observation is that in this case j_{min} is always 0. Using the same substitutions as for Lemma 3.19, we obtain the proof of the last lemma from the proof of Lemma 3.16.

3.13.3 Jordan Block of Size 2

Finally, we consider the case when

$$T = J_2(\lambda) = \begin{pmatrix} \lambda & 1 \\ 0 & \lambda \end{pmatrix}$$

If a system of functions $f_0, \dots f_n$ satisfies scaling relations (3.22) with $T = J_2(\lambda)$, we say that these functions satisfy $J_2(\lambda)$-scaling relations for λ'.

Applying $\partial_1^p \partial_2^{k-p}$ to $f_m(T\cdot)$ we obtain the following expression for the derivative:

$$\left(\partial_1^p \partial_2^{k-p} f_m(T\,\cdot)\right)(\xi) = \sum_{l=p}^{k} \binom{k-p}{l-p} \lambda^{k-l+p} \partial_2^{k-l} \partial_1^l f_m(T\xi)$$

Write each equation for $m > 0$ in the set of scaling relations in the matrix form:

$$\begin{pmatrix} \lambda^k & k\lambda^{k-1} & \binom{k}{2}\lambda^{k-2} & . & 1 \\ 0 & \lambda^k & (k-1)\lambda^{k-1} & . & \lambda \\ 0 & 0 & \lambda^k & . & \lambda \\ . & & & & . \\ . & & & & . \\ 0 & . & . & . & \lambda^k \end{pmatrix} \begin{pmatrix} \partial_2^k f_m(T\xi) \\ \partial_1^1 \partial_2^{k-1} f_m(T\xi) \\ \partial_1^2 \partial_2^{k-2} f_m(T\xi) \\ . \\ . \\ \partial_1^k f_m(T\xi) \end{pmatrix} = \begin{pmatrix} \partial_2^k(\lambda' f_m(\xi) + f_{m-1}(\xi)) \\ \partial_1^1 \partial_2^{k-1}(\lambda' f_m(\xi) + f_{m-1}(\xi)) \\ \partial_1^2 \partial_2^{k-2}(\lambda' f_m(\xi) + f_{m-2}(\xi)) \\ . \\ . \\ \partial_1^k f_m(\xi) \end{pmatrix} \tag{3.30}$$

Similar equation holds for f_0, with f_{m-1} removed. Denote the vector of derivatives $\tilde{f}_m(\xi) = [\partial_2^k f_m(\xi),\, \partial_1^2 \partial_2^{k-2} f_m(\xi), \ldots \partial_1^k f_m(\xi)]^T$ and let B be the matrix on the left side of (3.30). Then (3.30) becomes

$$B\tilde{f}_m(T\xi) = \lambda' \tilde{f}_m(\xi) + \tilde{f}_{m-1}(\xi)$$

Equations for all m can be written together as

$$\begin{pmatrix} B & & & & \\ & B & & & \\ & & . & & \\ & & & . & \\ & & & & B \end{pmatrix} \begin{pmatrix} \tilde{f}_n(T\xi) \\ \tilde{f}_{n-1}(T\xi) \\ . \\ . \\ \tilde{f}_0(T\xi) \end{pmatrix} = \begin{pmatrix} \lambda' I & I & & & \\ & \lambda' I & I & & \\ & & . & & \\ & & & . & \\ & & & & \lambda' I \end{pmatrix} \begin{pmatrix} \tilde{f}_n(\xi) \\ \tilde{f}_{n-1}(\xi) \\ . \\ . \\ \tilde{f}_0(\xi) \end{pmatrix}$$

multiplying by the inverse of the matrix on the right we get

$$\begin{pmatrix} \tilde{f}_n(T\xi) \\ \tilde{f}_{n-1}(T\xi) \\ . \\ . \\ . \\ \tilde{f}_0(T\xi) \end{pmatrix} = \begin{pmatrix} \lambda' B^{-1} & B^{-1} & & & & \\ & \lambda' B^{-1} & B^{-1} & & & \\ & & . & & & \\ & & & . & & \\ & & & & . & \\ & & & & & \lambda' B^{-1} \end{pmatrix} \begin{pmatrix} \tilde{f}_n(\xi) \\ \tilde{f}_{n-1}(\xi) \\ . \\ . \\ . \\ \tilde{f}_0(\xi) \end{pmatrix} \tag{3.31}$$

Let $\mathcal{B}$ be the matrix on the right, $\mathcal{B}_N$ be its Jordan form, P the matrix such that $P\mathcal{B}P^{-1} = \mathcal{B}_N$, and let $\tilde{f}$ be the vector $[\tilde{f}_n, \tilde{f}_{n-1} \dots \tilde{f}_0]^T$; then (3.31) can be written as

$$P\tilde{f}(T\xi) = \mathcal{B}_N P\tilde{f}(\xi)$$

Note that $\mathcal{B}$ is triangular with λ'/λ^k on the diagonal. Therefore, $\mathcal{B}$ has a single eigenvalue λ'/λ^k. The vector $P\tilde{f}$ can be separated into several sets of functions satisfying $J_2(\lambda)$-scaling relations for λ'/λ^k. If $|\lambda'| < |\lambda^k|$, all components of $P\tilde{f}$ and hence all derivatives $\partial_1^i \partial_2^j f_m$ for all $i + j \leq k$ and m are continuous at zero. If $|\lambda'| \geq |\lambda^k|$ all components of $P\tilde{f}$ are necessarily constant (zero if $\lambda' \neq \lambda^k$). We conclude that in this case the functions $f_m(\xi)$ have to be polynomials of degree no higher than k.

Next, we prove that all such polynomials have to be homogeneous. We start with the polynomial f_0. Any polynomial in two variables $(\xi_1, \xi_2) = \xi$ can be written as $f_0(\xi) = \sum_{j=0}^{k} H^j(\xi)$ where H_j is a homogeneous polynomial of degree j.

Note that $H^j(T\xi)$ is also homogeneous of degree j. Therefore, the scaling relation $f_0(T\xi) = \lambda' f_0(\xi)$ can be written separately for each homogeneous component

$$H^j(T\xi) = \lambda' H^j(\xi)$$

Write $H^j(\xi) = \sum_{i=0}^{j} \alpha_i \xi_1^i \xi - 2^{j-i}$. Then for $H^j(T\xi)$ we have

$$H^j(T\xi) = \sum_{i=0}^{j} \sum_{l=0}^{i} \binom{i}{l} \alpha_i \lambda^{l+j-i} \xi_1^l \xi^{j-l} = \sum_{l=0}^{j} \xi^l \xi_2^{j-l} \left(\sum_{i=l}^{j} \binom{i}{l} \alpha_i \lambda^{l+j-i} \right) \tag{3.32}$$

Using (3.32), we can write the scaling relation as

$$\sum_{l=0}^{j} \xi^l \xi_2^{j-l} \left(\sum_{i=l+1}^{j} \binom{i}{l} \alpha_i \lambda^{l+j-i} + (\lambda^j - \lambda') \alpha^l \right) = 0$$

For the polynomial to be identically zero, each coefficient has to be zero; therefore, α_i have to satisfy the linear system of equations

$$\sum_{i=l+1}^{j} \binom{i}{l} \alpha_i \lambda^{l+j-i} + (\lambda^j - \lambda') \alpha^l = 0, \quad l = 0 \dots j \tag{3.33}$$

Note that the matrix of the system is triangular with identical entries $\lambda' - \lambda^j$ on the diagonal. This system has a nontrivial solution if and only if $\lambda' = \lambda^j$ for some $j \leq k$. As $\lambda' = \lambda^j$ can hold only for one j, only one component $H^j(\xi)$ of $f_0(\xi)$ can be nonzero. Therefore, f_0 is a homogeneous polynomial. Moreover, if we assume that $\lambda' = \lambda^j$, then we can immediately solve the system: clearly, $\alpha = C$, $\alpha_m = 0$ for $m > 0$ is a solution for any C. The entries above the diagonal are all nonzero, therefore the rank of the system is j, with total size 1, and the space of solutions is one-dimensional. We conclude that $f_0(\xi) = C\xi^j$ if $\lambda' = \lambda^j$.

Our next task is to find expressions for $f_m(\xi)$. Suppose $f_m(\xi)$ is homogeneous of degree j and $\lambda' = \lambda^j$. Then the equations for a homogeneous component of f_{m+1} of degree p different from j are identical to the equations (3.33) with p instead of j. These systems have only trivial solutions, therefore, all polynomials f_m are homogeneous of the same degree j.

Let $f_m(\xi) = \sum_{i=0}^{j} \alpha_{mi} \xi_1^i \xi^{j-i}$. Then α_{mi} $i = 0 \dots j$ are solutions of the linear system of equations

$$\sum_{i=l+1}^{j} \binom{i}{l} \alpha_i \lambda^{l+j-i} = \alpha_{m-1\,l}, \quad l = 0 \dots j-1 \tag{3.34}$$

Note that the system has rank j and α_{m0} is not present in any equation. Therefore, once $\alpha_{m-1\,l}$ are fixed, all possible α_{ml} form a one-dimensional space. As f_0 linearly depends on 1 constant, then f_1 linearly depends on 2 constants, etc. If we construct a family of solutions with f_m depending on $m+1$ constant, we found all possible solutions.

Observe that we can formally write for any homogeneous polynomial of degree j

$$f_m(\xi_1, \xi_2) = \xi_2^j Q_m(\xi_1/\xi_2)$$

where $Q_m(t)$ is a polynomial with one variable. Note that $Q_0(t) = C$. Scaling relations can be written as

$$Q_m(t + \frac{1}{\lambda}) = Q_m(t) + \frac{1}{\lambda^j} Q_{m-1}(t)$$

for $m > 0$. Introduce polynomials $F_m(t) = \lambda^{mj} Q_m(\frac{t}{\lambda})$, i.e. $Q_m(t) = \frac{1}{\lambda^{mj}} F_m(\lambda t)$.

After substituting t instead of λt, we reduce the scaling relations to a form that does not depend on λ or j:

$$F_m(t+1) = F_m(t) + F_{m-1}(t); \quad F_0(t) = C \tag{3.35}$$

Note that if we have one solution of the recurrence (3.35), we can immediately obtain a solution with sufficient number of constants to span the whole space of sets homogeneous polynomials satisfying scaling relations: if $F_m(t)$, $m = 0 \ldots n$, is a solution, then $\sum_{i=0}^{m} C_i F_i(t), \quad m = 0 \ldots n$ is also a solution. A single solution of (3.35) can be guessed and is given for $F_0(x) = 1$ by

$$F_m(t) = \frac{1}{m!} \prod_{i=0}^{m-1} (x - i) \quad \text{for } m > 0 \tag{3.36}$$

This leads us to the following general expression for f_m:

$$f_m(\xi) = \sum_{i=0}^{m-l} C_{m-l-i} \frac{\xi_2^j}{\lambda^{mi}} F_i(\frac{\lambda \xi_1}{\xi_2})$$

where $l = \max(0, n - j)$.

We summarize our derivation in the following Lemma:

Lemma 3.21. *All functions $f_m(\xi)$ in a set satisfying $J_2(\lambda)$-scaling relations for λ' are C^k-continuous if and only if one of the following conditions holds:*

1. $|\lambda'| < |\lambda^k|$.

2. $\lambda' = \lambda^j$ *for* $j \leq k$ *and for* $m \geq n - j$

$$f_m(\xi) = \sum_{i=0}^{m-l} C_{m-l-i} \frac{\xi_2^j}{\lambda^{mi}} F_i(\frac{\lambda \xi_1}{\xi_2})$$

where $F_m(t) = \frac{1}{m!} \prod_{i=0}^{m-1}(x - i)$ *for* $m > 0$, $F_0(t) = 1$ *and* $l = \max(0, n - j)$. *For* $m < n - j$ $f_m(\xi) \equiv 0$.

3. *All* $f_m(\xi) \equiv 0$.

Chapter 4 Constructive Conditions for Smoothness

In this chapter we concentrate on constructive ways of proving C^1-continuity of subdivision schemes. As it was shown in Chapter 3 a generalization of Reif's sufficient condition is necessary for practical subdivision schemes unless they have eigenbasis functions with rather specific structure. All previous applications of Reif's criterion were restricted by necessity to the schemes that produce piecewise polynomial surfaces away from the extraordinary points. We develop methods that allow us to determine if a subdivision scheme is smooth even if there is no closed-form parameterization of the part of the surface away from the extraordinary points.

We start with several lemmas that show that injectivity and regularity of the a map generated by subdivision can be inferred from a sufficiently close linear approximation, due to the convergence of the linear approximations to the limit functions in the Lipschitz norm.

We show that a simple condition guarantees that the characteristic map is a covering, whether it is C^1-continuous or not, and thus the question of injectivity can be reduced to computing the winding number of a curve, leaving regularity as the only non-trivial part.

Next, we demonstrate how the difference between a linear approximation and the limit map can be estimated using contractivity with respect to a suitably chosen function, following [6] and [18]. We derive explicit formulas for the convergence rate for two classes of schemes: traditional uniform stationary schemes and a particular class of nonuniform schemes – schemes with creases. In particular, our estimates allow us to prove smoothness of a parameterized family of subdivision schemes on the regular complexes.

We conclude with an outline of the algorithm for checking smoothness of subdivision; details of the implementation for particular classes of schemes are discussed in the next chapter.

4.1 Injectivity of the Characteristic Map

In Section 3.10, the question of C^1-continuity of a subdivision scheme was reduced to checking local regularity of the parametric map and compatibility of eigenbasis functions once it is known that the scheme is tangent plane continuous. From the practical point of view, the schemes with regular injective characteristic maps are the most useful. If the characteristic map is injective with non-zero Jacobian everywhere it is defined, it is sufficient for C^1-continuity.

We show that, in general, injectivity of the characteristic map can be inferred from injectivity of a sufficiently close linear approximation.

4.1.1 Lipschitz Norms

In this section we state several simple facts about Lipschitz continuous functions with a special structure and prove a criterion for injectivity.

In the following lemmas we assume that f is a mapping from $\mathbf{R}^n$ to $\mathbf{R}^m$ ($\mathbf{C}^n$ can be identified with $\mathbf{R}^{2n}$ for our purposes).

It does not matter which particular norm from the family $\|\cdot\|_p$, $p = 1 \ldots \infty$ we use in a finite-dimensional space when examining convergence, as the topologies induced by all norms are identical. However, as we may have to compute certain norms explicitly, it is useful to make estimates for a general p and choose a norm which is most convenient computationally (typically, $\|\cdot\|_1$). We use the following general relation establishing equivalence between norms in $\mathbf{R}^n$:

$$\|x\|_q \leq \|x\|_p \leq n^{\frac{1}{p}-\frac{1}{q}} \|x\|_q, \quad \text{for} \quad p < q \tag{4.1}$$

the Lipschitz norm for functions from $\mathbf{R}^n$ to $\mathbf{R}^m$ can be defined for any given pair of norms on the domain and range. For our purposes it is sufficient to consider the same norm on both. Denote

$$\|f\|_{Lip,p} = \sup_{x_1,x_2} \frac{\|f(x_1) - f(x_2)\|_p}{\|x_1 - x_2\|_p} \tag{4.2}$$

Lemma 4.1. *For a C^1 function f defined on a compact convex domain,*

$$\|f\|_{Lip,p} \leq C \left\| \|\nabla f\|_p \right\|_\infty$$

where C depends only on p, and ∇f is the $n \times m$ Jacobi matrix of f, with the standard linear operator norm.

Proof. First, we prove this fact for the norm $\|\cdot\|_2$. Note that

$$\|f(x_2) - f(x_1)\|_2 = \frac{\partial}{\partial \tau} \|f(\widehat{x})\|_2 \|x_1 - x_2\|_2$$

where the direction of the derivative is $\tau = \frac{x_2 - x_1}{\|x_2 - x_1\|_2}$ and $\widehat{x}$ is a point of the line segment $[x_1, x_2]$.

$$\frac{\partial}{\partial \tau} \|f(\widehat{x})\|_2 = \frac{\left(f(\widehat{x}), \frac{\partial}{\partial \tau} f(\widehat{x})\right)}{\|f(\widehat{x})\|_2} \leq \left\| \frac{\partial}{\partial \tau} f(\widehat{x}) \right\|_2 = \|\nabla f(\widehat{x}) \tau\|_2 \leq \|\nabla f(\widehat{x})\|_2$$

Thus, $\|f\|_{Lip,2} \leq \| \|\nabla f\|_2 \|_\infty$. Using the bounds given by the norm equivalence, we get the statement of the lemma for $p \geq 2$:

$$\begin{aligned} \|f\|_{Lip,p} = \sup \frac{\|f(x_2) - f(x_1)\|_p}{\|x_2 - x_1\|_p} &\leq n^{\frac{1}{2} - \frac{1}{p}} \sup \frac{\|f(x_2) - f(x_1)\|_2}{\|x_2 - x_1\|_2} \leq n^{\frac{1}{2} - \frac{1}{p}} \| \|\nabla f\|_2 \|_\infty \\ &\leq n^{\frac{1}{2} - \frac{1}{p}} m^{\frac{1}{2} - \frac{1}{p}} \left\| \|\nabla f\|_p \right\|_\infty \end{aligned} \tag{4.3}$$

For $p = 1$, we get the estimate

$$\begin{aligned} \|f\|_{Lip,2} = \sup \frac{\|f(x_2) - f(x_1)\|_p}{\|x_2 - x_1\|_p} &\leq n^{\frac{1}{2}} \sup \frac{\|f(x_2) - f(x_1)\|_2}{\|x_2 - x_1\|_2} \\ &\leq n^{\frac{1}{2}} \| \|\nabla f\|_2 \|_\infty \leq (nm)^{\frac{1}{2}} \left\| \|\nabla f\|_p \right\|_\infty \end{aligned} \tag{4.4}$$

□

Lemma 4.2. *Assume that a function is piecewise C^1-continuous on a union of convex domains and on each domain it is C^1, with one-sided limits of the gradients existing on the boundary. In addition, assume that there is a constant B, such that for any x_1 x_2 there is a piecewise linear path in A connecting x_1 and x_2 of length no more than $B\|x_1 - x_2\|_p$. Then*

$$\|f\|_{Lip,p} < BC\left\|\|\nabla f\|_p\right\|_\infty$$

Proof. Let $b_0 = x_1', b_1, \ldots b_n = x_2'$ be intersections of a segment $[x_1', x_2']$ of a piecewise linear path connecting

with domain boundaries. Then

$$\begin{aligned}\left\|f(x_1') - f(x_2')\right\|_p &\le \sum_{i=0}^{n-1} \|f(b_{i+1}) - f(b_i)\|_p \\ &\le C\left\|\|\nabla f\|_p\right\|_\infty \sum_i \|b_{i+1} - b_i\|_p = C\left\|\|\nabla f\|_p\right\|_\infty \left\|x_1' - x_2'\right\|_p\end{aligned}$$

□

Summing the inequalities for all intervals of the path, we get the estimate of the lemma.

Lemma 4.3. *Let Ω be a compact set. Suppose f is Lipschitz continuous on Ω. If L^j is a sequence of functions converging to g in the Lipschitz norm, and*

$$0 < K' \le \left\|L^j(x_2) - L^j(x_1)\right\|_p / \|x_2 - x_1\|_p \le K$$

for some K and sufficiently large j. Then f is injective.

Proof. As for any x_1, x_2

$$0 < K' \le \frac{\left\|L^j(x_1) - L^j(x_2)\right\|_p}{\|x_1 - x_2\|_p} \le K$$

.

Suppose $\left\|L^j - f\right\|_{Lip,p} < \epsilon$.

Then

$$\frac{\|f(x_1) - f(x_2)\|_p}{\|x_1 - x_2\|_p} \ge \frac{\left\|L^j(x_1) - L^j(x_2)\right\|_p}{\|x_1 - x_2\|_p} - \left\|L^j - f\right\|_{Lip,p} \ge K' - \epsilon$$

.

Therefore, if $\epsilon < K'$, $\frac{\|f(x_1) - f(x_2)\|_p}{\|x_1 - x_2\|_p} \ge K'$ for $x_1 \ne x_2$, which means that g is invertible.

□

We call the ratio $\|f(x_2) - f(x_1)\|_p / \|x_2 - x_1\|_p$ the *Lipschitz ratio* of f.

4.1.2 Injectivity Criterion

In this section we show how injectivity of the characteristic map can be inferred from a sufficiently close linear approximation.

First, we note that Theorem 3.1 from [6] works also if the *Haar subdivision scheme* $H^{l,m}$, where (l, m) is one of six points adjacent to (0,0) on three-directional grid, used as a comparison scheme

Definition 4.1. *On a regular complex define Haar subdivision* $H^{l,m}$ *by*

$$\begin{aligned} p^{k+1}\left(m(v_{ij}, v_{i(j+m)})\right) &= \\ p^{k+1}\left(m(v_{ij}, v_{(i+l)j})\right) &= \\ p^{k+1}\left(m(v_{ij}, v_{(i+l)(j+m)})\right) &= \\ p^{k+1}(v_{ij}) &= p^k(v_{ij}) \end{aligned}$$

where $m(u, v)$ *denotes the midpoint of the edge* (u, v)*, and the pair* l, m *is one of* $(0, 1)$*,* $(1, 0)$*,* $(-1, -1)$*,* $(1, 1)$*,* $(-1, 0)$*,* $(0, -1)$*.*

In the formulas of the definition, we use notation $v(u, w)$ for the vertex of $D(\mathcal{R})$ inserted at the edge (u, w).

Note that the limit function is discontinuous (piecewise constant). Convergence, however, is obvious, and basis functions satisfy a trivial scaling relation. The domains of the basis functions are shown in 4.1; each function is constant and equal to 1 on its domain.

Stability of Haar subdivision is obvious.

If the comparison scheme B in Theorem 3.1 from [6] is taken to be $H^{l,m}$, $\mathcal{S}$ still converges and the estimate for the convergence rate is the same as in [6].

Theorem 4.4. *Suppose* $\mathcal{S}$ *is a convergent subdivision scheme on a complex* K *with* $|K|$ *being a subset of the plane satisfying the conditions of Lemma 4.2. Suppose for any vertex of* K *there is a piecewise linear one-to-one mapping* μ_v *from* $U_1(v)$ *to a subcomplex of the regular complex. Then the linear approximations converge to the limit surface in the Lipschitz norm, if* $\mathcal{S}$ *is* C^1 *on the regular complex.*

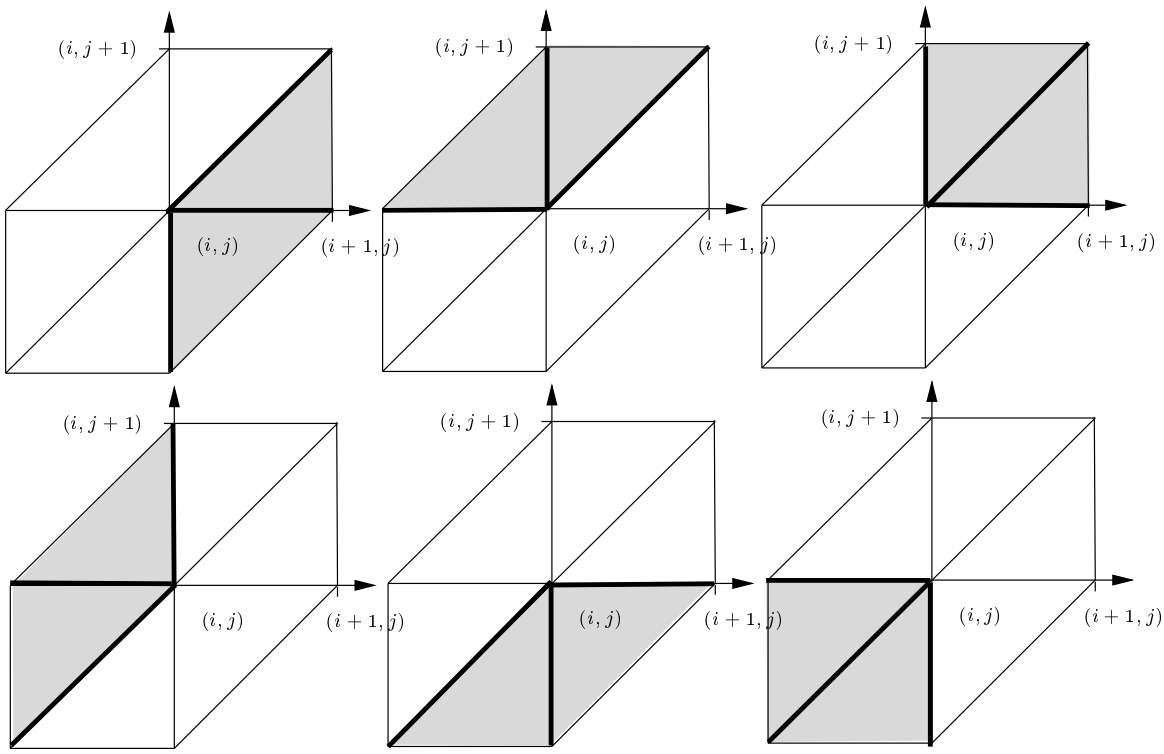

Figure 4.1: Domains of the basis functions $\varphi_{i,j}$ for $H^{l,m}$, $(l,m) = (1,0)$, $(0,1)$, $(1,1)$ (first row) $(-1,0)$, $(0,-1)$, $(-1,-1)$ (second row). Thick triangle boundaries are included in the domain; each function is 1 inside the domain and 0 outside.

Proof. For the regular complex we introduce the difference scheme d^1, following Dyn and Levin [18]:

$$\begin{aligned}(d^1p)(v_{ij})_1 &= 2^k(p^k_{(i+1)j} - p^k_{ij})\\ (d^1p)(v_{ij})_2 &= 2^k(p^k_{i(j+1)} - p^k_{ij})\end{aligned} \tag{4.5}$$

If $\mathcal{S}$ is C^1 there is a matrix subdivision scheme $\mathcal{S}^{(1)}$ such that

$$d^1p^{k+1} = S^{(1)}d^1p^k$$

is convergent.

By a straightforward generalization of the Lemma 2.7 to the matrix case, piecewise constant approximations of d^1p^k converge uniformly to $\nabla f[p^0]$ (for $f : \mathbf{R}^n \to \mathbf{R}^m$, $\nabla f = [\nabla f_1 \dots \nabla f_m]^T$).

Note that by construction $2^k d^1p^k$ is the gradient of the piecewise linear approximation on each triangle of $\mu_v(U_1(v))$ for any v. Consider two adjacent triangles of K. The limit function $f \circ \mu_v^{-1}$ is continuous and piecewise C^1, with limits of partial derivatives existing on the boundary. The difference scheme converges everywhere inside each triangle. On the boundary the limits on different sides exist, but may be different.

Consider $\nabla(f[p] - L^j)$ on each triangle. It is equal to $J_v(\nabla(f \circ \mu_v^{-1}) - d^1p^j)$ where J_v is the Jacobian matrix of μ_v on the triangle, and

$$\left\|\nabla(f[p] - L^j)\right\|_p \le \|J\|_p \left\|\nabla(f \circ \mu_v^{-1}) - d^1p^j\right\|_p$$

$\left\|f - L^j\right\|_p$ converges to 0 uniformly on K, as $\left\|\nabla(f \circ \mu_v^{-1}) - d^1p^j\right\|_p$ converges to 0 on a subcomplex of the regular complex, and $|K|$ is compact, therefore it can be covered by a finite number of neighborhoods $U_1(v)$ where μ_v are defined.

The conditions of Lemma 4.2 are satisfied for $|K|$; therefore,

$$\|f - L_j\|_{Lip} \le CB\left\|\|\nabla(f - L_j)\|_p\right\|_\infty$$

and $\|f - L_j\|_{Lip}$ also converges to 0. □

Now we observe that each layer defined in Section 2.4.1 is a complex satisfying the requirements of Theorem 4.4.

Suppose that we can establish that the Lipschitz ratio of a sufficiently close linear approximation is bounded from below by a positive number. Then the characteristic map is injective on each layer, and Reif's argument in Theorem 3.6 [55] applies in unchanged form.

We conclude that the following theorem holds:

Theorem 4.5. *Consider a subdivision scheme $\mathcal{S}$, which is C^1-continuous in the regular case. Suppose for a subdivision level j the following conditions are satisfied:*

1. *the Jacobian J of a piecewise linear approximation L_j to the characteristic map Φ for some valence k is within ϵ of the Jacobian of the limit function in L_∞ norm on the layer Lr_0, $\inf_x |J| > \epsilon$ for x in Lr_0;*

2. *the linear approximation is within ϵ' from Φ in Lipschitz norm of Lr_0, and the Lipschitz ratio $\|\Phi(x_2) - \Phi(x_1)\|_p / \|x_2 - x_1\|_p > \epsilon'$.*

Then Φ is injective and the scheme is C^1.

This theorem allows us to use the following procedure for asserting C^1-continuity of a subdivision scheme on the k-regular complex. First we estimate the rate of convergence of the scheme and the derivative scheme in the regular case. This allows us to estimate the precision of the approximation of the map and its derivatives after N subdivision steps. If the Jacobian of the linear approximation is greater than a sufficiently large positive constant everywhere, and so is the Lipschitz ratio, than we can guarantee that the characteristic map is injective. Special effort has to be made to ensure that the numerical error of the calculations does not affect correctness of our conclusions (see the next chapter for details).

Although the Lipschitz ratio for a piecewise linear function can be computed explicitly, it would be desirable to reduce the complexity of the problem. We will prove two lemmas in the next section; one reduces checking injectivity to computing the winding number of a curve under additional assumptions that are also easy to check; the second makes weaker assumptions but requires checking injectivity of the characteristic map on a curve. We describe a constructive procedure for this test.

4.2 Covering Conditions

We will prove the following lemma, which allows us to check injectivity with less effort.

Lemma 4.6. *Suppose a characteristic map $\Phi = (f_a, f_c)$ satisfies the following conditions:*

1. *the preimage $\Phi^{-1}(0)$ contains only one element, 0;*
2. *the characteristic map has a Jacobian of constant sign at all points where it is defined.*

Then the extension of the characteristic map is surjective and is a covering away from 0.

Proof. Three cases are possible:

1. the characteristic map is defined by a pair of real eigenvectors;
2. the characteristic map is defined by two generalized eigenvectors from the same Jordan block corresponding to a real eigenvector;
3. the characteristic map is defined by the real and imaginary parts of an eigenvector corresponding to a complex eigenvalue.

In the first case components satisfy the scaling relations of the simplest form

$$\begin{aligned} f_a(\frac{y}{2}) &= \lambda_a f_a(y) \\ f_c(\frac{y}{2}) &= \lambda_c f_c(y) \end{aligned}$$

First, we establish the following important fact: if a characteristic map satisfies the first two conditions of the lemma, then the map is continuous at infinity.

Consider two circles of radii r and $2r$ centered at 0 in the domain of Φ. The image of the ring R bounded by the two circles $\Phi(R)$ is compact, and does not contain 0. Thus, there is a constant $M > 0$ such that for any point p in the ring $\|\Phi(p)\| \geq M$ (Figure 4.2).

Consider any point p in the domain of Φ. There is a number $k \in \mathbf{Z}$ such that $2^k p$ is contained in the ring R. Thus, by scaling relations, $\|\Phi(p)\| > \min(|\lambda_a|, |\lambda_c|)^k M$. Clearly, as $\|p\| \to \infty$, $k \to \infty$, and for any C there is C' such that if $\|p\| > C'$, $\|\Phi(p)\| > C$.

Consider the stereographic map P from the plane into the sphere without one point. The map Φ gives rise to the map $\Phi_S = P\Phi P^{-1} : S^2 \setminus \{N\} \to S^2$, where N is the center

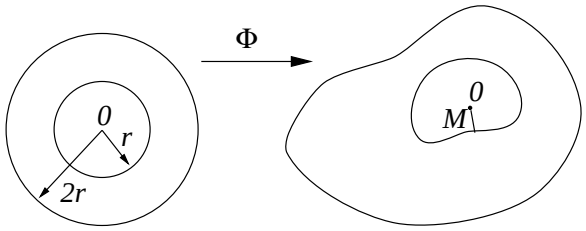

Figure 4.2:

of projection. From continuity of Φ at infinity it follows that if we extend the mapping by setting $\Phi_S(N) = N$, we get a continuous mapping. Thus, Φ_S is a continuous mapping of a sphere into the sphere. As we have assumed that the Jacobian of the characteristic map has constant sign where it is defined, the mapping is also a local homeomorphism away from 0. The sphere is compact, thus its image is compact, hence closed, i.e., contains its boundary. But under local homeomorphism the points on the boundary of the image can be images only of the points of the boundary of the domain. Therefore, the only points that can be contained in the boundary of the image are 0 and N. Therefore, the image has no boundary, i.e., the mapping is surjective.

Finally, for any p set $\Phi_S^{-1}(p)$ is finite: if it were not finite, it would have a limit point (S^2 is compact). As $\Phi_S^{-1}(p)$ is a discrete set for any local homeomorphism, the only limit points that it may have are 0 and N. But $\Phi(0) = 0$ and $\Phi(N) = N$, so this is impossible. We conclude that for any point p $\Phi_S^{-1}(p)$ is finite. As any point $y \in \Phi_S^{-1}(p)$, $p \neq 0, N$ has a neighborhood $U(y)$ such that $\Phi_S|_{U(y)}$ is a homeomorphism, then the intersection of all neighborhoods $V = \Phi_S(U(y))$ has inverse image consisting of disjoint homeomorphic images of V. This proves that Φ_S is a covering away from 0.

The case of the characteristic map generated by imaginary and real part of a complex eigenvector corresponding to a complex eigenvalue is similar to the case of two real eigenvectors; we proceed directly to the proof for the case of two generalized eigenvectors from a single Jordan block $\Phi = (f_0, f_1)$,

$$\begin{aligned} f_0(\frac{y}{2}) &= \lambda f_0(y) \\ f_1(\frac{y}{2}) &= \lambda f_1(y) + f_0(y) \end{aligned}$$

From these equations we immediately obtain

$$.\Phi(2^p y) = \frac{1}{\lambda^p} \begin{pmatrix} 1 & 0 \\ 1 & -p/\lambda \end{pmatrix} \Phi(y) = \frac{1}{\lambda^p} T\Phi(y) \tag{4.6}$$

Consider the image of a circle γ of radius r centered at 0. As $\Phi^{-1}(0)$ by assumption is $\{0\}$, then 0 is an interior point of the image of $\mathrm{Int}(\gamma)$ and there is an open disk centered at 0 of some radius r', which is contained in $\Phi(\mathrm{Int}\gamma)$. For any p the image of the disk bounded by $2^p\gamma$ is determined by the equations (4.6). It can be obtained from the image of the disk bounded by γ by affine transform $\frac{1}{\lambda^p}T$ from (4.6). If a disk D_r of radius r is contained in $\Phi(\mathrm{Int}\gamma)$, then the interior of the ellipse $\frac{1}{\lambda^p}TD_r$ is contained in $\Phi(\mathrm{Int}2^p\gamma)$. We can estimate the length of the minor axis of this ellipse: it can be represented parametrically as $(\frac{r}{\lambda^p}\cos(t), \frac{r}{\lambda^p}(\sin(t) - (p/\lambda)\cos(t)))$. The square of the distance from 0 to a point on the ellipse is

$$\frac{r^2}{\lambda^{2p}}(\cos^2(t) + (\sin(t) - \frac{p}{\lambda}\cos(t))^2) = \frac{r^2}{\lambda^{2p}}(1 + \frac{p^2}{2\lambda}(\cos(2t) + 1) - \frac{p}{\lambda}\sin(2t))$$

This quantity can be estimated from below by

$$\frac{r^2}{\lambda^{2p}}(1 + \frac{p^2}{\lambda} - \frac{p}{\lambda})$$

As $\lambda < 1$, the length of the minor axis increases with p for sufficiently large p. We conclude that as $p \to \infty$, the image of the exterior of $2^p\gamma$ is arbitrarily far from zero, and Φ is continuous at infinity. Then the rest of the argument that was used for the case of two eigenvectors applies. □

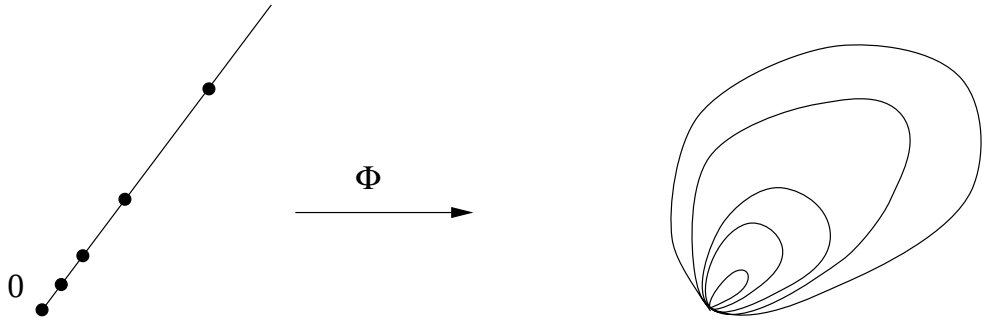

Figure 4.3: An example of a map which does not satisfy the conditions of Lemma 4.6. Infinitely many points on a line on the right map to 0, and the image of the line has to return to zero infinitely many times. While the points that map to zero do not have to be on one line, any regular characteristic map which has infinitely many points mapping to zero has to have similar structure for some curve.

Note. It is easy to see that if the first condition $\Phi^{-1}(0) = 0$ is violated, the structure of the characteristic map has to be quite complicated (Figure 4.3) and it is unlikely that any useful scheme may have such a map. Despite the fact that only "unreasonable" cases are excluded, it would be useful from a theoretical point of view to make the conditions of the lemma weaker.

Algorithm for checking injectivity. Lemma 4.6 is useful for checking injectivity of a characteristic map which is known to be regular. Indeed, suppose the conditions of the lemma are satisfied, and we have shown by some means that the map is regular and $\Phi^{-1}(0) = \{0\}$. Once the conditions of the lemma are established, we know that the map is a covering away from 0. Therefore, it is injective, if and only if the winding number of a simple curve around zero has winding number 1. This fact can be seen by looking at the fundamental groups of the domain and the image. The conditions of the Lemma 4.6 guarantee that both have fundamental group $\mathbf{Z}$. As for a covering the fundamental group of a covering space is a subgroup of the fundamental group of the base space, with a monomorphism induced by the covering map. A simple curve around zero is the generating element of the fundamental group of the domain. Thus, the mapping of fundamental groups is an isomorphism which is necessary and sufficient for the covering mapping to be an injection, if and only if the simple curve maps to a curve homotopic to a simple curve, i.e.,

one with winding number 1.

We summarize our observations in the following Proposition:

Proposition 4.7. *Suppose the characteristic map of a subdivision scheme is regular and satisfies* $\Phi^{-1}(0) = 0$. *Then if the winding number of the image* $\Phi(\gamma)$ *of a curve is 1, the characteristic map is injective and the scheme is* C^1*-continuous.*

Computing the winding number. In general, we do not have a closed-form expression for any curves on the limit surface. One way to compute the winding number of a curve is to choose a sufficiently close linear approximation and compute the winding number of the approximation. The linear approximation is sufficiently close if we can guarantee that the winding number of the approximation is equal to the winding number of the curve. This is a particular instance of the following problem:

> Consider two continuous curves $\gamma_1(t)$ and $\gamma_2(t)$. Suppose $\sup_t \|\gamma_1(t) - \gamma_2(t)\| = \epsilon$. What value of ϵ guarantees that the winding numbers of the curves are equal?

It is convenient to consider $\gamma_1(t)$ and $\gamma_2(t)$ as functions into the complex plane. Define $\alpha_1(t)$ to be the continuous phase of γ_1 and $\alpha_2(t)$ to be the continuous phase of $\gamma_2(t)$. Then $\alpha_1(0) = \alpha_2(0) = 0$, $\alpha_1(1) = 2\pi n_1$, $\alpha_2(1) = 2\pi n_2$, where n_1 and n_2 are the winding numbers. Consider $\alpha_1(t) - \alpha_2(t)$; this is a continuous function with values 0 and $2\pi(n_1 - n_2)$ on the endpoints. Suppose $n_1 \neq n_2$; then $\alpha_1(t_1) - \alpha_2(t) = \pi$ for some t_1, i.e., for some t_1 the points $\gamma_1(t_1)$ and $\gamma_2(t_1)$ are on the same line going through zero on different sides of zero.

Suppose that we have established that $\inf_t \|\gamma_1(t)\| > \epsilon$ and $\inf_t \|\gamma_2(t)\| > \epsilon$. Then the distance between $\gamma_1(t_1)$ and $\gamma_2(t_1)$ is at least 2ϵ. Therefore, if $\sup \|\gamma_1 - \gamma_2\|$ is less than 2ϵ, the winding numbers cannot be different.

The following proposition reduces computation of the winding number of a curve to the computation of the winding number of a linear approximation:

Proposition 4.8. *Suppose for some* ϵ

$$\begin{aligned} &\sup_t \|\Phi(\gamma(t)) - L_m(\gamma(t))\| \leq \epsilon \\ &\inf_t \|\Phi(\gamma(t))\| \geq 2\epsilon \end{aligned} \tag{4.7}$$

where $\gamma(t)$ is a curve in the domain of Φ, L_m is a piecewise linear approximation to Φ. Then the winding number of $L_m(\gamma(t))$ is equal to the winding number of $\Phi(\gamma(t))$.

The simplest way to compute the winding number is to count the number of intersections of a half-line starting at zero with the curve. However, when the curve is known only approximately and is represented by its linear approximation, this method is not very reliable numerically. The winding number of a piecewise linear curve can be computed in a more stable way using a projection of this curve to the unit square. Let $\gamma(t)$ be a piecewise linear curve with $\gamma(t_i) = y_i$, $i = 0 \dots n$, $\gamma(t)$ linear on each interval $[t_i, t_{i+1}]$, $t_0 = 0, t_n = 1$, and $y_0 = y_n$. A projection of the curve into the unit square can be defined using $P(y) = y/\|y\|_\infty$. Let $p_i = P(y_i)$, $i = 0 \dots n$. Suppose p_i and p_{i+1} end up on the different sides of the square $[-1, 1] \times [-1, 1]$. Then a corner of the square is contained in the projection of the line segment $[y_i, y_{i+1}]$. We split this interval in two, so that the projection of each subinterval is contained in only one side of the square. We assume that p_i and p_{i+1} both have one of the coordinates equal. Then $p_{i+1} - p_i$ has one of the forms $(p^1_{i+1} - p^1_i, 0)$ or $(0, p^2_{i+1} - p^2_i)$, i.e., can be characterized by a single number d_i. As the phase increases or decreases on each interval, depending on the sign of d_i, it is straightforward to show that the winding number is simply $(1/8)\sum_i d_i$.

Under additional assumptions, we can simplify the computation even further (see the next chapter).

4.3 Convergence Rates for Uniform Schemes on Regular Complexes

To apply Theorem 4.5 to a particular scheme, we need a way to estimate the rate of convergence of the scheme and the matrix schemes corresponding to the derivatives. As it was shown in [6], under sufficiently general assumptions subdivision converges geometrically. We derive estimates on the rate of convergence, and use them to determine the number of subdivision iterations that have to be performed to achieve sufficient approximation both to the limit surface and partial derivatives of the surface in the sense described in Section 4.1.

We use the contraction function

$$D(p) = \max(\left\|\Delta_{(1,0)}p\right\|_\infty, \left\|\Delta_{(0,1)}p\right\|_\infty)$$

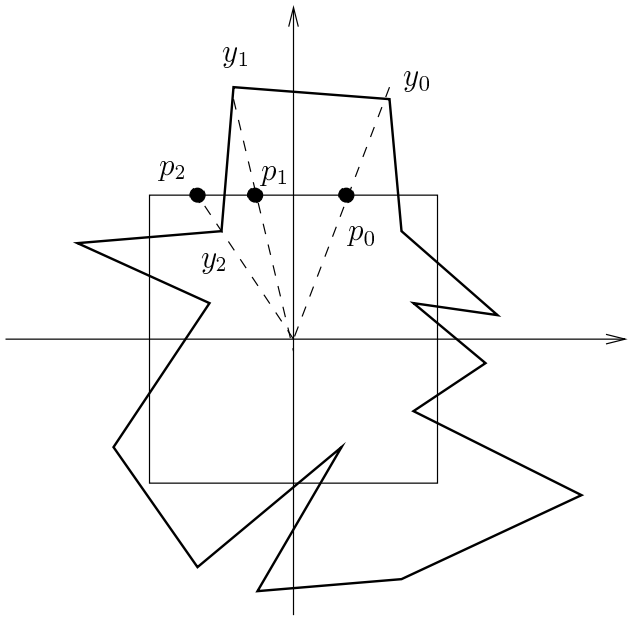

Figure 4.4: Computing the winding number of a piecewise linear curve.

, where $[\Delta_{(k,l)}p]_{ij} = p_{i+k\,j+l} - p_{ij}$, to be able to use convergence estimates of Theorem 3.1 [6].

Suppose that a subdivision scheme satisfies for any p

$$D(S^N p) < \gamma_N D(p) \text{ for some } N \text{ and } \gamma < 1 \tag{4.8}$$

$$\|(S-B)p\|_\infty < cD(p) \tag{4.9}$$

where B is a midpoint or piecewise constant subdivision scheme, then we have

$$\left\|L^{m+1} - L^m\right\|_\infty = \|(S-B)p^m\|_\infty < cD(p^m)$$

Suppose that $m = kN + q$; then $D(p^m) < \gamma^k D(p^q)$ and

$$\begin{aligned}\left\|L^{\infty}-L^{m}\right\|_{\infty} &\leq \sum_{j=0}^{\infty}\left\|L^{m+j}-L^{m+j}\right\|_{\infty}= \\ &= \sum_{j=0}^{\infty}\left\|(S-B)p^{j+m}\right\|_{\infty}\leq c\sum_{j=0}^{\infty}D\left(p^{m+j}\right)= \\ &= c\sum_{i=1}^{\infty}\sum_{q=1}^{N}D\left(p^{m+iN-q}\right)=\sum_{i=1}^{\infty}\left(\sum_{q=1}^{N-1}D\left(p^{m+iN-q}\right)+D\left(p^{m+(i-1)N}\right)\right)\end{aligned}$$

If $m \geq N$,

$$\left\|L^{\infty}-L^{m}\right\|_{\infty}\leq\frac{c}{1-\gamma}\left(\gamma\sum_{q=1}^{N-1}D\left(p^{m-q}\right)+D\left(p^{m}\right)\right) \tag{4.10}$$

If $m < N$,

$$\left\|L^{\infty}-L^{m}\right\|_{\infty}\leq\frac{c}{1-\gamma}\left(\gamma\sum_{q=1}^{m}D\left(p^{m-q}\right)+\sum_{q=m}^{N-1}D\left(p^{q}\right)\right) \tag{4.11}$$

Note that the formulas coincide for $m = N-1$. In particular, if $N = 1$, we get

$$\left\|L^{\infty}-L^{m}\right\|_{\infty}\leq\frac{c}{1-\gamma}D\left(p^{m}\right) \tag{4.12}$$

and for $N = 2$, $m \geq 1$

$$\left\|L^{\infty}-L^{2m}\right\|_{\infty}\leq c\left(\frac{c}{1-\gamma}\left(\gamma D\left(p^{m-1}\right)+D\left(p^{m}\right)\right)\right) \tag{4.13}$$

Note that piecewise constant approximations can be shown to satisfy the same estimate; this fact is important for characterizing convergence of the differences to partial derivatives. To calculate the number of steps necessary to approximate the limit surface to a given precision, we need to find an expression for constants γ and c.

Estimates of γ. For uniform stationary subdivision on regular complexes, we use the techniques of Cavaretta, Dahmen and Micchelli [6] and Dyn, Levin and Micchelli [21] to estimate the constants in the formulas above.

In this section we use notation S_a for a stationary uniform subdivision scheme with the Laurent polynomial $a(z)$. Consider a scheme S_a. Assume that $a(z)$ is divided by $1+z_1^{-1}$ and $1+z_2^{-1}$. In general, this is not necessary for C^1-continuity of subdivision and matrix schemes have to be considered. However, it is true for the particular instances of subdivision schemes that we are going to consider, and we restrict ourselves to the schemes with reduceable polynomials a to simplify exposition. We use the notation

$$a_1(z)=\frac{a(z)}{1+z_1^{-1}} \quad a_2(z)=\frac{a(z)}{1+z_2^{-1}} \tag{4.14}$$

Polynomials a_1 and a_2 correspond to difference subdivision schemes satisfying commutation formulas

$$S_{a_1}\Delta_{(1,0)}p=\Delta_{(1,0)}S_a p \quad S_{a_2}\Delta_{(0,1)}p=\Delta_{(0,1)}S_a p$$

Denote

$$a_{ij}=\frac{a_i}{1+z_j^{-1}} \quad a_{i3}=\frac{a_i}{1+z_2^{-1}z_1^{-1}} \quad i,j=1,2,\ i\neq j \tag{4.15}$$

It is easy to show for a symmetric scheme that if a_1 is finite, then $a_2, a_{12}, a_{21}, a_{13}, a_{23}$ are all finite. The polynomial $a(z)$ can be written in the following form:

$$a(z)=\frac{1}{2}\left(1+z_1^{-1}\right)\left(1+z_2^{-1}\right)\left(1+z_2^{-1}z_1^{-1}\right)q(z_1,z_2)z_1z_2 \tag{4.16}$$

with $q(z_1,z_2)$ satisfying $q(z_1,z_2)=q(z_2,z_1)=q(z_2^{-1},z_1z_2)$, as the rotation of the grid by $\pi/3$ corresponds to the transformation $z_1\to z_2^{-1}$, $z_2\to z_1z_2$. The polynomials $a_{12}, a_{21}, a_{13}, a_{23}$ satisfy

$$a_1(z_1, z_2) = a_2(z_2, z_1), \quad a_{12}(z_1, z_2) = a_{21}(z_1, z_2), \quad a_{13}(z_1, z_2) = a_{23}(z_2, z_1) \tag{4.17}$$

We can can find the estimate for γ in (4.8) using the L^∞ norms of the subdivision operators; for S we get

$$\begin{aligned} D(S^N p) &= \max(\left\|\Delta_{(0,1)} S^N p\right\|_\infty, \left\|\Delta_{(1,0)} S^N p\right\|_\infty) \\ &= \max(\left\|S^N_{a_2} \Delta_{(0,1)} p\right\|_\infty, \left\|S^N_{a_1} \Delta_{(1,0)} p\right\|_\infty) \leq \\ &\leq \max(\left\|S^N_{a_2}\right\|_\infty \left\|\Delta_{(0,1)} p\right\|_\infty, \left\|S^N_{a_1}\right\|_\infty \left\|\Delta_{(1,0)} p\right\|_\infty) \end{aligned}$$

As $a_1(z_1, z_2) = a_2(z_2, z_1)$, the norms of the corresponding subdivision operators are equal and

$$D(S^N p) \leq \left\|S^N_{a_1}\right\|_\infty D(p) \tag{4.18}$$

Thus, γ can be taken to be $\left\|S^N_{a_1}\right\|_\infty$ for any N. N should be chosen in such a way that the norm is less than 1; in addition we may try to improve our estimate of the convergence rate by choosing larger N, to minimize the number of subdivision steps required to guarantee the necessary precision. For any scheme an optimal N has to exist, as large N are clearly non-optimal (subdivision has to be evaluated for all levels at least up to N).

To prove that the characteristic map is regular, using Theorem 4.5 we need to estimate the Jacobian of the map, i.e., the partial derivatives of the limit functions of subdivision. In the case of schemes with Laurent polynomials that can be factored in the way described above, approximation of partial derivatives can be done using a similar approach applied to the schemes for the derivatives S_{2a_1} and S_{2a_2} (in a more general case we would have to use a single matrix subdivision scheme acting on the vector of differences).

When choosing the contraction functions, we have to ensure that there is a convenient commutation relation associated with this function. In the case of schemes for derivatives, the following contraction functions turn out to be convenient:

$$D_1(p) = \max(\Delta_{(1,1)}, \Delta_{(0,1)}) \text{ and } D_2(p) = \max(\Delta_{(1,1)}, \Delta_{(1,0)}) \tag{4.19}$$

For the scheme S_{2a_1} we get by triangle inequality

$$\begin{aligned} D_1(S^N_{2a_1}\Delta_{(1,0)}p) &= \max\left(\left\|\Delta_{(1,1)}S^N_{2a_1}\Delta_{(1,0)}p\right\|_\infty, \left\|\Delta_{(0,1)}S^N_{2a_1}\Delta_{(1,0)}p\right\|_\infty\right) = \\ &= \max\left(\left\|S^N_{2a_{13}}\Delta_{(1,1)}\Delta_{(1,0)}p\right\|_\infty, \left\|S^N_{2a_{12}}\Delta_{(0,1)}\Delta_{(1,0)}p\right\|_\infty\right) \leq \\ &\leq \max\left(\left\|S^N_{2a_{13}}\right\|_\infty, \left\|S^N_{2a_{12}}\right\|_\infty\right) D_1(\Delta_{(1,0)}p) \end{aligned}$$

Thus, the following estimate holds for the derivative scheme S_{2a_1}

$$D_1\left(S^N_{2a_1}\Delta_{(1,0)}p\right) \leq \max\left(\left\|S^N_{2a_{13}}\right\|_\infty, \left\|S^N_{2a_{12}}\right\|_\infty\right) D_1\left(\Delta_{(1,0)}p\right) = \gamma_1 D_1\left(\Delta_{(1,0)}p\right) \tag{4.20}$$

In a similar way, for the derivative scheme S_{2a_2} we get

$$D_2\left(S^N_{2a_2}\Delta_{(0,1)}p\right) \leq \max\left(\left\|S^N_{2a_{23}}\right\|_\infty, \left\|S^N_{2a_{21}}\right\|_\infty\right) D_2\left(\Delta_{(0,1)}p\right) = \gamma_2 D_2\left(\Delta_{(0,1)}p\right) \tag{4.21}$$

Estimates of c. Estimates of constant c in (4.8) can be obtained by considering the subdivision scheme S_{a-b}, where b is the Laurent polynomial for the midpoint subdivision given by the formula

$$b(z_1, z_2) = \frac{1}{2}\left(1 + z_1^{-1}\right)\left(1 + z_2^{-1}\right)\left(1 + z_2^{-1}z_1^{-1}\right) z_1 z_2$$

The following obvious fact plays an important role in our derivations, so we state it as a separate proposition:

Proposition 4.9. *For any pair of affine-invariant uniform schemes S and T with Laurent polynomials $s(z)$ and $t(z)$, the polynomial $s(z) - t(z)$ corresponding to their difference can be factored in the following ways:*

$$\begin{aligned} s(z) - t(z) &= p_1^1(z)(z_1^{-1} - 1) + p_2^1(z)(z_2^{-1} - 1) \\ s(z) - t(z) &= p_1^2(z)(z_1^{-1} - 1) + p_3^2(z)(z_1^{-1} z_2^{-1} - 1) \\ s(z) - t(z) &= p_2^3(z)(z_2^{-1} - 1) + p_3^3(z)(z_1^{-1} z_2^{-1} - 1) \end{aligned}$$

Proof. As both schemes are affine-invariant, they reproduce constants. Therefore, the following sums are 1:

$$\sum_{i,j} a_{2i+a\,2j+b} = 1, \quad a, b \in \{0, 1\}$$

Therefore, the sum of all coefficients of each Laurent polynomial is 4, and the sum of the coefficients of their difference is 0. This means that the pair $(1, 1)$ is a solution of the equation $s(z) - t(z) = 0$. It follows that the polynomial admits the first decomposition. Any Laurent polynomial in z_1 and z_2 can be rewritten as a polynomial in $y_1 = z_1$ and $y_2 = z_1 z_2$ or $y_1 = z_2$ and $y_2 = z_1 z_2$. If $z_1 = z_2 = 1$, then $y_1 = y_2 = 1$ in both cases, and we can obtain the second and the third decomposition. □

Using this proposition, we can write $a - b$ in the following form:

$$a(z_1, z_2) - b(z_1, z_2) = b(z_1, z_2) \left(p_1(z_1, z_2)(z_1^{-1} - 1) + p_2(z_1, z_2)(z_2^{-1} - 1) \right) \tag{4.22}$$

Note that $z_1 - 1$ is the Laurent polynomial for $\Delta_{(1,0)}$ and $z_2 - 1$ is the Laurent polynomial for $\Delta_{(0,1)}$. Define polynomials

$$b_1(z_1, z_2) = \frac{b(z_1, z_2)}{1 + z_1^{-1}}, \quad b_2(z_1, z_2) = \frac{b(z_1, z_2)}{1 + z_2^{-1}}, \quad b_3(z_1, z_2) = \frac{b(z_1, z_2)}{1 + z_1^{-1} z_2^{-1}} \tag{4.23}$$

Then we have the following estimate:

$$\|S_{a-b} p\|_\infty \leq \left(\|S_{b_1 p_1}\|_\infty + \|S_{b_2 p_2}\|_\infty \right) D(p) \tag{4.24}$$

For the derivatives, instead of using midpoint subdivision as a comparison scheme, we use one of the piecewise constant schemes corresponding to the polynomials b_1, b_2, b_3.

As $q(z_1, z_2)$ defined in (4.16) satisfies $q(z_1, z_2) = q(z_2^{-1}, z_1 z_2)$, $1 - q$ can be decomposed as $p_{12}(z_2^{-1} - 1) + (z_1^{-1} z_2^{-1} - 1)p_{13}$ or as $p_{21}(z_1^{-1} - 1) + (z_1^{-1} z_2^{-1} - 1)p_{23}$. Note that we can choose polynomials p_{12}, p_{13}, p_{21}, p_{23} to be $p_{12} = -z_1^{-1} p_1(z_1 z_2, z_1^{-1})$, $p_{13} = p_1(z_1 z_2, z_1^{-1})$, $p_{21} = -z_2^{-1} p_1(z_2^{-1}, z_1 z_2)$, $p_{23} = p_1(z_2^{-1}, z_1 z_2)$.

Similar to (4.24) we get

$$\left\| S_{2a_1 - 2b_1} \Delta_{(1,0)} p \right\|_\infty \le \left(\|S_{2b_{12} p_{12}}\|_\infty + \|S_{2b_{13} p_{13}}\|_\infty \right) D_1(\Delta_{(1,0)} p) = c_1 D_1(\Delta_{(1,0)} p) \tag{4.25}$$

where b_{ik} are defined similarly to b_k, with b replaced by b_i. For the other partial derivative, we have a similar expression and by symmetry $c_1 = c_2$.

Here is a summary of the estimates, $m \ge N - 1$:

- For the limit function f:

$$\|f - L^m\|_\infty \le \frac{c}{1 - \gamma} \left(\gamma \sum_{q=1}^{N-1} D\left(p^{m-q}\right) + D\left(p^m\right) \right) \quad \gamma = \left\| S_{a_1}^N \right\|_\infty, \quad c = \|S_{b_1 p_1}\|_\infty + \|S_{b_2 p_2}\|_\infty \tag{4.26}$$

- For the derivatives:

$$\begin{aligned} &\left\| \frac{\partial}{\partial x_1} f - L_1^m \right\|_\infty \le \frac{c_1}{1 - \gamma_1} \left(\gamma_1 \sum_{q=1}^{N-1} D_1\left(\Delta_{(1,0)} p^{m-q}\right) + D_1\left(\Delta_{(1,0)} p^m\right) \right) \\ &\gamma_1 = \max\left(\left\| S_{2a_{13}}^N \right\|_\infty, \left\| S_{2a_{12}}^N \right\|_\infty \right), \quad c_1 = \left(\|S_{2b_{12} p_{12}}\|_\infty + \|S_{2b_{13} p_{13}}\|_\infty \right) \end{aligned} \tag{4.27}$$

$$\begin{aligned} &\left\| \frac{\partial}{\partial x_2} f - L_2^m \right\|_\infty \le \frac{c_2}{1 - \gamma_2} \left(\gamma_2 \sum_{q=1}^{N-1} D_2\left(\Delta_{(0,1)} p^{m-q}\right) + D_2\left(\Delta_{(0,1)} p^m\right) \right) \\ &\gamma_2 = \max\left(\left\| S_{2a_{21}}^N \right\|_\infty, \left\| S_{2a_{23}}^N \right\|_\infty \right), \quad c_2 = \left(\|S_{2b_{21} p_{21}}\|_\infty + \|S_{2b_{23} p_{23}}\|_\infty \right) \end{aligned} \tag{4.28}$$

where $L_i^m = S_{2a_i}^m$ are the approximations of the derivatives generated using the basis

functions corresponding to S_{2b_i} (piecewise constant).

In all estimates above we need to compute the L-infinity norm of Laurent polynomials for powers of subdivision schemes. These norms can be computed using the formulas [6]

$$\left\|S^N\right\|_\infty = \max\left\{\widehat{a}^N_{i,j},\, 0 \le i,j \le 2^N - 1\right\}, \quad \widehat{a}^N = \sum_{k,l}\left|a^N_{i-2^N k, j-2^N l}\right| \tag{4.29}$$

where $a^N_{i,j}$ are the coefficients of $a(z)a(z^2)\cdots a(z^{2^{N-1}})$.

In particular, the Butterfly scheme is characterized by the polynomial $a(z_1, z_2)$ with $q(z_1, z_2)$ being

$$\begin{aligned} q(z_1,z_2) = 1 - \frac{1}{16}(&2z_1^{-2}z_2^{-1} + 2z_2^{-2}z_1^{-1} - 4z_1^{-1}z_2^{-1} - 4z_1^{-1} \\ &- 4z_2^{-1} + 2z_1^{-1}z_2 + 2z_1z_2^{-1} + 12 - 4z_1 - 4z_2 - 4z_1z_2 + 2z_1^2z_2 + 2z_1z_2^2) \end{aligned} \tag{4.30}$$

$$\|S_{a_1}\|_\infty = \frac{7}{8}, \quad \left\|S^2_{a_1}\right\|_\infty = \frac{31}{64}, \quad \left\|S^3_{a_1}\right\|_\infty = \frac{261}{1024}, \quad \|S_{b_1p_1}\|_\infty + \|S_{b_1p_1}\|_\infty = \frac{1}{2} \tag{4.31}$$

$$\|S_{2a_{12}}\|_\infty = 1, \quad \left\|S^2_{2a_{12}}\right\|_\infty = \frac{7}{8}, \quad \left\|S^3_{2a_{12}}\right\|_\infty = \frac{11}{16}, \tag{4.32}$$

$$\|S_{2a_{13}}\|_\infty = 1, \quad \left\|S^2_{2a_{13}}\right\|_\infty = \frac{7}{8}, \quad \left\|S^3_{2a_{13}}\right\|_\infty = \frac{11}{16}, \tag{4.33}$$

$$\|S_{2b_{12}p_{12}}\|_\infty + \|S_{2b_{13}p_{13}}\|_\infty = 2 \tag{4.34}$$

4.4 Convergence Rates for Schemes with Creases on Regular Complexes

It is often desirable to introduce a smooth or sharp one-dimensional feature on a surface. A common way of introducing sharp features is to separate the surface into several surface patches which match along an edge. When a smooth feature is introduced, it is typically done by increasing the number of control points on the surface near the crease. An alternative method of introducing sharp edges into a subdivision surface was proposed by Hoppe et al. [32]; the main idea of the approach is to modify the subdivision rules near tagged edges of the initial mesh so that the limit surface becomes non-smooth at that edge. A related idea was used by B. Barsky [3] for β-splines, who added tension parameters to the spline basis functions. In both cases it is not necessary to increases the number of control points of a surface to introduce a crease; only manipulation of the tags or tension parameters is required.

We extend the idea of modification of subdivision rules to add tension parameters to subdivision, and study C^1-continuity of the resulting families of schemes.

In this section we consider the behavior of subdivision schemes with modified rules along an edge on a regular complex.

To analyze C^1-continuity for extraordinary vertices, we need to derive estimates on convergence of the partial derivatives of a scheme similar to those in Section 4.3.

Note that we develop a method for asserting C^1-continuity of a particular parameterization of the surface (the dyadic parameterization over the plane). If this parameterization is not C^1-continuous, in general it does not mean that the surface is not C^1-continuous; our conditions are sufficient but it is not known if they are necessary.

4.4.1 Definitions

We restrict ourselves to the simplest class of schemes with creases defined as follows:

Definition 4.2. *A crease subdivision scheme S with uniform coefficients $a^0_{ij}, i,j \in \mathbf{Z}$ and crease coefficients $c_{i,2j}, \quad i,j \in \mathbf{Z}$ is a linear operator on sequences $p(v_{i,j}) = p_{ij}, i,j \in \mathbf{Z}$, such that*

$$[Sp]_{ij} = \sum_{l,m} a^0_{i-2m,j-2l} p_{lm} \quad for\ j \neq 0 \tag{4.35}$$

$$[Sp]_{i0} = \sum_{l,m} c_{i-2m,-2l} p_{lm} \tag{4.36}$$

In this definition special coefficients are used to compute values at vertices on the x-axis in the parametric plane. It is clear from this definition that the scheme is stationary but not uniform. The crucial observation for analysis of schemes of this type is that Theorem 3.1 from [6] and the estimates 4.10 do not use the assumption that the scheme is uniform. However, the lack of translation invariance does not allow us to use Laurent polynomials to represent the schemes. Nevertheless, we can derive convergence estimates for crease subdivision schemes in a similar way, considering several separate cases.

As we would like to introduce parameters into subdivision, we would like to estimate convergence rates for parametric families of subdivision schemes, rather than schemes with fixed coefficients. In order to do this efficiently, we further restrict the type of schemes that we consider, assuming that there is one parameter k, and the crease coefficients are computed using linear interpolation

$$c(k)_{ij} = a^k_{ij} = (1-k)a^0_{ij} + k a^1_{ij}, \quad 0 \leq k \leq 1 \tag{4.37}$$

where a^1_{ij} are coefficients for a sharp crease, that is, when the limits of the partial derivatives are different on the different sides of the x-axis.

The case $k = 0$ corresponds to the uniform scheme; the case $k = 1$ corresponds to a sharp crease.

We use notation S^k for the uniform scheme with coefficients a^k_{ij}. We denote by $a^k(z_1, z_2)$ the Laurent polynomial with coefficients a^k_{ij}. S_k is *not* the crease subdivision scheme; it is the uniform scheme that uses the coefficients of the crease scheme everywhere, rather than only at the x-axis. We use notation $D = S^0 - S^1$, with the Laurent polynomial $d(z) = a^0(z) - a^1(z)$.

As in Section 4.3, we assume that the Laurent polynomials a^0, a^1 have the form

$$a^l(z) = b(z)q^l(z) = \frac{1}{2}z_1 z_2(z_1^{-1}+1)(z_2^{-1}+1)(1+z_1^{-1}z_2^{-1})q^l(z) \tag{4.38}$$

In addition, we assume that

$$d(z) = (z_2^{-1}-1)\tilde{d}(z) \tag{4.39}$$

where $\tilde{z}$ is a finite Laurent polynomial. Both assumptions can be relaxed, but it would make the exposition somewhat more complex. The specific schemes that we consider satisfy this requirement, and we restrict our derivations to this special case.

In the case of crease schemes, it is not sufficient to consider scalar schemes for estimating the convergence rate even with the assumption (4.38), as we did in Section 4.3. Recall ([6], Section 2.4) that a matrix stationary uniform subdivision scheme is a linear operator on the sequences of vectors $p_{ij} \in \mathbf{R}^n$

$$[Sp]_{ij} = \sum_{l,m} a^T_{i-2l,j-2m}p_{lm}, \quad i,j \in \mathbf{Z} \tag{4.40}$$

where a_{ij} are $n \times n$ matrices. In general, there is no subdivision scheme that would allow to compute forward differences in a particular direction on a finer level from the forward differences in the same direction on the coarser level. However, if a scheme S is parametrically C^1-continuous, there is a matrix subdivision scheme S' that allows us to compute the gradient of the limit function starting with the vector of forward differences. This scheme satisfies the commutation formula

$$\Delta_{12}Sp_{ij} = S'\Delta_{12}p_{ij} \tag{4.41}$$

where $\Delta_{12}p_{ij} = [p_{i+1\,j} - p_{ij}, p_{i\,j+1} - p_{ij}]^T$. The index of Δ refers to the particular pair of forward differences that is used. The three direction vectors $(0,0)$, $(0,1)$ and $(1,1)$ are often used throughout the derivations; to make the notation less cumbersome, we assign numbers

1, 2,3 to $(1,0)$, $(0,1)$, $(1,1)$ respectively and use 1,2,3 in indices instead of direction vectors: $\Delta_{(1,0)} = \Delta_1$, $\Delta_{(0,1)} = \Delta_2$, $\Delta_{(1,1)} = \Delta_3$. Clearly, we can define Δ in (4.41) using any pair of independent forward differences; it is useful to consider $\Delta_{13}p_{ij} = [p_{i+1\,j} - p_{ij}, p_{i+1\,j+1} - p_{ij}]^T$ and $\Delta_{23}p_{ij} = [p_{i\,j+1} - p_{ij}, p_{i+1\,j+1} - p_{ij}]^T$.

We use three operators acting on schemes, both uniform and nonuniform, and on Laurent polynomials for uniform schemes.

1. For any scheme S, the scheme S'_l, $l = 1, 2, 3$, satisfies

$$\Delta_l S p = S'_l \Delta_l p \tag{4.42}$$

   Note that S' may not exist. Our assumptions guarantee existence of such schemes for S^k.

   If S is uniform, the polynomials $a'_l(z)$ corresponding to S'_l as in previous section satisfy

$$a'_1(z) = \frac{a(z)}{z_1^{-1} + 1}, \quad a'_2(z) = \frac{a(z)}{z_2^{-1} + 1}, \quad a'_3(z) = \frac{a(z)}{z_1^{-1} z_2^{-1} + 1} \tag{4.43}$$

2. Next we define for any scheme S $\bar{S}_l$, $l = 1, 2, 3$ a scheme

$$Sp = \bar{S}_l \Delta_l p \tag{4.44}$$

   Again, $\bar{S}$ need not exist. If S is uniform, the polynomials $\bar{a}(z)$ satisfy

$$\bar{a}_1(z) = \frac{a(z)}{z_1^{-2} - 1}, \quad \bar{a}_2(z) = \frac{a(z)}{z_2^{-2} - 1}, \quad \bar{a}_3(z) = \frac{a(z)}{z_1^{-2} z_2^{-2} - 1} \tag{4.45}$$

3. Finally, operator $\mathcal{Z}_{(a,b)}$ is defined by

$$\left[\mathcal{Z}_{(a,b)}p\right]_{ij} = p_{i+a\,j+b} \tag{4.46}$$

For (a,b) being one of $(0,1)$, $(1,0)$, $(1,1)$ we use the notation $\mathcal{Z}_1$, $\mathcal{Z}_2$, $\mathcal{Z}_3$. The corresponding polynomials are

$$\mathcal{z}_1(z) = z_1^{-1}, \quad \mathcal{z}_2(z) = z_2^{-1} \quad \mathcal{z}_3(z) = z_2^{-1}z_1^{-1}$$

The following list of relations allows us to manipulate schemes in a formal way:

$$\Delta_l \quad = \mathcal{Z}_l - 1 \tag{4.47}$$

$$\Delta_l S \quad = S'_l \Delta_l \tag{4.48}$$

$$S \quad = \bar{S}_l \Delta_l \tag{4.49}$$

$$S^k \quad = S^0 - kD \tag{4.50}$$

where $l = 1, 2, 3$. The relations above using S' and $\bar{S}$ are valid only when these schemes are defined for a given S.

4.4.2 Commutation Formulas

In this section our goal is to derive commutation formulas for the crease schemes and schemes for their partial derivatives under the assumptions (4.38) and (4.39). Once we have expressions for the schemes in commutation formulas, it is straightforward to obtain contractivity estimates necessary to apply (4.10), using formulas similar to the $\|\cdot\|_\infty$-norm expressions for polynomials.

In the following formulas we use i, j to specify the domain for the formulas defining nonuniform schemes; if A, B, C are uniform subdivision schemes, then the expression

$$S = \begin{cases} A & \text{if } j \neq 0, -1 \\ B & \text{if } j = 0 \\ C & \text{if } j = -1 \end{cases} \quad \text{is equivalent to} \quad [Sp]_{ij} = \begin{cases} [Ap]_{ij} & \text{if } j \neq 0, -1 \\ [Bp]_{ij} & \text{if } j = 0 \\ [Cp]_{ij} & \text{if } j = -1 \end{cases}$$

Expanding the definition of a crease scheme using $D_l = \mathcal{Z}_l - 1$, $S^k = S^0 - kD$, and the fact that Δ and $\mathcal{Z}$ commute, we get

$$\Delta_2 S = \begin{cases} \Delta_2 S^0 & \text{if } j \neq 0, -1 \\ \mathcal{Z}_2 S^0 - S^k & \text{if } j = 0 \\ \mathcal{Z}_2 S^k - S^0 & \text{if } j = -1 \end{cases} = \begin{cases} \Delta_2 S^0 & \text{if } j \neq 0, -1 \\ \Delta_2 S^0 + kD & \text{if } j = 0 \\ \Delta_2 S^0 - k\mathcal{Z}_2 D & \text{if } j = -1 \end{cases}$$

$$= \begin{cases} {S^0}'_2 \Delta_2 & \text{if } j \neq 0, -1 \\ {S^0}'_2 \Delta_2 + k\bar{D}_2 \Delta_2 & \text{if } j = 0 \\ {S^0}'_2 \Delta_2 - k\mathcal{Z}_2 \bar{D}_2 \Delta_2 & \text{if } j = -1 \end{cases}$$

Thus, we can define

$$S'_2 = \begin{cases} {S^0}'_2 & \text{if } j \neq 0, -1 \\ {S^0}'_2 + k\bar{D}_2 & \text{if } j = 0 \\ {S^0}'_2 - k\mathcal{Z}_2 \bar{D}_2 & \text{if } j = -1 \end{cases} \tag{4.51}$$

For S'_1 we get

$$\Delta_1 S = \begin{cases} \Delta_1 S^0 & \text{if } j \neq 0 \\ \Delta_1 S^k & \text{if } j = 0 \end{cases} = \begin{cases} S^{0\prime} \Delta_1 & \text{if } j \neq 0 \\ (1-k) {S^0}'_1 \Delta_1 + k {S^1}'_1 \Delta_1 & \text{if } j = 0 \end{cases} = S'_1 \Delta_1 \tag{4.52}$$

The motivation behind the assumptions (4.38) and (4.39) was to make it possible to define S'_1 and S'_2 as scalar, not matrix, subdivision schemes.

We outline briefly the derivation for the matrix scheme S' for the cases when the condition on D does not hold. It is not possible to use $\bar{D}_2$. Instead, we can apply Proposition 4.9 to $d(z)$: the polynomial $d(z)$ can be decomposed as $p_1^d(z)(z_1^{-1}-1)+p_2^d(z)(z_2^{-1}-1)$; combined with assumption that both $a^0(z)$ and $a^1(z)$ are divided by $b(z)$, we we obtain a decomposition

$$d(z) = q_1^d(z)(z_1^{-2}-1)+q_2^d(z)(z_2^{-2}-1)$$

We can factor Δ_1 out of the first term and Δ_2 out of the second term. Thus, we express $\Delta_2 S$ as $A\Delta_1 + B\Delta_2$ where A and B are some schemes. This gives us two components of the matrix. The other two components are easily obtained from the expression for S'_1 above.

Next, we derive commutation formulas for the schemes S'_1 and S'_2. Note that $2S'_1$ and $2S'_2$ converge to the partial derivatives of the limit function of subdivision when it is C^1-continuous. The goal of our calculations is to obtain estimates for convergence using contractivity functions; we are going to use the function $D_1(p) = \max\left(\|\Delta_1 p\|_\infty, \|\Delta_3 p\|_\infty\right)$ for S'_2 and $D_2(p) = \max\left(\|\Delta_2 p\|_\infty, \|\Delta_3 p\|_\infty\right)$ for S'_1. Thus we need commutation formulas for Δ_3.

For $\Delta_1 S'_2$ we obtain

$$\Delta_1 S'_2 = \begin{cases} \Delta_1 S^{0\prime}{}_2 & \text{if } j \neq 0,-1 \\ \Delta_1 S^{0\prime}{}_2 + k\Delta_1 \bar{D}_2 & \text{if } j = 0 \\ \Delta_1 S^{0\prime}{}_2 - k\mathcal{Z}_2 \Delta_1 \bar{D}_2 & \text{if } j = -1 \end{cases} = \begin{cases} S^{0\prime\prime}{}_{21}\Delta_1 & \text{if } j \neq 0,-1 \\ S^{0\prime\prime}{}_{21}\Delta_1 + k\bar{D}'_{21}\Delta_1 & \text{if } j = 0 \\ S^{0\prime\prime}{}_{21}\Delta_1 - k\mathcal{Z}_2 \bar{D}'_{21}\Delta_1 & \text{if } j = -1 \end{cases}$$

Define

$$S''_{21} = \begin{cases} S^{0\prime\prime}{}_{21} & \text{if } j \neq 0,-1 \\ S^{0\prime\prime}{}_{21} + k\bar{D}'_{21} & \text{if } j = 0 \\ S^{0\prime\prime}{}_{21} - k\mathcal{Z}_2 \bar{D}'_{21} & \text{if } j = -1 \end{cases} \tag{4.53}$$

Then $\Delta_1 S'_2 = S''_{21}\Delta_1$.

For $\Delta_3 S'_2$ we get

$$\Delta_3 S_2' = \begin{cases} \Delta_3 {S^{0'}}_2 & \text{if } j \neq 0, -1, -2 \\ \mathcal{Z}_3 {S^{0'}}_2 - {S^{0'}}_2 - k\bar{D}_2 & \text{if } j = 0 \\ \mathcal{Z}_3 {S^{0'}}_2 + k\mathcal{Z}_3\bar{D}_2 - {S^{0'}}_2 + k\mathcal{Z}_2\bar{D}_2 & \text{if } j = -1 \\ \mathcal{Z}_3 {S^{0'}}_2 - k\mathcal{Z}_3\mathcal{Z}_2\bar{D}_2 - {S^{0'}}_2 & \text{if } j = -2 \end{cases}$$

$$= \begin{cases} {S^{0''}}_{23}\Delta_3 & \text{if } j \neq 0, -1, -2 \\ {S^{0''}}_{23}\Delta_3 - k\Delta_3\bar{D}_2 & \text{if } j = 0 \\ {S^{0''}}_{23}\Delta_3 + k(\mathcal{Z}_3 + \mathcal{Z}_2)\Delta_3\bar{D}_2 & \text{if } j = -1 \\ {S^{0''}}_{23}\Delta_3 - k\mathcal{Z}_3\mathcal{Z}_2\Delta_3\bar{D}_2 & \text{if } j = -2 \end{cases}$$

As we have observed, $d(z)$ can be decomposed as

$$d(z) = q_1^d(z)(z_1^{-2} - 1) + q_3^d(z)(z_1^{-2}z_2^{-2} - 1)$$

Denote Q_1^d and Q_3^d the schemes corresponding to polynomials $q_1^d(z)$ and $q_3^d(z)$.

Thus, we can write the following commutation formula

$$\Delta_3 D = Q_1^d\Delta_1 + Q_3^2\Delta_3$$

Thus for $\Delta_3 S_2'$ we get

$$\Delta_3 S_2' = \begin{cases} {S^{0''}}_{23}\Delta_3 & \text{if } j \neq 0, -1, -2 \\ ({S^{0''}}_{23} - k[\bar{Q_3^d}]_2)\Delta_3 - k\bar{Q_{12}^d}\Delta_1 & \text{if } j = 0 \\ ({S^{0''}}_{23} + k(\mathcal{Z}_3 + \mathcal{Z}_2)[\bar{Q_3^d}]_2)\Delta_3 + k(\mathcal{Z}_3 + \mathcal{Z}_2)[\bar{Q_1^d}]_2\Delta_1 & \text{if } j = -1 \\ ({S^{0''}}_{23} - k\mathcal{Z}_3\mathcal{Z}_2[\bar{Q_3^d}]_2)\Delta_3 - k\mathcal{Z}_3\mathcal{Z}_2[\bar{Q_1^d}]_2\Delta_1 & \text{if } j = -2 \end{cases} \tag{4.54}$$

Define two difference schemes

$$S''_{23,3} = \begin{cases} S^{0\prime\prime}{}_{23} & \text{if } j \neq 0, -1, -2 \\ (S^{0\prime\prime}{}_{23} - k[\bar{Q}^d_3]_2) & \text{if } j = 0 \\ (S^{0\prime\prime}{}_{23} + k(\mathcal{Z}_3 + \mathcal{Z}_2)[\bar{Q}^d_3]_2) & \text{if } j = -1 \\ (S^{0\prime\prime}{}_{23} - k\mathcal{Z}_3\mathcal{Z}_2[\bar{Q}^d_3]_2) & \text{if } j = -2 \end{cases}$$

$$S''_{23,1} = \begin{cases} 0 & \text{if } j \neq 0, -1, -2 \\ -k\bar{Q}^d_{12} & \text{if } j = 0 \\ k(\mathcal{Z}_3 + \mathcal{Z}_2)[\bar{Q}^d_1]_2 & \text{if } j = -1 \\ -k\mathcal{Z}_3\mathcal{Z}_2[\bar{Q}^d_1]_2 & \text{if } j = -2 \end{cases} \tag{4.55}$$

Then

$$\Delta_3 S''_2 = S_{23,3}\Delta_3 + S_{23,1}\Delta_1$$

.

For $\Delta_2 S'_1$ and $\Delta_3 S'_1$ we have

$$S''_{12} = \begin{cases} S^{0\prime\prime}{}_{12} & \text{if } j \neq 0, -1 \\ S^{0\prime\prime}{}_{12} + k\bar{D}'_{12} & \text{if } j = 0 \\ S^{0\prime\prime}{}_{12} - k\mathcal{Z}_2\bar{D}'_{12} & \text{if } j = -1 \end{cases}$$

$$S''_{13} = \begin{cases} S^{0\prime\prime}{}_{13} & \text{if } j \neq 0, -1 \\ S^{0\prime\prime}{}_{13} + k\bar{D}'_{13} & \text{if } j = 0 \\ S^{0\prime\prime}{}_{13} - k\mathcal{Z}_3\bar{D}'_{13} & \text{if } j = -1 \end{cases} \tag{4.56}$$

The commutation formulas for S'_1 are $\Delta_2 S'_1 = S''_{12}\Delta_2$, $\Delta_3 S'_1 = S''_{13}\Delta_3$.

Commutation formulas could be derived in full generality for a matrix scheme with 4 components instead of the pair S'_1 and S'_2 and a matrix scheme with 16 components instead of S''_{12}, S''_{13}, S''_{21}, $S''_{23,1}$, $S''_{23,3}$ using polynomial decompositions of the type used for d. Whenever a scheme is affine-invariant, decompositions of this type are guaranteed to exist.

Further, for schemes with negative coefficients, the schemes S'_1 and S'_2 may be non

contractive (the Butterfly scheme being the primary example). Then it is necessary to consider powers of the scheme. The commutation formulas above have to be applied several times in such cases.

Comparison Schemes. The commutation formulas above allow us to estimate the rate of convergence (γ in the equation (4.10)) in the way described below; we also need to estimate the constant c, the measure of approximation by a comparison scheme. If we use piecewise linear subdivision scheme S_b as the comparison scheme for the limit function of S, it is natural to use piecewise constant schemes S_{b_1}, S_{b_2} defined in the previous section, as the comparison schemes for partial derivatives, as the limit functions of these schemes are derivatives of the piecewise linear function generated by S_b, whenever these derivatives are defined.

To estimate $S'_1 - S_{b_1}$ in terms of the contractivity function D_1 it is sufficient to factor out Δ_2 and Δ_3. Using Proposition 4.9, we can write the difference $a'_1 - b_1$ as $b_{12}p_{12}(z_1^{-1} - 1) + b_{12}p_{13}(z_2^{-1}z_1^{-1} - 1)$

Thus,

$$S'_1 - S_{b_1} = \begin{cases} S_{b_{12}p_{12}}\Delta_1 + S_{b_{13}p_{13}}\Delta_3 & \text{if } j \neq 0 \\ S_{b_{12}p_{12}}\Delta_1 + (S_{b_{13}p_{13}} + k\bar{D}'_{13})\Delta_3 & \text{if } j = 0 \end{cases} \tag{4.57}$$

and

$$S'_2 - B_2 = \begin{cases} S_{b_{21}p_{21}}\Delta_1 + S_{b_{23}p_{23}}\Delta_3 & \text{if } j \neq 0, -1 \\ (S_{b_{21}p_{21}} + k[\bar{Q}^d_1]_2)\Delta_1 + (S_{b_{23}p_{23}} + k[\bar{Q}^d_3]_2)\Delta_3 & \text{if } j = 0 \\ (S_{b_{21}p_{21}} - k\mathcal{Z}_2[\bar{Q}^d_1]_2)\Delta_1 + (S_{b_{23}p_{23}} - k\mathcal{Z}_2[\bar{Q}^d_3]_2)\Delta_3 & \text{if } j = -1 \end{cases} \tag{4.58}$$

Convergence parameters. Finally, we discuss how to compute convergence parameters γ and c given the commutation formulas. Suppose that a scheme S satisfies relations of the type

$$\begin{aligned}\Delta_i S &= S_{ii}\Delta_i + S_{ij}\Delta_j \\ \Delta_j S &= S_{ji}\Delta_i + S_{jj}\Delta_j\end{aligned}$$

Then we can make an estimate of the convergence rate using the function $D_{ij}(p) = \max(\|\Delta_i p\|_\infty, \|\Delta_j p\|_\infty)$:

$$\begin{aligned}D_{ij}(Sp) &= \max\left(\|S_{ii}\Delta_i p + S_{ij}\Delta_j p\|_\infty, \|S_{ji}\Delta_i p + S_{jj}\Delta_j p\|_\infty\right) \leq \\ &\leq \max\left(\max(\|S_{ii}\|_\infty, \|S_{ij}\|_\infty) D_{ij}(p), \max(\|S_{ji}\|_\infty, \|S_{jj}\|_\infty) D_{ij}(p)\right) \leq \\ &\leq \max\left(\|S_{ii}\|_\infty, \|S_{ij}\|_\infty, \|S_{ji}\|_\infty, \|S_{jj}\|_\infty\right) D_{ij}(p)\end{aligned} \tag{4.59}$$

The last question that we have to address is calculation of the operator norms for nonuniform subdivision schemes described above. An estimate of the norm from above is the maximum of the norms of the uniform schemes that are used to construct the scheme on each subdomain ($j \neq 0, -1$, $j = 0$, $j = -1$ for some of the schemes above). The norm can be calculated precisely, if we exclude the sums in the formulas (4.29) that correspond to the elements outside the domains: for example, if the scheme is used on the domain $j = 0$, the coefficients for odd j are never used.

4.5 The Algorithm for Checking C^1-continuity of a Subdivision Scheme

The following algorithm can be used to check C^1-continuity of a subdivision scheme on the regular part of the surface and near an extraordinary point of a fixed valence. Note that if this test fails, the scheme still can be C^1-continuous. It is likely, however, that the success of the test is necessary for C^1-continuity of a large class of schemes. This is a brief outline of the algorithm; details of the implementation for particular types of schemes are discussed in the next chapter.

1. Establish C^1-continuity of the scheme on the regular complex; this may be known *a priori*, as it is in the case of polynomial patches; otherwise, convergence estimates

derived in this section can be used to check C^1-continuity

2. Compute the convergence estimates for the scheme and the derivatives if they were not computed on the first step.

3. For the given valence, compute the eigenvectors with an initial precision.

4. Compute linear approximations to the characteristic map on a layer defined in Section 2.4 keeping track of the error bounds.

5. Test if the image of the layer is isolated from 0, using convergence estimates for the limit function of subdivision. The test can either fail (layer is not isolated from 0) or succeed (the layer is isolated from 0) or the result cannot be determined on this subdivision level. If this test fails, the whole test fails. If the test is successful, it is not repeated on the next subdivision level.

6. If the previous test is successful, compute the winding number of the approximation to the outer boundary curve as described in Section 4.1. If it is not 1, the whole test failed. If it is successful, this test is not repeated on the next subdivision level. This test always either fails or is successful, as the winding number can be determined from the linear approximation of the curve given that the previous test was successful.

7. Compute the lower and upper bounds for the minimum and maximum of the Jacobian using the Jacobians of the linear approximation and convergence estimates. If the minimal and maximal Jacobians have the same sign, the whole test is successful; if the minimal and maximal Jacobians have different signs, the whole test fails. If the signs of Jacobians cannot be determined, compute the next subdivision approximation and return to step 4.

4.6 Continuity with Respect to the Control Values

Convergence estimates derived in the previous sections allow us to examine smoothness of subdivision for fixed subdivision matrices; the estimates of Section 4.4 allow to analyze smoothness of particular parametric families of schemes on regular complexes. To extend this analysis of families to the neighborhoods of extraordinary points, we note that the limit functions generated by subdivision are linear combinations of the basis functions with

coefficients being the control values. Clearly, the same is true for the derivatives of the limit functions. Therefore, the limit functions and its derivatives are continuous functions of control values. If the control values of a characteristic map continuously depend on a parameter, as it is the case for crease schemes, it follows from regularity and injectivity of a characteristic map for a particular value of the parameter that all characteristic maps for nearby values of the parameter are also regular and injective, and corresponding schemes are C^1-continuous.

The same idea can be used to analyze smoothness of a given scheme on a k-regular complex for arbitrary value of k. Suppose the scheme is defined in such a way that some properly chosen affine transformations of control points of all sectors of the characteristic map converge to one of a set of fixed configurations as $k \to \infty$. If for these configurations we can prove regularity and if we can prove injectivity for all maps, then the scheme is smooth for arbitrary k.

It is clear that this approach does not always work: for example, if the dominant eigenvalues of the subdivision matrix approach 1 as $k \to \infty$, the limit configurations do not produce regular maps. However, in this case from practical point of view for sufficiently large k, the behavior of the scheme is be indistinguishable from non-C^1-continuous. More precisely, the convergence rate for the derivatives is very slow. When the scheme is "stably smooth" as $k \to \infty$ (for example, modified Butterfly and Loop schemes described in the next section), then smoothness for arbitrary k can be established by examining the limit configurations if they exist.

To implement this approach, we need an estimate of the change of the limit function and its derivatives given a change in the control values. As we cannot assume a closed-form expression for the basis function and its derivatives, two approaches are possible. The first approach is to use the decomposition

$$f(t) = \sum_{i,j} p_{ij} B(t - t_{ij}), \quad t_{ij} = (i, j)$$

where t is a point in the regular topological complex identified with the plane in the standard way, $B(t)$ is the basis (scaling) function corresponding to the scheme, p_i are the control values. For schemes with bounded support the basis function has compact support

so for a fixed t summation goes over a finite number of copies of the basis function. Let this number be K. Using subdivision we can compute B theoretically with arbitrary precision. Let the approximation error of our calculation be ϵ. Then we can easily obtain the following estimate:

$$\|f(t)\|_\infty \leq \sum_{i,j} \|B(t-t_{ij})\|_\infty \|p\|_\infty + K\epsilon \tag{4.60}$$

where p is the vector of control values. However, the error term for realistic $K\epsilon$ may be significant for derivatives. By necessity, our estimates of the error ϵ based on (4.10) are quite conservative, especially in the case of schemes with negative coefficients, such as Butterfly. For a reasonable number of subdivision levels (≤ 10) the error term may still be very large.

It is useful to derive a better estimate directly using contractivity functions.

$$\begin{aligned}
\|f(t)\|_\infty &= \|S^\infty p\|_\infty \leq \left\| \sum_{i=0}^{\infty} \left(S^{i+1} - S^i\right) p^m + p^m \right\|_\infty \leq \\
&\leq \left\| \sum_{i=0}^{\infty} (S-B) p^{m+i} \right\|_\infty + \|p^m\|_\infty \leq c \sum_{i=0}^{\infty} \sum_{q=0}^{N-1} D(p^{m+iN+q}) + \|p^m\|_\infty \leq \\
&\leq \frac{c}{1-\gamma} \sum_{q=0}^{N-1} D(p^{m+q}) + \|p^m\|_\infty
\end{aligned}$$

Suppose $m = kN + q_0$. Then

$$\begin{aligned}
\|f(t)\|_\infty &\leq \frac{c}{1-\gamma} \sum_{q=0}^{N-1} D(p^{kN+q_0+q}) + \|p^m\|_\infty \leq \\
&\leq \frac{c\gamma^k}{1-\gamma} \left(\sum_{q=q_0}^{N-1} D(p^q) + \gamma \sum_{q=0}^{q_0-1} D(p^q) \right) + \|p^m\|_\infty
\end{aligned}$$

Observe that $D(p) \leq 2\|p\|_\infty$ for all choices of $D(p)$ that we use. This leads to the following estimate

$$\|f\|_\infty \leq \left(\frac{2c\gamma^{\lfloor \frac{m}{N} \rfloor}}{1-\gamma} \Big(\gamma \sum_{q=0}^{m \bmod N-1} \|S^q\|_\infty + \sum_{q=m \bmod N}^{N-1} \|S^q\|_\infty \Big) + \|S^m\|_\infty \right) \|p\|_\infty \tag{4.61}$$

In the next chapter we will use this estimate to prove smoothness of the modified Butterfly and Loop schemes on arbitrary k-regular complex; see the next chapter for details.

Chapter 5 Algorithms for Verification of C^1-continuity

In this chapter we describe in detail the algorithms for checking C^1-continuity of subdivision schemes outlined in the previous chapter. These algorithms are used to establish C^1-continuity of several subdivision schemes in the next chapter.

The main idea of all algorithms is to use a sufficiently close linear approximation to the characteristic map to determine regularity and injectivity of the characteristic map or a family of sufficiently close maps.

5.1 Error Types

In this section we discuss the types of error that have to be taken into account in our algorithms.

Floating point error. Evaluating derivatives of subdivision schemes with slow convergence may require a large number of subdivision steps. For example, approximately 7 levels of subdivision are necessary to determine whether the Jacobian changes sign [1] In practically all cases there is little hope to perform more than 3-4 subdivision steps in symbolic form: the general data structures, memory management strategies and arbitrary precision floating point implementations used in common symbolic algebra packages make them difficult to use for extensive computations. In addition, the generalized eigenvectors of the subdivision matrix quite often can be represented only approximately. These factors suggest an implementation based on finite-precision arithmetics.

As the goal of our algorithms is to establish certain properties of the characteristic map precisely, we need to keep track of guaranteed lower and upper bounds for each number. One approach would be to encode the precision in the number of digits used

[1] After the work described in this thesis was completed, we have developed an improved method which allows us to determine if a map is regular with fewer subdivision steps; nevertheless, if the convergence of a scheme is slow, implementations using a symbolic algebra system is not feasible.

in the representation, as it is done in Maple or Mathematica. An alternative approach is to represent the numbers as intervals.

The ideas of interval arithmetic date back at least to Moore's work [43], [44]. The IEEE 754 standard made possible consistent and efficient implementations on a variety of hardware (e.g., PROFIL/BLAS package [34]).

A number of approaches can be used to implement this type of arithmetic. One approach would be to use IEEE standard operations "round to $+\infty$" and "round to $-\infty$" to compute the upper and lower bounds of the intervals, as suggested in [60].

Another approach was implemented in the `RealExpr` package described in [65] and in detail in [46] the `BigFloat` representation for numbers. A distinctive feature of this package is that it does not rely on the hardware floating point and uses an arbitrary-length integer representation for mantissas instead. Although this approach leads to significantly longer run times, it avoids the limitations on precision inherent in fixed-size representations. If our algorithm fails because the intervals for computed values grow too large before it is possible to determine whether the scheme is C^1-continuous or not, we can simply increase the precision and rerun the algorithm.

We have compared implementations of our algorithms based on these two approaches and found that at least for the examples that we have considered the hardware-based implementation is sufficient.

Linear approximation error. This error is defined by

$$\epsilon_{approx} = \|L_m - f\|_\infty$$

where L_m is the linear or piecewise constant approximation obtained after m steps of subdivision. The upper bounds on this error were derived in the previous chapter.

Control point approximation error. This type of error is defined by

$$\epsilon_{contr} = \|f[p] - f[\tilde{p}]\|_\infty$$

where p is the actual vector of control values, $\tilde{p}$ is the approximation of the vector of control values. This error was estimated in Section 4.6. The input of our algorithms

includes vectors of control points in interval representation; extending the intervals to include all initial configurations of control points that are of interest, we can simultaneously examine C^1-continuity of a parametric set of characteristic schemes for a sufficiently small ranges of parameters.

In all cases, the precise value is not known explicitly, and the error is not known either. In our calculations we track an upper bound for the error, rather than the error itself. Below we use the term "error" when referring to upper bounds.

The use of the interval representation allows us to obtain guaranteed bounds on the results; however, not all operations on real numbers can be extended to the interval representations. In the next subsections we define the representations precisely, introduce a set of operations defined on the interval representations and formulate the algorithms described in chapter 4 in terms of these operations.

5.2 Interval Representations

In our algorithms, we use the following set of operations on the interval numbers: binary $+$, $-$, $*$, $/$, min,max, unary $-$. In addition, for any number a, which has an exact representation, and for any interval number X we can check if a belongs to X. For any interval number X $ceil(X) = \overline{X}$ is the larger endpoint of the interval, and $floor(X) = \underline{X}$ is the smaller endpoint.

Conversion of a rational number to an interval number can be regarded as a special case of division. Also, given a floating point number with a known number of valid digits, we can easily compute a corresponding interval representation with the error being determined by the last valid digit.

Hardware-based interval representation. Each interval number X is a pair of machine floating point numbers $(\underline{X}, \overline{X})$. A real number a belongs to X if $\underline{X} \leq a \leq \overline{X}$. Following Moore, we define the operations on the interval numbers. In the formulas below the operations on hardware f.p. numbers performed in round-to-$+\infty$ mode are denoted with an arrow pointing up and operations performed in round-to-∞ with an arrow pointing down.

- addition

$$\underline{X+Y} = \underline{X} \downarrow + \underline{Y}, \quad \overline{X+Y} = \overline{X} \uparrow + \overline{Y}$$

- subtraction

$$\underline{X-Y} = \underline{X} \downarrow - \overline{Y}, \quad \overline{X-Y} = \overline{X} \uparrow - \underline{Y}$$

- multiplication

$$\underline{X \cdot Y} = \min(\underline{X \cdot Y}, \underline{X \cdot \overline{Y}}, \underline{\overline{X} \cdot Y}, \underline{\overline{X} \cdot \overline{Y}})$$
$$\overline{X \cdot Y} = \max(\underline{X} \cdot \underline{Y}, \underline{X} \cdot \overline{Y} \, \overline{X} \cdot \underline{Y}, \overline{X} \cdot \overline{Y})$$

- division (assuming $0 \notin Y$)

$$\underline{X/Y} = \min(\underline{X} \downarrow / \underline{Y}, \underline{X} \downarrow / \overline{Y}, \overline{X} \downarrow / \underline{Y}, \overline{X} \downarrow / \overline{Y})$$
$$\overline{X/Y} = \max(\underline{X} \uparrow / \underline{Y}, \underline{X} \uparrow / \overline{Y}, \overline{X} \uparrow / \underline{Y}, \overline{X} \uparrow / \overline{Y})$$

- minimum

$$\underline{\min(X,Y)} = \min(\underline{X}, \underline{Y}) \quad \overline{\min(X,Y)} = \min(\overline{X}, \overline{Y})$$

- maximum

$$\underline{\max(X,Y)} = \max(\underline{X}, \underline{Y}) \quad \overline{\max(X,Y)} = \max(\overline{X}, \overline{Y})$$

`BigFloat` Number Representation. Part of this section is adopted from the work of Ouchi [46].

Let $B = 2^c$, where $c = \lfloor L/2 \rfloor - 2$, L is the number of bits used for representing an integer. Each `BigFloat` number is a triple $\langle m, err, exp \rangle$ where

- $m \in \mathbf{Z}$ is mantissa, represented by an arbitrary-length integer;
- $err \in \mathbf{N}$ is the error *normalized*, i.e., be in the range $0 \ldots 2^L - 1$;
- exponent $exp \in \mathbf{Z}$, which is assumed to be in the range $-2^{L-1} \ldots 2^{L-1} - 1$.

We say that a real number X belongs to a `BigFloat` $x = \langle m, err, exp \rangle$ if

$$X \in [(m - err)B^{exp}, (m + err)B^{exp}]$$

The general definition of a binary operation @ on two numbers $x = \langle m_x, err_x, exp_x \rangle$ and $y = \langle m_y, err_y, exp_y \rangle$ is a number $z = \langle m_z, err_z, exp_z \rangle$, which satisfies the following condition:

if a real X belongs to x and a real Y belongs to y, then $X@Y$ belongs to z.

It would be desirable to minimize $err_z B^{exp_z}$ subject to the condition above and error normalization conditions. Unfortunately, this is not computationally feasible, and in some cases compromise formulas for computing z are adopted, which attempt to minimize the error without sacrificing the performance.

The formulas for the arithmetic operators are derived in [46]. Here we describe the formulas for addition/subtraction and multiplication; the formulas for division are quite complex and can be found in the cited work.

Addition/Subtraction. For the sum of two `BigFloat` numbers x and y, the sum is defined as follows.

Assume $exp_x \geq exp_y$. If $exp_x = exp_y$

$$\begin{aligned} m_z &= m_x + m_y \\ err_z &= err_x + err_y \\ exp_z &= exp_x \end{aligned}$$

If $exp_x > exp_y$ and $err_x = 0$,

$$\begin{aligned} m_z &= m_x B^{exp_x - exp_y} + m_y \\ err_z &= err_y \\ exp_z &= exp_y \end{aligned}$$

If $exp_x > exp_y$ and $err_x > 0$,

$$
\begin{aligned}
m_z &= m_x + \mathrm{sgn}(m_y) \left\lfloor |m_y| B^{exp_y - exp_x} \right\rfloor \\
err_z &= err_x + 5 \\
exp_z &= exp_x
\end{aligned}
$$

In the last case the error may have to be renormalized. The definition for the difference is similar.

Multiplication. The product of x and y is defined by

$$
\begin{aligned}
m_z &= m_x m_y \\
err_z &= |m_x| err_y + |m_y| err_x + err_x err_y \\
exp_z &= exp_x + exp_y
\end{aligned}
$$

The error has to be renormalized.

Min/Max. It is sufficient to define min. Several cases are possible (we assume that $exp_x \geq exp_y$):

1. $exp_x = exp_y$; if $m_x \geq m_y$,

$$
\begin{aligned}
m_z &= m_x \\
err_z &= \max(err_x, err_y - m_y + m_x) \\
exp_z &= exp_x
\end{aligned}
$$

The case $m_y < m_x$ is similar with x and y exchanged.

2. $exp_x > exp_y$, $m_x B^{exp_x - exp_y} \leq m_y$ and $(m_x - err_x) B^{exp_x - exp_y} > m_y - err_y$

$$m_z = m_x B^{exp_x - exp_y}$$
$$err_z = m_x B^{exp_x - exp_y} - m_y + err_y$$
$$exp_z = exp_y$$

If $(m_x - err_x)B^{exp_x - exp_y} <= m_y - err_y$ then $z = x$.

3. $exp_x > exp_y$, $m_x B^{exp_x - exp_y} > m_y$ and $(m_x - err_x)B^{exp_x - exp_y} \leq m_y - err_y$

$$m_z = m_y$$
$$err_z = m_y - (m_x - err_x)B^{exp_x - exp_y}$$
$$exp_z = exp_y$$

If $(m_x - err_x)B^{exp_x - exp_y} > m_y - err_y$, then $z = y$.

5.3 Input of the Algorithms

In our description of the algorithms we do not assume any specific data structures for representing the mesh; we assume that there is a way to iterate through all values in the mesh and compute forward differences and second differences at all vertices where they are defined.

The algorithms compute linear approximation errors for the function and derivatives using formulas (4.26), (4.27) and (4.59).

The input is a collection of 2D control points G_0, typically a part or a whole control set for the characteristic map, and constants $\gamma, C, \gamma_j, C_j,\ j = 1, 2$ estimating the convergence rate of subdivision.

Formally, let $G_0 \in \mathcal{P}(P, \mathbf{R}^2 \times \mathbf{R}^2)$ be a vector of 2D control points defined on a subset P of the regular complex identified with the plane with coordinates (t_1, t_2) in the usual manner (Section 2.2). The values of G_0 are represented using 2-vectors of interval numbers, thus the range is $\mathbf{R}^2 \times \mathbf{R}^2$ (pairs of intervals) rather than $\mathbf{R}^2$ (pairs of numbers).

Let $\Phi = (f_1, f_2)$ be the limit function corresponding to these control points, defined on

a maximal subset D of $|P|$ such that $\mathrm{Ctrl}^0(D) \in P$. Note that Φ is an interval function with values in $\mathbf{R}^2 \times \mathbf{R}^2$. The range of such a function in $\mathbf{R}^2$ is the union all points $y \in \mathbf{R}^2$ such that $y \in \Phi(y)$ for some y. When Φ is defined by interval approximations to dominant generalized eigenvectors of a subdivision scheme, we call it an *interval characteristic map.*

Let $\tilde{P}^i$ be the maximal subcomplex of P^i (i-th subdivision of P) such that $\mathrm{Ctrl}^0(\tilde{P}^i) \subset P$. Let $\tilde{G}^i$ be the restriction of G^i to $\tilde{P}^i$. $\tilde{L}^i$ is the linear or piecewise constant extension of $\tilde{G}^i$ to D.

The functions $\epsilon_j(C, \gamma, \tilde{G}^i, i)$, $j = 1, 2$, $\epsilon_{jk}(C_j, \gamma_j, \tilde{G}^i, i)$,$j = 1, 2$, $k = 1, 2$, compute linear approximation errors at level i for the functions f_1 and f_2 and their partial derivatives, using formulas (4.26), (4.27) and (4.59).

$$\|f_j - L_i\|_\infty < \epsilon_j, \quad j = 1, 2$$

$$\left\| \frac{\partial f_j}{\partial t_m} - L_i \right\|_\infty < \epsilon_{jm}, \quad m = 1, 2 \quad j = 1, 2$$

To define the initial control net G^0 more specifically, we consider the characteristic map of a subdivision scheme on a k-regular complex $\mathcal{R}_k$, with k fixed.

As input to our algorithm we use the control set for a ring of triangles Ring_k of $\mathcal{R}_k$, which have vertices v_{ijl} with $i = 0 \ldots k-1$, $j = r_1 \ldots r_2$, $l < j$ (see Figure 2.3 for notation). We refer to this control set as the control net of the ring.

The inner and outer radii r_1 and r_2 are defined by the following conditions:

- For any triangle T of Ring_k
$$v_{000} \notin \mathrm{Loc}^0(T)$$
- If ρ^m is the identification of $\mathcal{R}_k^0$ and $\mathcal{R}_k^m$, then
$$(\cup_{m=0}^{\infty} |\rho^m(\mathrm{Ring}_k)|) \cup \{0\} \quad \text{contains a neighborhood of } 0$$
- r_1 is the minimal value such that the ring satisfying the first two conditions exist; r_2 is the minimal value of r_2 for r_1.

Informally speaking, this means that the subdivision rules that are used to subdivide

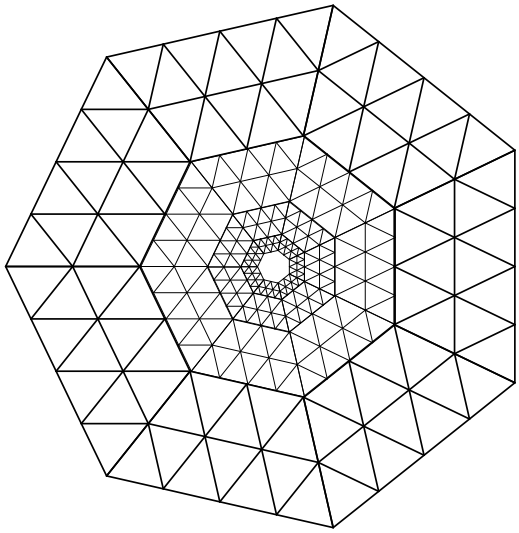

Figure 5.1: The ring Ring_7 for the Loop scheme and 3 scaled copies of the ring; the ring coincides with the domain of the characteristic map in the sense of Reif. The union of all scaled copies is the interior of the 7-gon bounded by the outer boundary of Ring_7 excluding 0.

Ring_k are the subdivision rules that are used on the regular complex, and a neighborhood of zero is covered by scaled copies of the ring as shown in the Figure 5.1.

The characteristic map in our sense restricted to Ring_k coincides with the characteristic map in the sense of Reif whenever it is defined.

Note that although the only meaningful input to the whole algorithm is the control net of the ring of the characteristic map, the subalgorithms (regularity test, isolation from zero test, winding number calculation) can be used to determine properties of other maps generated by subdivision, which need not be characteristic maps. In particular, we use isolation from zero test and winding number computation to establish that the Butterfly scheme does *not* satisfy a necessary condition for regularity.

5.4 Algorithm for Testing C^1-Continuity for Fixed Valence

We define the algorithm for testing C^1-continuity of subdivision on a k-regular complex for fixed k starting with the top level. The main algorithm uses a number of subalgorithms, which will be described in subsequent sections. The following subalgorithms are used:

`TestRegular` tests whether the map defined by the control net G^0 has Jacobian of constant

sign.

`TestIsolZero` tests whether the map has value 0.

`TestInjective` tests if the boundary curve of the map has winding number 1 or -1. Assuming that the first two tests succeeded, this means that the map is injective.

Assumptions: We assume that the dominant generalized eigenvectors defining the characteristic map are eigenvectors, to be able to apply Lemma 4.6.

Input:

$\tilde{G}^0_k$, the control net for Ring_k;

convergence rate estimates C, γ, C_i, γ_i^N, $i = 1, 2$. N is the number of levels of subdivision used in (4.26) and (4.27). (For simplicity, we assume that it is the same for the function and both derivatives.)

maxlevel The maximal number of levels of subdivision to perform.

If the algorithm is able to establish C^1-continuity, it is established for all maps with convergence described by the input constants or better, and with control points of the characteristic maps belonging to the interval control points of $\tilde{G}^0$. This fact can be used to establish C^1-continuity of certain types of schemes for arbitrary valence as explained in Section 6.2.1.

Output:

`true` if the scheme is C^1-continuous,

`false` if the scheme is not C^1-continuous or the assumption
$\Phi^{-1}(0) = \{0\}$ of Lemma 4.6 is not satisfied.

`undefined` if the algorithm cannot determine whether the scheme is C^1-continuous, but it might be possible to give a definite answer with more subdivision steps, and

`fail` if the algorithm could not determine C^1-continuity and increasing the number of subdivision steps does not help because the precision of the arithmetic is insufficient.

```
TestC1cont( G̃^0_k, C, γ, C_{1,2}, γ^N_{1,2}, maxlevel)

isolationTestOK := injectiveTestOK := regularTestOK := undefined
for i = 0 to maxlevel
  compute G̃^i_k
  if isolationTestOK≠ true then
    isolationTestOK := TestIsolZero(G̃^i_k, C,γ,max(ε_1, ε_2))
    if (isolationTestOK= false) then return false
  endif

  if (injectiveTestOK ≠ true) and (isolationTestOK = true) then
    injectiveTestOK := TestInjective(G̃^i_k, C,γ)
    if (injectiveTestOK= false) or (injectiveTestOK= fail) then return injectiveTestOK
  endif

  if regularTestOK≠ true then
    regularTestOK := TestRegular(G̃^i_k, C_{1,2},γ_{1,2})
    if (regularTestOK= false) then return false
  endif

  if injectiveTestOK= true and isolationTestOK= true and regularTestOK= true then
    return true
endfor
return undefined
```

5.5 Algorithm for Testing Regularity

This algorithm attempts to check if the limit function f has non-zero Jacobian everywhere on D. This algorithm does not rely on any assumptions about the nature of $\tilde{G}^0$ and can be used on any initial control net.

Input: $\tilde{G}^0$, γ_j, C_j, $j = 1, 2$ as defined above.

Denote $Int(A)$ the subset of a set A of vertices of the regular complex such that if $v_{kl} \in \mathrm{Int}(A)$, then $v_{k+1\,l} \in A$ and $v_{k\,l+1} \in A$, i.e., forward differences at this point can be computed.

Output: `true` if the function is regular, `false` if not, `undefined` if the algorithm could not make a decision.

For brevity, we omit the arguments of ϵ_{jk} which are clear from the context.

```
TestRegular( G̃^0, γ_{1,2}, C_{1,2})

  J_{min min} := +∞, J_{min max} := +∞
  J_{min min} := −∞, J_{max max} := −∞
  foreach v_{kl} ∈ Int(G̃^i)
    d^1 := G̃^i(i+1, j) − G̃^i(i, j)
    d^2 := G̃^i(i, j+1) − G̃^i(i, j)
    compute 16 numbers J_l, l = 1...16
    choosing signs in (d^1_1 ± ε_{11})(d^2_2 ± ε_{22})(d^1_2 ± ε_{12})(d^2_1 ± ε_{21})
    J_min := min(J_l, l = 1...16)
    J_max := max(J_l, l = 1...16)
    J_{min min} := min(J_min, J_{min min})   J_{min max} := min(J_max, J_{min max})
    J_{max min} := max(J_min, J_{max min})   J_{max max} := max(J_max, J_{max max})
    if 0 ∉ J_{min max} and 0 ∉ J_{max min}
       and J_{min max} and J_{max min} have different signs then
      return false
  endforeach
if 0 ∉ J_{min min} and 0 ∉ J_{max max}
   and J_{min min} and J_{max max} have the same sign then
  return true
return undefined
```

If we can make the precision of $\tilde{G}_k^0$ arbitrarily high, our algorithm returns `undefined` only if the Jacobian is zero at some points, but never changes the sign for all maps in the set defined by the intervals of the initial control points (assuming infinite amounts of time and memory available).

Note that the algorithm never returns `fail`. It seems to be reasonable to expect that further refinement does not help if $0 \in J_{min}$ and $0 \in J_{max}$ or $0 \in \epsilon$. Proving if this is indeed the case is rather difficult, so we do not use this condition for termination.

5.6 Algorithm For Testing Isolation from Zero

This algorithm determines if the range of the limit interval function produced by $\tilde{G}_k^0$ is further than δ from $(0,0)$ in $\|\cdot\|_\infty$ norm. This algorithm does not rely on any assumptions about the nature of $\tilde{G}^0$ and can be used on any initial control net. The idea of the algorithm is straightforward: if it is known that the function is approximated within ϵ, and if all values of the approximation are further than $\epsilon + \delta$ from zero, the limit function cannot have value zero.

Input: $\tilde{G}^0$, γ, C, as defined above; δ.

Output: `true` if the function has no value $f(y)$ with $\|f(y)\|_\infty < \delta$, `false` if it does, `undefined` if the algorithm could not make a decision.

```
TestIsolZero( G̃^i, C, γ, δ)

  foreach v_kl ∈ G̃^i
    d_1 := |G̃^i_1(v_kl)| − δ − ε_1
    d_2 := |G̃^i_2(v_kl)| − δ − ε_2
    if d_1 and d_2 are both negative  then return false
    if 0 ∈ d_1  and 0 ∈ d_2  then return undefined
  endforeach
  return true
```

This algorithm can be made considerably more efficient if additional information is

known: for example, if the map is regular on the domain, and the domain is a union of triangles of the initial complex, then we can check these conditions by scanning only the points on the boundary.

5.7 Algorithm for Testing Injectivity

Unlike the previous two algorithms, this algorithm is specific for characteristic maps. Here we use the assumption that Lemma 4.6 can be applied. The generalized eigenvectors have to be known in advance; the condition $\Phi^{-1}(0) = \{0\}$ is tested by the algorithm. Given that both components of Φ satisfy scaling relations, checking this condition is equivalent to checking isolation from zero for a layer, which can be done using the algorithm from the previous section. If we have established regularity for every top level triangle, we know that the map has to be a covering. In this case it is sufficient to estimate the winding number for the image of a simple curve that has zero in its interior region; the winding number can be computed using projected length as described above.

Input: $\tilde{G}_k^0$, the interval control net for the characteristic map restricted to Ring_k, γ, C, as defined above.

Output: `true` if the interval characteristic map is injective, `false` if it is not, `undefined` if the algorithm could not determine the result.

Projected length is computed in the following way: for each linear segment of the piecewise linear approximation to the image of the boundary, we compute the projections of the endpoints, determine on which sides of the square they ended up and compute the length accordingly. We need not determine precisely the side of the square where the point is; it is sufficient to determine a pair of adjacent sides. Number the sides of the square from 0 to 4 starting from the side on the line $y = 1$ (Figure 5.2). Note that this calculation may fail as shown in the figure.

We define a function `ComputeProj` which computes the interval projective length of the image of the outer boundary of the Ring at level i.

The function returns either the length or `undefined` or `fail`.

We use an auxiliary function `Sides`(x), which returns the set of sides of the unit square that an interval point x intersects.

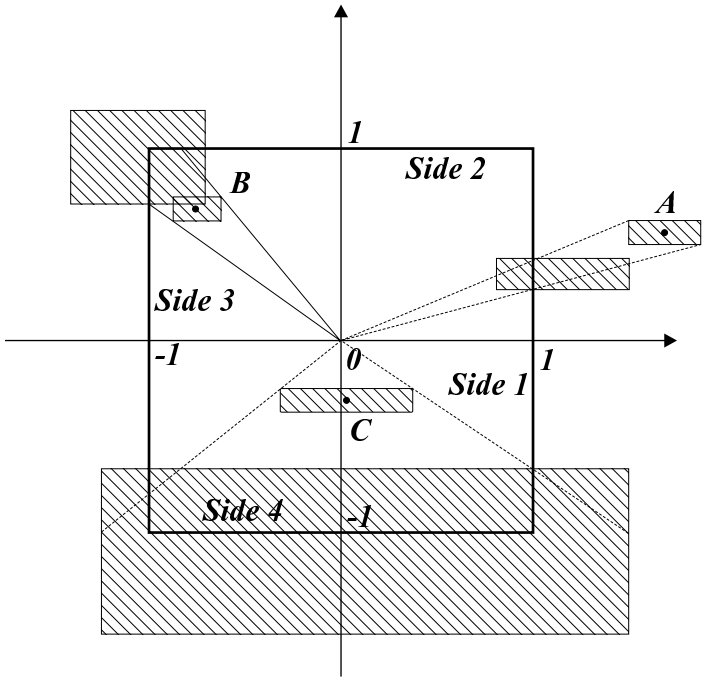

Figure 5.2: Projecting an interval point onto the unit square. For the interval point A unique side is defined; for the interval point B two adjacent sides intersect the projection. For the point C there are 3 sides intersecting projection. In this case, precision is insufficient, and the algorithm fails completely: it is unlikely that the problem disappears with further subdivision. The absence of cases of this type can be guaranteed if the characteristic map on the ring is sufficiently well separated from 0 and the intervals for the control points are small.

A side i is in $\texttt{Sides}(x)$ if and only if the corresponding predicate is true:

$$\begin{aligned}
&\text{for 1: } (0 \in x_1 - 1) \ \texttt{and} \ (0 \notin x_1 + 1)\\
&\text{for 2: } (0 \in x_2 - 1) \ \texttt{and} \ (0 \notin x_2 + 1)\\
&\text{for 3: } (0 \in x_1 + 1) \ \texttt{and} \ (0 \notin x_1 - 1)\\
&\text{for 4: } (0 \in x_2 + 1) \ \texttt{and} \ (0 \notin x_2 - 1)
\end{aligned} \tag{5.1}$$

we also define $\texttt{Next}(v_{m\,r_2\,j}) := \texttt{Next}(v_{m\,r_2\,j+1})$ if $j < r_2 - 1$, and

$\texttt{Next}(v_{m\,r_2\,r_2-1}) := \texttt{Next}(v_{m+1 \bmod r_2\,0})$.

```
ComputeProj(G̃^i)

  projLength := 0
  for m := 0 to k − 1
    for j := 0 to r_2 − 1
      n^s := G̃^i_k(v_{m r_2 j}) / max(G̃^i_1(v_{m r_2 j}), G̃^i_2(v_{m r_2 j}))
      n^f := G̃^i(Next(v_{m r_2 j})) / max(G̃^i_1(Next(v_{m r_2 j})), G̃^i_2(Next(v_{m r_2 j})))
      if |Sides(n^s)| > 2 or |Sides(n^f)| > 2 then
return fail
      intervSides := Sides(n^s) ∪ Sides(n^f)
      if |intervSides| > 2 then return undefined
      case intervSides
        {1}:projLength += n^f_2 − n^s_2
        {2}:projLength += n^s_1 − n^f_1
        {3}:projLength += n^s_2 − n^f_2
        {4}:projLength += n^f_1 − n^s_1
        {1,2}:projLength += n^s_1 − n^f_1 + n^f_2 − n^s_2
        {2,3}:projLength += n^s_1 − n^f_1 + n^s_2 − n^f_2
        {3,4}:projLength += n^f_1 − n^s_1 + n^s_2 − n^f_2
        {4,1}:projLength += n^f_1 − n^s_1 + n^f_2 − n^s_2
      endcase
    endfor
  endfor
return projLength
```

The test is illustrated in Figure 5.3.

Now we can describe the algorithm for checking injectivity. As we compute the winding number of the linear approximation to the image of the curve, we need to check that the image is sufficiently far from zero using the function `TestIsolZero`.

For the winding number to be 0, projected length has to be 8 (the perimeter of the square).

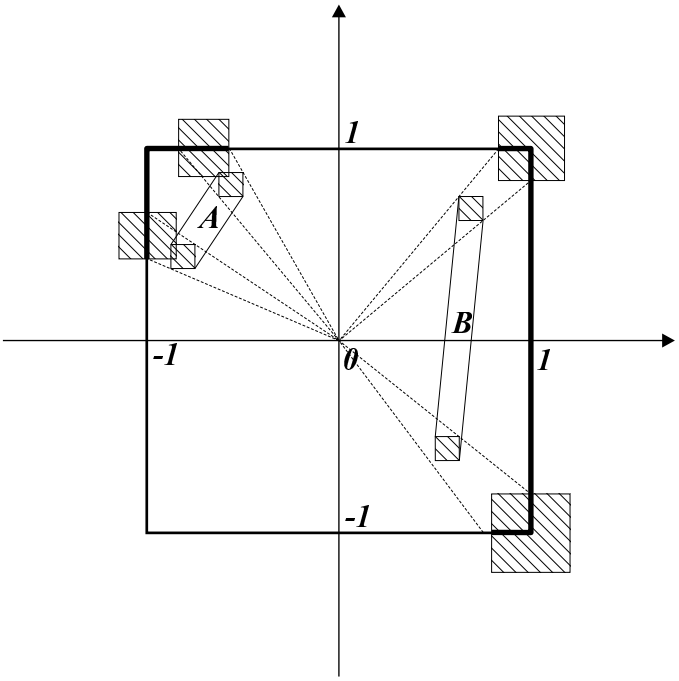

Figure 5.3: Projecting an interval into the unit square. The algorithm computes projected length for interval A, but not for the interval B. It is possible to estimate the upper and lower bounds for projected length in some cases of type B, but it may also happen that the interval passes through 0 and its projected length is undefined. Rather than further analyzing this case, we choose to refine the mesh further to reduce the length of the interval.

```
TestInjective(G̃_k^i, C, γ)

ProjLength= ComputeProj(G̃_k^i)
if (ProjLength= fail) or (ProjLength= undefined) then return ProjLength
if (0 ∈ ProjLength − 8) and (0 ∉ ProjLength) and ( 0 ∉ ProjLength − 16) then
  return true
```

This is the only subalgorithm that can return `fail`.

5.8 Conditions for Successful Completion

We say that the algorithm `TestC1cont` was successful if it returned `true` or `false`. Assuming unlimited memory and time available, as well as arbitrary precision arithmetic (note that we need arbitrary but finite precision, rather than exact arithmetic), the algorithm is guaranteed to return `true` or `false` for a finite value of *maxlevel* if

- the Jacobian of the characteristic map either has constant sign or changes signs;
- or 0 is a value of the characteristic map in an internal point of the ring;
- or 0 is not the value of the characteristic map on the ring and the winding number of the image of the bounding curve is not 1 or -1.

The time and/or space required to execute algorithms above grows linearly with the valence k and size of the initial mesh G^0. Dependence of the complexity on other parameters is more difficult to determine. Intuitively, it is clear that the number of subdivision steps to be performed is proportional to $|\log \gamma|^{-1}$.

Arbitrary Valence. The algorithm that we have described in this section works for fixed valence k. For practical purposes it is typically sufficient to prove C^1-continuity for a finite number of valences. It is, however, desirable to be able to obtain more complete results and prove C^1-continuity for a scheme for arbitrary valence. It turns out that it is possible with for certain classes of schemes; we describe the algorithm for verifying C^1-continuity of invariant schemes for arbitrary valence in Section 6.2.1; in the same section we also explain how a similar approach can be used for a more general class of schemes.

Chapter 6 Analysis of Specific Schemes

In this chapter we present analysis of several subdivision schemes. In each case, we present a brief description of the scheme and its properties. Eigenvalues and generalized eigenvectors of the subdivision matrices play an important role in our analysis. Most of the analysis techniques developed in previous chapters apply to G-invariant schemes, which are invariant with respect to sets G of isomorphisms of complexes described in Section 2.2.1. For invariant schemes, that is, schemes that are invariant with respect to all possible isomorphisms of complexes, we can establish necessary conditions for C^1-continuity. that are easier to evaluate. We derive some general formulas for the eigenstructure of invariant schemes that allow us to understand the behavior of the schemes and synthesize new and improved schemes.

In the case of Modified Butterfly and Modified Loop schemes, we establish C^1-continuity for complexes with vertices of arbitrary valence.

C^1-continuity of the Butterfly scheme on arbitrary complexes was not rigorously analyzed before, as all previous work on the analysis of subdivision surfaces relies on closed-form expressions for the surface on the regular complex.

C^1-continuity of the original Loop scheme was analyzed in [59] for complexes with extraordinary vertices of valence up to 100. We show that Loop scheme is C^1-continuous for all valences. We use Loop scheme as an example to identify the origin of some common problems with subdivision surfaces and discuss a modification of the scheme that corrects some of the problems. We prove that our modification of the Loop scheme is C^1-continuous for all valences of extraordinary vertices.

Finally, we present a parametric family of schemes based on Loop that allows us to create "soft creases" on the surface.

6.1 Invariant Schemes

Before discussing properties of particular schemes, we discuss some properties of a general class of *invariant schemes*. General algorithms for verifying C^1-continuity can be simplified for invariant schemes and extended to handle all valences.

All well-known subdivision schemes (Loop, Butterfly, Catmull-Clark, Doo-Sabin) belong to this class (although some changes in notation are required to describe quadrilateral-based schemes, essential properties are preserved). Useful examples of non-invariant schemes are Hoppe's piecewise smooth Loop scheme and Loop's scheme with creases proposed in this work.

The constructions of this section follow the ideas of Ball and Storry [2]; some of them were presented in [66]. Similar constructions are presented by Peters and Reif [49].

However, in most common situations there is no restriction on isomorphisms that can be used. For a k-regular complex there is a set of automorphisms that add additional constraints on the subdivision rules that can be used. For a regular complex this set is even larger and the number of degrees of freedom in such schemes is considerably reduced. In most general form, such conditions can be written as

$$S^i[K, v](p) = S^i[K, \rho(v)](p \circ \rho^{-1}) \quad \text{for any } p \in \mathcal{P}(K) \tag{6.1}$$

where $S^j[K, v]$ is the subdivision function at a vertex v, ρ is an automorphism of the complex K.

By linearity, any subdivision function can be written as

$$S^i[K, v](p) = \sum_w a(v, w)p(w),$$

where $a(w, v)$ are the coefficients of subdivision. Expanding (6.1) and substituting $w = \rho(w)$, we get

$$\sum_w a(v, w)p(w) = \sum_w a(\rho(v), w)p(\rho^{-1}(w)) = \sum_w a(\rho(v), \rho(w))p(w) \quad \text{for any } p \in \mathcal{P}(K)$$

Taking $p(w) = \delta(w)$ (1 at w, 0 elsewhere) we get explicit conditions on coefficients of subdivision

$$a(v, w) = a(\rho(v), \rho(w)) \tag{6.2}$$

In particular, for k-regular complexes with three-index numbering shown in Figure 2.6, the set of automorphisms consists of rotations around the extraordinary vertex, mirror reflections and their combinations; we start with considering only rotations, adding restrictions following from mirror symmetries later. We will use notation (sjl) for the vertex with indices s,j and l. In our notation the formulas for rotations are particularly simple:

$$R^m\left([sjl]\right) = [s \bmod k \; jl]$$

where R^m is the automorphism of the k-regular complex corresponding to the rotation of the plane by $2m\pi/k$.

This leads to the condition on the coefficients of the scheme

$$a\left((s'j'l'),(sjl)\right) = a\left(\left[(s'+m) \bmod k \; j'l'\right],[(s+m) \bmod k \; jl]\right) \quad \text{for any } m,\ j,j' > 0$$

In the cases when $j = 0$ or $j' = 0$ (one of v, w is the extraordinary vertex), we get

$$\begin{aligned} a\left([0\,0\,0],[sjl]\right) &= a\left([0\,0\,0],\left[s'jl\right]\right) \quad \text{for any } s,s' \\ a\left([sjl],[0\,0\,0]\right) &= a\left(\left[s'jl\right],[0\,0\,0]\right) \quad \text{for any } s,s' \end{aligned} \tag{6.3}$$

This means that the coefficients are functions of j,l,j',l' and $(s-s') \bmod k$ only.

This fact allows us to simplify analysis of subdivision matrices, in particular for schemes with small control and localization sizes, for which the range of j and l that we have to consider is small.

Let $n = (j,l)$ for $j >= 1$. We introduce notation $a\left([sjl],[s'j'l']\right) = a_{nn'}(s-s')$. It follows from (6.3) that $a\left([0\,0\,0],[sjl]\right)$ and $a\left([sjl],[0\,0\,0]\right)$ and do not depend on s. This allows us to introduce notation

$$\begin{aligned} b_n &= a\left([0\,0\,0],[sjl]\right) \\ c_n &= a\left([sjl],[0\,0\,0]\right) \\ a_{00} &= a\left([0\,0\,0],[0\,0\,0]\right) \end{aligned}$$

Let M be the localization size for the subdivision scheme on a k-regular complex. In this case, the control set of U_1 is a M-neighborhood of the extraordinary vertex. One sector of this neighborhood (center excluded) contains $M(M+1)/2 = N$ vertices, the total number of vertices being $Nk+1$.

To write the subdivision matrix explicitly, we need to convert triple indices into single indices. The matrix will have a convenient block form if we use the following rule for translating indices

$$(s,j,l) \to k(\frac{j(j+1)}{2}+l)+1+s \quad \text{for } j>0,\ l<j,\ s=0\dots k-1$$

Effectively, we arrange the vertices "by symmetry class": first we enumerate all vertices that can be obtained by rotation from the vertex $(0,1,0)$, then $(0,2,0)$, $(0,2,1)$, etc.

The index $(0,0,0)$ corresponds to index 0. For double indices $n=(j,l)$ inside one sector, we use the rule $(j,l) -> j(j+1)/2 \quad \text{for } j>0, l<j$

With this ordering of vertices, the subdivision matrix has the form

$$S = \left(\begin{array}{c|ccc} a_{00} & \mathbf{b}_0^T & \cdots & \mathbf{b}_{N-1}^T \\ \hline \mathbf{c}_0 & A_{00} & \cdots & A_{0\,N-1} \\ \vdots & \vdots & \ddots & \vdots \\ \mathbf{c}_{N-1} & A_{N-1\,0} & \cdots & A_{N-1\,N-1} \end{array}\right) \tag{6.4}$$

where $A_{nn'}$ are $k \times k$ matrices with entries $a_{nn'}(s-s')$, $s,s' = 0\dots$. Clearly, these matrices are cyclic. $\mathbf{b}_n$ denotes the vector $[b_n,\dots b_n]^T$ of size k with equal entries; similarly, $\mathbf{c}_n$ is the vector $[c_n,\dots c_n]^T$.

A cyclic matrix can be reduced to a diagonal form using the DFT. As the subdivision matrix has cyclic blocks, we can simplify the matrix applying DFT to each block. Let

$$\mathcal{D} = \left(\begin{array}{c|ccc} 1 & \mathbf{0}^T & \cdots & \mathbf{0}^T \\ \hline \mathbf{0} & \frac{1}{k}D_k & \cdots & 0 \\ \vdots & \vdots & \ddots & \vdots \\ \mathbf{0} & 0 & \cdots & \frac{1}{k}D_k \end{array}\right)$$

where D_k is the DFT matrix with entries $e^{-2\pi jl/k}$, $j,l = 0\ldots k-1$, and $\mathbf{0}$ is the zero vector of length k. The number of DFT blocks in $\mathcal{D}$ is N. We choose to include the normalization factor $\frac{1}{k}$ in $\mathcal{D}$ rather than in $\mathcal{D}^{-1}$ because it will slightly simplify the calculations later.

The inverse of this matrix is

$$\mathcal{D}^{-1} = \left(\begin{array}{c|ccc} 1 & \mathbf{0}^T & \cdots & \mathbf{0}^T \\ \hline \mathbf{0} & \bar{D}_k & \cdots & 0 \\ \vdots & \vdots & \ddots & \vdots \\ \mathbf{0} & 0 & \cdots & \bar{D}_k \end{array}\right)$$

Applying a similarity transform to S, we obtain a matrix with diagonal blocks $\widehat{A}_{nn'} = \frac{1}{k} D_k A_{nn'} \bar{D}_k$:

$$\mathcal{D}\, S\, \mathcal{D}^{-1} = \left(\begin{array}{c|ccc} a_{00} & \mathbf{b}_0^T \bar{D}_k & \cdots & \mathbf{b}_{N-1}^T \bar{D}_k \\ \hline \frac{1}{k} D_k \mathbf{c}_0 & \frac{1}{k} D_k A_{00} \bar{D}_k & \cdots & \frac{1}{k} D_k A_{0\,N-1} \bar{D}_k \\ \vdots & \vdots & \ddots & \vdots \\ \frac{1}{k} D_k \mathbf{c}_{N-1} & \frac{1}{k} D_k A_{N-1 \bar{D}_k\, 0} & \cdots & \frac{1}{k} D_k A_{N-1\, N-1} \bar{D}_k \end{array}\right)$$

The matrices $(1/k) D_k A \bar{D}_k$ are diagonal with entries on the diagonal $D_k \mathbf{a}_{nn}$, where $\mathbf{a} = [a_{nn'}(0) \ldots a_{nn'}(k-1)]$. Note that vectors $D^k \mathbf{b}_n$ and $D_k \mathbf{c}_n$ have zeros in all positions except the first: $D^k \mathbf{b} = [k b_n 0 \ldots 0]^T$.

Finally, the subdivision matrix can be reduced to block diagonal form by applying a permutation. Let P be the permutation matrix mapping the index $r = pk + q + 1$, where $q \in \{0 \ldots k-1\}$ $p \in \{0 \ldots N-1\}$, to $r' = qN + p + 1$; if we write an $Nk+1$ vector v as $[f\ v_0^T\ \ldots v_{N-1}^T]^T$ where v_j are vectors of length k and f a scalar, then Pv will be a vector with f in the first position, followed by N first components of $v_0 \ldots v_{N-1}$, followed by N second components, etc.

Applying this permutation reduces the subdivision matrix to the block-diagonal form:

$$P\,\mathcal{D}\,S\,\mathcal{D}^{-1}P^{-1} = \left(\begin{array}{c|cccccc} a_{00} & \mathbf{b} & 0 & \cdots & 0 & 0 \\ \hline \frac{1}{k}\mathbf{c} & B(0) & 0 & \cdots & & 0 \\ 0 & 0 & B(\frac{2\pi}{k}) & \cdots & & 0 \\ \vdots & \vdots & & \ddots & & \vdots \\ 0 & 0 & & \cdots & B(\frac{2\pi}{k}) & 0 \\ 0 & 0 & & \cdots & 0 & B(\frac{2(k-1)\pi}{k}) \end{array}\right) \tag{6.5}$$

The matrix has k $N \times N$ blocks $B(2\omega)$ where $\omega = 0, \pi/k, 2\pi/k, \ldots (k-1)\pi/k$. Each $B(2m\pi/k)$ has entries $[D\mathbf{a}_{nn'}]_m$, i.e., is composed of m-th entries of DFT transforms of all vectors $\mathbf{b}_{nn'}$. For $m = 0$ we have to analyze a larger $(N+1) \times (N+1)$ matrix Z with vectors $\mathbf{b} = [b_0, \cdots b_{N-1}]^T$ and $(1/k)\mathbf{c} = (1/k)[c_0, \cdots c_{N-1}]^T$ added on two sides. Note that $B(2m\pi/k) = B(2(k-m)\pi/k)$ and the eigenvalues of these blocks are conjugate. If an eigenvalue happens to be real, and corresponds to the block $B(2m\pi/k)$ with $m \neq k/2$, it necessarily has an eigenspace of dimension at least 2. If x is its complex eigenvector obtained from an eigenvector of $B(2m\pi/k)$, a pair of real eigenvectors in this subspace can be taken to be $\Re\, x$ and $\Im\, x$. If an eigenvalue λ is complex, the two-dimensional real eigenspace corresponding to λ and $\bar{\lambda}$ is also spanned by $\Re\, x$ and $\Im\, x$.

This representation of the subdivision matrix allows one to find eigenvectors and eigenvalues of the matrix using eigenvalues and eigenvectors of smaller matrices $B(\omega)$ and the matrix Z. For example, in the case when $M = 3$ which will be considered in greater detail in the next section, the matrices $B(2\omega)$ are 6×6 and can be further reduced to 3×3; eigenvalues and eigenvectors of 3×3 matrices and one 4×4 matrix can be computed explicitly.

Each eigenvalue of the subdivision matrix is an eigenvalue of a block $B(2m\pi/k)$,$m = 1 \ldots k-1$ or Z. Each eigenvector can be obtained by taking an eigenvector of one of the blocks, setting the rest of the entries to 0, and transforming it using $\mathcal{D}P$. This means that the eigenvectors have symmetries that can be used to establish necessary conditions on location of dominant eigenvalues of the subdivision matrix.

A condition of this type was proposed in [49] (Theorem 3.1). Unfortunately, the proof of that theorem is not formally correct as reported in the paper; some assumptions on

the characteristic map, which are difficult to verify, are implicitly used in the proof. The theorem of Peters and Reif states that the dominant eigenvalues for a subdivision scheme with injective characteristic map necessarily have to be the eigenvalues of the blocks $B(1)$ and $B(2\pi(k-1)/k)$. Intuitively, it appears that this is true for any "reasonable" subdivision scheme. However, it is possible to construct examples of C^1-continuous schemes with dominant eigenvalues in other blocks. Typically, such schemes would have noninjective characteristic map. As it was shown in Chapter 3, injectivity of a characteristic map is not strictly necessary for C^1-continuity of the scheme. This contradicts Theorem 2.2 of [49] which has several errors in the proof. However, the cases when the scheme is C^1-continuous and the characteristic map is not injective, are quite degenerate and are unlikely to be practically useful.

We prove a weaker version of the conditions of Peters and Reif under some additional assumptions. These additional assumptions are quite technical, and it would be desirable to come up with more natural conditions.

Lemma 6.1. *Let $\mathcal{S}$ be a invariant scheme, S its subdivision matrix for valence k. Suppose that the subdivision matrix has a dominant pair of cyclic subspaces J_b^a, J_d^c corresponding to the blocks $B(2\pi m/k)$ and $B(2\pi(k-m)/k)$, $m \neq 1$, the characteristic map of this pair of cyclic subspaces has Jacobian which is not identically zero, and dimension of $J_b^a \oplus J_d^c$ is 2.*

Let λ be an eigenvalue of the block $B(2\pi/k)$ and x a corresponding complex eigenvector. Suppose that for the limit map $f : U_1 \to R^2$ generated by the pair $\Re x$, $\Im x$ the following two conditions hold:

1. *$f^{-1}(0) = \{0\}$*
2. *there is a simple curve $\gamma(t) : S^1 \to \dot{U}_1$ such that the winding number of $f(\gamma(t))$ is 1 or -1, and $\mathrm{Im}(\gamma)$ is invariant with respect to rotations of the plane by $2m\pi/k$, for integer m.*

Then the scheme is not C^1-continuous.

Proof. Suppose the scheme is C^1-continuous. It follows from the conditions of the lemma that the parametric map Φ has to correspond to the pair of cyclic subspaces J_b^a and J_d^c and coincide with the characteristic map. If the scheme is C^1-continuous, $f \circ \Phi^{-1} : \Phi(U_1) \to \mathbf{R}^2$

is well-defined. U. This means that the curve $f(\gamma(t))$ can be written as $f(\Phi^{-1}(\Phi(\gamma(t))))$. As $f^{-1}(0) = 0$, $\Phi^{-1}(0) = 0$ also, and the winding number for the curve $\Phi(\gamma(t))$ is well-defined.

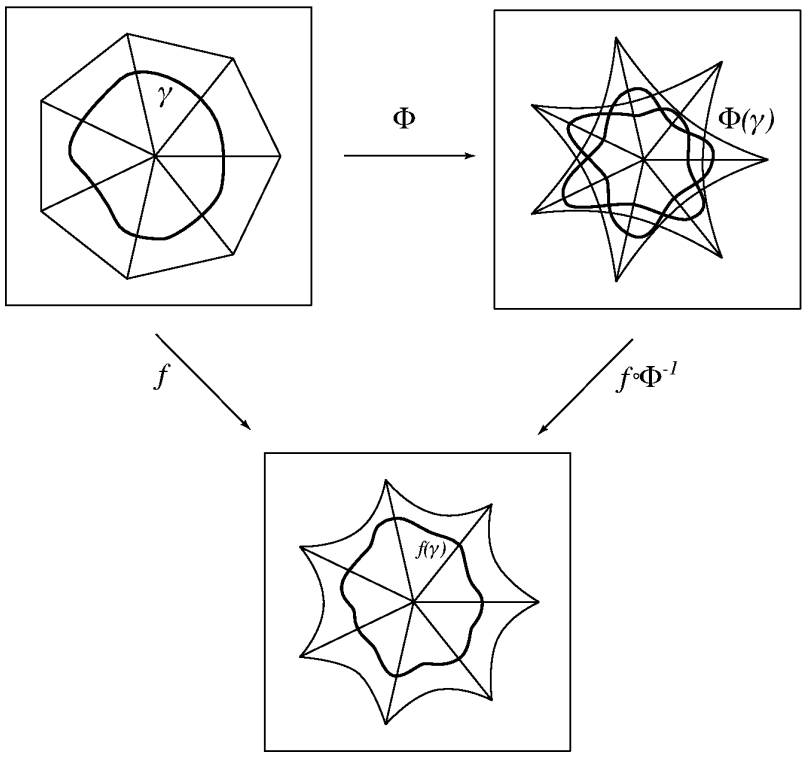

Figure 6.1: This diagram shows the maps used in the proof of Lemma 6.1 for the case $k = 7$. In this case the characteristic map Φ is generated by the eigenvectors of the blocks $B(4\pi/7)$ and $B(10\pi/7)$.

The idea of the proof is to show that the curve $f(\gamma)$ cannot be parameterized over the image of $\gamma'(t) = \Phi(\gamma(t))$ (Figure 6.1).

Consider $\Phi(\gamma(t))$ on the part of the curve contained in one triangle of U_1. It follows from the invariance of the curve and structure of the generalized eigenvectors generating Φ that the difference of the arguments at the endpoints is $2m\pi/k$; the change in the argument of $\Phi(\gamma(t))$ is $2m\pi/k+2\pi l$ for some l. By symmetry, the total change of argument is $2\pi(m+lk)$ and the winding number of $\gamma' = \Phi(\gamma(t))$ is $2\pi(m + lk)$.

As it was shown in Lemma 2.13, the mapping $\Phi : U_1 \to \mathbf{R}^2$ can be extended to the mapping $\Phi : \mathbf{R}^2 \to \mathbf{R}^2$. Note that Φ satisfies the conditions of Lemma 4.6 for a C^1-continuous scheme. Thus, it is a surjection from $\mathbf{R}^2\setminus\{0\}$ to $\mathbf{R}^2\setminus\{0\}$. f is a homeomorphism $\mathbf{R}^2 \setminus \{0\}$ to $\mathbf{R}^2 \setminus \{0\}$. Clearly, $f \circ \Phi^{-1}$ which is well-defined, is also a homeomorphism of

the same type. Moreover, it is not nullhomotopic because the image of $f(\gamma(t))$ is a curve in $\mathbf{R}^2 \setminus \{0\}$ not homotopic to 0.

The mappings

$$\mathbf{R}^2 \setminus \{0\} \xrightarrow{\Phi} \mathbf{R}^2 \setminus \{0\} \xrightarrow{f \circ \Phi^{-1}} \mathbf{R}^2 \setminus \{0\}$$

induce a pair of homomorphisms of fundamental groups, which are all $\mathbf{Z}$:

$$\mathbf{Z} \xrightarrow{\Phi^*} \mathbf{Z} \xrightarrow{(f \circ \Phi^{-1})^*} \mathbf{Z}$$

any homomorphism $\mathbf{Z} \to \mathbf{Z}$ is of the form $n \to rn$, where $n \in \mathbf{Z}$, r is an integer. This means that the combined homomorphism is of the form $n \to r_1 r_2 n$. Recall that the winding number of the curve in $\mathbf{R}^2 \setminus \{0\}$ is the index of the corresponding element of the fundamental group. As $\gamma(t)$ is a simple curve, it corresponds to the element 1 of the fundamental group. We have shown that $\Phi(\gamma(t)) = \gamma'(t)$ has index $m + lk$. The winding number of the composition $f\left(\Phi^{-1}(\gamma'(t))\right)$ must be a multiple of $m + lk$. However, by assumption of the Lemma it is 1 or -1; as $k \geq 3$ and $m < k$, this is possible only if $m = 1$. □

It would be desirable to improve on the last lemma in a number of ways. Conditions like Lemma 6.1 are primarily useful for proving non-C^1-continuity of a scheme. Although it is possible to check the condition on the winding number above using the techniques that we have developed, the check is relatively complex and has to be performed for all valences. It would be desirable to have a simpler procedure for rejecting schemes that are not C^1-continuous. For example, this potentially can be achieved describing constraints on the coefficients of the schemes and eigenvectors that would imply conditions of the Lemma.

6.2 Single Ring Schemes

Schemes with localization and control sizes ≤ 3 are particularly important in practice: all well-known schemes belong to this class or its analog for the quadrilateral-based schemes. It follows from the definition of the localization and control sizes that the stencils $\mathrm{St}(K^j, v)$ of such subdivision schemes may include 1-neighborhoods for even vertices $V \in V^j$ and 1-neighborhoods of the two even neighbors of an odd vertex $v \in V^{j+1} \setminus V^j$. Examples of

such stencils are shown in Figure 6.3. The name "single ring" was suggested by the shape of stencils. Several reasons make this class of schemes particularly important:

Efficiency Small stencils allow efficient subdivision.

Simplicity If the stencils were larger, we would have to design rules for a variety of cases: for example, if we were to include two rings into the stencil for an odd vertex, at least on the top level we would have to define rules for a k-vertex surrounded by vertices of valences $n_1 \dots n_k$; instead of a family of rules parameterized by a single parameter k, we need a family of rules with infinite number of parameters.

Generality This family of schemes includes both interpolating and approximating C^1 schemes; there are no C^1-continuous interpolating schemes in the family of schemes with support size 2.

Schemes from this family have sufficiently small number of parameters to make achievable the goal of complete characterization of C^1-continuity properties of all schemes in this family; the tools developed in this thesis can serve as a foundation for such characterization, and we hope that a more or less complete analysis will be done in the nearest future.

Single ring schemes have subdivision matrices with blocks of size $N = 6$. It is possible to show that the blocks have a particular form that allows us to reduce the analysis of their structure to the analysis of the structure of 3×3 blocks.

We start by making several simple observations about the coefficients of the scheme in the regular case; the number of symmetries in this case is higher than in the k-regular case, and all possible schemes are fully characterized by 4 coefficients a, b, c, e as shown in Figure 6.2 (by affine invariance $d = 1/2 - a - b - 2c$). The number of parameters can be further reduced by considering C^1-continuity requirements, but this is not our goal at this point.

Figure 6.3 shows the 6 symmetry types of vertices for single ring schemes. One can see that the stencils for vertices of types (3,0), (3,1) and (3,2) do not contain the extraordinary vertex; by definition of the localization size, the coefficients used in this case have to be the coefficients for the regular case.

Considering the stencil for each type we can see that the blocks of the subdivision matrix have the following form:

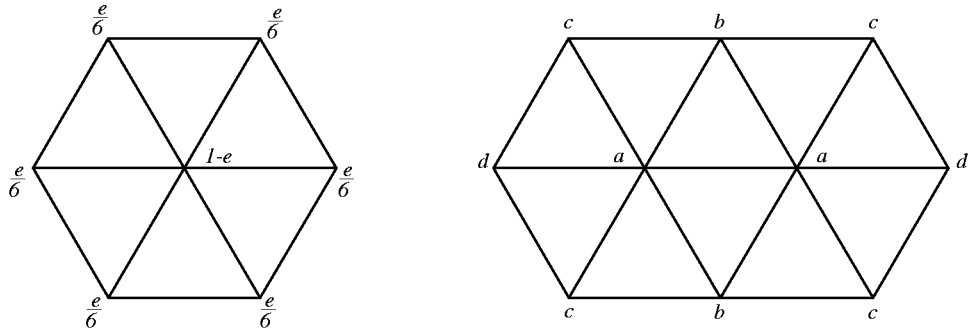

Figure 6.2: Coefficients for a single ring scheme in the regular case; a,b,c,d satisfy $2a + 2b + 4c + 2d = 1$ by affine invariance.

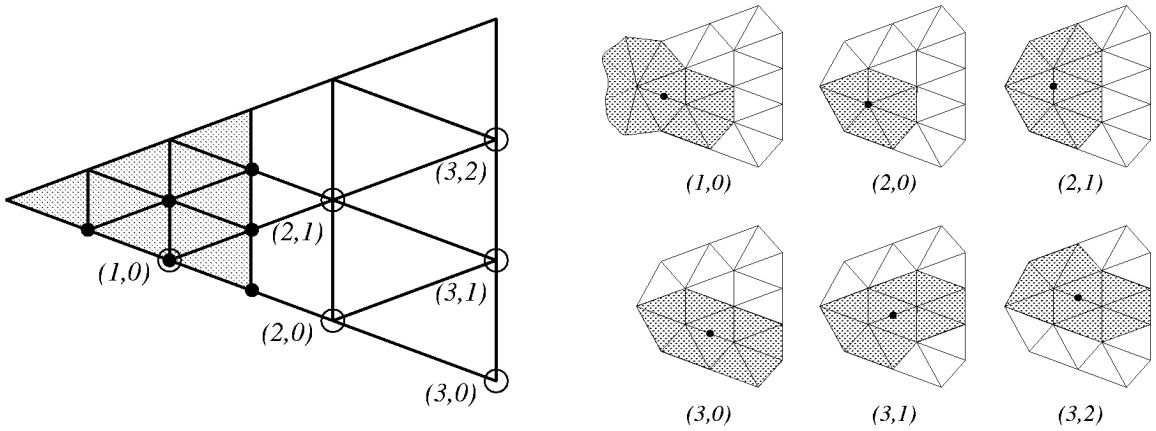

Figure 6.3: 6 symmetry types of vertices with respect to rotations for single ring schemes and stencils for each type.

$$
\begin{array}{cccccc}
* & * & * & 0 & 0 & 0 \\
* & * & * & 0 & 0 & 0 \\
* & * & * & 0 & 0 & 0 \\
* & * & * & d & c & ce^{-2\pi/k} \\
* & * & * & 0 & c & d \\
* & * & * & 0 & d & c
\end{array}
$$

where $*$ denotes potentially non-zero entries. Some of the $*$-entries could be made explicit, but it is not important for our purposes. It is immediately clear that the matrix has two sets of eigenvectors and eigenvalues; the first is defined by the 3×3 matrix in the upper left corner; the rest are defined by a 3×3 matrix in the lower left corner which depends only on the coefficients of the scheme in the regular case; the eigenvalues and eigenvectors of this matrix are easy to compute. The eigenvalues are d, $c - d$ and $c + d$. Eigenvectors may have different expressions depending on the Jordan type of the matrix. Given that the eigenvalues do not depend on the block number, if one of them happens to be dominant, the scheme is not C^1-continuous excluding several exceptional cases; in general, the primary reason to examine these eigenvalues is to make sure that they are not dominant.

Finally, the structure of the block Z is

$$\begin{array}{ccccccc} * & * & 0 & 0 & 0 & 0 & 0 \\ * & * & * & * & 0 & 0 & 0 \\ * & * & * & * & 0 & 0 & 0 \\ * & * & * & * & 0 & 0 & 0 \\ * & * & * & * & d & c & ce^{-2\pi/k} \\ * & * & * & * & 0 & c & d \\ * & * & * & * & 0 & d & c \end{array}$$

In this case a 4×4 matrix in the upper left corner has to be considered.

We conclude that analysis of the structure of any single ring scheme with explicit coefficients can be done in closed form although the expressions for the eigenvalues may be quite complicated as we will see in Section 6.3.

6.2.1 Algorithms for Testing C^1-Continuity of Invariant Schemes

It is easy to see that for an invariant scheme it is sufficient to test regularity on one out of k identical segments surrounding the k-vertex. The same applies to the test of isolation from zero — testing one sector of the ring is sufficient. In the injectivity test, if the projected length of the part of the boundary curve contained in one segment may be $8/k$ and is not 0 or $16/k$, then the total length should be 8. Thus, the algorithms `TestRegular` and

`TestIsolZero` don't have to be changed at all (their input becomes the control net for one segment rather than for the whole ring). The only change that is required in `TestIsolZero` is replacing the lengths 8 and 16 with $8/k$ and $16/k$.

Arbitrary valence. An important observation about all algorithms described in this section is that the input is always a set of interval control points; thus, each time the algorithms are successful in establishing C^1-continuity of subdivision, we actually have established C^1-continuity not for one scheme but for a collection of schemes with sufficiently close eigenvectors of the subdivision matrix.

As we have observed, for invariant schemes we need to check regularity and compute projective length for a boundary curve only on one segment. If r_1 and r_2 are constant for all $k > k_0$ for some k_0, and the control set does not contain the whole ring for $k > k_0$, then the initial data for all $k > k_0$ are defined on the same subcomplex of the regular complex, i.e. are elements of one space $\mathcal{P}(P)$. As our schemes are affine-invariant, proving C^1-continuity for initial data $G^0 \in \mathcal{P}(P, \mathbf{R}^2 \times \mathbf{R}^2)$ is equivalent to proving C^1-continuity for any affine transformation A $A \circ G^0 \in \mathcal{P}(P, \mathbf{R}^2 \times \mathbf{R}^2)$, where A is extended to act on the space of interval vectors in the obvious way. The algorithms don't have to be changed in any way, except for the value of the projected length, which have to be scaled in an appropriate way. It is worth noting that it can be deduced from symmetry that if the projected length for one segment is less than 8, it is less than $8/k$, so even this scaling is not really necessary.

Suppose we can choose affine transformations of the initial data $G^0(k)$ in such a way that the sequence of vectors $G^0(k)$ converges to a limit $G^0(\infty)$. Further, assume that for any k the pair of dominant eigenvalues is unique and satisfies conditions of Lemma 4.6. Then for any n-dimensional interval I containing $G^0(\infty)$, there is a k_0 such that for all $k > k_0$ the initial data vectors $G^0(k)$ are in I. Then if we can test regularity for the limit set of initial data, and an interval around it, we need to test C^1-continuity only for finitely many valences $k \leq k_0$ to prove C^1-continuity for arbitrary valence. Note that in the limit eigenvalues of the scheme need not be well-behaved and for example, may approach 1. In these cases, however, C^1-continuity for large k has mostly theoretical interest, because of extremely slow convergence of derivatives to the limit.

We describe the algorithm for testing C^1-continuity of a invariant scheme for arbitrary valence using an additional function `ControlNet`(i, *interval_size*) which computes the nor-

malized interval control net for one segment of the ring of the characteristic map with each interval point having size at least *interval_size*.

Normalization is given by an appropriately chosen affine transform of the map, the one for which the sequence $G^0(k)$ converges and the limit net is nondegenerate. The particular choice of the transform depends on the way in which the coefficients are specified. As we will see in Sections 6.3 and 6.5, a simple scaling by $1/\sin(\pi/k)$ works for most invariant schemes.

The function `TestC1contSymmetricNormalized` differs from the function `TestC1cont` described in Chapter 5 in two aspects: the control net that is used in all algorithms is the net for one segment and the constant that is used for checking projected length is scaled using the normalization transform.

We omit the usual arguments C, γ, $C_{1,2}$, $\gamma_{1,2}$.

```
TestAllValences(interval_size)

current_mesh  := ControlNet(3,interval_size)
limit_mesh    := ControlNet(∞,interval_size)
if TestC1contSymmetricNormalized(current_mesh) ≠ true then return fail
if TestC1contSymmetricNormalized(limit_mesh) ≠ true then return fail
i := 4
loop
  mesh := := ControlNet(i,interval_size)
  if Distance(mesh, limit_mesh) < interval_size
   then return true
  if Distance(mesh, current_mesh) >= interval_size  then
    current_mesh  := mesh
    if TestC1cont(current_mesh) ≠ true then return fail
    endif
  endif
endloop
```

The argument *interval_size* should be chosen as large as possible without making the algorithm fail.

This algorithm can be further generalized to non-invariant schemes, crease schemes in particular.

In this case all k segments of the ring may be different. However it is reasonable to expect that control segments in fixed positions (e.g. 0 and $\lfloor k/4 \rfloor$) also admit suitable affine transforms such that as $j \to \infty$ their control nets converge to a nondegenerate limit control net. It is also reasonable to expect that the control net of each segment changes "continuously" with the number of segment; by "continuous change we mean that as $k \to \infty$ the maximal difference between normalized control meshes of any two adjacent segments is approaching zero. It is clear that if the scheme behaves in this way, it is possible to apply the algorithm above; however, now we have to use two parameters: one corresponding to the valence, the other to angular position of the segment ($2\pi m/k$ for segment number m). In addition, we have to be careful about estimating the projected length correctly. However, the general structure of the algorithm remains the same although the details become more complicated.

6.3 Butterfly Scheme

In this section we analyze the C^1-continuity of the Butterfly scheme of Dyn, Gregory and Levin [20, 21]. It turns out that this scheme produces C^1 surfaces only for extraordinary vertices of valences 4, 5 and 7. We examine the behavior of the scheme when it is not smooth; the non-C^1-continuous appearance of the surfaces is primarily due to the clustering of eigenvalues for large valences. This observation suggests an approach for constructing C^1-continuous schemes which will be further developed in the following sections.

6.3.1 Definition of the Scheme

An attractive feature of the Butterfly scheme is that the same set of coefficients is used for all odd vertices. The scheme is interpolating, which means that for each vertex we need to compute only one value in $\mathbf{R}^3$ which is the same for all subdivision levels. The coefficients of the scheme are shown in Figure 6.4.

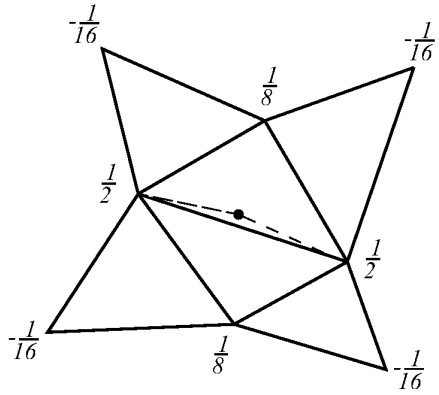

Figure 6.4: The stencil of the Butterfly scheme.

6.3.2 Analysis of the Eigenvalues

As in Sections 6.1 and 6.2, we apply the DFT to obtain a general forma for the blocks of the subdivision matrix near a vertex of valence k. As it was observed in Section 6.2, the eigenvalues of the subdivision matrix are the eigenvalues of a 4×4 matrix, a family of 3×3 matrices and three eigenvalues $d = 0$, $c - d = -1/16$ and $c + d = -1/16$. As the scheme is interpolating, the matrix Z, is block diagonal with 1 and $B(0)$ on the diagonal, so we may consider $B(0)$ instead of Z. By abuse of notation we denote the 3×3 matrices in the top left corner of 6×6 matrices $B(2m\pi/k)$, $m = 0 \dots k-1$ by the same letter B.

For the Butterfly scheme these matrices have the form

$$B(\omega) = \begin{pmatrix} \frac{1}{2} + \frac{1}{4}\cos(2\,\omega) - \frac{1}{8}\cos(4\,\omega) & -\frac{1}{16}\,e^{-2\,i\omega} - \frac{1}{16} & 0 \\ \frac{1}{2} + \frac{1}{2}\,e^{2\,i\omega} - \frac{1}{16}\,e^{-2\,i\omega} - \frac{1}{16}\,e^{4\,i\omega} & \frac{1}{8} & -\frac{1}{16} - \frac{1}{16}\,e^{2\,i\omega} \\ 1 & 0 & 0 \end{pmatrix}$$

where $\omega = m\pi/k$. Denote $x^\omega, y^\omega, z^\omega$ the coordinates corresponding to the block $B(\omega)$. Using a change of coordinates, $y^\omega = y^\omega e^{i\omega}$, we can reduce the matrix to a real form:

$$\begin{bmatrix} 1/2 + 1/4\,\cos(2\,\omega) - 1/8\,\cos(4\,\omega) & -1/8\,\cos(\omega) & 0 \\ -1/8\,\cos(3\,\omega) + \cos(\omega) & 1/8 & -1/8\,\cos(\omega) \\ 1 & 0 & 0 \end{bmatrix}$$

Expanding the cosines as functions of $\cos(\omega)$ and denoting $\cos(\omega) = z$, we get

$$\begin{bmatrix} 1/8 + 3/2\,z^2 - z^4 & -1/8\,z & 0 \\ -1/2\,z^3 + \frac{11}{8}\,z & 1/8 & -1/8\,z \\ 1 & 0 & 0 \end{bmatrix}$$

The characteristic polynomial of this matrix is

$$\lambda^3 + \left(-1/4 - 3/2\,z^2 + z^4\right)\lambda^2 + \left(\frac{1}{64} + \frac{23}{64}\,z^2 - 3/16\,z^4\right)\lambda - \frac{1}{64}\,z^2$$

Using the standard substitution $\mu = \lambda - r/3$, where r is the coefficient of the quadratic term, we can eliminate the quadratic term

$$\begin{aligned} &\mu^3 + \left(-\frac{1}{192} + \frac{7}{64}\,z^2 - \frac{37}{48}\,z^4 + z^6 - 1/3\,z^8\right)\mu \\ &\quad + \frac{1}{6912} + \frac{55}{1152}\,z^4 + \frac{73}{144}\,z^8 + \frac{2}{27}\,z^{12} - 1/3\,z^{10} - \frac{19}{64}\,z^6 + \frac{1}{768}\,z^2 \\ &= \mu^3 + p(z)\mu + q(z) \end{aligned}$$

The number of real roots is determined by the sign of $D = (p/3)^3 + (q/2)^2$. It can be shown that $p(z) \le 0$ for all z. If $D \le 0$ the three real roots of this polynomial are

$$y_1 = -2R\cos\frac{\varphi}{3} \quad y_2 = -2R\cos(\frac{\varphi}{3} + \frac{2\pi}{3}) \quad y_3 = -2R\cos(\frac{\varphi}{3} + \frac{4\pi}{3})$$

where $R = \mathrm{sign}(q)\sqrt{|p|/3}$, $\cos\varphi = q/2R^3$.

If $D > 0$, then there are two complex and one real root:

$$y_1 = -2R\cosh\frac{\varphi}{3} \quad y_2 = R\cosh\frac{\varphi}{3} + i\sqrt{3}R\sinh\frac{\varphi}{3} \quad y_2 = R\cosh\frac{\varphi}{3} + i\sqrt{3}R\sinh\frac{\varphi}{3}$$

where $R = \text{sign}(q)\sqrt{(}|p|/3)$, $\cosh\varphi = q/2R^3$.

The eigenvalues of the matrix can be expressed as functions of $z = cos(\omega)$, which changes in the range from -1 to 1; the eigenvalues for a subdivision matrix for valence k are obtained by substituting $z = 1$, $\cos(\pi/k), \cos(2\pi/k) \ldots \cos(\pi)$ into the expressions for the roots of the equation above. The graphs of the roots are shown in Figures 6.5-6.8.

To characterize the eigenstructure of the matrix completely, we also need to determine the size of the Jordan blocks for all values of z in the range $-1 \ldots 1$. These sizes can be determined using the following argument. Given a fixed eigenvalue λ of$B(\omega)$ an eigenvector x_λ is a solution of the equation $(B(\omega) - \lambda I)x = 0$. Directly solving this system, we can see that 2 cases are possible.

1. $z = cos(\omega) = 0$. In this case for a given $\lambda \neq 0$ the solution of the system is unique up to a scaling constant. This means that for a given value of λ there is only one eigenvector. If the characteristic polynomial happens to have a double or triple root, necessarily there is only one Jordan block for that eigenvalue, which has to have size 2 or 3. The characteristic polynomial has a triple eigenvalue 1/4 for $z = 1$ ($z = -1$ can be excluded as it does not occur for any valence), a double eigenvalue 1/4 for $z = \pm 0.5$ and a double eigenvalue for $z \approx \pm 0.9212389505$. The latter value of z is unlikely to be the value of $\cos 2m\pi/k$ for any m and k, although we did not establish this rigorously. z may have value 0.5 for valences $3, 6, 9 \ldots$. For all valences the 0th block has $z = 1$, i.e., has a triple eigenvalue 1/4.

2. $z = 0$. In this case the matrix is simply

$$\begin{bmatrix} 1/8 & 0 & 0 \\ 0 & 1/8 & 0 \\ 1 & 0 & 0 \end{bmatrix}$$

and has a double eigenvalue 1/8 with 2 Jordan blocks and a simple eigenvalue 0.

Using the algorithm of Sections 5.6 and 5.7, we can verify the conditions of Lemma 6.1 for all valences except 3.

We will describe the calculations in greater detail in the next section where they are

performed for the Modified Butterfly scheme. We conclude that the scheme is C^1-continuous only if the largest eigenvalues, excluding 1, all belong to the blocks $B(1)$ and $B(k-1)$.

Figures 6.5-6.8 show the magnitudes of eigenvalues for valences 3, 6 and 8. The magnitudes of eigenvalues can be visualized as intersections of vertical lines $z = 1$, $\cos(\pi/k)$, $\cos(2\pi/k)$ ... $\cos(\pi)$ with the plots of the magnitudes of roots of the characteristic polynomial as functions of z.

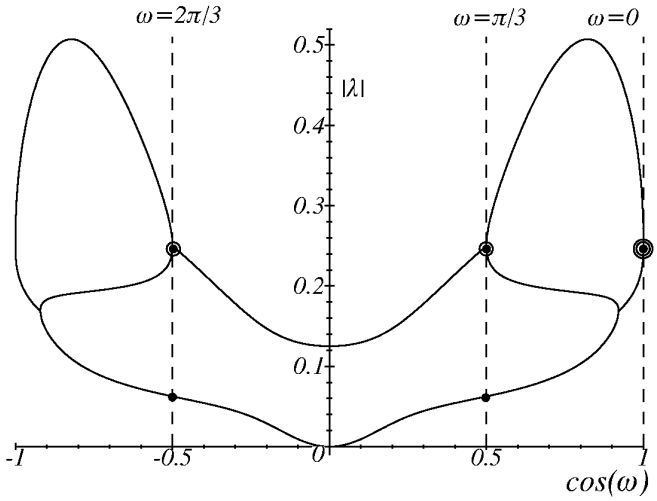

Figure 6.5: Eigenvalues of the subdivision matrix for the Butterfly scheme for valence 3. There are 2 eigenvalues with Jordan blocks of size 2 (dots with circles), 1 eigenvalue with a Jordan block of size 3 (the dot with a double circle) and 2 single eigenvalues. All eigenvalues with nontrivial Jordan blocks happen to coincide and are equal to 1/4. The dominant eigenvalue in this case is the one with the largest Jordan cell and belongs to $B(0)$.

As shown in Figure 6.5, necessary conditions of Lemma 3.9 for tangent plane continuity fail for valence 3 (additional assumptions are verified computing sufficiently close approximations of the appropriate Jacobians). As a result, the surfaces produced by the butterfly scheme have a singularity whenever there is a vertex of valence 3 (Figure 6.11).

Eigenvalues satisfy necessary conditions for valences 4,5,6,7. Due to symmetry we need to consider only one out of k segments of the characteristic maps for $k = 4, 5, 7$. Once the eigenvalues are known, the pair of dominant eigenvectors is completely defined, up to a scaling factor, by 2 real parameters a and c and a complex parameter l, as shown in Figure 6.6.

The equations for finding the values of a, c and l can be obtained by applying subdivision

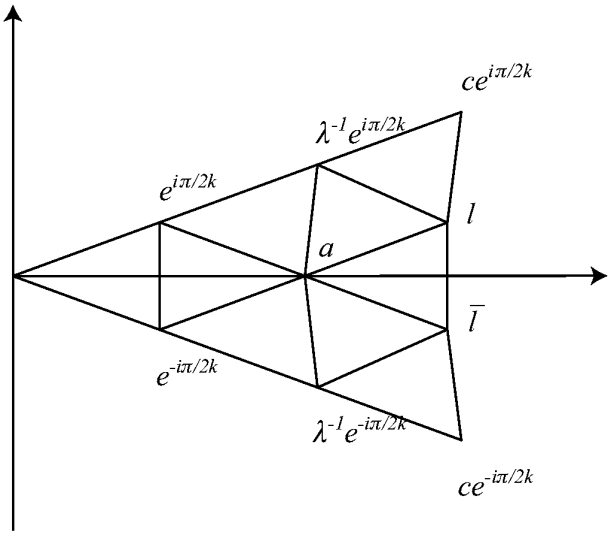

Figure 6.6: One sector of the control net of the characteristic map for the Butterfly scheme.

and using the fact that the central 2 rings of the subdivided mesh should be scaled versions of the rings of the initial mesh with scaling factor λ. In this way we find

$$
\begin{aligned}
a &= -\frac{8\lambda}{z} + \frac{1}{z} + 12z - 8z^3 \\
c &= \frac{5}{8\lambda} + \frac{1}{2\lambda^2} + \frac{az}{4\lambda} - \frac{z^2}{4\lambda} - \frac{\Re l z}{8\lambda} \\
\Im l &= -\sin\frac{\pi}{k}\frac{6\lambda - 3 + 2az\lambda}{\lambda(16\lambda+1)} \\
\Re l &= -\frac{-10\lambda z - 9\lambda a - z + 2az^2\lambda}{\lambda(16\lambda+1)}
\end{aligned}
$$

Control nets for the rings of the characteristic maps for valences 4,5 and 7 are shown in Figure 6.9. The characteristic map can be shown to be regular and injective using our algorithm. We don't reproduce the details here; an example of detailed analysis of regularity and injectivity is given in the next section where we prove that our modification of the butterfly scheme is C^1-continuous for all valences.

It is not necessary to check C^1-continuity for the valence 6, but this is an important boundary case (Figure 6.7) and it helps to understand the eigenstructure for other cases. Necessary conditions fail for valence 8: the largest eigenvalue for $\omega = \pi/8$ is smaller than

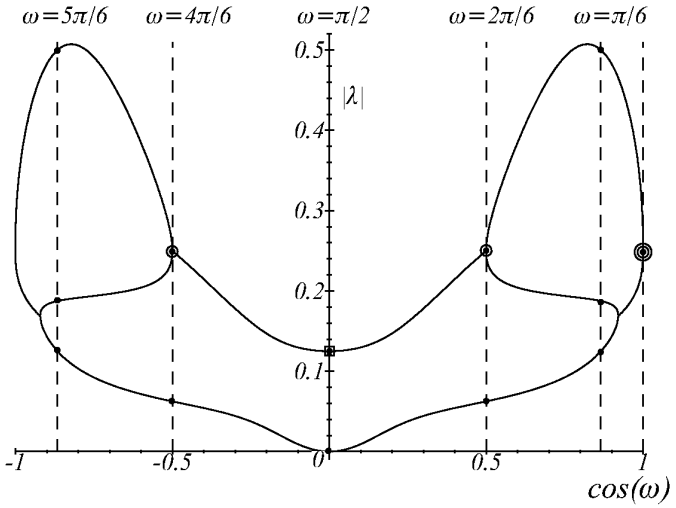

Figure 6.7: Eigenvalues of the subdivision matrix for the Butterfly scheme for valence 6.

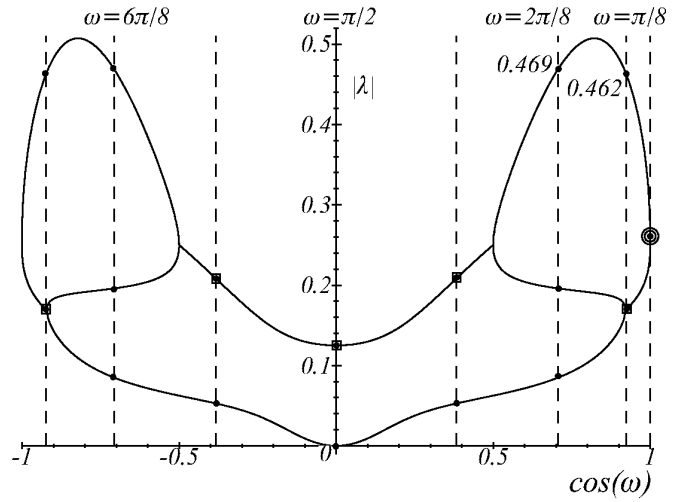

Figure 6.8: Eigenvalues of the subdivision matrix for the Butterfly scheme for valence 8. The magnitude for the largest eigenvalue of the first block $B(\pi/8)$ is less than the magnitude of the largest eigenvalue for the second block $B(2\pi/8)$.

the largest eigenvalue for $\omega = \pi/4$. Moreover, it is clear from Figure 6.8 that for higher valences the situation will be the same: the vertical line $z = cos(\pi/k)$ will move to the right as z increases and the magnitude of the largest eigenvalue will decrease. $z = cos(2\pi/k)$ will intersect the upper curve at a point to the left of $z = cos(\pi/k)$ and to the right of $z = cos(\pi/4)$ for $k > 8$. Therefore, the eigenvalues of block $B(\pi/k)$ will be always less than the largest eigenvalue of $B(2\pi/k)$. This fact can be established precisely analyzing the expressions for the roots of the characteristic polynomial.

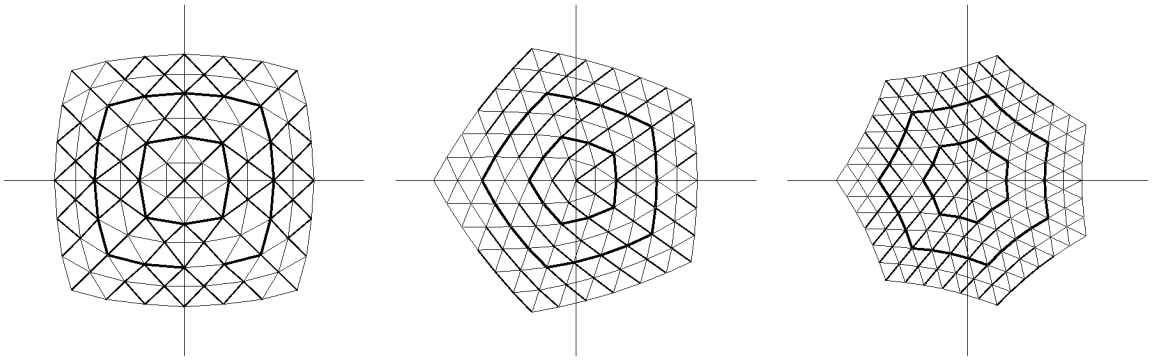

Figure 6.9: Characteristic maps for the Butterfly scheme, valences 4,5,7.

Formally, failure of the eigenvalues to satisfy the necessary conditions precludes the scheme from being C^1-continuous. However, it is useful to examine the behavior of surfaces generated by the scheme near extraordinary points. From the fact that the dominant eigenvalues of the scheme are located in the second block of the subdivision matrix, one might infer that in a small neighborhood of the extraordinary vertex, the surface will behave in a similar way to the map generated by a pair of eigenvectors corresponding to the second block. These eigenvectors produce a mapping $U_1 \rightarrow \mathbf{R}^2$ that is not injective and is a double covering on a sufficiently small neighborhood of the extraordinary vertex. However, this effect often cannot be observed even after a few subdivision steps.

The reason for this is that for many surfaces the decomposition with respect to the eigenbasis of the subdivision matrix contains only small components corresponding to the dominant eigenvectors; and large components corresponding to the eigenvalues of the first block which are not dominant, but close to dominant. If we consider a surface which is known to contain components of sufficiently large magnitude corresponding to the second block (Figure 6.10a), then the twist starting to appear in the surface becomes apparent. Note the difference between behavior of the Butterfly scheme and the Modified Butterfly

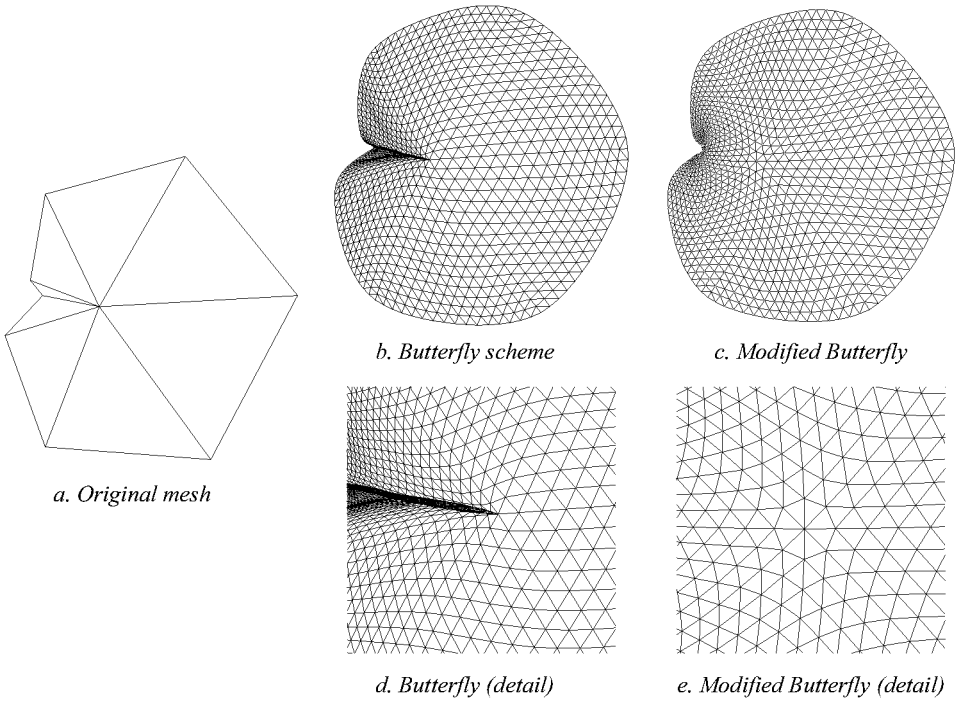

Figure 6.10: The difference in the behavior of a C^1-continuous scheme (Modified Butterfly) and non-C^1-continuous scheme (Butterfly). The latter has close eigenvalues in $B(\pi/8)$ and $B(2\pi/8)$. The ring of points around the vertex of valence 8 was generated using the formula $e^{2m\pi/8} + 0.7e^{4m\pi/8+0.2}$, to introduce a significant component at the "frequency" $4\pi/8$.

scheme (Figure 6.10bc) which is C^1-continuous near extraordinary point of valence 8 as it will be shown in the next section. For other initial meshes the Butterfly can produce smooth-looking surfaces even for valences for which it is not formally smooth (Figure 6.12a). On the other hand, in the particularly degenerate case of valence 3, the Butterfly scheme never produces surfaces that look smooth (Figure 6.11).

For large valences, the appearance of the meshes generated by the Butterfly scheme is primarily determined by the fact that the largest eigenvalues of the blocks $B(m\pi/k)$ are clustered together (Figure 6.12b) rather than by the number of the block which has the largest eigenvalues. It is particularly important for common "cap-like" configurations that the eigenvalues of the block $B(0)$ are close to the eigenvalues in the block $B(2\pi/k)$. This results in a surface very close to conical near a vertex with large valence.

As we will see in the next section, for Loop's scheme the formal requirements for C^1-continuity are satisfied, but the surfaces produced by the scheme don't look smooth for

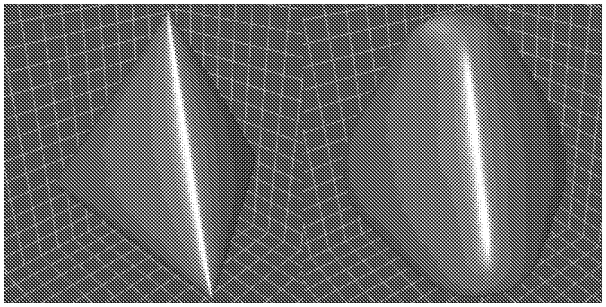

Figure 6.11: A tetrahedron is subdivided according to the original Butterfly scheme (on the left) and with our modified Butterfly scheme (right).

large valences due to a similar clustering of eigenvalues.

These observation indicate that for practical schemes it is important to consider relative magnitudes of eigenvalues rather than only the dominant eigenvalues and characteristic maps generated by the dominant eigenvectors.

In the next section we discuss how the Butterfly scheme has to be modified to ensure C^1-continuity for all valences and avoid eigenvalue clustering.

6.4 Modified Butterfly Scheme

In this section we describe and analyze a modification of the Butterfly scheme that corrects some of the problems of the original scheme while keeping the support of the scheme small and coefficients easy to compute. Some examples of surfaces generated using our scheme are shown in Figure 6.13

6.4.1 Definition of the Scheme

As we have observed, the appearance of the surfaces generated by the Butterfly scheme is largely determined by the behavior of the eigenvalues of the subdivision matrix. We can improve the Butterfly scheme by choosing the coefficients near extraordinary points in such a way that the eigenvalues of the subdivision matrix have desired behavior. It would be nice to be able to preserve the size of the stencil of the scheme; however, it is easy to show that if the stencil does not change, the eigenvalues inevitably will be clustered; formal C^1-continuity in this case will have little relevance. We allow the stencil to include 1-neighborhoods of both neighbors of the vertex were the value is computed, i.e., the whole stencil for single

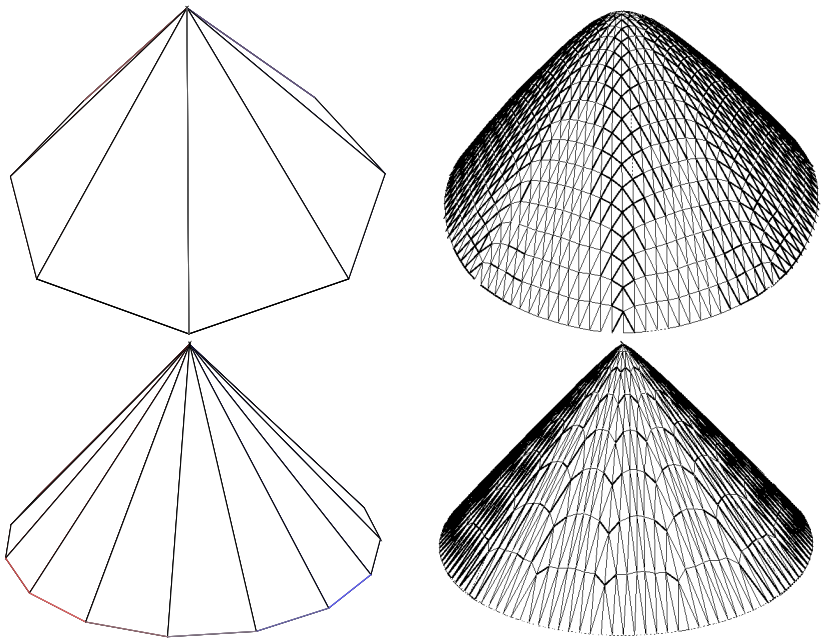

Figure 6.12: Left: for this initial mesh (all vertices around the extraordinary vertex of valence 8 are on a circle) the Butterfly scheme generates a smooth-looking surface, although it is not formally C^1-continuous. Right: for valence 17, the surface generated by the Butterfly scheme is close to conical.

ring schemes. Using this stencil, it is possible to find coefficients for subdivision for any prescribed set of eigenvalues of the subdivision matrix. In fact, it is sufficient to use a smaller stencil, including only one ring (Figure 6.14). Note that this stencil is asymmetric. For vertices on level finer than 0, this is not a problem: we are modifying coefficients of the scheme only for neighbors of extraordinary vertices, and only one of the two neighbors can be extraordinary after one subdivision step. On the top level both neighbors can be extraordinary. The choice that we make on the top level does not affect C^1-continuity, but affects the appearance of the surface. As we don't have enough degrees of freedom to apply a meaningful optimization procedure, we make an *ad hoc* choice to take the average of the results produced by each of the two possible choices. In our experience, this choice has produced satisfactory results, but a better one may be possible.

For the stencil shown in the Figure 6.14, the eigenvectors of the subdivision matrix are completely defined by the eigenvalues. The eigenvalues of the subdivision matrix can be chosen using the following considerations. The Butterfly scheme does not generate C^2 surfaces on the regular complex, and it is possible to show that no other interpolating scheme

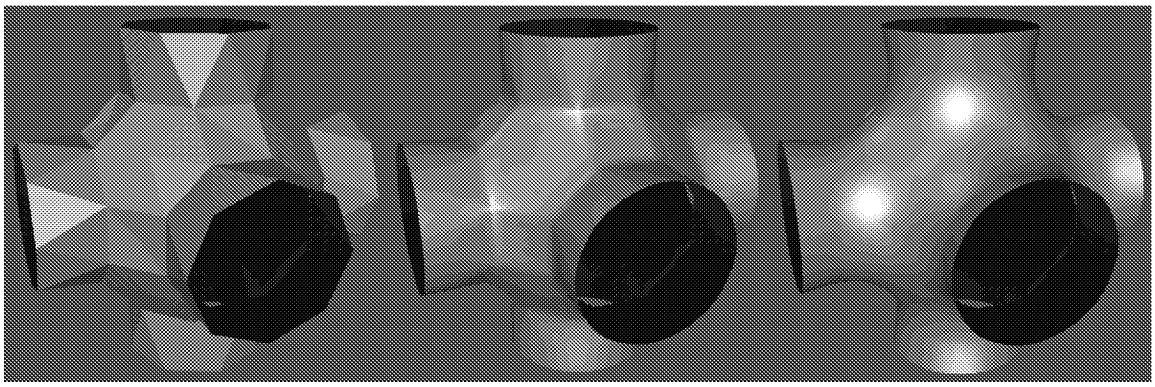

Initial mesh Butterfly interpolation Modified Butterfly interpolation

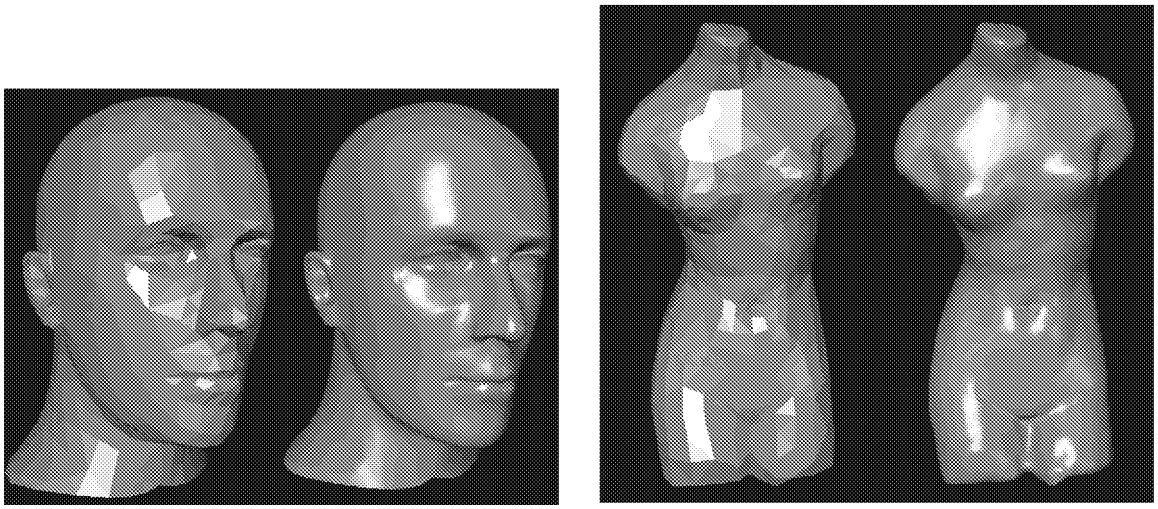

Initial mesh Modified Butterfly interpolation Initial mesh Modified Butterfly interpolation

Figure 6.13: Top row: pipe joint. Note the difference between Butterfly and Modified Butterfly. Lower left: mannequin head. Lower right: torso.

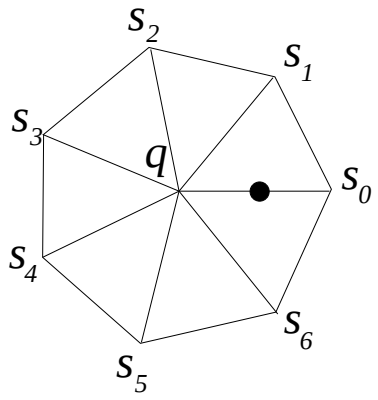

Figure 6.14: Stencil for a vertex in the 1-neighborhood of an extraordinary vertex

on a Butterfly or ten-point (Figure 6.2) does. We can try to approximate the behavior of a C^2 surface. Suppose a C^2 surface is generated by a symmetric scheme with all eigenvalues having trivial Jordan blocks.

If the scheme is not flat at the extraordinary vertex, it is necessary that the second largest eigenvalue is the eigenvalue of $B(0)$, $B(4\pi/k)$ (and, by symmetry of $B(2(k-2)\pi/k)$) and is λ^2. It is possible to make any scheme which is C^2 on the regular complex into a C^2 scheme on an arbitrary complex by making it flat, i.e., make the distance to the tangent plane decrease as $O(h^3)$ as we approach the extraordinary vertex. However, this is undesirable: one of the reasons for using C^2 surfaces is their natural local behavior; for generic points C^2-surfaces have either parabolic or saddle shape, while a flat surface will always closely approximate a plane or a cylinder.

If the surface is not C^2 at the extraordinary vertex but is C^2 elsewhere, picking the eigenvalues λ^2 as largest eigenvalues for $B(0)$, $B(4\pi/k)$ and $B(2(k-2)/k)$ ensures that the second derivatives of the parameterization given by the characteristic map stay bounded near the extraordinary point, without diverging to infinity or converging to zero.

Finally, it is useful to have the dominant eigenvalues the same for the regular and extraordinary case. The magnitude of the eigenvalue does not affect C^1-continuity as long as all other eigenvalues are scaled with it, but it determines how fast the size of the triangles near an extraordinary point decreases with each subdivision step. In Section 6.5 we will see how the magnitude of the eigenvalues affect the quality of the approximating meshes.

In the regular case, the dominant eigenvalues of the subdivision matrix are both 1/2.

This leads us to the following choice of the eigenvalues: $1/4, 1/2, 1/4, 1/4, 1/2$ for blocks $B(0)$, $B(2\pi/k)$, $B(4\pi/k)$, $B(2(k-2)\pi/k)$, $B(2(k-1)\pi/k)$. The only condition that we have to impose on the eigenvalues for other blocks is that their magnitude should be less than $1/4$. The simplest choice is to set them to 0. This appears to work quite well in practice. The two cases that have to be treated separately are $k = 3$ and $k = 4$. We choose eigenvalues $1/2, 1/2$ in the first case and $1/2, 1/4, 1/2$ in the second.

These conditions immediately determine the choice of coefficients of the scheme for computing the values at vertices that have one regular and one extraordinary neighbor.

For $K \geq 5$ the coefficients are given by the equations

$$s_j = \frac{1}{k}\left(1/4 + \cos(2\pi/k) + 1/2\cos(4\pi/k)\right) \tag{6.6}$$

with $j = 0, \ldots, k-1$. For $k = 3$ we use $s_0 = 5/12$, $s_{1,2} = -1/12$, and for $k = 4$, $s_0 = 3/8$, $s_2 = -1/8$, $s_{1,3} = 0$.

To summarize, the proposed scheme uses the following rules:

1. For all edges with both endpoints of valence 6, compute the value for the midpoint using the coefficients of the Butterfly scheme.

2. For every edge that is adjacent to an extraordinary vertex, compute the value for the midpoint using coefficients of Equation (6.6).

3. For every edge that connects two extraordinary vertices, compute values for the midpoint using coefficients (6.6) for each vertex and take the average.

6.4.2 Subdivision Matrices, Eigenvectors and Convergence Rates

As in the case of the Butterfly scheme, we primarily have to analyze the eigenstructure of the blocks $B(2m\pi/k)$ which in this case have the form

$$B(2\omega) = \begin{pmatrix} \lambda_\omega & 0 & 0 \\ 1/2 + 1/2\, e^{2\,i\omega} - 1/16\, e^{-2\,i\omega} - 1/16\, e^{4\,i\omega} & 1/8 & -1/16 - 1/16\, e^{2\,i\omega} \\ 1 & 0 & 0 \end{pmatrix}$$

with eigenvalues λ_ω, $1/8$ and 0, where λ_ω are the prescribed eigenvalues. Therefore, the dominant eigenvalues are guaranteed to be the prescribed eigenvalues $1/2$.

The eigenvectors can be determined in the same way as it was done for the Butterfly scheme using the parameters λ, a, c, l shown in Figure 6.6. For the Modified Butterfly scheme $\lambda = 1/2$, $c = 3$, a and l are given by

$$a = \frac{8}{3}\left(\frac{3}{4}\cos\frac{\pi}{k} - \frac{1}{8}\cos\frac{3\pi}{k}\right)$$
$$l = a\left(\frac{8}{9} - \frac{1}{9}e^{-\frac{2\pi i}{k}}\right) + \frac{4}{3}e^{-\frac{\pi i}{k}}$$

In order to analyze C^1-continuity using the algorithms of Chapter 5, we need to find the control net for a ring of patches; the size of the ring is determined by two conditions:

- No stencil of the net contains the extraordinary vertex as an internal vertex; in our case this is guaranteed by choosing the internal radius to be 2. This is due to the fact that the extraordinary vertex has stencil of size 1 on all subdivision levels finer than the top level. In general, this radius for a single ring scheme is 3.
- The union of the ring and it scaled images with scaling factors $1/2^i$, $i > 0$, cover $\dot{U}_1$. This means that the outer radius should be no less than twice the inner radius, i.e., at least 4.

The control net for the ring consists of 6 rings of vertices around the central vertex as shown in Figure 6.15.

The algorithms of Chapter 5 require the constants C, C_1, C_2, γ, γ_1, γ_2 characterizing the convergence of the scheme on the regular grid. These constants can be computed using Equations (4.26) and (4.27) and formulas for the $\|\cdot\|_\infty$ norm of Laurent polynomials (4.29). For the Butterfly scheme, as it was already mentioned in Section 4.3, we obtain

$$\begin{array}{llll} C = \frac{3}{4} & \gamma^1 = \frac{7}{8} & \gamma^2 = \frac{31}{64} & \gamma_3 = \frac{261}{1024} \\ C_{1,2} = \frac{11}{8} & \gamma^1_{1,2} = 1 & \gamma^2_{1,2} = \frac{7}{8} & \gamma^3_{1,2} = \frac{11}{16} \end{array} \tag{6.7}$$

We have chosen to use γ for 3 levels of subdivision as after 3 levels of subdivision the convergence rate estimate is close enough to what we would get if we were to use more

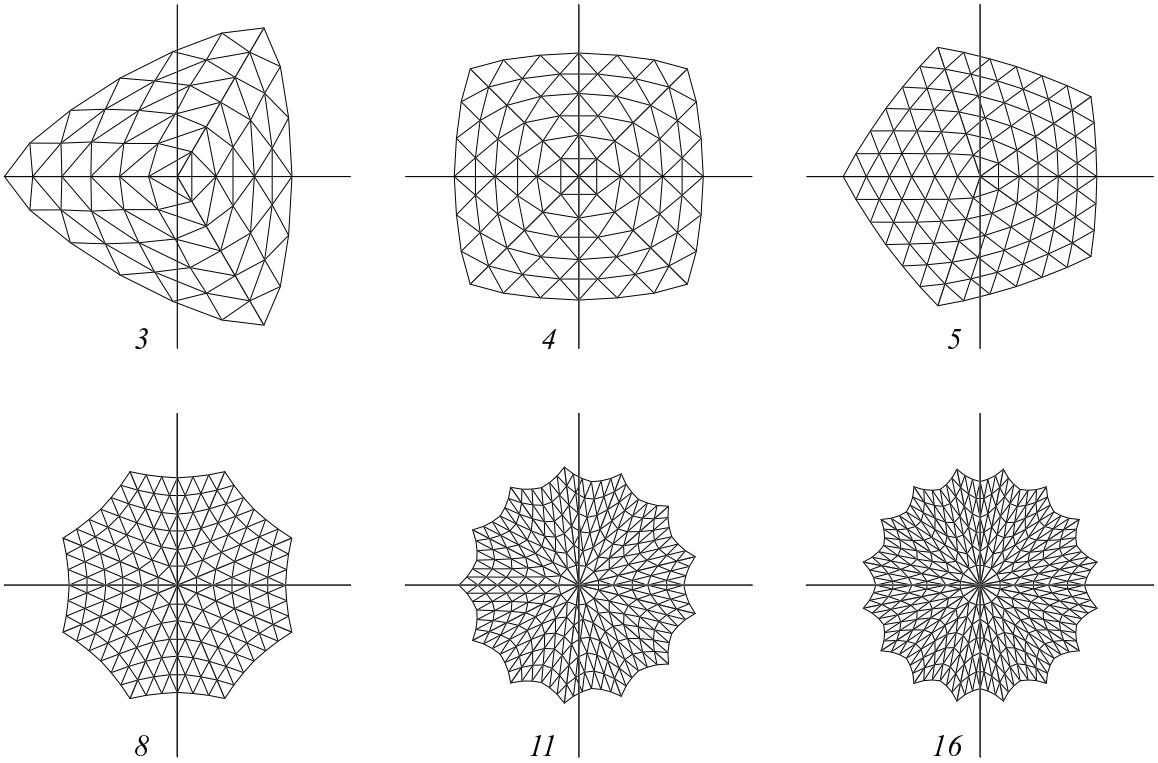

Figure 6.15: Control nets of the rings of characteristic maps for the Modified Butterfly scheme.

levels: $\gamma_3^{1/3}$ is close to $(\gamma_4)^{1/4}$. These estimates indicate that the convergence for derivatives is quite poor: γ stays close to 0.9 per level. However, this is a worst case estimate and in practice the scheme behaves quite well. The reason for this is that for schemes with negative coefficients, the "worst case" happens when the initial values have changing signs, i.e., consist primarily out of high frequency components, which is uncommon for surfaces. These overly conservative estimates result in a relatively large number of subdivision steps that have to be performed to establish C^1-continuity of the Modified Butterfly scheme. Potential ways of improving the situation are discussed below.

6.4.3 C^1-Continuity Analysis

To prove C^1-continuity of the Modified Butterfly scheme for vertices of arbitrary valence, we use the algorithms of Chapter 5. As discussed in Section 6.2.1, it is possible to prove convergence for arbitrary valence if suitably chosen affine transforms of the control nets for one segment of the characteristic map converge to a limit as $k \to \infty$ and the normalized segment in the limit is regular and injective. This is the case for the Modified Butterfly

scheme; the affine transform that we use is simply scaling along the y-axis by $sin(\pi/k)$. The values of a and l for the limit configuration are

$$a = \frac{5}{3}; \quad l = \frac{71}{27} - \frac{26}{27}i$$

The control net for one segment of the characteristic map before normalization consists out of parts of 3 segments of the control net for the whole map; the middle segment is the one shown in Figure 6.6; the other two can be obtained from the middle one by rotation by $2\pi/k$ and $-2\pi/k$. After scaling, the transformation for obtaining the normalized segments from the normalized middle segment are given by the matrix

$$\begin{pmatrix} \cos\frac{2\pi}{k} & \mp\sin\frac{2\pi/k}{\sin}\frac{\pi}{k} \\ \pm\sin\frac{2\pi}{k}/\sin\frac{\pi}{k} & \cos\frac{2\pi}{k} \end{pmatrix}$$

The limit of this transformation as $k \to \infty$ is

$$\begin{pmatrix} 1 & 0 \\ \pm 2 & 1 \end{pmatrix}$$

Normalized control nets for several valences and the limit net are shown in Figure 6.16

The algorithm of Section 6.2.1 steps through the valences, verifying C^1-continuity for each valence which has sufficiently different control net. In the case of the Modified Butterfly scheme we were able to use only a relatively small step size 2.6×10^{-6}, with all tests passing only after 7 steps of subdivision. However, our implementation based on hardware floating point operation is quite efficient and the algorithm spends around 30 sec. performing all tests for 7 levels of subdivision; as the test has to be one only once for a given scheme, time becomes a concern only for multiparameter schemes.

The plot in Figure 6.17 shows the valences used by the algorithm; Figure 6.18 shows how the normalized control nets approach the limit as function of valence.

The lower and upper bounds of the Jacobians computed by the algorithm are shown in Figure 6.19. Each upper and lower bound is an interval number; the error bars indicate the size of the interval.

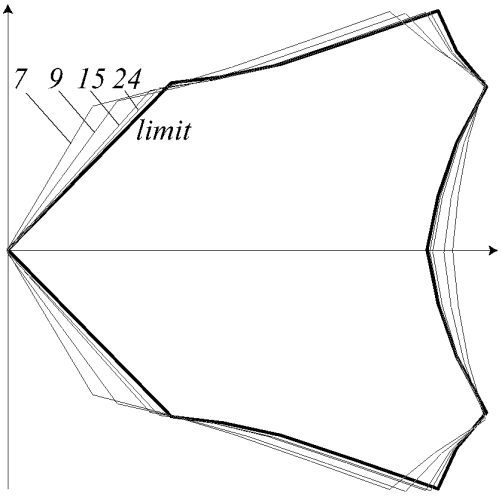

Figure 6.16: Convergence of normalized control nets of one segment of the characteristic maps for the Modified Butterfly scheme as valence increases. Only the boundaries of the nets are shown.

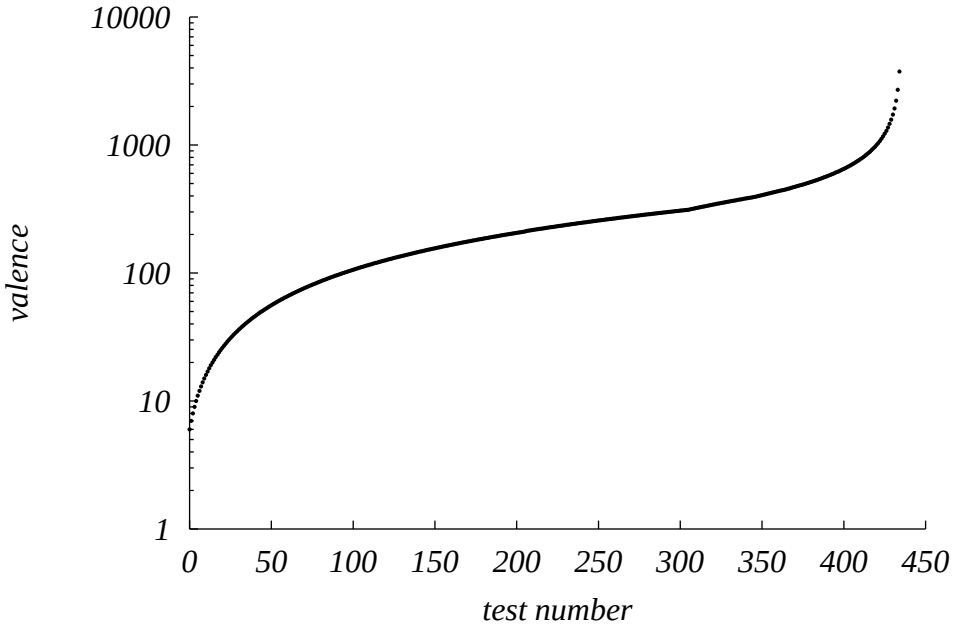

Figure 6.17: Valences tested by algorithm; note that only few large valences need to be tested. Total number of tested valences is 440. Data for valences 3, 4, 5 are not shown.

The jumps in the plot occur when the algorithm has to increase the number of levels used for estimating Jacobians.

It is clear from the appearance of the control nets that the estimates for the convergence rate of the Butterfly scheme are overly pessimistic; clearly, for this initial configurations the linear approximations to the Jacobians approach their limit values much faster. A possible approach to improving the performance of the algorithm is to refine analysis of Chapter 4; rather than using worst case estimates, one can try to decompose surfaces on regular grids into suitably chosen combinations of basis functions corresponding to different frequencies; as it was observed by Taubin [61], high-frequency components of surfaces are typically small. The same observation applies to characteristic maps of practically useful subdivision schemes. One may expect that significantly better convergence estimates can be obtained for interpolating schemes restricted to low-frequency initial data. This will lead to better estimates for general surfaces. In particular, one may expect a significant improvement simply by decomposing the control net into a linear component and an offset. For the linear part the convergence rate is very fast; in fact, the Butterfly scheme degenerates into midpoint subdivision and we can get rid of that component altogether, in error estimation, adding fixed constants to the derivatives.

Finally, the plot in Figure 6.20 shows the behavior of 6 error estimates ϵ_j^i, ϵ_{jk}^i as functions of valence.

The tests for isolation from zero and injectivity succeeded after 3 or less subdivision steps.

6.4.4 Tangents, Normals and Degeneracy Conditions

To complete the description of the Modified Butterfly scheme, we state the formulas for tangents and normals for the scheme. As discussed in Section 3.10.1 the tangent vectors can be computed using left eigenvectors of a submatrix of the subdivision matrix, which is obtained by restricting the matrix to the minimal invariant neighborhood. For the Modified Butterfly scheme, this is a 2-neighborhood for regular vertices and 1-neighborhood for extraordinary vertices. The latter is due to the fact that the immediate neighbors of an extraordinary vertex can be computed using only immediate neighbors of the same vertex on the coarser level.

The left eigenvectors required to compute tangent vectors are dual to the subvectors of

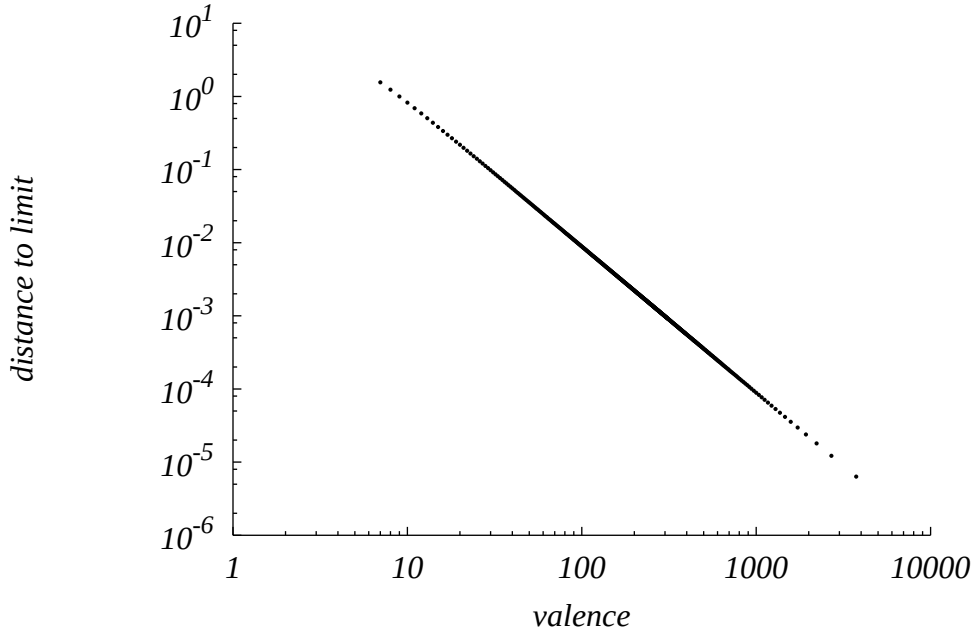

Figure 6.18: Distance from normalized control net to the limit control net as a function of valence.

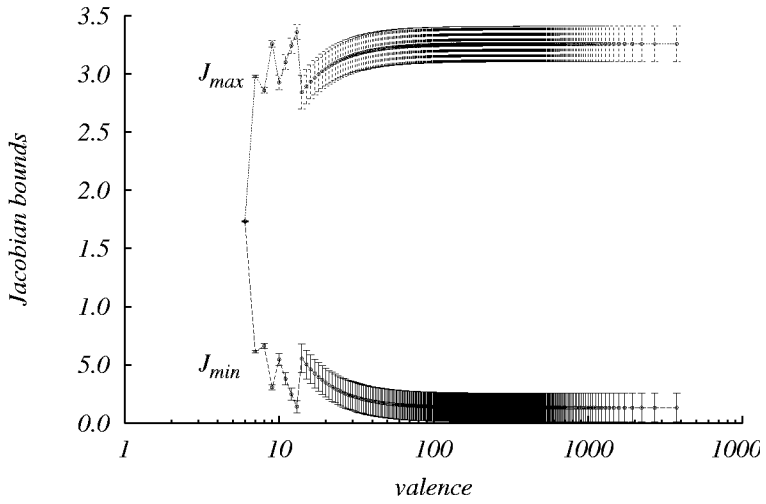

Figure 6.19: Upper and lower bounds for the Jacobians; error bars indicate the size of the interval; the *interval_size* argument for the algorithm was chosen to be 2.6^{-6} so that lower bound of the interval for J_{min} is close to zero.

the dominant eigenvectors. For extraordinary vertices the calculation is trivial: the matrix is cyclic (with one column and row added on the left and top) so it is reduced to the diagonal form by the DFT matrix. The left eigenvectors are the rows of the inverse DFT matrix.

Therefore, for the extraordinary vertices the tangent vectors are given by

$$t_1 = \sum_{m=0}^{k-1} x^m \cos\frac{2m\pi}{k}, \quad t_2 = \sum_{m=0}^{k-1} x^m \sin\frac{2m\pi}{k} \tag{6.8}$$

x_m, $m = 0 \dots k-1$ denote the control points at the vertices of 1-neighborhood of the vertex of valence k, the vertex itself excluded. The numbering can start from any vertex (tangent vectors are not unique). The normal is just the cross-product $t_1 \times t_2$; this product is unique up to a scaling factor. This is not obvious from the expressions above; to understand this, it is useful to consider the expression for the normal which is obtained from $t_1 \times t_2$ by expanding the product and rearranging the terms:

$$t_1 \times t_2 = \sum_{m<n} \sin\frac{2(n-m)\pi}{k} x^n \times x^m = \sum_{p=0}^{k} \sin\frac{2p\pi}{k} \sum_{n=0} x^n \times x^{(n+p) \bmod k}$$

In this form one can see that the cross product is a sum of normals of all triangles adjacent to the vertex plus a scaled sum of normals of triangles formed by edges adjacent to the vertex which are separated by another edge etc. Clearly, this sum does not depend on the particular choice of indexes of the vertices. This construction also shows the relation between the exact normal and approximate normal computed using the standard technique of averaging normals.

The same formulas can be used for any other scheme for which the subdivision matrix for minimal invariant neighborhood is diagonalized by DFT, such as Loop and Modified Loop schemes described in Sections 6.5 and 6.6.

For regular vertices the situation is somewhat more complicated; the minimal invariant neighborhood in this case has size 2, and the eigenvectors are larger: as the valence is 6, the number of points in the invariant neighborhood is 19. the left eigenvectors corresponding to the dominant eigenvalues have the following form using indexing described in Section 6.1:

$$l_0 = [16, -8, -8, 16, -8, -8, -\frac{8\sqrt{3}}{3}, \frac{4\sqrt{3}}{3}, \frac{4\sqrt{3}}{3}, -\frac{8\sqrt{3}}{3}, \frac{4\sqrt{3}}{3}, \frac{4\sqrt{3}}{3}, 1, -\frac{1}{2}, -\frac{1}{2}, 1, -\frac{1}{2}, -\frac{1}{2}]$$
$$l_1 = [0, 8, -8, 0, 8, -8, 0, -\frac{4\sqrt{3}}{3}, \frac{4\sqrt{3}}{3}, 0, -\frac{4\sqrt{3}}{3}, \frac{4\sqrt{3}}{3}, 0, \frac{1}{2}, -\frac{1}{2}, 0, \frac{1}{2}, -\frac{1}{2}]$$

The tangent vectors are obtained by multiplying the vector of control points on the 2-neighborhood of a vertex by the vectors l_1 and l_2.

As the surfaces generated by subdivision are not necessarily C^1-continuous if $a_1 \times a_2 = 0$ it is desirable to have a geometric condition which would guarantee that this does not happen.

For the case of extraordinary vertices (as well as for Loop-like schemes) it is possible to formulate a natural sufficient condition for a configuration of control points to be nondegenerate.

For any integer $j \in [0 \dots k-1]$ the set of indices $\{0..k-1\}$ of vertices in the invariant neighborhood can be separated into two sets: $H_1(j) = \{j, \dots j + \lfloor \frac{k}{2} \rfloor\}$ and its complement $H_2(j) = \{j + \lfloor \frac{k}{2} \rfloor + 1 \dots k-1\} \cup \{0 \dots j\}$

Proposition 6.2. *For any direction in space d consider the projections Px^m, of control points x^m, $m \in \{0 \dots k-1\}$ onto this direction. Fix an origin and a positive direction on d. If there is a real number C and an integer j, $0 \le j \le k-1$, such that for all $m \in H_1(j)$ $P_m^d < C$ and for $m \in H_2(j)$ $P_m^d > C$, then the normal $t_1 \times t_2$ is not a zero vector.*

Informally speaking, this condition means that there is a plane such that $\lfloor \frac{N}{2} \rfloor$ consecutive points of the invariant neighborhood are above this plane and the other $\lceil \frac{N}{2} \rceil$ are below.

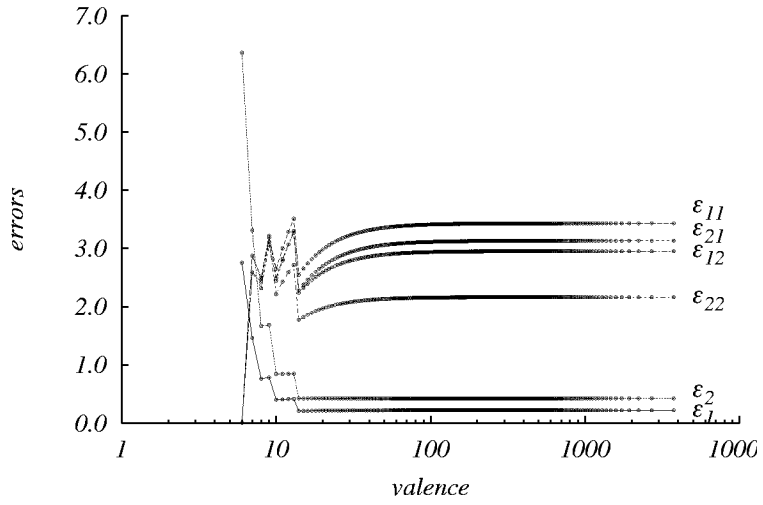

Figure 6.20: Linear approximation errors for Modified Butterfly scheme; ϵ_1, ϵ_2 are errors for components of the map, ϵ_{12}, ϵ_{12}, ϵ_{12}, ϵ_{12} are errors for the partial derivatives. Note that errors level out quite quickly; this indicates that the difference between normalized maps for large valences is quite small.

6.5 Loop Scheme

This scheme was introduced in C. Loop's thesis [40]. This is one of the simplest known C^1-continuous subdivision schemes. On the regular mesh this scheme generates degree 4 triangular splines. Tangent plane continuity (existence of limit normals) of this scheme was analyzed in Loop's thesis. C^1-Continuity as defined in Section 3.1 was established using Reif's criterion and analytic methods for valences up to 100 by J. Schweitzer [59]. In this section we use our algorithms to establish C^1-continuity of Loop scheme for arbitrary valence. Observations that we make in this section lead to improved versions of Loop scheme described in the next section.

6.5.1 Eigenvalues, Eigenvectors, Convergence Rates

Many facts stated in this section can be found in [40] and [59]. We reproduce these facts here for completeness.

The Loop scheme was defined in Section 2.2. The control and localization sizes for Loop scheme are both 2.

The eigenvectors of Loop scheme are determined by two parameters λ and a shown in Figure 6.21.

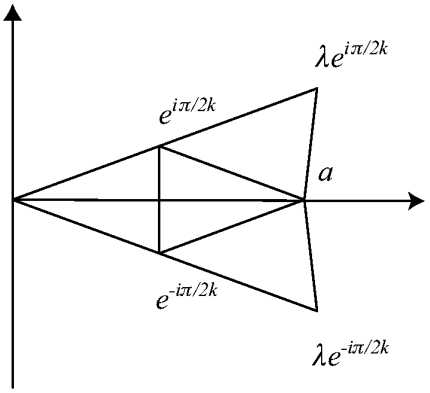

Figure 6.21: One sector of the control net of the characteristic map for Loop scheme.

The subdivision matrix in this case has particularly simple blocks

$$B(2\omega) = \begin{pmatrix} \frac{3}{8} + \frac{1}{4}\cos(2\,\omega) & 0 & 0 \\ \frac{3}{4}\cos(\omega) & \frac{1}{8} & 0 \\ \frac{5}{8} + \frac{1}{8}\cos(2\,\omega) & \frac{1}{8}\cos(\omega) & \frac{1}{16} \end{pmatrix} \tag{6.9}$$

where $\omega = 2m\pi/k$, $m = 1 \ldots k-1$. The eigenvalues of this matrix are $3/8+(1/4)\cos(2\omega)$, $1/8$ and $1/16$. The first changes in the range $1/8$ to $5/8$. In particular, the eigenvalue of the first block increases from $1/4$ to $5/8$ as ω goes through values $\pi/3$, $\pi/4$, $\pi/5$ ...

The 0-th block Z has the form

$$Z = \begin{pmatrix} c_0 & 1-c_0 & 0 & 0 \\ \frac{3}{8} & \frac{5}{8} & 0 & 0 \\ 0 & \frac{3}{4} & \frac{1}{8} & 0 \\ 0 & \frac{3}{4} & \frac{1}{8} & \frac{1}{16} \end{pmatrix} \tag{6.10}$$

The eigenvalues of Z are 1, $1/8$, $1/16$ and $c_0 - 3/8$ (see Figure 2.8 for definition of c_0).

It can be easily established by direct calculation that the dominant eigenvalues are both $3/8 + (1/4)\cos(2\pi/k)$ for all k and are eigenvalues of blocks $B(2\pi/k)$ and $B(2(k-1)\pi/k)$.

For Loop scheme Ring_k has the same size as for the Modified Butterfly; the control nets, however, are smaller and contain only the vertices (s, j, l) with $j = 1 \ldots 5$. Several control nets for rings are shown in Figure 6.30.

We choose the same normalization for the control nets of one segment of the characteristic map as we used for the Modified Butterfly scheme, i.e., scaling by factor $1/\sin(2\pi/k)$ along the y-axis. As a result, we get a converging sequence with nondegenerate limit, similar to the one shown in Figure 6.28; see also Figure 6.16.

Convergence rate estimates for Loop scheme are much better than for the Modified Butterfly; not only all coefficients of Loop scheme on the regular grid are positive, but all coefficients of the schemes generating derivatives are positive too. It turns out that this results in convergence rate $1/2$.

The values of the convergence constants for Loop scheme are

$$C = \frac{7}{8} \quad C_{1,2} = \frac{3}{2} \quad \gamma = \gamma_{1,2} = \frac{1}{2}$$

The plots in Figures 6.22-6.25. show that the algorithm is able to establish C^1-continuity of Loop scheme with significantly less effort: only 55 valences have to be tested, and only 3 subdivision steps were required in the worst case. The primary reason for this is that the estimates for convergence rates for schemes with non-negative coefficients are much more realistic. This allowed us to use the interval size 0.0004, considerably larger than the interval size for the Modified Butterfly.

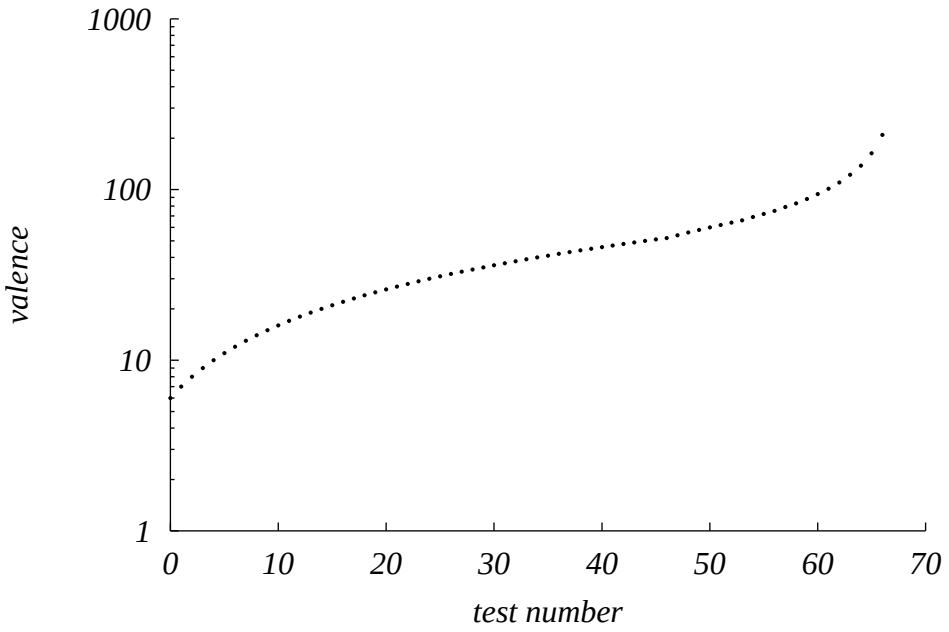

Figure 6.22: Valences tested by algorithm; note that only few large valences need to be tested. Total number of tested valences is 55. Data for valences 3,4,5 are not shown.

Behavior for large valences. Eigenvalue clustering for large valences also occurs for Loop scheme. Clearly, as $k \to \infty$ largest eigenvalues of blocks $B(2\pi/k)$ and $B(4\pi/k)$ both approach 5/8. However, the limit values of the eigenvalues of block Z are 1, 1/8, 1/16 and 25/64; thus, the "zero-frequency" eigenvalues are away from the cluster; as a result, as $k \to \infty$, the surfaces generated by the scheme don't approach cones, unlike the Butterfly scheme (Figure 6.12). Note that this becomes possible for a scheme which uses the regular rule for immediate neighbors of the central vertex only if it is not interpolating.

However, a milder problem coming from eigenvalue clustering persists: an example is shown in Figure 6.26 on the right. This problem can be solved as it is described in the next section; it is worth mentioning that in some cases this behavior may be desirable, but our goal is to make it controllable rather than let the artifacts appear by chance.

The other problem, presence of ripples in the surface close to an extraordinary point, shown in Figure 6.26. It is not clear to what extent this problem can be eliminated, as it appears to be related to the fact that Loop scheme is not C^2 at extraordinary vertices. There is no C^2-stationary non-flat symmetric scheme with same stencils as Loop, and it is

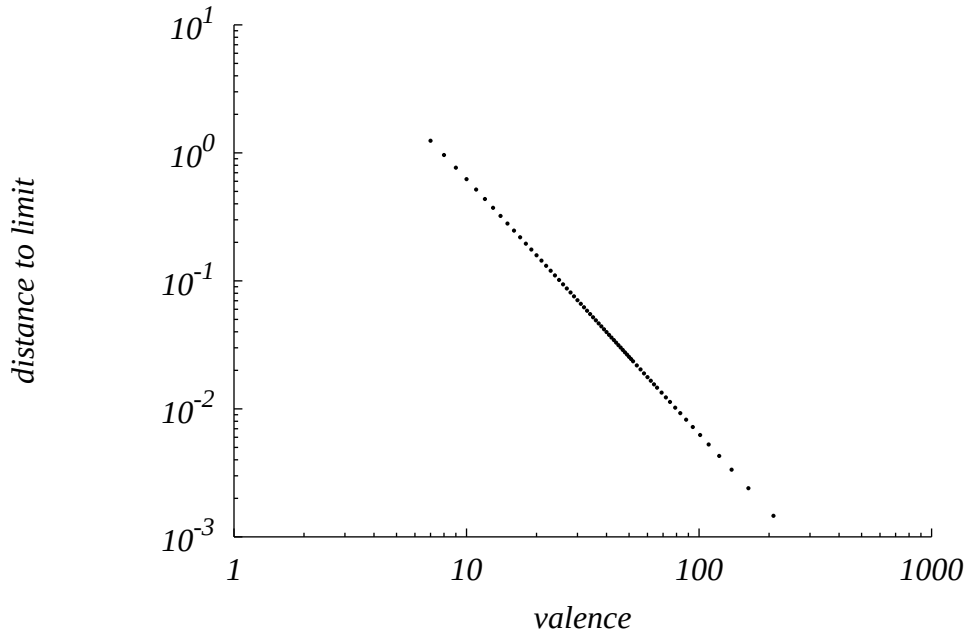

Figure 6.23: Distance from normalized control net to the limit control net as a function of valence.

unlikely that the problem can be eliminated completely if we use stationary schemes.

It turns out that there is a trade-off between the two types of artifacts described above; we discuss this problem further in the next section.

6.6 Modification of Loop Scheme

In this section we describe a modification of Loop scheme that does not have eigenvalue clusters.

We construct the new scheme in the same way we have constructed the Modified Butterfly scheme: we prescribe eigenvalues and compute coefficient using inverse DFT. An additional property of Loop scheme that we would like to preserve is non-negativity of coefficients. When coefficients are nonnegative, the surfaces generated by the scheme have the convex-hull property, that is, are contained inside the convex hull of the initial control points.

The only eigenvalues that we would like to fix are the free eigenvalues of Z, $B(2\pi/k)$, $B(2(k-1)\pi/k)$, $B(4\pi/k)$, $B(2(k-2)\pi/k)$; it is desirable to have eigenvalues 1/4, 1/2, 1/4,1/4

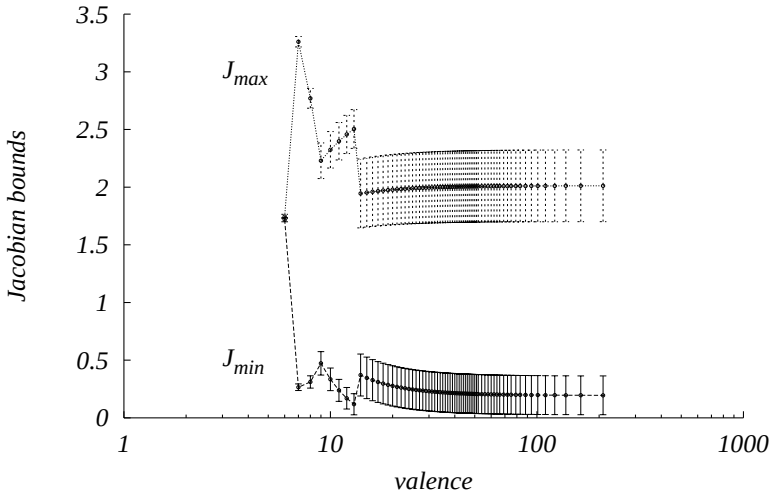

Figure 6.24: Upper and lower bounds for the Jacobians; error bars indicate the size of the interval; the *interval_size* argument for the algorithm was chosen to be 0.0004 so that lower bound of the interval for J_{min} is close to zero.

and 1/2 in these blocks as explained in Section 6.4. As can be seen from the formulas of the previous section, we have no control over the eigenvalues except one eigenvalue in block Z if we use the stencil of Loop scheme and require the scheme to coincide with Loop on the regular complex. We increase the stencil in a minimal way, including all vertices around a k-vertex into the stencil for an immediate odd neighbor, as we did for the Butterfly scheme. Formally, this increases the control and localization sizes of the scheme to 3; however, as the change is made only for neighbors of extraordinary vertices, the size of the subdivision matrix does not have to be increased for analysis.

It turns out that it is possible to obtain a scheme with prescribed eigenvalues and positive coefficients using eigenvalues $(1/2)^m$ for blocks $B(2m\pi/k)$ and $B(2(k-m)\pi/k)$, for $m = 1 \dots \lfloor k/2 \rfloor$. Let the (0,0) entry of $B(0)$ be a. Using notation of Figure 6.14, the coefficients of the scheme for immediate neighbors of extraordinary vertices are for $k > 4$

$$\begin{aligned} s_j &= \frac{1}{k}\left(a - 1 + \frac{3 + (-1)^j 2^{-(k+1)/2} \cos\frac{m\pi}{k}}{9 - 8\cos^2\frac{j\pi}{k}}\right) \text{ for } j = 0 \dots k, \text{ odd } k \\ s_j &= \frac{1}{k}\left(a - 1 + \frac{3 + 3(-1)^j 2^{-k/2} \cos\frac{m\pi}{k}}{9 - 8\cos^2\frac{j\pi}{k}}\right) \text{ for } j = 0 \dots k, \text{ even } k \end{aligned} \tag{6.11}$$

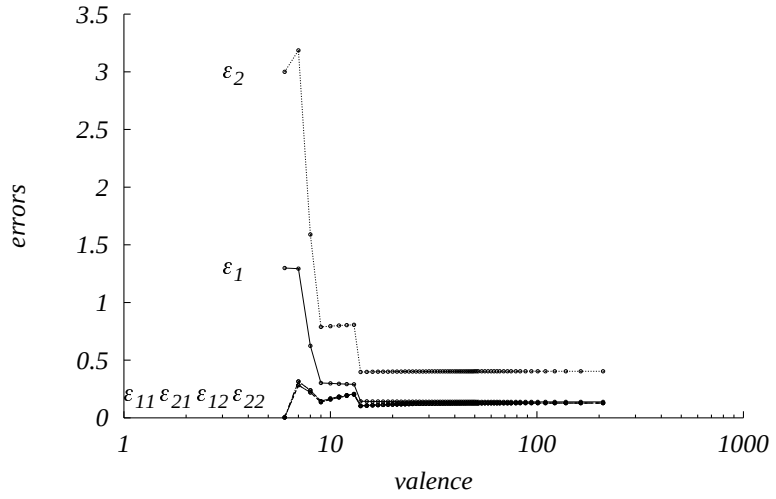

Figure 6.25: Linear approximation errors for Loop scheme; ϵ_1, ϵ_2 are errors for components of the map, and ϵ_{12}, ϵ_{12}, ϵ_{12}, ϵ_{12} are errors for the partial derivatives. ϵ_1 and ϵ_2 for valences close to 6 are large because J_{min} is sufficiently far away from zero, and the errors were computed using fewer subdivision levels.

For valences 3 and 4 we cannot have all prescribed eigenvalues because the subdivision matrix has too few blocks. In these cases we use spectra $1/4, 1/2, 1/2$ and $1/4, 1/2, 1/4, 1/2$ obtaining coefficients $13/24, 1/24, 1/24$ and $1/2, 1/16, 0, 1/16$ respectively, assuming the coefficient in the center is $3/8$.

If we ignore the variable terms in the denominator of the second term of the formulas (they vanish as $k \to \infty$), it is easy to see that the coefficients are nonnegative if $a > 2/3$. More detailed analysis shows that it is sufficient to use values for a above $5/6 + \sqrt{61}/48$.

For given a we can choose the coefficients of the scheme for the central vertex to be $(1/k)(a - 1/4)$ for the immediate neighbors and $5/4 - a$ for the vertex itself to guarantee that the free eigenvalue of Z is $1/4$.

The tests required to prove C^1-continuity of this scheme are very similar to the tests for Loop scheme; 60 valences had to be tested; the interval size used was 0.0013. Behavior of lower and upper bounds of the Jacobians is shown in Figure 6.27.

As expected, the meshes generated by this scheme have better structure near extraordinary points (Figure 6.29). However, the ripples become larger, so one kind of artifact is traded for another. The reason for this can be understood intuitively from the form of the

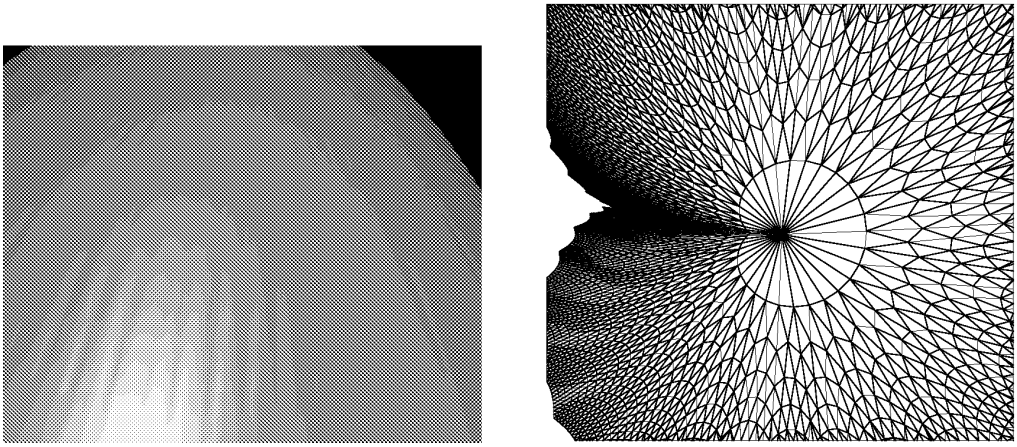

Figure 6.26: Left: ripples on a surface generated by Loop scheme near a vertex of large valence; Right: mesh structure for Loop scheme near an extraordinary vertex with significant "high-frequency" component; a crease starting at the extraordinary vertex appears.

expressions for the coefficients and eigenvalues: eigenvalues can be computed as DFT of coefficients. One can hypothesize that ripples are amplified by non-zero coefficients s_j with j far from 0 and k. Thus, it is desirable to make these coefficients as small as possible. However, for large k having distinct eigenvalues in adjacent blocks $B(2\pi/k)$ and $B(4\pi/k)$ is similar to having a δ-function for the continuous Fourier transform. This means that coefficients s_j may be significantly different from zero for values of j far from 0 and k. This reflects the standard duality between properties of a function and its Fourier transform.

It is, however, possible to seek an optimal solution or one close to optimal; alternatively, one may resort to a family of schemes that would allow to control the tradeoff between the two artifacts.

6.7 Crease Subdivision

In this section we briefly discuss a simple one-parametric family based on Loop scheme, with rules modified to create a smooth crease. This family of schemes is shown to be C^1-continuous for regular vertices and extraordinary vertices for certain ranges of tension parameters. Further work is needed to achieve controlled behavior near extraordinary vertices.

As discussed in Section 4.4, one can analyze C^1-continuity of a particular type of non-

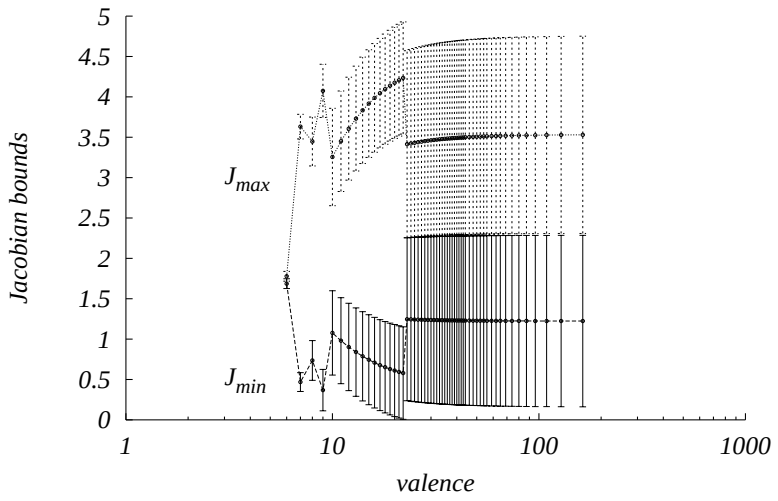

Figure 6.27: Upper and lower bounds for the Jacobians for Modified Loop scheme; error bars indicate the size of the interval; the *interval_size* argument for the algorithm was chosen to be 0.0013 so that lower bound of the interval for J_{min} is close to zero.

uniform schemes, constructed as a linear combination of two uniform subdivision schemes.

For Loop scheme the natural choice of coefficients satisfying Definition 4.2 is shown in Figure 6.31.

Direct computation using (4.59) and commutation formulas derived in Section 4.4 gives the following estimates for convergence rates γ: 1/2 for the derivative in x direction; $(k{+}1)/4$ in y-direction. Clearly, the scheme is C^1-continuous for all $k < 1$ on the regular complex.

It is instructive to analyze the eigenstructure of the subdivision matrix in the regular case; the matrix has the form

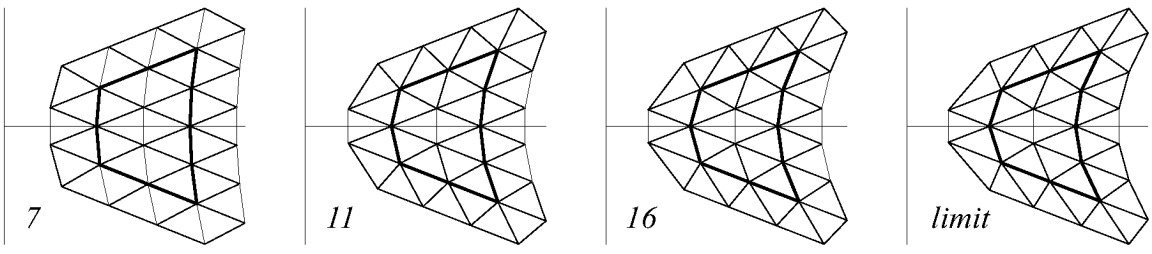

Figure 6.28: Normalized control nets for Modified Loop scheme and the limit control net.

$$\begin{bmatrix}
\frac{k}{8}+5/8 & \frac{k}{16}+1/16 & 1/16-\frac{k}{16} & 1/16-\frac{k}{16} & \frac{k}{16}+1/16 & 1/16-\frac{k}{16} & 1/16-\frac{k}{16} \\
\frac{k}{8}+3/8 & \frac{k}{8}+3/8 & 1/8-\frac{k}{8} & 0 & 0 & 0 & 1/8-\frac{k}{8} \\
3/8 & 1/8 & 3/8 & 1/8 & 0 & 0 & 0 \\
3/8 & 0 & 1/8 & 3/8 & 1/8 & 0 & 0 \\
\frac{k}{8}+3/8 & 0 & 0 & 1/8-\frac{k}{8} & \frac{k}{8}+3/8 & 1/8-\frac{k}{8} & 0 \\
3/8 & 0 & 0 & 0 & 1/8 & 3/8 & 1/8 \\
3/8 & 1/8 & 0 & 0 & 0 & 1/8 & 3/8
\end{bmatrix}$$

An additional parameter can be introduced to adjust the shape of the crease near a vertex; it will affect only the first row of the matrix, and won't have any impact on the C^1-continuity analysis; the coefficients for the central vertex change to

$$\begin{aligned}
&5/8 + k/8 + 3k_p(1-k)/8, \\
&(k+1)(1-k_p)/16,\ (1-k)(1-k_p)/16, (1-k)(1-k_p)/16, \\
&(k+1)(1-k_p)/16, (1-k)(1-k_p)/16,\ (1-k)(1-k_p)/16
\end{aligned}$$

where k_p is the "parallel" tension, i.e., tension along the crease. For $k_p = 1$ the crease interpolates the vertex and has a sharp corner. For $k \neq 1$ it does not mean that the surface is not C^1-continuous.

Remarkably, in the regular case the eigenvectors and eigenvalues of the subdivision matrix also linearly interpolate between eigenvectors and eigenvalues of the two limit cases $k = 0$ and $k = 1$.

The eigenvalues are

$$1, \frac{1}{4}, \frac{1}{4}, \frac{1}{2}, \frac{1}{2}, \frac{k+1}{8}, \frac{k+1}{4}$$

If we choose to interpolate coefficients linearly for extraordinary vertices, the behavior of eigenvectors and eigenvalues is much more complicated. Although we were able to analyze

C^1-continuity for a range of valences using our algorithms, this analysis relies on numerically computed eigenvalues; precision of such calculations is difficult to estimate, in most cases, and the analysis without such estimates cannot be regarded as rigorous. Additionally, our analysis indicates that the surface may become non-C^1-continuous at an extraordinary vertex for $k < 1$.

A better way to determine coefficients for the crease scheme near extraordinary vertex is to derive them from predefined eigenvalues and eigenvectors. It would be undesirable to use matrix inversion to compute coefficients; this imposes an additional constraint of having an orthogonal system of eigenvectors for all values of the tension parameter. Note that the standard crease scheme as introduced by Hoppe does not have an orthogonal system of eigenvectors for valences different from 6. It can be made orthogonal, however, by appropriate modification of coefficients. Interpolation inside the class of orthogonal matrices is also a difficult task, and the resulting expressions for coefficients are likely to be quite complicated. We leave construction and analysis of such schemes as a direction for future work.

As the expressions for eigenvalues and eigenvectors of the crease scheme for $k = 1$ are known [59], we were able to prove one-sided C^1-continuity of Loop scheme with sharp creases for arbitrary valence. The results are very similar to those obtained in the previous sections of r symmetric schemes, with the only difference that two parameters have to be considered.

Shapes generated by the scheme for various values of the tension parameter are shown in Figure 6.32.

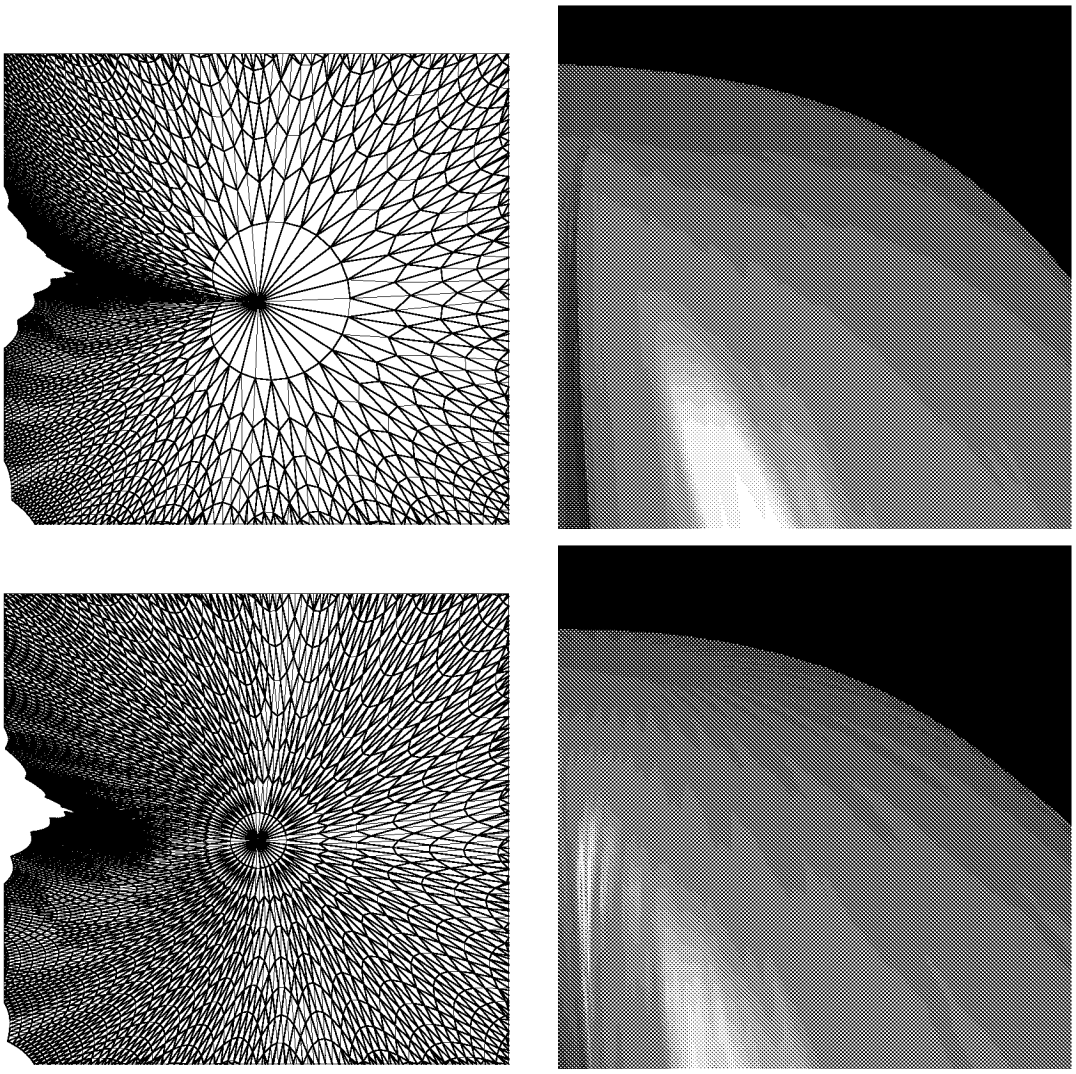

Figure 6.29: Left: mesh structure for Loop scheme and Modified Loop scheme near an extraordinary vertex; a crease does not appear for the Modified Loop. Right: shaded images of the surfaces for Loop and Modified Loop; ripples are more apparent for Modified Loop.

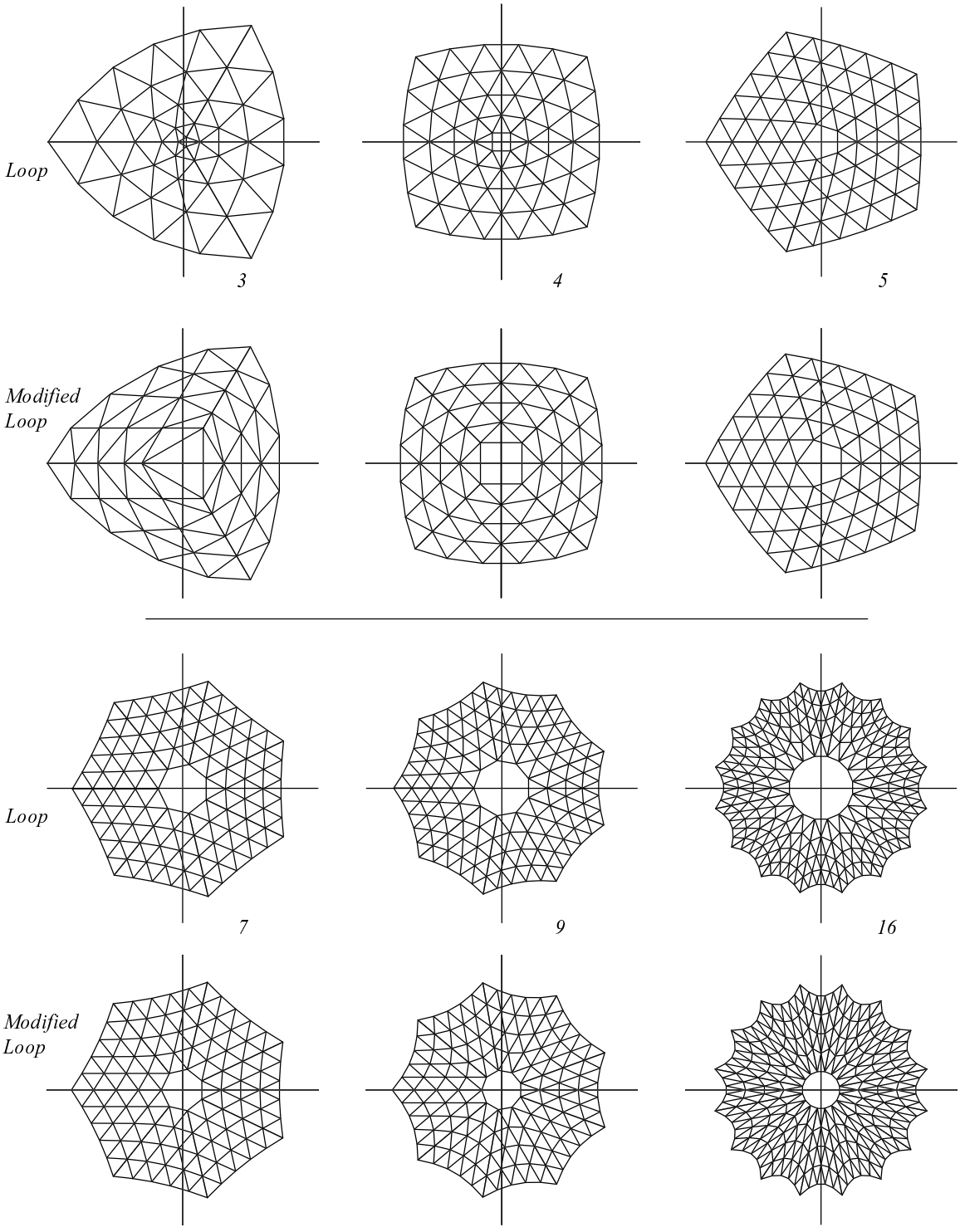

Figure 6.30: Comparison of control nets for Loop scheme and Modified Loop scheme. Note that for Loop scheme the size of the hole in the ring (1-neighborhood removed) is very small relatively to the surrounding triangles for valence 3 and becomes larger as k grows. For Modified Butterfly this size remains constant.

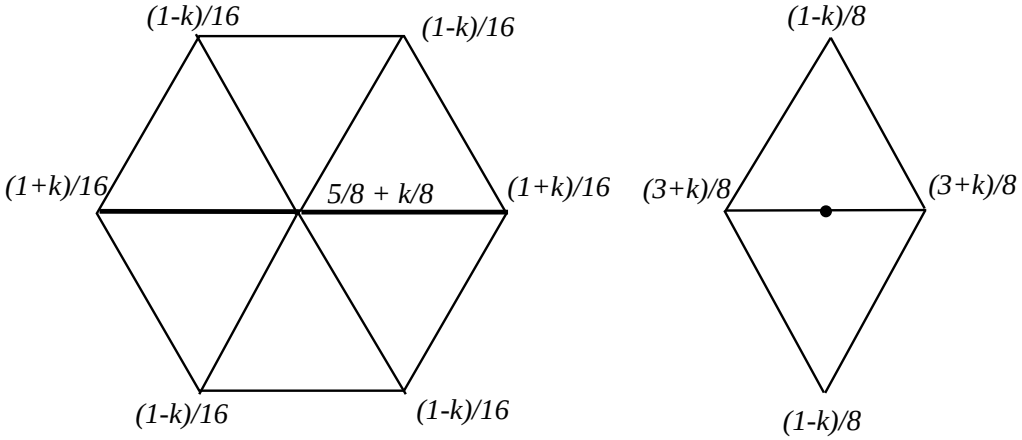

Figure 6.31: Coefficients for Loop scheme with creases (regular case).

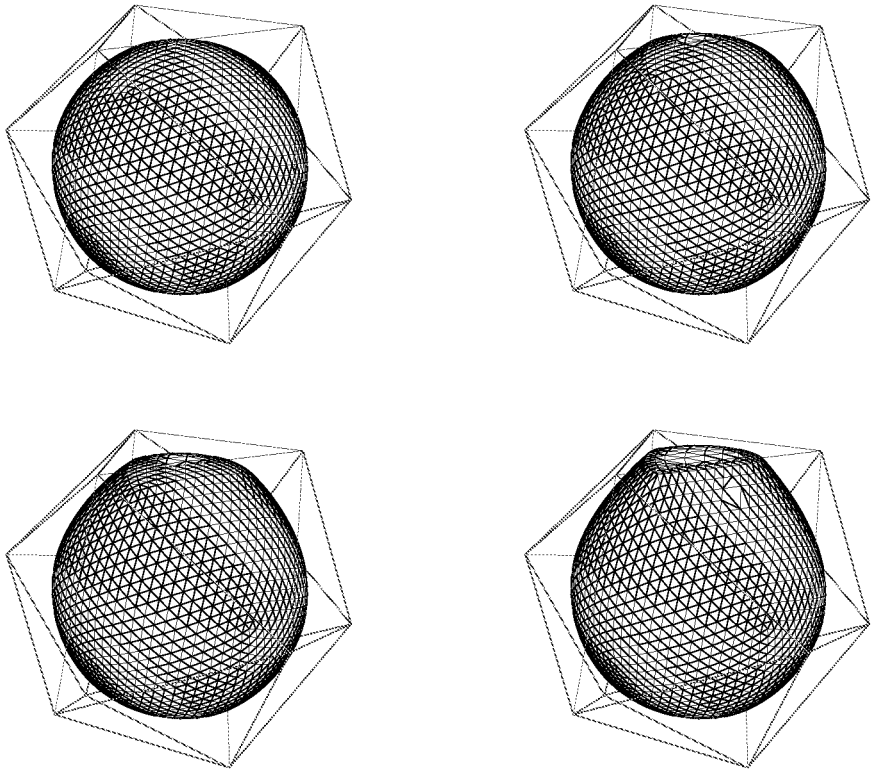

Figure 6.32: Three edges were assigned tensions 0.2, 0.5 (top row), and 0.7, 0.9 (bottom row).

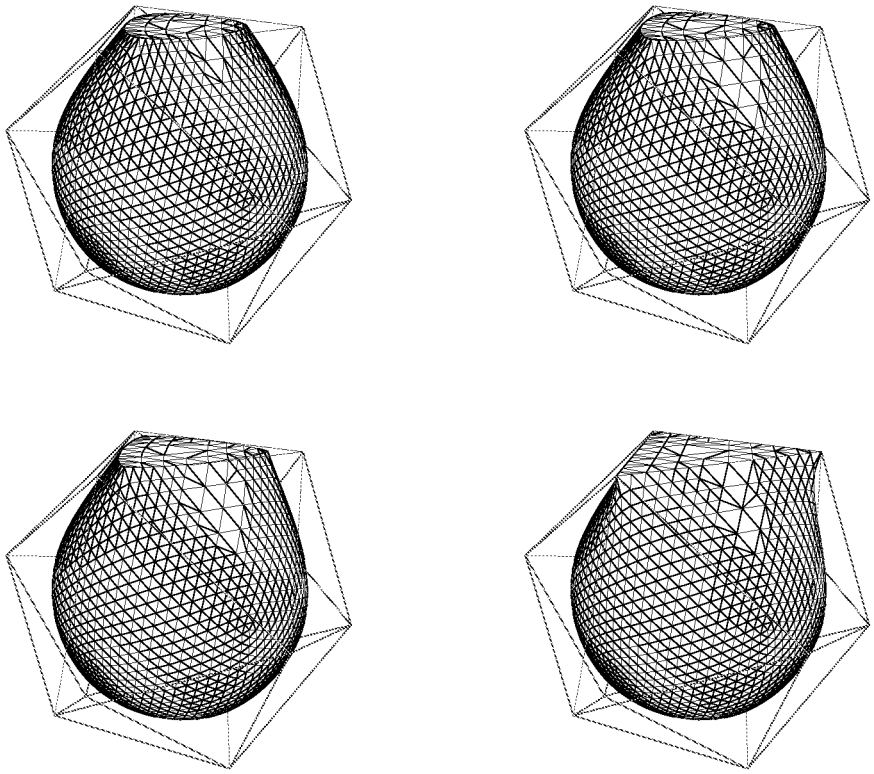

Figure 6.33: Three edges were assigned "parallel" tensions 0.2, 0.5 (top row), and 0.7, 0.9 (bottom row).

Chapter 7 Multiresolution Representations

In the previous chapters we have concentrated on theoretical properties of subdivision. In this chapter we describe algorithms for implementing subdivision and a multiresolution representation closely related to subdivision. Combining subdivision and the smoothing algorithms of Taubin [61] allows us to construct a set of algorithms for interactive multiresolution editing of complex hierarchical meshes of arbitrary topology. The simplicity of the underlying algorithms for refinement and coarsification enables us to make them local and adaptive, thereby considerably improving their efficiency. These algorithms take advantage of some basic properties of subdivision:

- **Smoothness** of the subdivision scheme used in the representation ensures that the changes made to the surface are blended with the rest of the surface.
- **Locality** of subdivision makes it possible to design algorithms which typically traverse only a small part of the data when recomputation is required.
- **Topological Generality:** Vertices in a triangular (resp. quadrilateral) mesh need not have valence 6 (resp. 4). Almost all generated surfaces are C^1-continuous everywhere, and efficient algorithms exist for computing normals and limit positions of points on the surface.
- **Multiresolution:** Because they are the limit of successive refinement, subdivision surfaces support multiresolution algorithms, such as level-of-detail rendering, multiresolution editing, compression, wavelets, and numerical multigrid.
- **Uniformity of Representation:** Subdivision provides a single representation of a surface at all resolution levels. Boundaries and features such as creases can be resolved through modified rules reducing the need for trim curves.

Although all algorithms are presented for multiresolution representations, they can be used for rendering and manipulation of pure subdivision surfaces, which are a special case of our representation.

For reasons of efficiency the algorithms should be highly adaptive and dynamically adjust to available resources. Our goal is to have a single, simple, uniform representation with scalable algorithms. The system should be capable of delivering multiple frames per second update rates even on small workstations taking advantage of lower resolution representations.

7.0.1 Structure of the Editng System

The particulars of the algorithms will be given later, but Figure 7.1 already gives a preview of how the different algorithms make up the editing system. In the next sections we first talk in more detail about subdivision, smoothing, and multiresolution transforms.

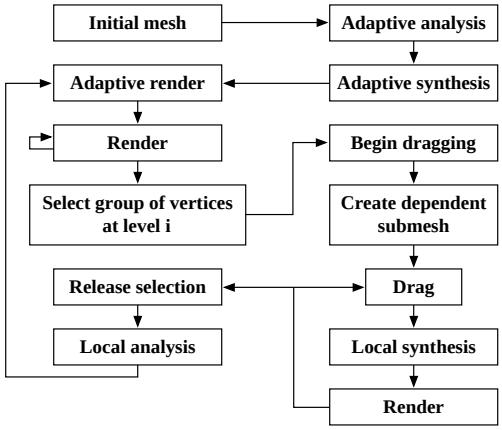

Figure 7.1: The relationship between various procedures as the user moves a set of vertices.

7.1 Multiresolution Representation

We begin by fixing our notation which is slightly different from the notation used in previous chapters. As usual, K denotes the initial complex, K^i, $i \geq 1$ subdivided complexes. Recall that the vertex sets are nested as $V^j \subset V^i$ if $j < i$. We define *odd* vertices on level i as $M^i = V^{i+1} \setminus V^i$. V^{i+1} consists of two disjoint sets: *even* vertices (V^i) and *odd* vertices (M^i). We define the *level* of a vertex v as the smallest i for which $v \in V^i$. The level of v is $i+1$ if and only if $v \in M^i$.

With each set V^i we associate a map to $\mathbf{R}^3$., i.e., for each vertex v and each level i, we have a 3D point $s^i(v) \in \mathbf{R}^3$. The set s^i contains all points on level i, $s^i = \{s^i(v) \mid v \in V^i\}$.

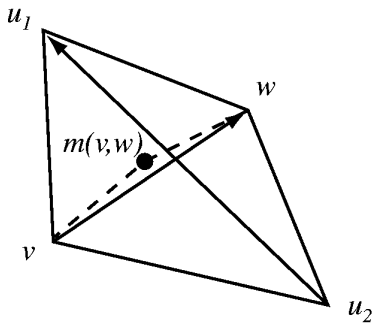

Figure 7.2: Computing approximate frame; the tangents at $m(v, w)$ are taken to be $t_1 = w - v$ and $t_2 = u_2 - u_1$; the normal n is their cross-product; the frame is the coordinate system obtained from (t_1, T_2, n) by orthonormalization.

A subdivision scheme S takes the points from level i to points on the *finer* level $i + 1$: $s^{i+1} = S\, s^i$.

Assuming that the subdivision converges, $\sigma(v) \in \mathbf{R}^3$ denotes the point on the limit surface associated with vertex $v \in V^\infty$.

In order to define our offsets with respect to a local frame, we also need tangent vectors and a normal. For the subdivision schemes that we use, such vectors can be defined through the application of linear operators Q and R acting on s^i so that $q^i(v) = (Qs^i)(v)$ and $r^i(v) = (Rs^i)(v)$ are linearly independent tangent vectors at $\sigma(v)$. Together with an orientation they define a local orthonormal frame $F^i(v) = (n^i(v), q^i(v), r^i(v))$. It is important to note that , in general, it is not necessary to use precise normals and tangents during editing; as long as the frame vectors are affinely related to the positions of vertices of the mesh, we can expect intuitive editing behavior.

The simplest possible formula that can be used for odd vertices is illustrated in Figure 7.2; it is important to note that while the approximate frame is adequate for representing details, the approximate normal vector computed in this way is not adequate for lighting calculations at coarsest levels of resolution. A precise subdivision surface normal using the formulas from the previous chapter can be used; in the case of a scheme with localization size 3, such as Butterfly, 2-ring neighborhoods have to be used for this calculation which makes them expensive to compute. In practice, formulas for schemes with support size 2, which don't depend on the coefficients of the scheme as long as it is symmetric, provide an adequate approximation to the normal for lighting.

For our implementation we have chosen the Loop scheme, since more performance optimizations are possible in it. However, the algorithms we discuss later work for any single ring scheme.

So far we have only discussed subdivision, i.e., how to go from coarse to fine meshes. In this section we describe analysis which goes from fine to coarse.

We first need *smoothing*, i.e., a linear operation H to build a smooth coarse mesh at level $i-1$ from a fine mesh at level i:

$$s^{i-1} = H\, s^i.$$

Several options are available here:

- **Least squares:** One could define analysis to be optimal in the least squares sense,

$$\min_{s^{i-1}} \| s^i - S\, s^{i-1} \|^2.$$

  The solution may have unwanted undulations and is too expensive to compute interactively [24].

- **Fairing:** A coarse surface could be obtained as the solution to a global variational problem. This is too expensive as well. An alternative is presented by Taubin [61], who uses a *local* non-shrinking smoothing approach.

Because of its computational simplicity, we decided to use a version of Taubin smoothing. As before let $v \in V^i$ have k neighbors $v_m \in V^i$. Use the average, $\overline{s}^i(v) = k^{-1} \sum_{m=1}^{k} s^i(v_m)$, to define the discrete Laplacian $\mathcal{L}(v) = \overline{s}^i(v) - s^i(v)$. On this basis Taubin gives a Gaussian-like smoother which does not exhibit shrinkage

$$H := (I + \mu\, \mathcal{L})\, (I + \lambda\, \mathcal{L}).$$

With subdivision and smoothing in place, we can describe the transforms needed to support multiresolution editing. Recall that for multiresolution editing we want the difference between successive levels expressed with respect to a frame induced by the coarser level, i.e., the offsets are relative to the smoother level.

With each vertex v and each level $i > 0$ we associate a *detail vector*, $d^i(v) \in \mathbf{R}^3$. The

set d^i contains all detail vectors on level i, $d^i = \{d^i(v) \mid v \in V^i\}$. As indicated in Figure 7.3 the detail vectors are defined as

$$d^i = (F^i)^t\,(s^i - S\,s^{i-1}) = (F^i)^t\,(I - S\,H)\,s^i,$$

i.e., the detail vectors at level i record how much the points at level i differ from the result of subdividing the points at level $i-1$. This difference is then represented with respect to the local frame F^i to obtain coordinate independence.

Since detail vectors are sampled on the fine level mesh V^i, this transformation yields an overrepresentation in the spirit of the Burt-Adelson Laplacian pyramid [4]. The only difference is that the smoothing filters (Taubin) are not the dual of the subdivision filter (Loop). Theoretically, it would be possible to subsample the detail vectors and only record a detail per odd vertex of M^{i-1}. This is what happens in the wavelet transform. However, subsampling the details severely restricts the family of smoothing operators that can be used.

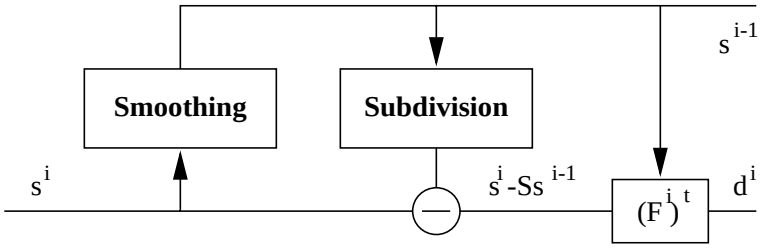

Figure 7.3: Wiring diagram of the multiresolution transform.

7.2 Algorithms and Implementation

Before we describe the algorithms in greater detail, let us recall the overall structure of the mesh editor (cf. Figure 7.1). The analysis stage builds a succession of coarser approximations to the surface, each with fewer control parameters. Details or offsets between successive levels are also computed. In general, the coarser approximations are not visible; only their control points are rendered. These control points give rise to a *virtual surface* with respect to which the remaining details are given. Figure 7.4 shows wireframe representations of

virtual surfaces corresponding to control points on levels 0, 1, and 2.

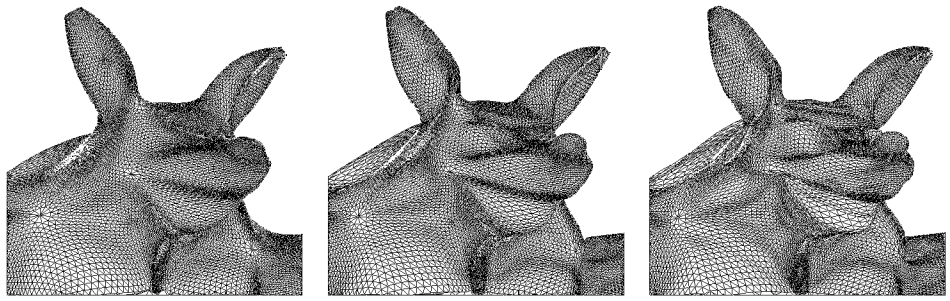

Figure 7.4: Wireframe renderings of virtual surfaces representing the first three levels of control points.

When an edit level is selected, the surface is represented internally as an approximation at this level, plus the set of all finer level details. The user can freely manipulate degrees of freedom at the edit level, while the finer level details remain unchanged relative to the coarser level. Meanwhile, the system will use the synthesis algorithm to render the modified edit level with all the finer details added in. In between edits, analysis enforces consistency on the internal representation of coarser levels and details (cf. Figure 7.5).

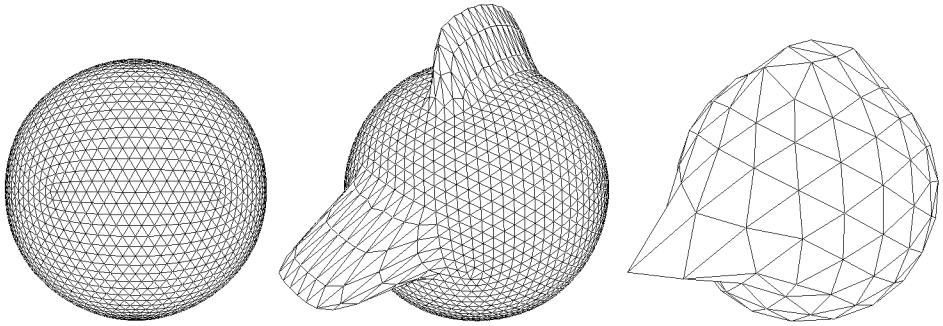

Figure 7.5: Analysis propagates the changes on finer levels to coarser levels, keeping the magnitude of details under control. Left: The initial mesh. Center: A simple edit on level 3. Right: The effect of the edit on level 2. A significant part of the change was absorbed by higher level details.

The basic algorithms `Analysis` and `Synthesis` are very simple, and we begin with their description.

Let $i = 0$ be the coarsest and $i = n$ the finest level with N vertices. For each vertex v and all levels i finer than the first level where the vertex v appears, there are storage locations $v.s[i]$ and $v.d[i]$, each with 3 floats. With this the total storage adds to $2 * 3 * (4N/3)$ floats.

In general, $v.s[i]$ holds $s^i(v)$ and $v.d[i]$ holds $d^i(v)$; temporarily, these locations can be used to store other quantities. The local frame is computed by calling $v.F(i)$.

Global analysis and synthesis are performed levelwise:

```
Analysis

  for i = n downto 1
     Analysis(i)
```

```
Synthesis

  for i = 1 to n
     Synthesis(i)
```

With the action at each level described by

```
Analysis(i)

  ∀v ∈ V^{i-1} : v.s[i-1] := smooth(v, i)
  ∀v ∈ V^i     : v.d[i] := v.F(i)^t * (v.s[i] - subd(v, i-1))
```

and

```
Synthesis(i)

  ∀v ∈ V^i : s.v[i] := v.F(i) * v.d[i] + subd(v, i-1)
```

Analysis computes points on the coarser level $i-1$ using smoothing (`smooth`), subdivides s^{i-1} (`subd`), and computes the detail vectors d^i (cf. Figure 7.3). Synthesis reconstructs level i by subdividing level $i-1$ and adding the details.

So far we have assumed that all levels are uniformly refined, i.e., all neighbors at all levels exist. Since time and storage costs grow exponentially with the number of levels, this approach is unsuitable for an interactive implementation. In the next sections we explain how these basic algorithms can be made memory and time efficient.

Adaptive and *local* versions of these generic algorithms (cf. Figure 7.1 for an overview of their use) are the key to these savings. The underlying idea is to use lazy evaluation and pruning based on thresholds. Three thresholds control this pruning: ϵ_A for adaptive analysis, ϵ_S for adaptive synthesis, and ϵ_R for adaptive rendering. To make lazy evaluation fast enough, several caches are maintained explicitly and the order of computations is carefully staged to avoid recomputation.

7.2.1 Adaptive Analysis

The generic version of analysis traverses entire levels of the hierarchy starting at some finest level. Recall that the purpose of analysis is to compute coarser approximations and detail offsets. In many regions of a mesh, for example, if it is flat, no significant details will be found. *Adaptive analysis* avoids the storage cost associated with detail vectors below some threshold ϵ_A by observing that small detail vectors imply that the finer level almost coincides with the subdivided coarser level. The storage savings are realized through *tree pruning.*

For this purpose we need an integer $v.\mathit{finest} := \max_i\{\|v.d[i]\| \geq \epsilon_A\}$. Initially $v.\mathit{finest} = n$ and the following precondition holds before calling `Analysis(i)`:

- The surface is uniformly subdivided to level i,
- $\forall v \in V^i \ : \ v.s[i] = s^i(v)$,
- $\forall v \in V^i \mid i < j \leq v.\mathit{finest} \ : \ v.d[j] = d^j(v)$.

Now `Analysis(i)` becomes:

```
Analysis(i)

  ∀v ∈ V^{i-1} : v.s[i-1] := smooth(v, i)
  ∀v ∈ V^i :
    v.d[i] := v.s[i] − subd(v, i-1)
    if v.finest > i or ||v.d[i]|| ≥ ε_A then
      v.d[i] := v.F(i)^t * v.d[i]
    else
      v.finest := i − 1
  Prune(i − 1)
```

Triangles that do not contain details above the threshold are unrefined:

```
Prune(i)

  ∀t ∈ T^i :  If all middle vertices m have m.finest = i − 1
              and all children are leaves, delete children.
```

This results in an adaptive mesh structure for the surface with $v.d[i] = d^i(v)$ for all $v \in V^i$, $i \leq v.\mathit{finest}$. Note that the resulting mesh is not restricted, i.e., two triangles that share a vertex can differ by more than one level. Initial analysis has to be followed by a synthesis pass which enforces restriction.

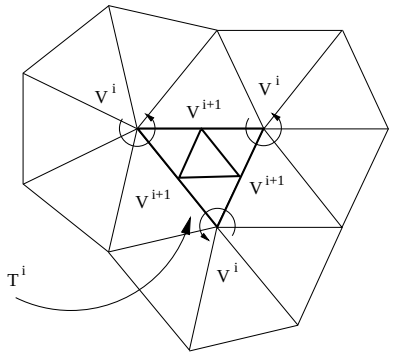

Figure 7.6: A restricted mesh: the center triangle is in T^i and its vertices in V^i. To subdivide it we need the 1-rings indicated by the circular arrows. If these are present the graph is restricted and we can compute s^{i+1} for all vertices and middle vertices of the center triangle.

7.2.2 Adaptive Synthesis

The main purpose of the general synthesis algorithm is to rebuild the finest level of a mesh from its hierarchical representation. Just as in the case of analysis we can realize savings from noticing that in flat regions, for example, little is gained from synthesis and one might as well save the time and storage associated with synthesis. This is the basic idea behind *adaptive synthesis*, which has two main purposes. First, ensure the mesh is restricted on each level, (cf. Figure 7.6). Second, refine triangles and recompute points until the mesh has reached a certain measure of local flatness compared against the threshold ϵ_S.

The algorithm recomputes the points $s^i(v)$ starting from the coarsest level. Not all neighbors needed in the subdivision stencil of a given point necessarily exist. Consequently, adaptive synthesis lazily creates all triangles needed for subdivision by temporarily refining their parents, then computes subdivision, and finally deletes the newly created triangles unless they are needed to satisfy the restriction criterion. The following precondition holds before entering `AdaptiveSynthesis`:

- $\forall t \in T^j \mid 0 \leq j \leq i$: t is restricted

- $\forall v \in V^j \mid 0 \leq j \leq v.depth$: $v.s[j] = s^j(v)$

where $v.depth := \max_i\{s^i(v)\text{has been recomputed}\}$.

```
AdaptiveSynthesis

  ∀v ∈ V^0 : v.depth := 0
  for i = 0 to n − 1
    temptri := {}
    ∀t ∈ T^i :
      current := {}
      Refine(t, i, true)
    ∀t ∈ temptri : if not t.restrict then
      Delete children of t
```

The list *temptri* serves as a cache holding triangles from levels $j < i$ which are temporarily refined. A triangle is appended to the list if it was refined to compute a value at a vertex. After processing level i these triangles are unrefined unless their $t.restrict$ flag is set, indicating that a temporarily created triangle was later found to be needed permanently to ensure restriction. Since triangles are appended to *temptri*, parents precede children. Deallocating the list tail first guarantees that all unnecessary triangles are erased.

The function `Refine`(t, i, dir) (see below) creates children of $t \in T^i$ and computes the values $Ss^i(v)$ for the vertices and middle vertices of t. The results are stored in $v.s[i+1]$. The boolean argument *dir* indicates whether the call was made directly or recursively.

```
Refine(t, i, dir)

  if t.leaf then  Create children for t
  ∀v ∈ t : if v.depth < i + 1 then
    GetRing(v, i)
    Update(v, i)
    ∀m ∈ N(v, i + 1, 1) :
      Update(m, i)
      if m.finest ≥ i + 1 then
        forced := true
  if dir and Flat(t) < ε_S and not forced then
    Delete children of t
  else
    ∀t ∈ current : t.restrict := true


Update(v, i)
  v.s[i + 1] := subd(v, i)
  v.depth := i + 1
  if v.finest ≥ i + 1 then
    v.s[i + 1] += v.F(i + 1) ∗ v.d[i + 1]
```

The condition $v.depth = i+1$ indicates whether an earlier call to `Refine` already recomputed $s^{i+1}(v)$. If not, call `GetRing`(v, i) and `Update`(v, i) to do so. In case a detail vector lives at v at level i ($v.finest \geq i + 1$) add it in. Next compute $s^{i+1}(m)$ for middle vertices on level $i+1$ around v ($m \in N(v, i + 1, 1)$, where $N(v, i, l)$ is the l-ring neighborhood of vertex v at level i). If m has to be calculated, compute `subd`(m, i) and add in the detail if it exists and record this fact in the flag *forced* which will prevent unrefinement later. At this point, all s^{i+1} have been recomputed for the vertices and middle vertices of t. Unrefine t and delete its children if `Refine` was called directly, the triangle is sufficiently flat, and none of the middle vertices contain details (i.e., *forced* = `false`). The list *current* functions as a cache holding triangles from level $i - 1$ which are temporarily refined to build a 1-ring around the vertices of t. If after processing all vertices and middle vertices of t it is decided that t will

remain refined, none of the coarser-level triangles from *current* can be unrefined without violating restriction. Thus $t.restrict$ is set for all of them. The function `Flat`(t) measures how close to planar the corners and edge middle vertices of t are.

Finally, `GetRing`(v, i) ensures that a complete ring of triangles on level i adjacent to the vertex v exists. Because triangles on level i are restricted triangles all triangles on level $i-1$ that contain v exist (precondition). At least one of them is refined, since otherwise there would be no reason to call `GetRing`(v, i). All other triangles could be leaves or temporarily refined. Any triangle that was already temporarily refined may become permanently refined to enforce restriction. Record such candidates in the *current* cache for fast access later.

```
GetRing(v, i)

  ∀t ∈ T^{i-1} with v ∈ t :
    if t.leaf then
      Refine(t, i − 1, false); temptri.append(t)
      t.restrict := false; t.temp := true
    if t.temp then
      current.append(t)
```

7.2.3 Local Synthesis

Even though the above algorithms are adaptive, they are still run everywhere. During an edit, however, not all of the surface changes. The most significant economy can be gained from performing analysis and synthesis only over submeshes which require it.

Assume the user edits level l and modifies the points $s^l(v)$ for $v \in V^{*l} \subset V^l$. This invalidates coarser level values s^i and d^i for certain subsets $V^{*i} \subset V^i$, $i \leq l$, and finer level points s^i for subsets $V^{*i} \subset V^i$ for $i > l$. Finer level detail vectors d^i for $i > l$ remain correct by definition. Recomputing the coarser levels is done by *local incremental analysis* described in Section 7.2.4; recomputing the finer level is done by *local synthesis* described in this section.

The set of vertices V^{*i} which are affected depends on the support of the subdivision scheme. If the support fits into an m-ring around the computed vertex, then all modified

vertices on level $i+1$ can be found recursively as

$$V^{*i+1} = \bigcup_{v \in V^{*i}} N(v, i+1, m).$$

We assume that $m = 2$ (Loop-like schemes) or $m = 3$ (Butterfly type schemes). We define the *subtriangulation* T^{*i} to be the subset of triangles of T^i with vertices in V^{*i}.

`LocalSynthesis` is only slightly modified from `AdaptiveSynthesis`: iteration starts at level l and iterates only over the submesh T^{*i}.

```
LocalSynthesis

  ∀v ∈ V^{*l} : v.depth := l
  for i = l to n − 1
    temptri := {}
    ∀t ∈ T^{*i} :
      current := {}
      Refine(t, i, true)
    ∀t ∈ temptri :
      if t.leaf and not t.restrict then
        Delete children of t
```

7.2.4 Local Incremental Analysis

After an edit on level l, *local incremental analysis* will recompute $s^i(v)$ and $d^i(v)$ locally for coarser level vertices ($i \leq l$) which are affected by the edit. As in the previous section, we assume that the user edited a set of vertices v on level l and call V^{*i} the set of vertices affected on level i. For a given vertex $v \in V^{*i}$, we define $R^{i-1}(v) \subset V^{i-1}$ to be the set of vertices on level $i-1$ affected by v through the smoothing operator H. The sets V^{*i} can now be defined recursively starting from level $i = l$ to $i = 0$:

$$V^{*i-1} = \bigcup_{v \in V^{*i}} R^{i-1}(v).$$

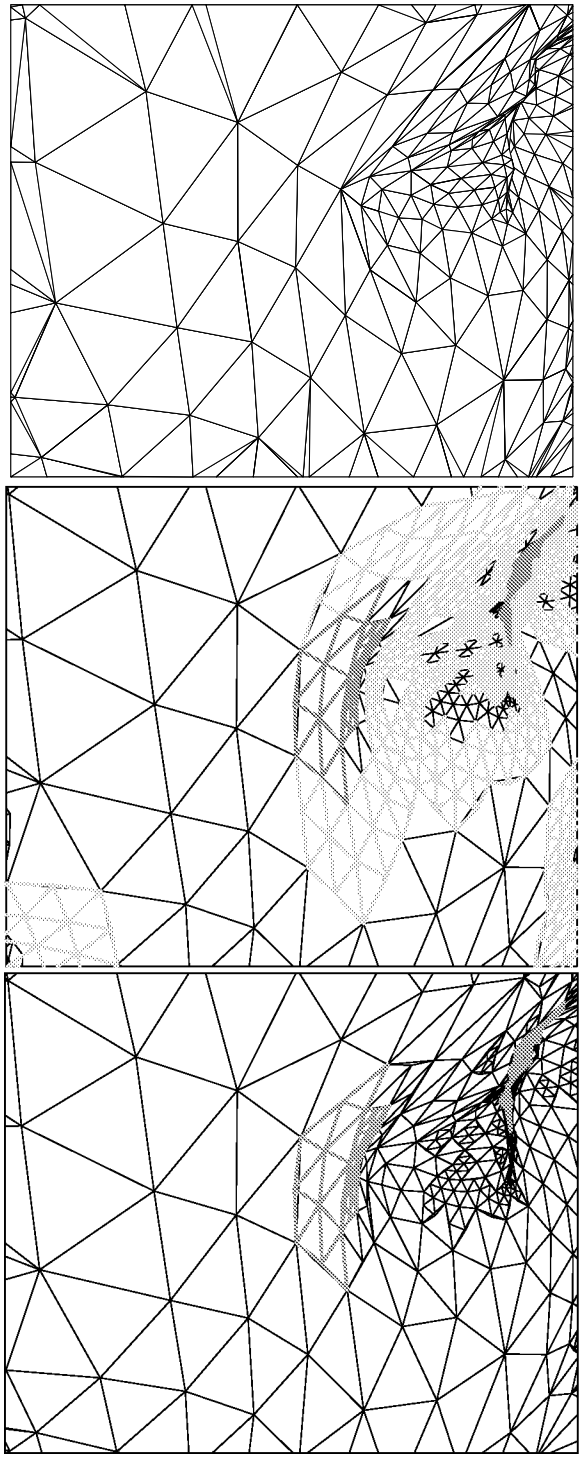

Figure 7.7: The mesh on the top is adaptively subdivided; middle image shows the mesh after subdivision but before any temporary triangles are removed; in the bottom image the mesh has all temporary triangles removed. Temporary triangles are shown in light gray; temporary triangles that were fixed due to restriction and subdivided triangles are shown in dark gray.

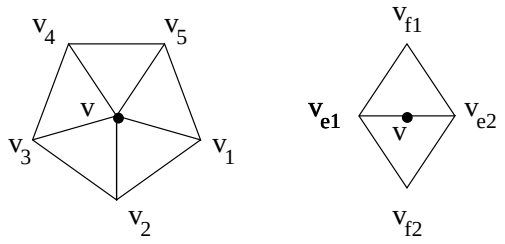

Figure 7.8: Sets of even vertices affected through smoothing by either an even v or odd m vertex.

The set $R^{i-1}(v)$ depends on the size of the smoothing stencil and whether v is even or odd (cf. Figure 7.8). If the smoothing filter is 1-ring, e.g., Gaussian, then $R^{i-1}(v) = \{v\}$ if v is even and $R^{i-1}(m) = \{v_{e1}, v_{e2}\}$ if m is odd. If the smoothing filter is 2-ring, e.g., Taubin, then $R^{i-1}(v) = \{v\} \cup \{v_m \mid 1 \leq m \leq k\}$ if v is even and $R^{i-1}(m) = \{v_{e1}, v_{e2}, v_{f1}, v_{f2}\}$ if v is odd. Because of restriction, these vertices always exist. For $v \in V^i$ and $v' \in R^{i-1}(v)$ we let $c(v, v')$ be the coefficient in the analysis stencil. Thus

$$(H\, s^i)(v') = \sum_{v | v' \in R^{i-1}(v)} c(v, v') s^i(v).$$

This could be implemented by running over the v' and each time computing the above sum. Instead we use the dual implementation, iterate over all v, accumulating (+=) the right amount to $s^i(v')$ for $v' \in R^{i-1}(v)$. In the case of a 2-ring Taubin smoother, the coefficients are given by

$$\begin{aligned} c(v, v) &= (1-\mu)\,(1-\lambda) + \mu\lambda/6 \\ c(v, v_k) &= \mu\,\lambda/6K \\ c(m, v_{e1}) &= ((1-\mu)\lambda + (1-\lambda)\mu + \mu\lambda/3)/K \\ c(m, v_{f1}) &= \mu\,\lambda/3K, \end{aligned}$$

where for each $c(v, v')$, K is the degree of v'.

The algorithm first copies the old points $s^i(v)$ for $v \in V^{*i}$ and $i \leq l$ into the storage location for the detail. Then it propagates the incremental changes of the modified points from level l to the coarser levels and adds them to the old points (saved in the detail

locations) to find the new points. Then it recomputes the detail vectors that depend on the modified points.

We assume that before the edit, the old points $s^l(v)$ for $v \in V^{*l}$ were saved in the detail locations. The algorithm starts out by building V^{*i-1} and saving the points $s^{i-1}(v)$ for $v \in V^{*i-1}$ in the detail locations. Then the changes resulting from the edit are propagated to level $i-1$. Finally, $S\, s^{i-1}$ is computed and used to update the detail vectors on level i.

```
LocalAnalysis(i)

  ∀v ∈ V^{*i} : ∀v' ∈ R^{i-1}(v) :
    V^{*i-1} ∪= {v'}
    v'.d[i-1] := v'.s[i-1]
  ∀v ∈ V^{*i} : ∀v' ∈ R^{i-1}(v) :
    v'.s[i-1] += c(v,v') * (v.s[i] - v.d[i])
  ∀v ∈ V^{*i-1} :
    v.d[i] = v.F(i)^t * (v.s[i] - subd(v, i-1))
    ∀m ∈ N(v,i,1) :
      m.d[i] = m.F(i)^t * (m.s[i] - subd(m, i-1))
```

Note that the odd points are actually computed twice. For the Loop scheme this is less expensive than trying to compute a predicate to avoid this. For Butterfly type schemes this is not true and one can avoid double computation by imposing an ordering on the triangles. The top level code is straightforward:

```
LocalAnalysis

  ∀v ∈ V^{*l} : v.d[l] := v.s[l]
  for i := l downto 0
    LocalAnalysis(i)
```

It is difficult to make incremental local analysis adaptive, as it is formulated purely in terms of vertices. It is, however, possible to adaptively clean up the triangles affected by the edit and (un)refine them if needed.

7.2.5 Adaptive Rendering

The *adaptive rendering* algorithm decides which triangles will be drawn depending on the rendering performance available and level of detail needed.

The algorithm uses a flag $t.draw$ which is initialized to `false`, but set to `true` as soon as the area corresponding to t is drawn. This can happen either when t itself gets drawn, or when a set of its descendents, which cover t, is drawn. The top level algorithm loops through the triangles starting from the level $n-1$. A triangle is always responsible for drawing its children, never itself, unless it is a coarsest-level triangle.

```
AdaptiveRender

  for i = n − 1 downto 0
    ∀t ∈ T^i : if not t.leaf then
      Render(t)
  ∀t ∈ T^0 : if not t.draw then
    displaylist.append(t)
```

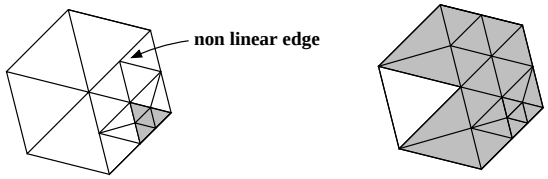

Figure 7.9: Adaptive rendering: On the left 6 triangles from level i, one has a covered child from level $i+1$, and one has a T-vertex. On the right the result from applying `Render` to all six.

The `Render`(t) routine decides whether the children of t have to be drawn or not (cf. Figure 7.9). It uses a function `edist`(m) which measures the distance between the point corresponding to the edge's middle vertex m, and the edge itself. In the case when any of the children of t are already drawn or any of its middle vertices are far enough from the plane of the triangle, the routine will draw the rest of the children and set the draw flag for all their vertices and t. It also might be necessary to draw a triangle if some of its middle vertices are drawn because the triangle on the other side decided to draw its children. To avoid cracks, the routine `cut`(t) will cut t into 2, 3, or 4 triangles depending on how many

middle vertices are drawn.

```
Render(t)

  if (∃ c ∈ t.child | c.draw = true
   or ∃ m ∈ t.mid_vertex | edist(m) > ε_D) then
    ∀c ∈ t.child :
      if not c.draw then
        displaylist.append(c)
        ∀v ∈ c : v.draw := true
    t.draw := true
  else if ∃ m ∈ t.mid_vertex | m.draw = true
    ∀t' ∈ cut(t) : displaylist.append(t')
    t.draw := true
```

7.2.6 Data Structures and Code

The main data structure in our implementation is a forest of triangular quadtrees. Neighborhood relations within a single quadtree can be resolved in the standard way by ascending the tree to the least common parent when attempting to find the neighbor across a given edge. Neighbor relations between adjacent trees are resolved explicitly at the level of a collection of roots, i.e., triangles of a coarsest level graph.

Finding neighborhoods. One can observe that the algorithms described above rely on a fast algorithm for finding neighborhoods of a set of vertices in the mesh (submeshes). An obvious solution can be described recursively: find a neighborhood $N_{m-1}(V_0)$ of size $m-1$; for each vertex of v N_{m-1}, insert all vertices of $N_1(v)$ into $N_m(V_0)$. This procedure requires time which is quadratic in the size of the neighborhood. Complexity is even worse if we use a representation of the mesh that does not allow us to determine if a triangle is already in the mesh in constant time. In addition to improving speed, we would like to solve this problem under several additional constraints:

- We avoid using markers associated with triangles to indicate whether a triangle is in the submesh that we are constructing or not. We take this approach for two main

reasons: it is useful to be able to maintain more than one submesh at the same time and it is desirable to avoid an extra cleanup step, which would reset markers to zero once the submesh is constructed.

- We would like to reduce as much as possible the number of searches for a 1-neighborhood and the number of times we test if a triangle is in the submesh, as well as the time required for each test.

In order to avoid markers we need a container that stores the triangles of the submesh and allows fast iteration and fast tests for existence of a given element.

Our solution is to maintain an explicit representation of the boundary of a submesh. In this way in order to extend N_{m-1} to N_m, we have to iterate only over the boundary which has average size proportional to $\sqrt{m}$. The size of the container is reduced, which also decreases the time for non-constant time operations with the container.

The algorithm is based on the following function, which, given a vertex v on the boundary, adds all triangles in $N_1(v)$ to the submesh. The vertex is specified as a triple (T, e, v) where T is a triangle already in submesh with edge e on the boundary, and v indicates which of the two vertices of e we are using.

Variables used in the algorithm are shown in Figure 7.10.

The function takes as an argument the boundary of the old submesh B and adds edges to the boundary of the new submesh $Bnew$. Containers representing boundaries are assumed to have operations *insert* and *erase*. The algorithm uses functions `Neighbor` and `link` to find neighbors and to create links to adjacent triangles.

```
ExpandMesh( T, e, v, B, Bnew)
prevTri:=T  prevEdge:=e
Neighbor:=v
currentTri  :=Neighbor(prevTri, prevEdge)
currentEdge:=edge of  currentTri  containing Neighbor which is not prevEdge

while  currentTri  exists  and ( currentTri , prevEdge) ∉ B
  nextTri:= Neighbor( currentTri ,currentEdge)
  nextEdge:=edge of nextTri containing Neighbor which is not currentEdge
  if ( currentTri ,currentEdge) ∉ B  then
    link( prevTri,  currentTri )
    Bnew.erase(prevTri,prevEdge)
    if nextTri exists  and (nextTri, currentEdge) ∈ B  then
      link(nextTri,  currentTri )
      Bnew.erase(nextTri,currentEdge)
    else
      Bnew.insert( currentTri ,currentEdge)
    endif
    outerTri  := Neighbor( currentTri ,outerEdge)
    if outerTri  exists  and (outerTri , outerEdge) ∈ B  then
      link( currentTri , outerTri )
      Bnew.erase(outerTri ,outerEdge)
    else
      Bnew.insert( currentTri ,outerEdge)
    endif
  prevTri:=  currentTri     prevEdge:=currentEdge
  currentTri  :=nextTri     currentEdge:=nextEdge
endwhile
```

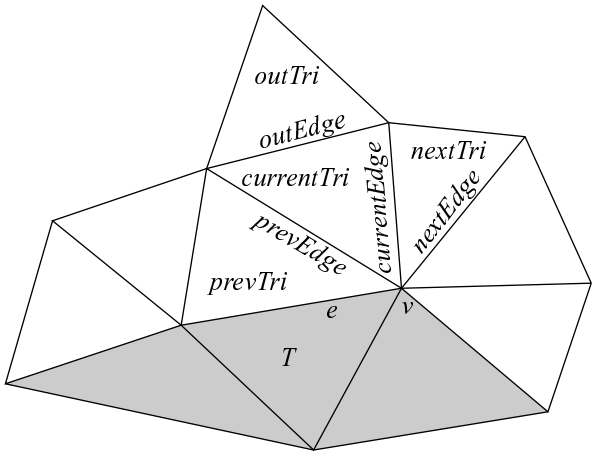

Figure 7.10: Notation of the function `ExpandMesh`.

We have used the C++ Standard Template Library implementation of sets based on red-black tree which has $log(m)$ time for search, insertion and deletion of elements to implement containers for edges.

7.3 Results

In this section we show some example images to demonstrate various features of our system and give performance measures.

Figure 7.11 shows two triangle mesh approximations of the Armadillo head and leg. Approximately the same number of triangles are used for both adaptive and uniform meshes. The meshes on the left were rendered uniformly, and the meshes on the right were rendered adaptively. (See also color plate 7.13).

Locally changing threshold parameters can be used to resolve an area of interest particularly well, while leaving the rest of the mesh at a coarse level. An example of this "lens" effect is demonstrated in Figure 7.12 around the right eye of the Mannequin head. (See also color plate 7.14).

We have measured the performance of our code on two platforms: an Indigo R10000, 175MHz with Solid Impact graphics, and a PentiumPro@200MHz with an Intergraph Intense 3D board. We used the Armadillo head as a test case. It has approximately 172000 triangles on 6 levels of subdivision. Display list creation took 2 seconds on the SGI and

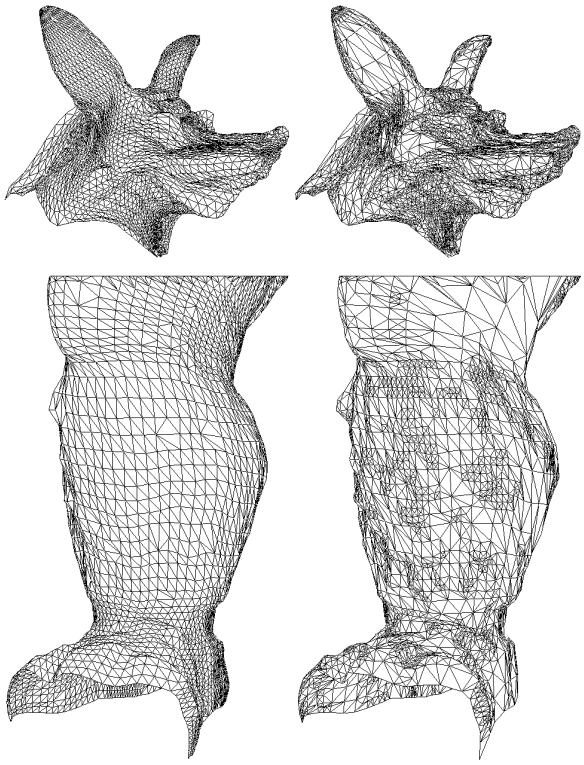

Figure 7.11: On the left are two meshes which are uniformly subdivided and consist of 11k (upper) and 9k (lower) triangles. On the right another pair of meshes mesh with approximately the same numbers of triangles. Upper and lower pairs of meshes are generated from the same original data but the right meshes were optimized through suitable choice of ϵ_S. See the color plates for a comparison between the two under shading.

3 seconds on the PC for the full model. We adjusted ϵ_R so that both machines rendered models at 5 frames per second. In the case of the SGI approximately 113,000 triangles were rendered at that rate. On the PC we achieved 5 frames per second when the rendering threshold had been raised enough so that an approximation consisting of 35000 polygons was used.

The other important performance number is the time it takes to recompute and re-render the region of the mesh which is changing as the user moves a set of control points. This submesh is rendered in immediate mode, while the rest of the surface continues to be rendered as a display list. Grabbing a submesh of 20-30 faces (a typical case) at level 0 added 250 mS of time per redraw, at level 1 it added 110 mS and at level 2 it added 30 mS in case of the SGI. The corresponding timings for the PC were 500 mS, 200 mS and 60 mS

respectively.

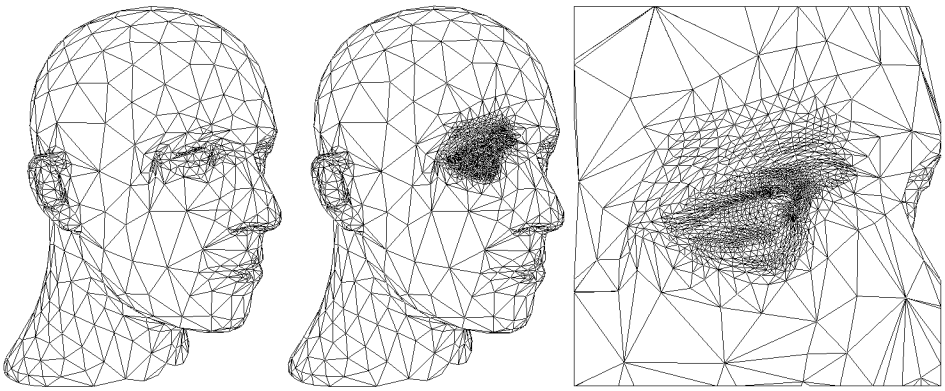

Figure 7.12: It is easy to change ϵ_S locally. Here a "lens" was applied to the right eye of the Mannequin head with decreasing ϵ_S to force very fine resolution of the mesh around the eye.

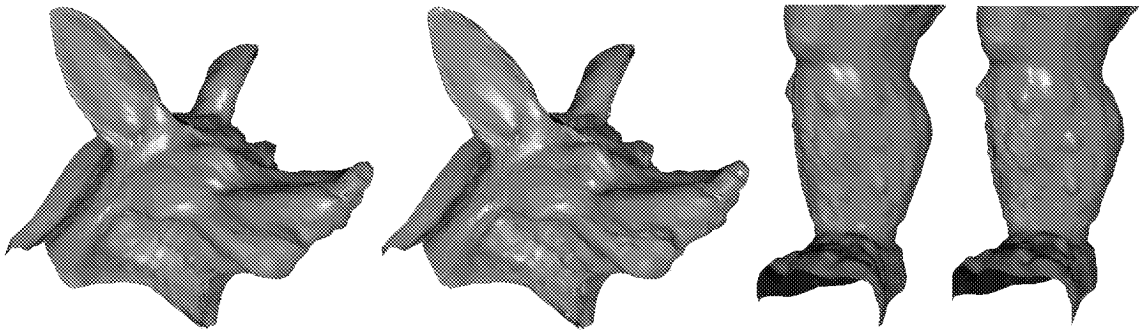

Figure 7.13: Shaded rendering (OpenGL) of the meshes in Figure 7.11.

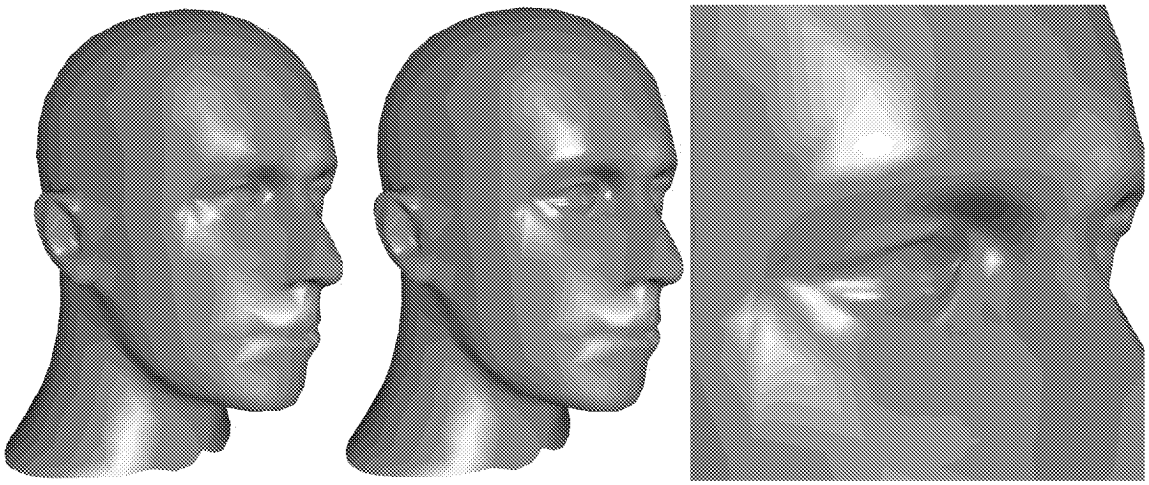

Figure 7.14: Shaded rendering (OpenGL) of the meshes in Figure 7.12.

Chapter 8 Conclusions and Future Work

8.1 Summary

8.1.1 Subdivision Theory

In Chapters 2 and 3 we develop a foundation for analysis of general subdivision schemes. Our results extend and put into a common context most previously known results on C^1-continuity of stationary subdivision surfaces.

We prove necessary and sufficient conditions for tangent plane continuity and C^1-continuity of subdivision. One of the important observations we can make is that for almost any C^1-continuous subdivision scheme a small generic perturbation of the coefficients of the scheme near an extraordinary vertex will not destroy C^1-continuity, as long as the coefficients for each subdivision rule sum up to 1.

We establish necessary and sufficient conditions for C^k-continuity of subdivision surfaces, relating C^k-continuity and reproduction of certain polynomials in a parameterization given by the characteristic map. These conditions show that requirements for C^k schemes are quite different from C^1 schemes: unless the surface is flat, a small perturbation of coefficients is likely to destroy C^1-continuity. Our results demonstrate both the potential and limitations of stationary subdivision methods: while C^k-subdivision schemes can be constructed for $k \geq 2$, the support of the schemes is likely to be large.

In Chapters 4 and 5 we establish explicit estimates on convergence rates of subdivision along with constructive sufficient conditions for C^1-continuity and used them to develop algorithms for verification of C^1-continuity. We implement these algorithms using interval arithmetic, which allows us to prove C^1-continuity for all valences simulataneously, and for parametric families of subdivision schemes.

8.1.2 Multiresolution Editing

We have built a scalable system for interactive multiresolution editing of arbitrary topology meshes. The user can either start from scratch or from a given fine detail mesh *with*

subdivision connectivity. We use smooth subdivision combined with details at each level as a uniform surface representation across scales and argue that this forms a natural connection between fine polygonal meshes and patches. Interactivity is obtained by building both local and adaptive variants of the basic analysis, synthesis, and rendering algorithms, which rely on fast lazy evaluation and tree pruning. The system allows interactive manipulation of meshes on a variety of hardware, with rendering quality adapting to the available resources while maintaining acceptable frame rates.

8.2 Future Work

8.2.1 Subdivision

It is immediately obvious how to extend our constructions in several directions.

Different topological rules. We have considered only schemes defined using the simplest topological subdivision rule; schemes using different types of topological rules are also of considerable interest. A topological rule for a stationary scheme is typically based on a tiling of a plane that admits a refinement procedure that produces a similar tiling from the original one. If we would like to use a tiling consisting of identical regular polygons, only few cases are possible: triangular tiling (this is the tiling that we were using), quadrilateral and hexagonal tiling. It does not make a lot of sense to consider refinements that create more than 4 polygons per each polygon of the initial tiling. If we restrict ourselves to regular tilings and dyadic refinements, not that many topological rules are possible. Excluding rather arcane, but possible case of honeycomb refinement, we have 3 main cases: midpoint refinement of triangular and quadrilateral grids and dual refinement of the quadrilateral grid (Doo-Sabin-type rule), as shown in Figure 8.1.

In each case we can reduce the scheme to an equivalent scheme defined on simplicial complexes as explained in Appendix A. However, while this is acceptable for theoretical purposes, analysis of specific schemes would be more difficult than it is necessary if we adopt this approach. Instead, we might develop a similar formalism for each refinment type.

Generalization of our formalism to the refinement of quadrilaterals of Catmull-Clark type is straightforward: vertices of refined complexes still form a hierarchy of nested sets; one case can be reduced to the other by splitting each quadrilateral into two. The only

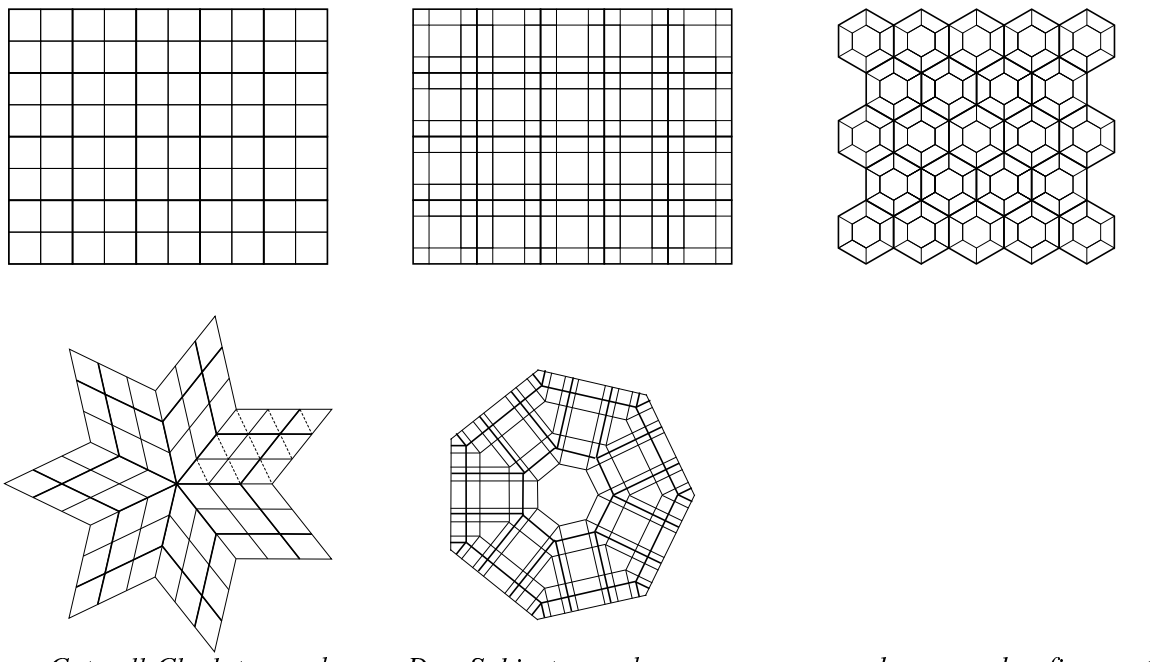

Figure 8.1: Several different topological rules on regular grids and near an extraordinary vertex of valence 7.

difference between these cases is the number of symmetries in the group of automorphisms of regular complexes, and hence the number of constraints on symmetric schemes.

Doo-Sabin-type schemes are different from triangle-based schemes in a more fundamental way. The vertices of the refined complexes do not form a hierarchy, but the polygons do. Thus it would be more natural to define neighborhoods on the dual complexes.

Boundary case. All derivations in Chapter 3 were performed for an extraordinary vertex in the interior of the surface. The same methods can be used to consider the vertices on the boundary; although Schweitzer [59] applied Reif's conditions to vertices on the boundary, a careful theoretical analysis was never performed in that case. In the case of C^k continuity, the fact that the classifications of singularities of smooth functions are different for the boundary case suggests that there might be subtle differences in the conditions.

Convergence estimates in the general case. In Chapter 4 we made some simplifying assumptions on factorizations of Laurent polynomials in our derivations of convergence estimates. Convergence estimates using matrix schemes can be derived without these additional assumptions.

Better convergence estimates. As already mentioned in Section 6.3, the estimates that we have obtained for schemes with negative coefficients are unnecessarily pessimistic. A simple way to improve these estimates is to subtract suitably chosen closed-form functions that the scheme is known to reproduce (quadratic in the simplest case) from the coordinate control points and perform the estimates only on the residual term. It is likely that some improvement can be achieved for most schemes.

Single ring schemes. A more difficult problem that appears to be within close reach is sufficiently complete description (in terms of coefficients) of all possible C^1-continuous symmetric single ring schemes based either on a triangular or quadrilateral topological rule. Such a description would allow us to search for small-support schemes satisfying certain requirements.

While the polynomial degree estimate leads to the conclusion that C^k-continuous polynomial schemes have large support, it does not require all other schemes to have large support. Intuitively, it appears that polynomial schemes have maximal smoothness among

all schemes with given support. A proof of this fact in the one-dimensional case can be found in [6]. We are not aware of a proof in the two-dimensional case; a theorem like this would finally answer the question of the minimal possible support for a C^2 scheme.

Limitations of stationary subdivision make it desirable to extend the theory to some classes of non-stationary schemes. However, in the case of non-stationary schemes, smoothness analysis alone is unlikely to be sufficient. The remarkable fact that C^k-continuity of subdivision surfaces is related to polynomial reproduction also leads to a particular dependence between global (fairness) and local (smoothness) properties. It is unlikely to be the case for most non-stationary schemes, so it might be necessary to consider fairness directly.

All smoothness criteria that we have described reduce verification of smoothness of all surfaces generated by a subdivision rule to verification of certain properties of the eigenbasis functions. The eigenbasis functions are still defined as a limit of the subdivision process; in some important cases we found a way to verify the properties of the limit function using a sufficiently close linear approximation. It would be desirable to have sufficiently general smoothness criteria formulated entirely in terms of the coefficients of the scheme (0-th linear approximation).

8.2.2 Multiresolution Representations and Editing

There are several avenues for future research:

- Multiresolution transforms readily connect with compression. We want to be able to store the models in a compressed format and use progressive transmission.

- Features such as creases, corners, and tension controls can easily be added into our system and expand the users' editing toolbox.

- Presently no real time fairing techniques, which lead to higher quality coarse levels, exist.

- In our system coarse level edits can only be made by dragging coarse level vertices. The locations of the vertices control the on coarse levels cannot be controlled directly. Ideally the user should be able to dynamically choose control points and their areas of influence (direct manipulation).

- The system allows topological edits on the coarsest level. Algorithms that allow topological edits on all levels are needed.

- An important area of research relevant for this work is generation of meshes with subdivision connectivity from scanned data or from existing models in other representations.

Appendix A Reduction of Subdivision of Polyhedra to Subdivision of Complexes

In this thesis we have considered schemes defined on simplicial complexes; most theoretical constructions and algorithms are more transparent for this type of schemes. For a variety of reasons some of the popular types of schemes are defined on general polyhedral meshes (Catmull-Clark, Doo-Sabin). With minor modifications, constructions of Chapter 2 also apply to these schemes. Rather than redoing all derivations for each type of refinement rules, we can show that schemes using these refinement rules are equivalent to other schemes defined on simplicial complexes. This can be achieved using tagged complexes.

The goal of this reduction is not to propose a new way to implement Catmull-Clark or Doo-Sabin subdivision, but to demonstrate that the theoretical results of Chapter 3 equally apply to schemes of other types. To simplify the exposition, we assume that all polyhedra are closed.

Catmull-Clark refinement. Refinement rules of this type can be defined on polyhedra in the same way as we defined refinement of simplicial complexes. In addition to inserting vertices in the middle of each edge, we also insert a vertex at the barycenter of each polygonal face. For any subdivision scheme using subdivision rules of this type defined on a polyhedron P, we construct a subdivision scheme defined on a suitably simplicial complex $\Sigma(P)$, which produces the same limit surfaces.

Subdivide a polyhedron P once to obtain P^1; after this, no extraordinary vertices are adjacent, all faces of the subdivided complex are quadrilateral, and each face has no more than two extraordinary vertices. Consider one of the quadrilaterals (v_1, v_2, v_3, v_4). Suppose v_1 is extraordinary. If the quadrilateral has two extraordinary vertices, the other can be only v_3. We split the quadrilateral along the diagonal (v_2, v_4) into two triangles; as a result, we obtain a simplicial complex $\Sigma(P)$. In addition, we tag all edges of the resulting simplicial complex $\Sigma(P)$ that are also edges of P^1. The process is shown in Figure A.1.

Finally, we define a rule to propagate the tags from $\Sigma(P)$ to $D(\Sigma(P))$. Note that each

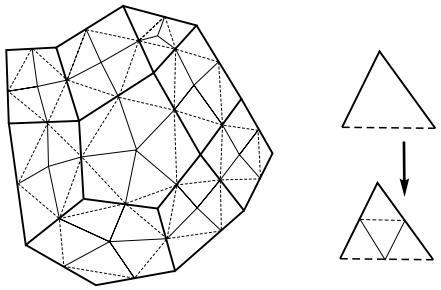

Figure A.1: Reducing refinement rules of the Catmull-Clark scheme to simplicial complex refinement.

triangle in $\Sigma(P)$ has exactly two tagged edges. a new edge of the refined complex $D(\Sigma(P))$ (we use simplicial refinement defined in Chapter 2) is tagged if it connects a midpoint of a tagged edge with the midpoint of an edge that is not tagged.

Now the standard Catmull-Clark rules [5] (vertex, edge and face rule) are used as follows: the vertex rule is used to compute the values $p^{j+1}(v)$ at vertices $v \in V^j$, the edge rules are used to compute midpoints of tagged edges, and the face rule is used to compute the midpoint of edges that are not tagged.

We define the set of admissible isomorphisms G as the set of all isomorphisms that map tagged edges to tagged edges; it is easy to show that it satisfies our requirements for admissible sets (Section 2.2.1) and that the simplicial complex equivalent of the Catmull-Clark scheme is G-invariant and stationary.

Doo-Sabin scheme. Because the refinement of the type used by the Doo-Sabin scheme removes vertices from the polyhedron, it is more difficult to reduce it to simplicial refinement. We show how to reduce it to the Catmull-Clark refinement with vertex tags. Then it can be reduced to simplicial refinement using edge tags as above.

Note that defining the domain for Doo-Sabin surfaces is less straightforward than for simplicial refinement or Catmull-Clark refinement. One possible way of doing this is to introduce additional vertices into the polyhedra generated by the scheme. For each polygonal face, we add the center of the face and connect it to all vertices of the face (Figure A.2a). Then we eliminate all the edges of the original polyhedron, retaining only the edges introduced on the previous level (Figure A.2a). Initially we tag all centers. Then we propagate vertex tags as shown in the figure.

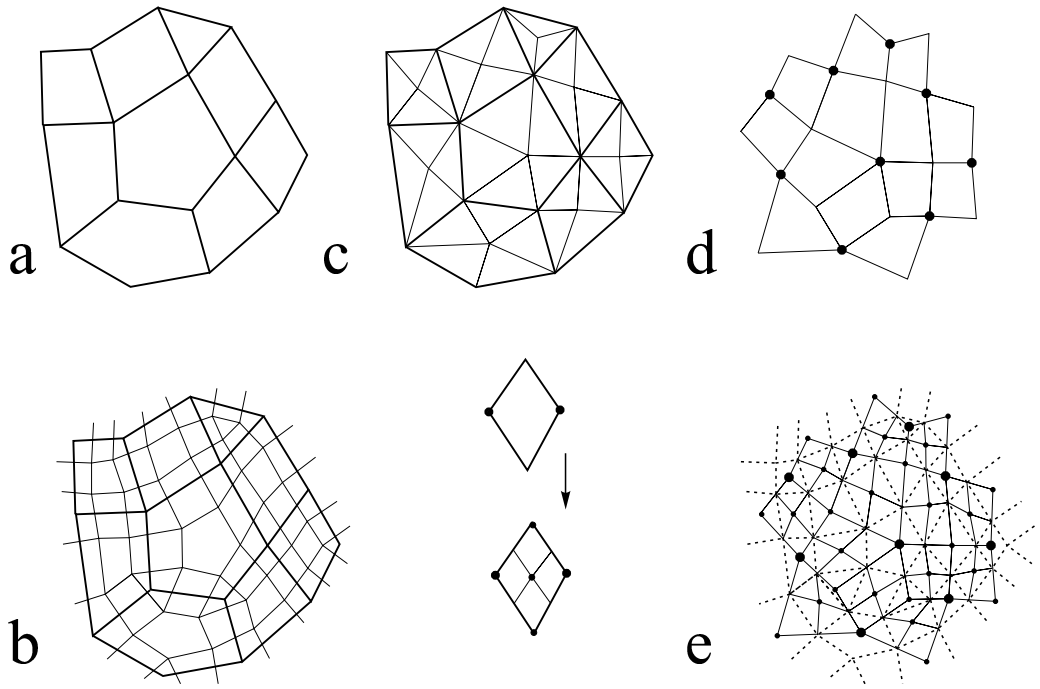

Figure A.2: Reducing refinement rules of the Doo-Sabin scheme to the Catmull-Clark refinement. a. The original polyhedron. b. One step of the Doo-Sabin subdivision. c. The original polyhedron with the centers of the faces added. d. The polyhedron subdivided using the Catmull-Clark refinement, with the edges of the polyhedron obtained using Doo-Sabin refinement (b) shown as dashed lines. e. The polyhedron converted to a simplicial complex. The picture in the center shows how vertex tags are propagated. Each quadrilateral has two tagged vertices; in the subdivided quadrilateral all old vertices are tagged, all new vertices are not tagged.

The new mesh can be subdivided using the Catmull-Clark refinement. Note that all tagged vertices always correspond to the centers of the faces of polyhedra that we would obtain using the Doo-Sabin refinement.

Clearly, the values at the centers on subdivision level $j+1$ can be computed from the values on level j. These formulas give us vertex rules for tagged and untagged vertices; the rule for tagged vertices is the rule for centers of faces on level $j+1$ that correspond to faces of level j; the rule for untagged vertices is the rule for centers of faces that correspond to new faces on level $j+1$ created for vertices. The vertex rules are derived from the formulas for the centers of new faces. The edge rules are the standard Doo-Sabin rules. The tagged vertex (exactly one vertex of each edge is tagged) is used to determine which values to use in the rule.

Appendix B Classification of Quasihomogeneous Polynomials

The conditions provided by Lemmas 3.16 and 3.20 are not explicit in one aspect: they use implicitly defined sets of polynomials $\mathbf{P}(p,q)$. If a set $\mathbf{P}(p,q)$ consists of more than one polynomial, it is possible to enumerate all polynomials in this set as points on a line with a rational slope in the Newton plane. It would be of some interest however, to find classes of polynomials that can be reduced to each other with suitable coordinate transformations.

Polynomials in these sets play an important role in singularity theory. In this section we will briefly touch on the subject; the nature of the relation between quasihomogeneous functions and eigenbasis functions of subdivision requires further study.

First we make the connection between functions satisfying scaling relations and quasihomogeneous functions explicit.

Definition B.1. *A function satisfying relation*

$$f(\lambda^{q_1}\xi_1, \lambda^{q_2}\xi_2) = \lambda f(\xi_1, \xi_2) \tag{B.1}$$

where $q_1 + q_2 = 1$, is called quasihomogeneous function of degree 1 with exponents q_1, q_2.

It is clear that whenever the set $P(p,q)$ is not spanned by one monomial, there is a non-zero pair of integers p_1, p_2 such that $\lambda_1^{p_1}\lambda_2^{p_2} = 1$. Therefore, all scaling factors in the corresponding relation can be expressed in terms of $\lambda_1^p\lambda_2^q$, resulting in the relation of the type (B.1). The exponents q_1 and q_2 in this case will be positive and rational, which means that any smooth quasihomogeneous function satisfying (B.1) has to be a polynomial.

Thus, the set of quasihomogeneous functions with given positive rational exponents is exactly one of the sets $P(p,q)$.

With each monomial of a quasihomogeneous polynomial, we can associate a pair of integer points in the plane, similar to the way it was done in Figure 3.12.

All such points (i, j) are on the line $q_1 i + q_2 j = 1$. Monomials corresponding to these points are called diagonal. Monomials below the line are called lower; monomials above the line are called upper.

An important quantity characterizing quasihomogeneous functions is *intrinsic modality.* To define intrinsic modality, we first define the local algebra of a quasihomogeneous function f. This algebra is the factor algebra of all formal power series with respect to the ideal generated by the partial derivatives of f.

The local algebra has a basis of monomials, and the number of upper, lower and diagonal monomials in the basis does not depend on the choice of the basis.

The *intrinsic* or *inner* modality is the number of upper and diagonal monomials of any basis of the local algebra. There is a simple geometric method for calculating modality on the exponent plane.

Any quasihomogeneous polynomial of given type can be represented in the form $f_0 + \sum c_k e_k$, where f_0 is a fixed quasihomogeneous polynomial of the same type, e_k are diagonal monomials of the basis of the local algebra and c_k are some coefficients.

The sets $\mathbf{P}(p, q)$ can be specified by presenting the diagonal monomials of the basis of the local algebra and one quasihomogeneous polynomial with given exponents.

The equivalence of quasihomogeneous functions is given by the group of quasihomogeneous diffeomorphisms. The classification of the quasihomogeneous functions of intrinsic modality 0 up to equivalence is particularly simple: all such functions are listed in the table below (up to renaming of variables):

Type	Normal Form	q_1	q_2
A_k	$ax^{k+1} + by^1$	$k+1$	$\frac{1}{2}$
D_k	$ax^2y + by^{k-1}$	$\frac{k-2}{2k-2}$	$\frac{2}{2k-2}$
E_6	$ax^3 + by^4$	$\frac{1}{3}$	$\frac{1}{4}$
E_7	$ax^3 + bxy^3$	$\frac{1}{3}$	$\frac{2}{9}$
E_8	$ax^3 + by^5$	$\frac{1}{3}$	$\frac{1}{5}$

The same five classes occur in various classifications, such as classifications of simple Lie algebras, braid groups and regular polyhedra.

Many references to the singularity theory literature can be found in Arnold [1].

Bibliography

[1] V. I. Arnold, S. M. Gusein-Zade, and A. N. Varchenko. *Singularities of differentiable maps*, volume 1. Birkhauser, 1985.

[2] A. A. Ball and D. J. T. Storry. Conditions for tangent plane continuity over recursively generated B-spline surfaces. *ACM Transactions on Graphics*, 7(2):83–102, 1988.

[3] B. Barsky. *Computer Graphics and Geometric Modeling Using Beta-splines*. Springer Verlag, 1988.

[4] P. J. Burt and E. H. Adelson. Laplacian pyramid as a compact image code. *IEEE Trans. Commun.*, 31(4):532–540, 1983.

[5] E. Catmull and J. Clark. Recursively generated B-spline surfaces on arbitrary topological meshes. *Computer Aided Design*, 10(6):350–355, 1978.

[6] A. S. Cavaretta, W. Dahmen, and C. A. Micchelli. Stationary subdivision. *Memoirs Amer. Math. Soc.*, 93(453), 1991.

[7] A. Certain, J. Popović, T. DeRose, T. Duchamp, D. Salesin, and W. Stuetzle. Interactive multiresolution surface viewing. In H. Rushmeier, editor, *SIGGRAPH 96 Conference Proceedings*, Annual Conference Series, pages 91–98. ACM SIGGRAPH, Addison Wesley, Aug. 1996. held in New Orleans, Louisiana, 04-09 August 1996.

[8] W. Dahmen, C. A. Micchelli, and H.-P. Seidel. Blossoming begets B-splines bases built better by B-patches. *Mathematics of Computation*, 59(199):97–115, July 1992.

[9] G. Deslauriers and S. Dubuc. Interpolation dyadique. In *Fractals, dimensions non entières et applications*, pages 44–55. Masson, Paris, 1987.

[10] G. Deslauriers and S. Dubuc. Symmetric iterative interpolation processes. *Constr. Approx.*, 5(1):49–68, 1989.

[11] D. L. Donoho. Interpolating wavelet transforms. Preprint, Department of Statistics, Stanford University, 1992.

[12] D. Doo. A subdivision algorithm for smoothing down irregularly shaped polyhedrons. In *Proceedings on Interactive Techniques in Computer Aided Design*, pages 157–165, Bologna, 1978.

[13] D. Doo and M. Sabin. Analysis of the behaviour of recursive division surfaces near extraordinary points. *Computer Aided Design*, 10(6):356–360, 1978.

[14] S. Dubuc. Interpolation through an iterative scheme. *J. Math. Anal. Appl.*, 114:185–204, 1986.

[15] T. Duchamp, A. Certain, A. DeRose, and W. Stuetzle. Hierarchical computation of PL harmonic embeddings. Technical report, University of Washington, 1997.

[16] N. Dyn, J. A. Gregory, and D. Levin. A four-point interpolatory subdivision scheme for curve design. *Computer Aided Geometric Design*, 4:257–268, 1987.

[17] N. Dyn, S. Hed, and D. Levin. Subdivision schemes for surface interpolation. In A. C. et al., editor, *Workshop in Computational Geometry*, pages 97–118. World Scientific, 1993.

[18] N. Dyn and D. Levin. Interpolating subdivision schemes for the generation of curves and surfaces. In *Multivariate approximation and interpolation (Duisburg, 1989)*, volume 94 of *Internat. Ser. Numer. Math.*, pages 91–106, 1989.

[19] N. Dyn and D. Levin. The subdivision experience. In P. Laurent, A. L. Méhauté, and L. L. Schumaker, editors, *Wavelets, Images and Surface Fitting*, pages 229–244. A. K. Peters, Wellesley, MA, 1994.

[20] N. Dyn, D. Levin, and J. A. Gregory. A butterfly subdivision scheme for surface interpolation with tension control. *ACM Transactions on Graphics*, 9(2):160–169, April 1990.

[21] N. Dyn, D. Levin, and C. A. Micchelli. Using parameters to increase smoothness of curves and surfaces generated by subdivision. *Computer Aided Geometric Design*, 7:129–140, 1990.

[22] M. Eck, T. DeRose, T. Duchamp, H. Hoppe, M. Lounsbery, and W. Stuetzle. Multiresolution analysis of arbitrary meshes. In *Computer Graphics Proceedings*, Annual Conference Series, pages 173–182. ACM Siggraph, 1995.

[23] A. Finkelstein and D. H. Salesin. Multiresolution curves. In *Computer Graphics* Proceedings, Annual Conference Series, pages 261–268. Siggraph, July 1994.

[24] D. Forsey and D. Wong. Multiresolution surface reconstruction for hierarchical B-splines. Technical report, University of British Columbia, 1995.

[25] D. R. Forsey and R. H. Bartels. Hierarchical B-spline refinement. *Computer Graphics (SIGGRAPH '88 Proceedings)*, 22(4):205–212, August 1988. held in Atlanta, Georgia; 1-5 August 1988.

[26] P. J. Giblin. *Graphs, Surfaces and Homology.* Chapman and Hall, London, 1981.

[27] S. J. Gortler and M. F. Cohen. Hierarchical and variational geometric modeling with wavelets. In *Proceedings Symposium on Interactive 3D Graphics.* Siggraph, May 1995.

[28] A. Habib and J. Warren. Edge and vertex insertion for a class of subdivision surfaces. Preprint. Computer Science, Rice University, 1996.

[29] M. Halstead, M. Kass, and T. DeRose. Efficient, fair interpolation using Catmull-Clark surfaces. In *Computer Graphics Proceedings*, Annual Conference Series, pages 35–44. ACM Siggraph, 1993.

[30] G. H. Hardy and E. M. Wright. *An Introduction to the Theory of Numbers.* Oxford at the Clarendon Press, Oxford, 1938.

[31] H. Hoppe. Progressive meshes. In H. Rushmeier, editor, *SIGGRAPH 96 Conference Proceedings*, Annual Conference Series, pages 99–108. ACM SIGGRAPH, Addison Wesley, August 1996. held in New Orleans, Louisiana, 04-09 August 1996.

[32] H. Hoppe, T. DeRose, T. Duchamp, M. Halstead, H. Jin, J. McDonald, J. Schweitzer, and W. Stuetzle. Piecewise smooth surface reconsruction. In *Computer Graphics Proceedings*, Annual Conference Series, pages 295–302. ACM Siggraph, 1994.

[33] H. Hoppe, T. DeRose, T. Duchamp, J. McDonald, and W. Stuetzle. Mesh optimization. In J. T. Kajiya, editor, *Computer Graphics (SIGGRAPH '93 Proceedings)*, volume 27, pages 19–26, August 1993.

[34] O. Knüppel. Profil – programmer's runtime optimized fast interval library. Technical report, Technische Universität Hamburg-Hamburg, Technische Informatik III, 1993. preprint.

[35] L. Kobbelt. Interpolatory subdivision on open quadrilateral nets with arbitrary topology. In *Proceedings of Eurographics 96*, Computer Graphics Forum, pages 409–420, 1996.

[36] L. Kobbelt. Interpolatory subdivision on open quadrilateral nets with arbitrary topology. *Computer Graphics Forum*, 15(3), 1996. Eurographics '96 Conference issue.

[37] V. Krishnamurthy and M. Levoy. Fitting smooth surfaces to dense polygon meshes. In H. Rushmeier, editor, *SIGGRAPH 96 Conference Proceedings*, Annual Conference Series, pages 313–324. ACM SIGGRAPH, Addison Wesley, August 1996. held in New Orleans, Louisiana, 04-09 August 1996.

[38] T. Kurihara. Interactive surface design using recursive subdivision. In *Proceedings of Communicating with Virtual Worlds*. Springer Verlag, June 1993.

[39] A. G. Kušnirenko. A criterion for the existence of a nondegenerate quasihomogeneous function with given weights. *Uspehi Mat. Nauk*, 32(3 (195)):169–170, 1977.

[40] C. Loop. Smooth subdivision surfaces based on triangles. Master's thesis, University of Utah, Department of Mathematics, 1987.

[41] C. Loop. Smooth spline surfaces over irregular meshes. In *Computer Graphics Proceedings*, Annual Conference Series, pages 303–310. ACM Siggraph, 1994.

[42] M. Lounsbery, T. DeRose, and J. Warren. Multiresolution analysis for surfaces of arbitrary topological type. *Transactions on Graphics*, 16(1):34–73, January 1997.

[43] R. Moore. *Interval arithmetic and automated error analysis in digital computing*. PhD thesis, Stanford University, 1962.

[44] R. E. Moore. *Methods and Applications Of Interval Analysis*. SIAM, Philadelphia, 1979.

[45] A. H. Nasri. Surface interpolation on irregular networks with normal conditions. *Computer Aided Geometric Design*, 8:89–96, 1991.

[46] K. Ouchi. `Real/Expr`: Implementation of an exact computation package. Master's thesis, New York University, Department of Computer Science, 1997.

[47] J. Peters. C^1 surface splines. *SIAM J. Numer. Anal.*, 32(2):645–666, 1995.

[48] J. Peters. Curvature continuous spline surfaces over irregular meshes. *Computer Aided Geometric Design*, to appear.

[49] J. Peters and U. Reif. Analysis of generalized B-spline subdivision algorithms. *SIAM Jornal of Numerical Analysis*, 1997.

[50] H. Prautzsch. Analysis of C^k-subdivision surfaces at extraordianry points. Preprint. Presented at Oberwolfach, June, 1995, 1995.

[51] H. Prautzsch and U. Reif. Necessary conditions for subdivision surfaces. 1996.

[52] K. Pulli and M. Lounsbery. Hierarchical editing and rendering of subdivision surfaces. Technical Report UW-CSE-97-04-07, Dept. of CS&E, University of Washington, Seattle, WA, 1997.

[53] U. Reif. A degree estimate for polynomial subdivision surface of higher regularity. Technical report, Universität Stuttgart, Mathematisches Institut A, 1995. preprint.

[54] U. Reif. Some new results on subdivision algorithms for meshes of arbitrary topology. In C. K. Chui and L. Schumaker, editors, *Approximation Theory VIII*, volume 2, pages 367–374. World Scientific, Singapore, 1995.

[55] U. Reif. A unified approach to subdivision algorithms near extraordinary points. *Computer Aided Geometric Design*, 12:153–174, 1995.

[56] U. Reif. A degree estimate for polynomial subdivision surfaces of higher regularity. *Proc. Amer. Math. Soc.*, 124:2167–2174, 1996.

[57] M. Sabin. *The Use of Piecewise Forms for the Numerical Representation of Shape*. PhD thesis, Hungarian Academy of Sciences, Budapest, 1976.

[58] P. Schröder and W. Sweldens. Spherical wavelets: Efficiently representing functions on the sphere. In *Computer Graphics Proceedings*, Annual Conference Series, pages 161–172. ACM Siggraph, 1995.

[59] J. E. Schweitzer. *Analysis and Application of Subdivision Surfaces*. PhD thesis, University of Washington, Seattle, 1996.

[60] J. M. Snyder. *Generative Modeling for Computer Graphics and CAD*. Academic Press, 1992.

[61] G. Taubin. A signal processing approach to fair surface design. In R. Cook, editor, *SIGGRAPH 95 Conference Proceedings*, Annual Conference Series, pages 351–358. ACM SIGGRAPH, Addison Wesley, August 1995.

[62] J. Warren. Binary subdivision schemes for functions over irregular knot sequences. In *Mathematical methods for curves and surfaces (Ulvik, 1994)*, pages 543–562. Vanderbilt Univ. Press, Nashville, TN, 1995.

[63] J. Warren. Subdivision methods for geometric design. Unpublished manuscript, November 1995.

[64] W. Welch and A. Witkin. Variational surface modeling. In E. E. Catmull, editor, *Computer Graphics (SIGGRAPH '92 Proceedings)*, volume 26, pages 157–166, July 1992. held in Chicago, Illinois; 26-31 July 1992.

[65] C. Yap and T. Dubé. The exact computation paradigm. In D. Z. Du and F. K. Hwang, editors, *Computing in Euclidean Geometry*, pages 452–486. World Scientific Press, 1995.

[66] D. Zorin, P. Schröder, and W. Sweldens. Interpolating subdivision for meshes with arbitrary topology. *Computer Graphics Proceedings (SIGGRAPH 96)*, pages 189–192, 1996.

Index

C^1-continuity, 64
  conditions, 99
  criterion, 95
C^2-continuity
  conditions, 99
C^k-continuity
  criterion, 95, 98

affine invariance, 32
analysis, 238
  adaptive, 240
  incremental, 245
arbitrary valence
  Modified Butterfly scheme, 212

basis function, 41
Butterfly scheme, 181
  C^1-continuity, 199
  characteristic maps, 200
  convergence rate, 146, 210
  definition, 196
  modified, 161
  subdivision matrix, 197
    eigenvalues, 198

category
  of complexes, 29
Catmull-Clark scheme, 30, 181, 258, 263
characteristic map, 93, 96, 126, 132
  definition, 90
  injectivity, 133, 137
  linear approximation, 133, 136, 137
commutation formula, 151
complex, 234
  k-regular, 25, 27, 40, 44, 72
  abstract simplicial, 23
  isomorphism, 44
  refinement, 26
  regular, 25, 27, 72
  self-similar, 27
  simplicial, 39
    isomorphism, 40
    refinement, 39
  with boundary, 25
Condition A, 73, 76, 77
Condition C, 96
contraction function, 138, 142
contractivity function, 160
control set
  definition, 34
  of a triangle,size, 34
control size, 183, 189
convergence rate, 260
covering, 133, 137, 187
creases, 147
cyclic subspace, 50, 104
  decay exponent, 92
  enumeration, 20, 50

decay exponent, 92
degree estimate, 101

detail vector, 236
directional set, 85
    definition, 81
    nondegenerate, 84
Discrete Fourier Transform, 184
Doo-Sabin scheme, 30, 181, 260, 263
dyadic, 44

eigenbasis function, 73
    definition, 50
    extension to the whole plane, 57
    trivial, 52
eigenbasis functions
    constant, 52
    linear independence of Jacobians, 86
eigenvalue, 81
    1, 52
    complex, 103
    of subdivision matrix, 50
    trivial, 52
eigenvalues, 50
    enumeration, 20, 50
eigenvector, 81
    constant, 52

finite support, 31
functions on complex, 28
fundamental group, 187

Gauss map, 81
generalized eigenvector
    complex, 50
    decay exponent, 92
    decay exponent of a pair, 92
generalized eigenvectors, 55, 74
    real, 51

injectivity, 136
injectivity criterion, 129
invariance
    with respect to a set of isomorphisms, 182
isomorphism
    of complexes, 24

Jacobian, 67, 76, 132
    of a pair of eigenbasis functions, 73
    linear combinations, 94
    of characteristic map, 90
Jordan block, 75
Jordan normal form, 54, 85
Jordan subspace
    enumeration, 20, 50

Laplacian pyramid, 237
Laurent polynomial, 141, 148
    L^∞-norm, 146
layer, 49
limit function
    basis function decomposition, 41, 42
linear approximation
    of a curve, 137
link
    of a vertex, 23
Lipschitz norm, 126, 129
local definition, 32

local frame, 235
local isomorphism, 24
localization set, 74
    definition, 35
    of a triangle,size, 36
localization size, 32, 35, 47, 183, 189
Loop scheme, 161, 181, 235
    characteristic maps, 218
    convergence rates, 219
    definition, 32
    eigenvalues, 218
    eigenvectors, 218
    mesh structure near extraordinary vertices, 224
    modifications, 222
    subdivision matrix, 48
    with creases, 225

Modified Butterfly scheme, 205, *see* definition
    C^1-continuity, 211
    arbitrary valence, 212
    characteristic maps, 210, 212
    convergence rate, 146, 210
    subdivision matrix, 209
modified Butterfly scheme, 161
multiresolution editing, 234

neighborhood
    computing, 250
    definition, 24
    properties, 36
Newton diagram, 112
nondegeneracy condition, *see* Condition A
normal, 67, 100
    as wedge product, 67
    orientation, 67

order
    definition, 50

parametric map
    definition, 87
partition of U_1, 93
piecewise linear approximation, 129, 132
point
    dyadic, 44
    internal, 44

quasihomogeneous, 267
quasihomogeneous polynomials, 97, 112

refinement
    complex, 26
refinement rule, 263
regular, 63
rendering
    adaptive, 249
restriction, 240
Riesz basis, 102

scaling relation, 76
    tangents, 80
scaling relations, 53, 75, 96, 108
sharp features, 147
simplical map, 24
simplicial complex
    closed, 24

local isomorphism, 24
tagged, 29, 263
singular parameterization, 72
stationarity, 47
stencil, 31, 189
Loop scheme, 31
subdivision
adaptive, 241
analysis for arbitrary valence, 159
as projection, 74
convergence
criterion, 56
estimate, 140
rate, 138
limit function, 18, 40, 50
basis function decomposition, 41, 42
linear approximation, 41
piecewise constant approximation, 42
subdivision function, 31
subdivision matrix, 74
block-diagonal form, 185
cyclic, 184
definition, 47
eigenvalues, 50
for single ring schemes, 190
Jordan normal form, 54
tangent, 80, 104
eigenstructure, 86
Jordan structure, 104
tangents, 80
subdivision scheme
C^1-continuity, 157
C^1-continuous
criterion, 95
C^k-continuous
criterion, 95, 98
affinely invariant, 32
algorithm for testing C^1-continuity, 193
arbitrary valence
C^1-continuity, 193
Butterfly, *see* Butterfly scheme
Catmull-Clark, *see* Catmull-Clark scheme
comparison, 156
computing normals, 100
convergence
rate, 156
convergent, 40
crease, 147, 225
definition, 30
derivative, 143, 145
difference, 131, 154
Doo-Sabin, *see* Doo-Sabin scheme
finitely supported, 31
Haar, 129
invariant, 182
conditions for C^1-continuity, 187
with respect to a set of isomorphisms, 182
Laurent polynomial, 141
locally defined, 32
Loop, 161, *see* Loop scheme
matrix, 142, 149, 260
Modified Butterfly, *see* Modified Butterfly scheme

modified Butterfly, 161
nonstationary, 261
piecewise constant, 129, 139, 156
single ring, 189, 260
stationary, 47
stencil, 189
tangent plane continuity, 77
sufficient conditions, 88, 91
support size, 31
surface
C^1-continuous, 63, 64
self-intersections, 63
singular parameterization, 72
tangent plane continuous, 67
tangent plane continuous in $\mathbf{R}^p$, 69
synthesis, 238
adaptive, 241
local, 244

tangent plane continuity, 67
criterion, 83, 87
necessary condition, 92
of universal surface, 76
tangent plane continuity in $\mathbf{R}^p$, 69
Taubin's smoothing, 233, 236, 247
tension, 147
tension parameter, 147, 225

universal surface
definition, 76
reparameterization, 76

vector
normal, 100
tangent, 100

wedge product, 67
winding number, 137, 187
computation, 137